ACTIVE ADAPTIVE CANCELLATION OF SOUND IN DUCTS

A thesis by
Ian David McNicol
B.E.(Hons)

Submitted for Degree
of
Master of Engineering
Science
Department of Electrical
and
Electronic Engineering
University of Adelaide

Submitted 28th June 1985

Awarded 27-11-1985

TABLE OF CONTENTS

SYNOPSIS

In this thesis we consider the Active Adaptive Cancellation of Low Frequency Sound propagating down a duct. Active Sound Cancellers operate by injecting into a duct an anti-phase copy (anti-sound) of the primary sound propagating down the duct. Cancellation results when the primary sound and the anti-sound destructively interfere.

We have conducted a theoretical analysis of a practical Active Adaptive Sound Canceller based on the time domain LMS algorithm. This Adaptive Sound Canceller generates an estimate of the anti-sound by convolving an input signal (obtained from a microphone placed to sense the primary sound in the duct) with the tap weights of a transversal filter. The tap weights are updated using the LMS algorithm. We have further constructed and tested such an LMS Adaptive Sound Canceller.

We have recognised that the active cancellation of sound involves conditions additional to those of conventional electrical noise cancellation systems (i.e. the Adaptive Noise Canceller). In the case of the LMS Adaptive Sound Canceller, the adaptive algorithm does not have direct access to the sound that is to be controlled, but must sense this sound using electro-acoustic transducers. The cancelling sound cannot simply be subtracted from the sound in the duct, but must be added acoustically using a loudspeaker. Also, the algorithm only has access to a delayed error signal sensed by a microphone. The additional electro-acoustic transfer functions can be allowed for if known, but in most cases they will not be known accurately. We call this difference between the actual and estimated transfer functions mismatch.

The effect of the delayed error signal is to reduce the stability limit on the convergence constant of the LMS algorithm by a factor $\mathrm{Sin}(\pi/2(2d_2+1))$ where d_2 is the discrete delay between the loudspeaker and error sensing microphone. For a general mismatch it is found that the algorithm will become unstable if a mismatch in phase of greater than $\pm 90^{o}$ occurs between the actual and estimated transfer functions at any frequency of operation.

The work on the delayed error signal is an application of the work undertaken by Kabal on the stability of LMS adaptive Equalizers with delayed adjustment, to the LMS Adaptive Sound Canceller. The work on mismatch is an extension of the work of Morgan on the stability of Multiple Correlation Cancellation Loops with filters in their auxiliary paths. We have recognised that the "filter in the auxiliary path" as proposed by Morgan is the same as the mismatch for the Adaptive Sound Canceller. We have extended Morgans work to consider the effect of mismatch on the stability of our system.

As a result of our theoretical analysis, a control unit for a time domain LMS Adaptive Sound Canceller has been built using two TMS32010 Digital Signal Processing chips. The design incorporates a compensating filter that is used to reduce the effect of mismatch. Tests of this system have been conducted at the CSIRO Division of Energy Technology in Melbourne.

We have also conducted a theoretical analysis of an Adaptive Sound Canceller based on the frequency domain LMS algorithm. It is found that each frequency channel of the frequency domain LMS Adaptive Sound Canceller is similar to a time domain LMS A.S.C. with only two taps and a narrowband input signal. The stability conditions applicable to the time domain LMS Adaptive Sound Canceller can be applied to the

frequency domain LMS Adaptive Sound Canceller on a channel by channel basis.

This thesis contains no material which has been accepted for the award of any other degree or diploma in any University.

To the best of my knowlege and belief, this thesis contains no material previously published or written by another person except where due reference is made in the text of the thesis.

Name: IAN DAVID MCNICOL Course: M.ENG.SC.

I give consent to this copy of my thesis, when deposited in the University Library, being available for loan and photocopying.

Date: 5/7/85 Signed: .....

ACKNOWLEDGEMENTS

Firstly, I would like to thank my Supervisor Professor R.E. Bogner for not only suggesting the topic of "Active Adaptive Sound Cancellation" but also for providing support, encouragement and understanding during the lifetime of the project, and for a few pointers along the way. My thanks also go to Dr. B.R. Davis who acted as Supervisor for six months in Professor Bogners absence.

I gratefully acknowledge the assistance of Dr. Andre Cabelli, Frank La Fontain and Ian Shepherd of the CSIRO Division of Energy Technology in regard to conducting tests of the Adaptive Sound Canceller Control Unit. In particular I am grateful to Frank La Fontain for providing valuable assistance and cheerful support when conducting the tests. My thanks also go to Harry Timtschenko for writing interface programs for the Sorcerer mini-computer as part of the tests.

I would also like to express my thanks to Rod Bryant and Justin Johansson for many discussions, and some useful suggestions when the Adaptive Sound Canceller Control Unit was being constructed and tested in the laboratory.

Finally, I would like to acknowledge the assistance of the following bodies in providing funds to support the research; Adelaide University Research Grants, Radio Research Board, and the CSIRO Division of Energy Technology. Throughout the lifetime of the project, I have been supported by a Commonwealth Postgraduate Research Award scholarship.

1. INTRODUCTION

1.1 LOW FREQUENCY NOISE IN DUCTS

There are many examples of high level low frequency sound sources in the range 0-500Hz that occur in everyday life. Some of these sources are man made such as compressors, transformers, airconditioners, cars, ships and planes, and some are natural such as wind, turbulence, storms and earthquakes(0).

In this thesis we shall be concentrating on the cancellation of low frequency sound that is propagating down a duct. The classic example of this is sound propagating down an airconditioning duct however the duct may also be some form of exhaust, ventillation shaft, or chimney stack. For the case of sound propagating down a duct the low frequency noise is usually generated by a turbine or fan, and this noise will propagate through the duct until it reaches an outlet(0).

A typical fan sound power spectrum consists of a broadband portion with superimposed discrete peaks at the blade passage frequency and subsequent harmonics. The relative contribution of the broadband and discrete components depends upon the type and geometry of the fan used(75). Figure 1.1 shows typical sound power spectra for axial and centrifugal fans.

There has been considerable research into the effects of low frequency noise on people. It is generally accepted that exposure to high levels of low frequency noise result in nausia, fatigue, disorientation, pain and general disturbance. However, there is still much debate about the level of noise and the exposure period that is required to bring about these effects(0).

It has also been suggested by some researchers that even low

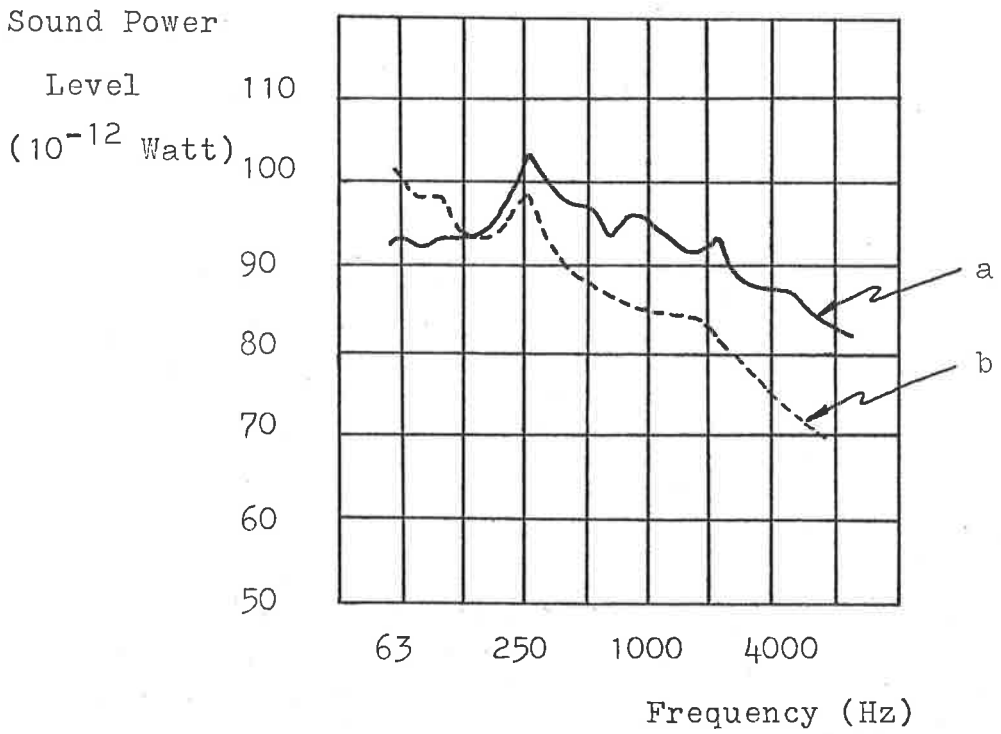

FIG 1.1: Typical Fan Sound Power Spectra*

a: A 10 blade vaneaxial fan at 1470 RPM.

b: An 8 backward curved blade centrifugal fan at 1750 RPM.

* Taken from Ref(75)

levels of some specific frequencies can affect bodily functions such as speech, eyesight, balance and thought processes. Here again, there is a good deal of contention as to the level and duration of the exposure that produce these effects(0).

Although there may be some dispute about the more drastic effects of low frequency sound, most people would agree that it can be quite annoying in too large a dose. It is for this reason that quite a bit of effort has gone into the design and development of systems that can attenuate the level of low frequency noise.

1.2 ACTIVE SOUND ATTENUATION IN DUCTS

In general, there have been two types of systems that have been designed to attenuate sound propagating down ducts; systems that employ passive techniques, and systems that employ active techniques.

Passive, or conventional systems are still in wide use today. They consist of such measures as lining ducts with absorbent sheeting, plenum chambers, splitters and helmholtz resonators(2, 42,75).

A plenum chamber is a large enclosed space containing some sound absorbent material which is inserted into the duct, usually just after the fan. The inlet and outlet are displaced relative to each other so that only some of the incident sound passes directly to the outlet, the rest being internally reflected and absorbed(75). A lined duct simply uses special absorbent sheeting on the inside of the duct to absorb the sound, and a splitter is a device formed from absorbent material that is inserted into the duct, dividing it up into a number of smaller sections, thus giving a larger surface area to absorb the sound(75). A helmholtz resonator is a resonant acoustic

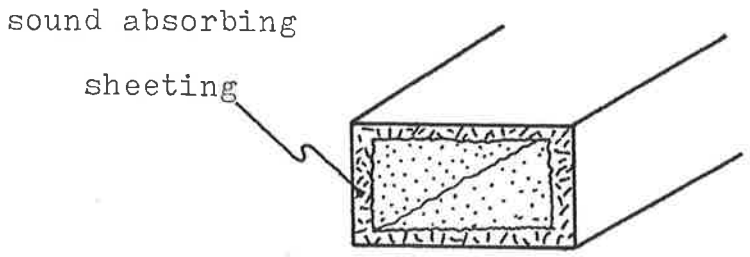

(a) A Lined Duct*

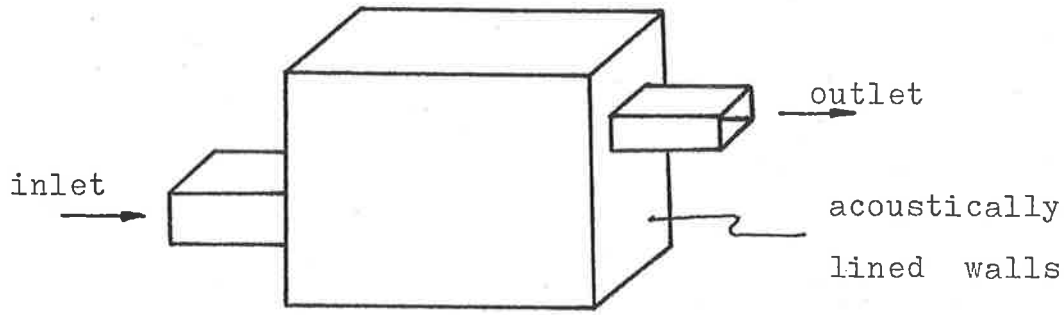

(b) A Plenum Chamber*

* Taken from Ref(75)

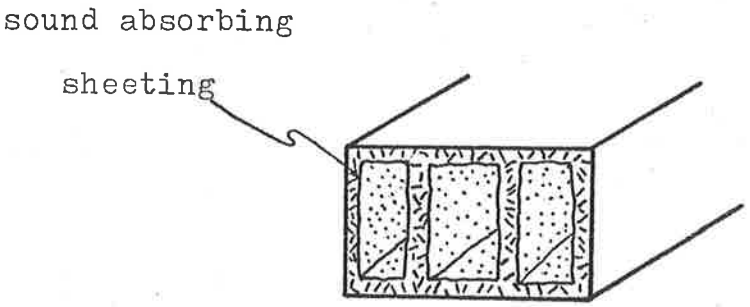

(c) A Splitter

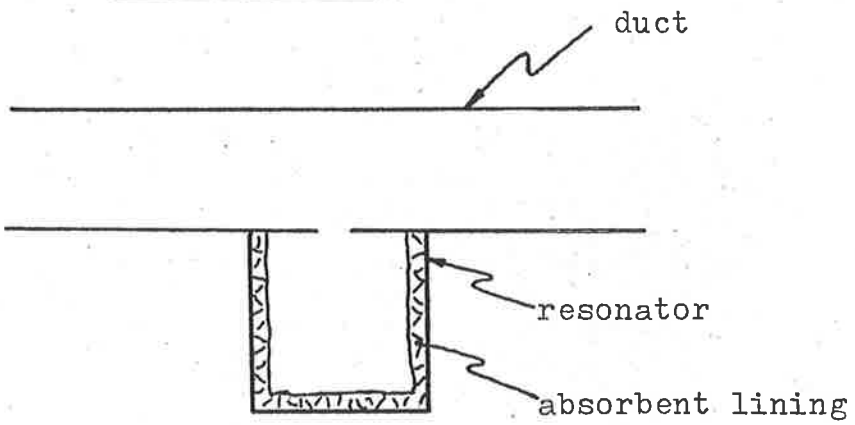

(d) A Helmholtz Resonator

FIG 1.2: Passive Techniques of Sound Attenuation

cavity that is coupled to the duct, and lined with sound absorbing sheeting(2). Figure 1.2 shows the main passive techniques for obtaining sound attenuation in ducts.

The conventional attenuators are inexpensive to manufacture, but have the disadvantage of giving poor performance at low frequencies. This is due to the low absorption coefficients of the sound absorbing material at low frequencies(2). The poor low frequency performance leads to the need to install much bulkier absorbing sheets than would be required to achieve satisfactory performance at the middle and upper frequencies, that is, above 500Hz(25).

Other disadvantages of passive absorbers at low frequencies are that if they are too bulky they can obstruct the airflow down the duct, and also plenum chambers and helmholtz resonators become too large at low frequencies(2,25).

To overcome the problems of passive sound absorption systems, Active Sound Cancellation systems have been proposed and tested. As yet however these systems have not found wide application in industry. Active sound cancellation systems operate by injecting into the duct an anti-phase copy (anti-sound) of the offending sound which cancels out this sound by destructively interfering with it. Active sound cancellation systems have the potential of yielding considerably improved low frequency performance over passive systems, a reduction of size and weight in comparison with the passive systems, and zero or very low back pressure as there are no obstructions in the duct(5,25). A block diagram of a general Active Sound Cancellation system is shown in Fig. 1.3.

In general, there are two types of active system that have been proposed. The first of these injects the anti-sound into the duct so that it propagates in both the upstream and downstream directions. In this case the sound will be cancelled

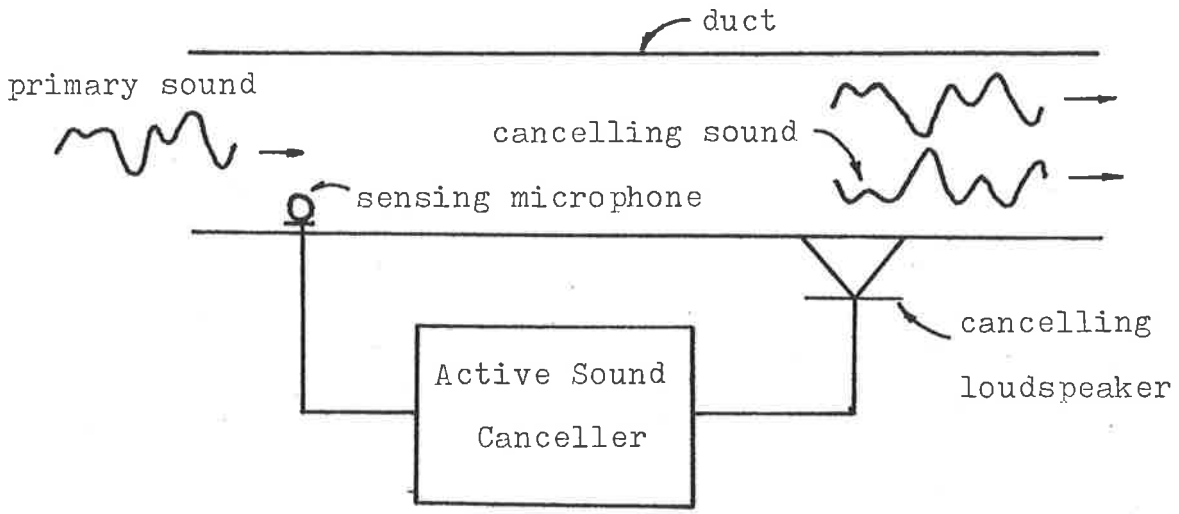

FIG 1.3: A General Active Sound Canceller

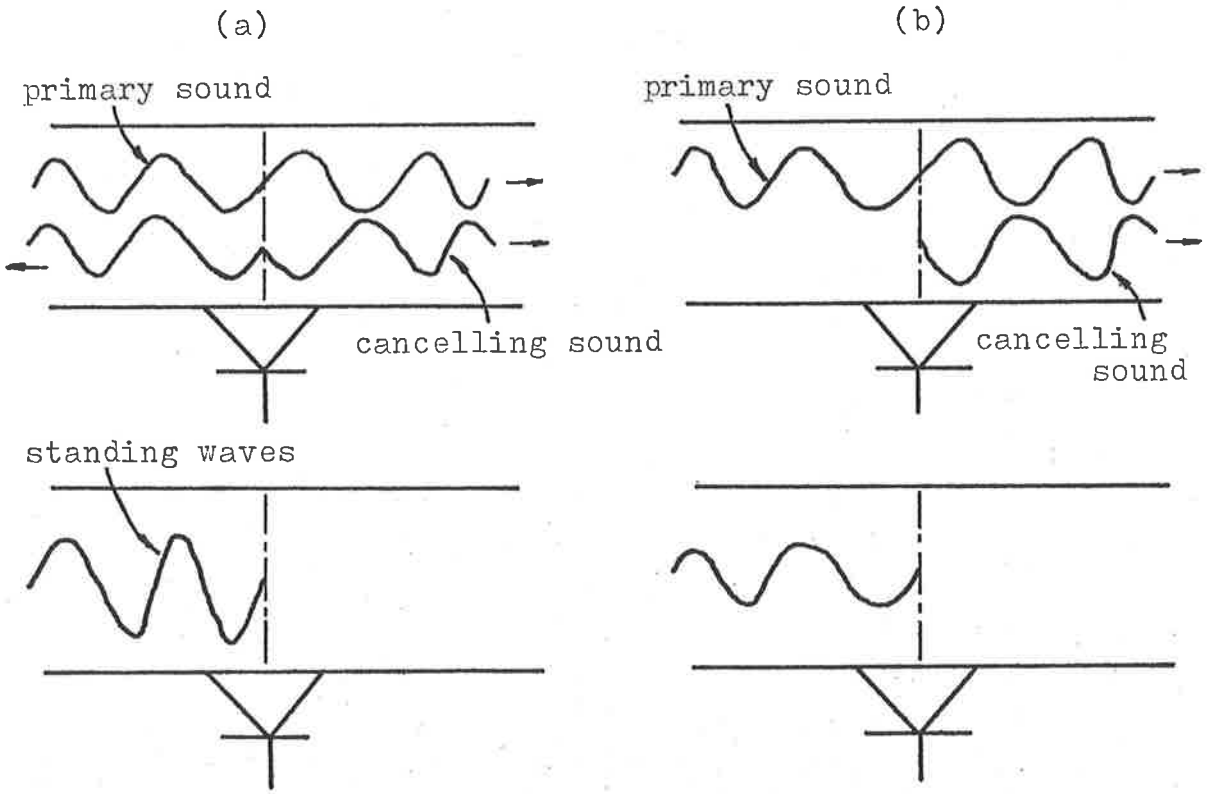

FIG 1.4: Two Types of Active Sound Cancellation

(a) Reflection of primary sound wave

(b) Absorption of primary sound wave

in the downstream direction but will cause a standing wave to be produced in the upstream direction. In effect, the incident sound has simply been reflected back upstream.

The second system injects the anti-sound into the duct so that it propagates in the downstream direction only. In this case, the sound is cancelled in the downstream direction but there are no standing waves in the upstream direction, and so effectively the incident sound has been absorbed. The two different types of active cancellation systems are shown in Fig 1.4.

Passive attenuation systems give good performance at higher frequencies (i.e. above 500Hz), and active systems have shown promising performance at low frequencies. For this reason, it has been suggested that future systems for the attenuation of sound in ducts will be a combination of active and passive systems(5). The projected performance of such a hybrid active-passive sound attenuation system taken from a recent review(5) is shown in Fig 1.5.

1.3 OVERVIEW OF THESIS

In this thesis we will be considering the active adaptive cancellation of low frequency sound propagating down a duct. As an introduction to this topic in Chapter 2 and Chapter 3 we consider the development of Active Sound Cancellers.

Chapter 2 follows the development of non-adaptive Active Sound Cancellers from when they were first proposed by Leug in 1933, up until modern times when practical systems were being tested. There is a discussion of the first attempts to construct active sound cancellers by Olson and May, and Conover in the 1950's and the theoretical work of Jessel in the

1960's which resulted in his "Principle of Active Absorption".

A major section of Chapter 2 is a discussion of the work undertaken by various researchers in the 1970's as they attempted to build practical sound cancellers. The discussion of this work is split up into the development of Monopole, or Sound Reflecting Systems, and the development of Active Sound Absorbers.

Chapter 3 follows the development of Active Adaptive Sound Cancellers, and also takes a look at the future directions that this field may take. There is a discussion of the work undertaken by the "Essex Team" on the cancellation of repetitive, and random noise, and the adaptive algorithm proposed by Ross.

A major section of Chapter 3 is a discussion of the development of LMS Adaptive Sound Cancellers. These systems developed from work by Sondhi and Presti on the Adaptive Echo Canceller, and Widrow et al on the Adaptive Noise Canceller. Burgess in 1981 based his Adaptive Sound Canceller (ASC) on a blend of these two systems, and conducted computer simulations on a simplified model. Warnaka et al have since developed a working system, the Adaptive Acoustic Canceller that is similar to the ASC proposed by Burgess, but more sophisticated.

In Chapter 4 we undertake a mathematical analysis of a practical Active Adaptive Sound Canceller based on the time domain LMS algorithm. The Adaptive Sound Canceller that is studied is an extension of the simplified ASC proposed by Burgess to take into consideration all of the practical effects.

The mathematical analysis concentrates on the stability and convergence of the LMS algorithm used to update the weights of the transversal filter which forms part of the ASC. The

stability of this algorithm is found to be dependent on a convergence constant, certain acoustic delays, and a quantity known as mismatch. This work is based on the work of Kabal on the stability of adaptive LMS Equalizers using delayed adjustment, and also the work of Morgan on Multiple Correlation Cancellation Loops (LMS algorithms) with a filter in the auxiliary path.

In a truly practical ASC system the Noisy Gradient LMS (NGLMS) algorithm would be employed rather than the LMS algorithm which requires the calculation of a data correlation matrix. In Chapter 4 we also consider the stability of an ASC based on the NGLMS algorithm. This turns out to be a very similar problem to the stability of the LMS Adaptive Sound Canceller.

In the final section of Chapter 4 we consider extensions that can be made to the practical ASC to improve its performance.

In Chapter 5 the design and construction of a practical Active Adaptive Sound Canceller based on the TMS32010 Digital Signal Processing chip is considered. The ASC uses a normalized form of the time domain LMS algorithm to update a 32 tap transversal filter that is used to model the anti-phase path. The design also incorporates a compensating filter that is used to condition the error signal and reduce the effects of mismatch.

A description, and results are given for tests conducted at the CSIRO Division of Energy Technology in Melbourne, and also tests conducted using a simulation circuit.

In Chapter 6 we consider the implementation of an Adaptive Sound Canceller based on a frequency domain adaptive algorithm. This includes a discussion of frequency domain LMS algorithms,

Transform domain algorithms, and Frequency Sampling Filters.

The final section of Chapter 6 considers the implementation of a frequency domain Adaptive Sound Canceller employing Frequency Sampling Filters.

We conclude the thesis in Chapter 7 with a summary of the main points arising from the theoretical work undertaken in Chapters 4 and 6, and comments and conclusions based on the theoretical work, and tests performed on the time domain LMS Adaptive Sound Canceller.

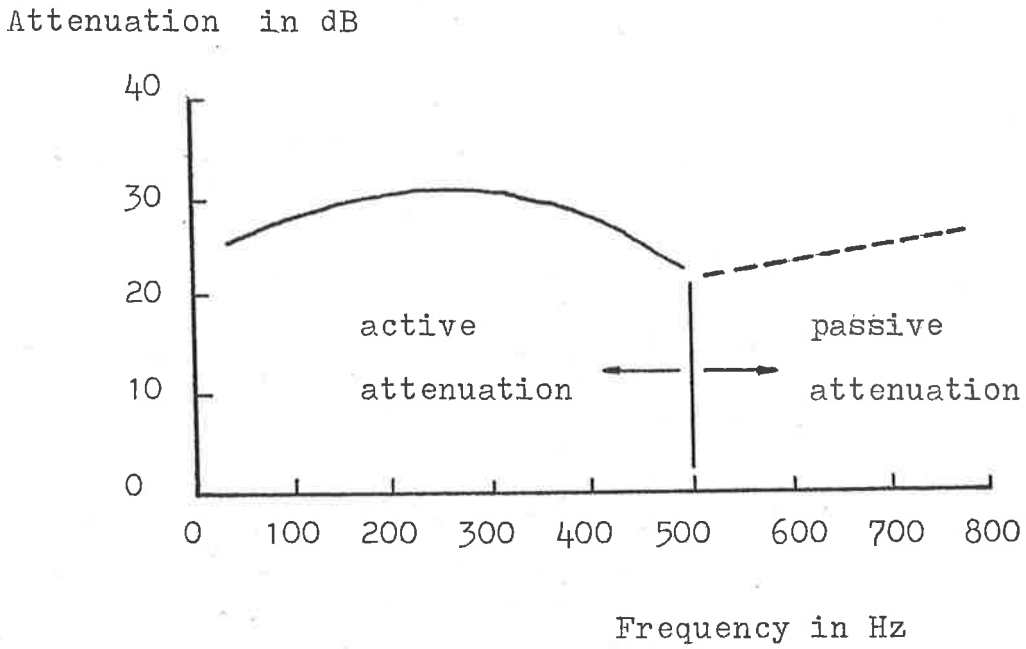

FIG 1.5: Projected Performance of Hybrid Sound Attenuator for a Duct*

* Taken from Ref(5)

2. DEVELOPMENT OF ACTIVE SOUND CANCELLERS

2.1 OVERVIEW

In this chapter we will be looking at the development of Active Sound Cancellation systems from when they were first proposed by Leug in 1933, up until modern times when practical systems were being tested in the laboratory and in the field.

Leug's proposals for active sound cancellation contained many features that are evident in modern cancellers, however they were somewhat ahead of their time. Leug lacked the technology to realize his system and his ideas lay dormant for over twenty years. These first steps in the development of active sound cancellers are described in Section 2.2.

In 1953, Olson and May revived the field of active sound cancellation with the introduction of their Electronic Sound Absorber. This system was tested in the laboratory, and although they could achieve some attenuation, their results were by and large unsatisfactory. Olson and May's work inspired other researchers such as Conover to investigate active sound cancellation, but yet again due to inadequate technology satisfactory results could not be obtained and by the late 1950's interest in active cancellers had died down. The work of Olson and May, and Conover was the first attempt to build and test practical sound cancellers. This work is described in Section 2.3.

The first attempts at sound cancelling were based on rather inexact theory. In 1968, Jessel introduced his "Principle of Active Absorption" based on Huygens Theory of Wave Propagation, and this set the field of active sound cancellation on a more solid base. The development of this principle, and its application to the cancellation of sound in ducts is described

in Section 2.4.

The 70's saw a period of increased interest in active sound cancellation, and there was considerable effort aimed at developing a practical wide band sound canceller. This interest was partly due to Jessels work in 1968, and a theoretical study by Swinbanks in 1973, but was also due to the fact that technology had finally caught up with theory. Researchers were now able to obtain encouraging results in the laboratory, and work began on the development of practical systems that would find applications in industry. The work of Swinbanks and the various other researchers who worked to produce a practical active sound cancellation system is described in Section 2.5.

2.2 ANCIENT HISTORY - THE BIRTH OF ACTIVE SOUND CANCELLATION

The field of Active Sound Cancellation first came into being in 1933 when Paul Leug filed for a patent in Germany. Leug filed for a U.S. patent in the following year, "Process of Silencing Sound Oscillations", and this was granted in 1936(4, 5).

An inspection of Leug's patent application shows that he was aware of the two main principles on which active sound cancellation is based(5).

Firstly, he made use of the well known Principle of Superposition of acoustic waves, and the constructive and destructive interference that results when two waves mix(5).

Secondly, it is obvious that he understood the concept of "negative time"(28). In leug's own words this is(5):-

> "The speed of sound in air is very much less than the speed of electrical impulses. This means that while a relatively slow sound wave is moving from a location

> where it is detected to a location where it can be attenuated, there is ample time available within the electronic circuit for signal processing and activation of the control elements, to a greater or lesser degree depending on the frequency range, the type of noise, and the physical extent of the system."

Although Leug did not build or test his proposed canceller, he discussed several applications in which it could be used. These include the cancellation of sound propagating down a duct, the cancellation of sound in a limited area around a loudspeaker, and noise reduction in an open space(5). A diagram showing Leug's proposal for the cancellation of noise in a duct is shown in Fig. 2.1.

Unfortunately, the electronic technology of the 1930's was not adequate to meet the needs placed upon it by Leug's proposals, and he took their development no further. In particular, this was true of the amplifier whose phase characteristics could not be controlled adequately to meet the requirements of active sound cancellation(5). Active Sound Cancellers would have to wait another 20 years until Leug's ideas in some sense became a reality.

2.3 THE MIDDLE AGES - A BRIEF REVIVAL

2.3.1 OLSON & MAY'S ELECTRONIC SOUND ABSORBER:-

Olson and May first introduced their Electronic Sound Absorber in 1953(1), and Olson extended these initial ideas in 1956(2) to cover more applications. Their work heralded a brief period of renewed interest in the field of active sound cancellation.

The basic Electronic Sound Absorber unit consisted of a microphone, amplifier and loudspeaker combination connected in an inverse feedback manner, the feedback being acoustic in nature(1,2). Olson and May went to considerable trouble

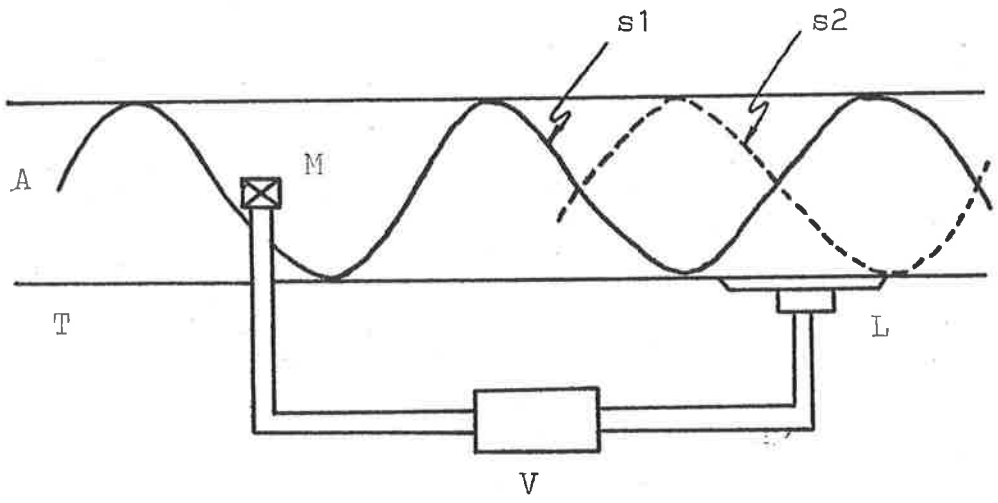

FIG 2.1: Leug's Proposed Active Sound Canceller*

* Taken from Ref(5)

with the system components, especially the microphones and loudspeakers which were designed for low frequency operation (1). A schematic diagram of the basic Electronic Sound Absorber unit is shown in Fig. 2.2.

The Electronic Sound Absorber (ESA) system was connected so that for an incident sound pressure wave the pressure at the microphone was reduced, and the system could be used in two basic ways:-

(i) In its most simple form the ESA could be used as a sound pressure reducer. In this way it was used to reduce the pressure in a zone around the microphone by destructively interfering with the incident pressure wave(1,2,5).

(ii) The ESA could be used to absorb the sound falling on the microphone. This required the addition of a special acoustic barrier around the microphone and loudspeaker(1,2,5).

Starting with these two basic configurations, Olson and May suggested many applications in which their ESA could be used. These applications include:-

(a) Spot type sound reducers for reducing the sound level over a limited space. They suggested that this would find applications in the reduction of noise in airplanes, automobiles, trains, factories, ships and offices. Their idea was to place the ESA unit in a position such that it reduced the noise in the vicinity of a persons ears(1,2).

(b) Noise reduction for ducts and exhausts. Applications here include the reduction of noise at the outlet of a duct or exhauxt, and the cancellation of noise propagating down a duct. Diagrams showing the way in which Olson and May proposed to construct these systems

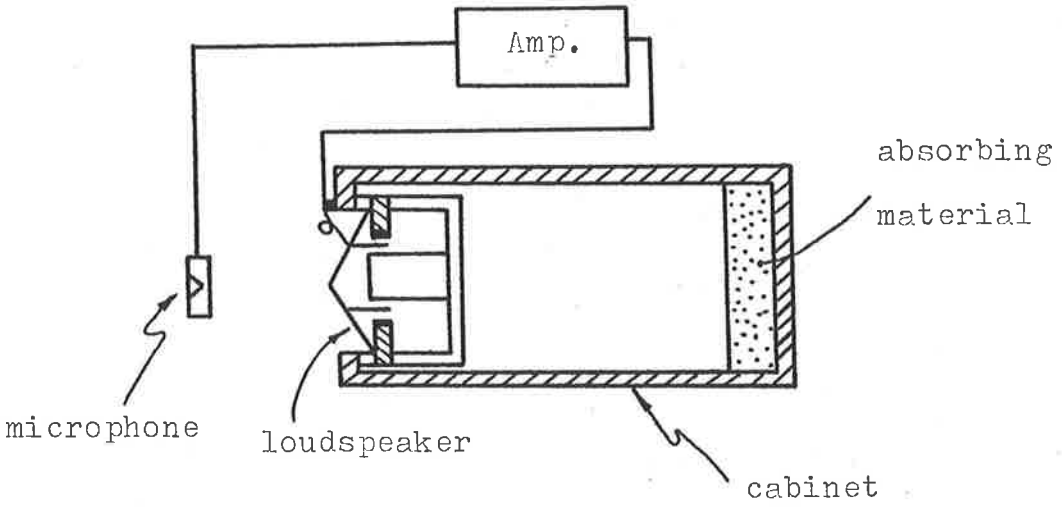

FIG 2.2: Olson and May's Electronic Sound Absorber*

* Taken from Ref(2)

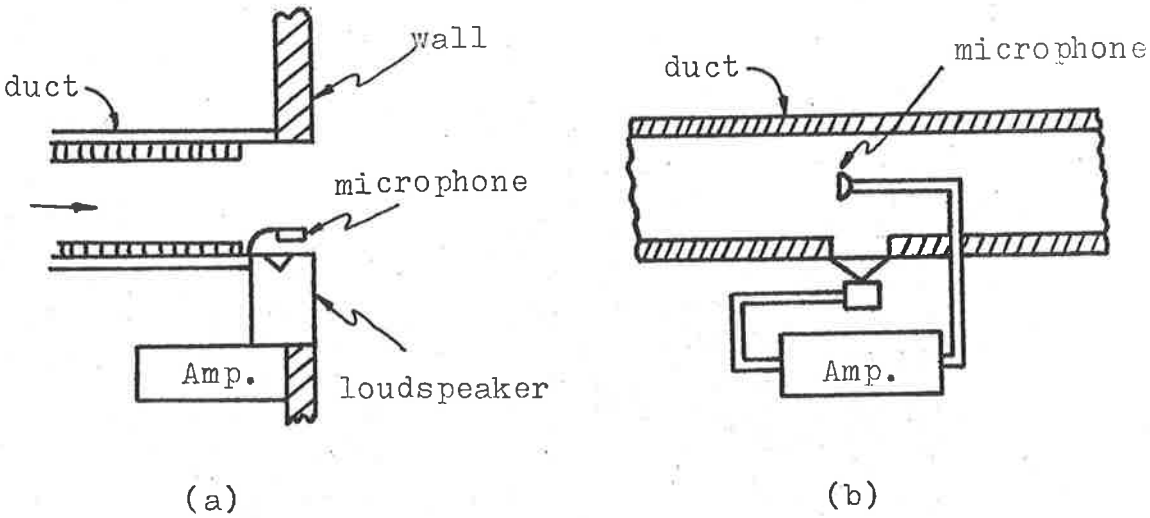

FIG 2.3: Olson and May's Proposed Sound Cancellers*

(a) At outlet of duct

(b) In duct

are shown in Fig. 2.3 (1,2).

(c) Noise reduction in closed places. Suggested applications here were a noise reducing helmet, and a noise reducing headset(2).

Olson and May tested many of these proposed devices in the laboratory, but found that their performance was limited by the performance of the basic ESA unit. The noise reduction that could be obtained by this unit was limited to a fairly narrow frequency band, and the performance dropped off rapidly only a short distance from the microphone. At a distance of only 30cm, the system was of marginal utility(1,2,5). The performance of Olson and May's Electronic Sound Absorber as it varies with distance is shown in Fig. 2.4.

Olson and May's accomplishment lies in the fact that they were the first to test an active sound canceller in the laboratory, and were able to suggest many ways in which such a device could be used. The limited usefulness of the ESA in practical applications was due in part to the poor low frequency response of the loudspeaker(5), phase problems and limitations of the amplifier electronics(5), and also the fact that the ESA in essence was only a narrow band canceller by virtue of its construction. This final point is dealt with in more detail in Section 2.5.2 when Monopole Systems are investigated.

2.3.2 THE REDUCTION OF TRANSFORMER NOISE:-

In 1956, William Conover(3) in work undertaken for General Electric was the first to investigate the attenuation of transformer hum by active means. This has now become the classic three dimensional active sound cancellation problem.

Conover's work differed from that of Leug, and Olson and May

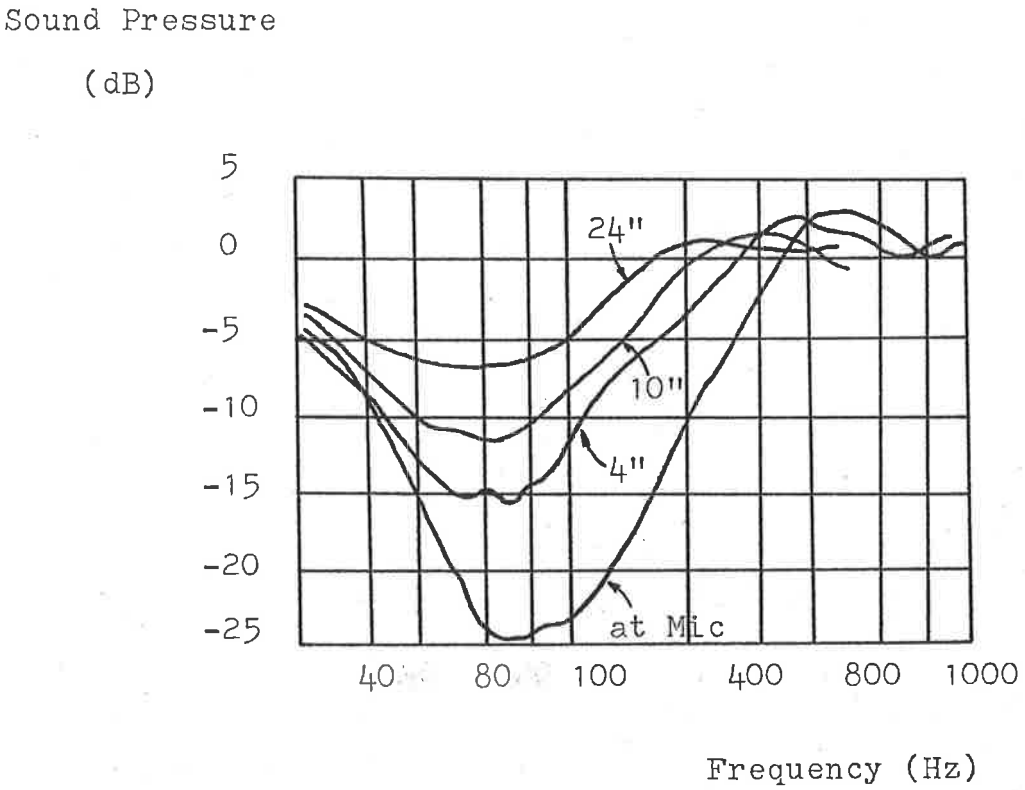

FIG 2.4: Performance of Olson and May's E.S.A.*

* Taken from Ref(5)

in that he did not drive the cancelling source from the incident sound that was to be cancelled. Transformer hum consisted of several harmonic components (120,240,360Hz etc), and the driving signal was obtained by filtering out these components from the power supply(3,4,5).

Conover aimed to reduce the hum directly infront of the transformer. To achieve this he placed his cancelling loudspeaker very close to the surface of the offending transformer so that in the far field good cancellation could be obtained (3,5).

The system was set up by recording the residual sound and analysing each frequency component in turn. For instance, the phase and amplitude of the filtered 120Hz component was adjusted so that a null was obtained in the residual sound(3,4,5).

In preliminary tests Conover found that he could obtain reasonably good results, 20-25dB of attenuation at 100ft, but that the attenuation fell away as he moved off axis, and that after about 25^{o} the sound level was increased rather than reduced(3,4,5). As it turned out Conover was only able to produce a beam of attenuation.

After these initial tests, Conover attempted to apply his technique in several field tests, but was disappointed with the results. He found that the transformers had a sound output that varied with time, and that it would be necessary to keep adjusting his controller to maintain good performance(3). Another interesting observation was that, "It was noted that reduction at maximum position varied between 15 and 35dB, and appeared to be a function of wind velocity"(3).

Thus Conover found that the attenuation that could be achieved was a function of the type of sound that was to be attenuated, and also on system parameters such as wind velocity, and that there was a possibility (probability) that they

would change with time.

Conover suggested that an adaptive controller could be used to meet changes in the sound output, but considered its construction too difficult and expensive. Due to the expense involved with upgrading the performance of Conover's Transformer Noise canceller that had performed poorly in field tests, further experiments with Conover's techniques were postponed by General Electric(3).

Olson and May, and Conover were the first to attempt the practical implementation of Active Sound Cancellers. Although they did have some success, they were still limited by the technology that was available, and they found that their results were not good enough to warrant further investigation. Thus work on active sound cancellaton came to a halt yet again.

2.4 THE RENAISSANCE - AT LAST A THEORETICAL BASIS

2.4.1 INTRODUCTION:-

Leug realized that Active Sound Cancellation was based on the principle of destructive interference of sound waves(5). Olson and May's understanding of it was based on an equivalent circuit and impedence description of the acoustic system(1,2). Conover noted the importance of the placement of the cancelling source, and the possible necessity of multiple cancellation sources if good attenuation was to be achieved(3), but as yet there was no unified theoretical basis on which active sound cancellation could be placed.

In 1968, Jessel introduced his "Principle of Active Absorption". This was based on a lemma on Field Perturbation(6) from which both Huygens Principle of Wave Propagation, and

Jessels principle could be deduced as special cases(6).

2.4.2 HUYGENS PRINCIPLE OF WAVE PROPAGATION:-

Huygens introduced his general theory of wave propagation in 1690. With reference to Fig 2.5, this can be stated as follows(6,8,10):-

> "Consider primary sound sources s_1 that are contained in the space v_1, and bounded by the surface E. These sources radiate a sound field F_1 into the space v_2. Then, a set of secondary sources s^H exist such that when properly distributed over E they will radiate a field F^H which sums to zero in the space v_1, and is equal to F_1 in the space v_2. Thus the primary sources s_1 can be replaced by the Huygens sources s^H with no effect on the radiated field in v_2."

These Huygens sources are infinitesimal and are distributed over the surface E. To compute the sources the primary field, and the partitioning surface must be known(6,8,9,10).

2.4.3 THE PRINCIPLE OF ACTIVE ABSORPTION:-

Now, let us consider the case when we have a set of secondary sources s^A obtained simply by reversing the sign of the Huygens sources s^H. Due to linearity these sources will radiate a field $F^A = -F^H = -F_1$ into the space v_2(6,8,10).

If we now let the sources s^A interfere with the primary sources s_1, the resulting field $F_T = F_1 + F^A$ will be equal to F_1 $(F_1 + 0)$ in v_1, and zero $(F_1 - F_1)$ in v_2(6,8,10). This is shown diagramatically in Fig. 2.6.

Thus the principle of active absorption shows that it is possible to cancel a sound field in any given domain by using

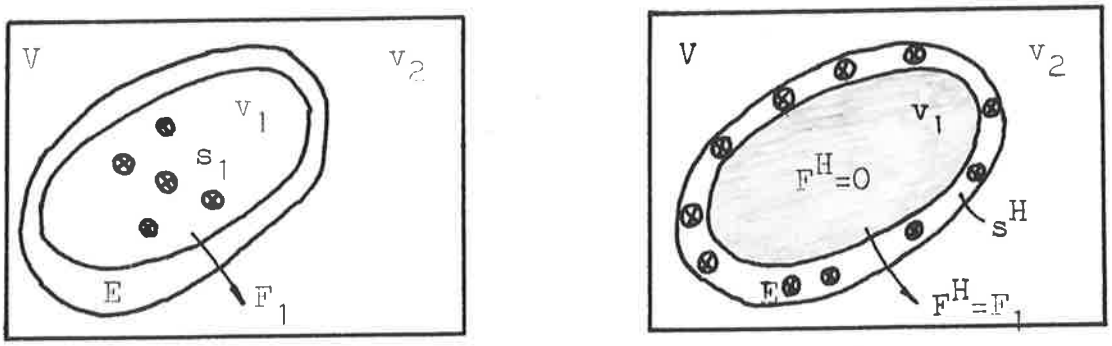

(a) Primary Sources (b) Huygens Sources

FIG 2.5: Huygens Principle*

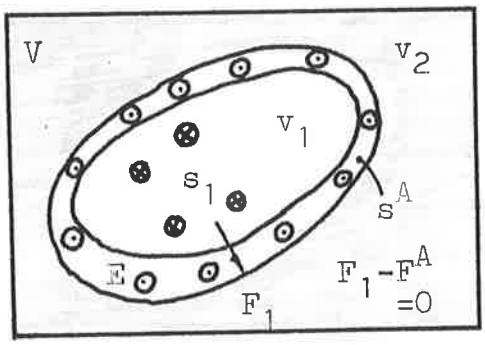

FIG 2.6: The Principle of Active Absorption*

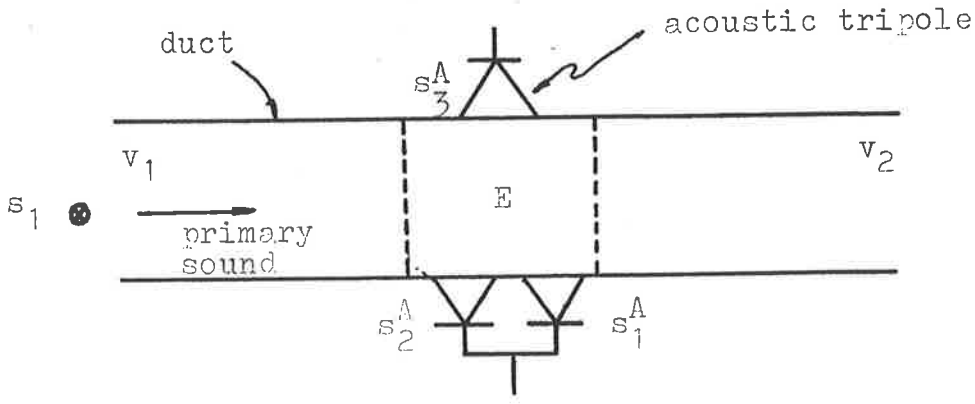

FIG 2.7: Jessel's Active Sound Absorber

* Taken from Ref(10)

a suitable distribution of secondary sources over a surface enclosing that domain.

2.4.4 THE NATURE OF THE SECONDARY SOURCES:-

The absorbing sources s^A are continuously distributed, and can be calculated exactly only when the primary field and absorbing surface are known(9,10).

In (9), Canevet notes that the Principle of Active Absorption has established that for perfect absorption to take place, the boundary E must contain an infinite number of sources, the characteristics of which are highly dependent on the noise to be cancelled.

In practice a continuous distribution cannot be obtained and therefore perfect sound absorption is unobtainable. However, by using an array of discrete sources distributed around the boundary E it will be possible to attenuate the noise to a certain extent over the region v_2 depending on the number, distribution and the nature of the secondary sources used(9, 10).

In general Jessel and Mangiante(6) have shown that there are three types of sources that are required for use as the secondary absorbing sources; monopoles, dipoles, and quadropoles(9). The monopole and dipole sources may be combined to form a tripole source which has a cardoid radiation pattern (8,9).

2.4.5 THE PRINCIPLE OF ACTIVE ABSORPTION APPLIED TO DUCT NOISE:-

Although the Principle of Active Absorption was formulated for the three dimensional case, the practical problems associated with implementing a three dimensional cancelling

system are large(9). For this reason many researchers have considered the simpler one dimensional problem of cancelling sound propagating down a duct.

When the Principle of Active Absorption is applied to this problem, the region v_1 becomes the upstream section of the duct from whence the sound propagates, and v_2 becomes the downstream section of the duct where it is required that the sound be cancelled. The absorbing region E is the region in which the absorbing sources are placed(6,9).

Jessel and Mangiante(6) proposed an active sound absorption system for the cancellation of sound in a duct that used an acoustic tripole as the absorbing source. A diagram of this system is shown in Fig. 2.7.

Due to the cardoid radiation pattern of the tripole there is radiation in the downstream direction, but not in the upstream direction. Although Jessel and Mangiante do not indicate how the tripole is driven in (6), the principle of active absorption tells us that it must radiate a field in the downstream direction that is equal in magnitude, but opposite in phase to the primary sound field.

Although the fine detail of Jessel's theory can become mathematically complicated, the principle is in essence simple. All that needs to be understood is that for active absorption to take place in a duct, the secondary sources must be unidirectional and must reproduce the incident sound in anti-phase.

2.5 MODERN HISTORY - THE QUEST FOR A PRACTICAL SOUND CANCELLER

2.5.1 INTRODUCTION:-

Once the Principle of Active Absorption proposed by Jessel

had laid a solid basis for the theory of active sound absorption, the task that still lay ahead was to implement a practical sound canceller based on this theory and to obtain satisfactory experimental results. The aim was to produce a canceller that could achieve a high level of attenuation over a considerable frequency range; that is, to produce a broadband sound canceller.

An alternative approach that was taken was to construct a broadband monopole canceller instead of an active sound absorber. Such a system would not absorb sound but rather reflect the incident wave upstream. Although monopole systems were first proposed by Leug(4,5), and Olson and May(1,2) they soon fell out of favour because they could only produce narrowband attenuation. More recently however Eghtesadi and Leventhall (24) have shown that the narrowband nature of the monopole system is due mainly to the acoustic feedback from the monopole to the sensing microphone. In an attempt to increase the bandwidth of the monopole systems, recent work has attempted to reduce the effects of the acoustic feedback(24,25).

In the 70's a number of researchers attempted to construct broadband active sound cancellers that would perform well in practical applications. Initial attempts to improve the bandwidth of the systems, (whether monopole or active absorbers), have involved the use of compensation circuits to account for the nature of the secondary sources used. In this section we will look at the major developments that have taken place in the 70's and early 80's as researchers have gone in search of the practical active sound canceller. We will treat the development of monopole systems and active sound absorbers separately as there is a fundamental difference between the two in the way in which the sound is cancelled. In this sec-

tion we will not consider the recent development of adaptive active sound cancelling systems, but this will be dealt with separately in the next chapter. The work on adaptive systems was based largely on the work carried out on non-adaptive systems during the 70's, and the need for adaptive systems became evident from this work.

Monopole Systems:

The renewed interest in monopole systems has been led largely by Eghtesadi, Leventhall and Hong(24,25). These researchers proposed a system known as the Chelsea Monopole that aimed to compensate for the acoustic feedback (that limits system bandwidth) by feeding back an electrical signal to negate its effect. We begin our treatment of monopole systems in Section 2.5.2 with a look at conventional monopole systems such as those proposed by Leug, and Olson and May. This is followed in Section 2.5.3 with a discussion of the Chelsea Monopole system.

The Chelsea Monopole idea was taken further by Eghtesadi, Hong and Leventhall(25), and independently by Trinder and Nelson(26) with the development of the tight coupled active attenuator. This consisted of a Chelsea Monopole in which the sensing microphone had been shifted to be placed directly over the secondary source. In this way it was possible to produce a very simple system consisting only of a loudspeaker, a microphone and a high gain amplifier. The tight coupled attenuator is dealt with in section 2.5.4.

Another unusual system that was proposed by Eghtesadi and Leventhall(20,21,22) was the Chelsea Dipole. Although this system used two secondary sources, it was monopole in nature as it radiated in both the upstream and downstream directions. A unique feature of this system was that the sensing

microphone was placed between the two secondary sources, and the sources phased so that the microphone sensed only the incident primary wave. The Chelsea Dipole is discussed in Section 2.5.5.

Active Sound Absorbers:

In recent times there have been two main approaches taken to implement active sound absorbers based on Jessels theory. The first approach was to implement a system using Jessels acoustic tripole to obtain unidirectional radiation. This system was developed by Jessel and Mangiante(6), and further by Canevet(9). The general properties of Jessels acoustic tripole are discussed in Section 2.5.6, and the practical implementation of sound cancelling systems using this tripole in Section 2.5.7.

The second approach was based on the work of Swinbanks(11), who conducted a thorough investigation into the cancellation of sound propagating down a duct. Swinbanks set out by assuming that his system required unidirectional sources, and working from a general source arrangement deduced a source array to meet his requirements. The secondary source arrays devised by Swinbanks were not tripoles such as Jessel had proposed but consisted of two or three rings of secondary sources placed symmetrically around the duct. Swinbanks theoretical investigations are summarized in Section 2.5.8.

Swinbanks initial proposals were developed experimentally by Poole and Leventhall(12,13), and this work is discussed in Section 2.5.9. These authors then went on to extend Swinbanks basic concepts to general N-source arrays, and this work is dealt with in Section 2.5.10.

Finally, in Section 2.5.11 we look at some new work that has been conducted in the early 80's. Although this work is

in part based on that of Jessel and Swinbanks, it shows a subtle shift of emphasis that has largely been made possible by the development of digital technology.

Instead of starting with a theoretically proposed system and compensating it to overcome inherent shortcomings, the aim of this new work(15,18,19) has been to generate an anti-phase path for the sound incident at the sensing microphone.

2.5.2 CONVENTIONAL MONOPOLE SYSTEMS:-

The conventional monopole canceller as proposed by Leug(4, 5), and Olson and May(1,2) consists of a microphone located upstream from the secondary source with a suitable time delay in between. Such a system is shown in Fig. 2.8. The radiation from the single secondary source S propagates in both the upstream and downstream directions. In the downstream direction the secondary sound acts to cancel out the primary sound but in the upstream direction standing waves are formed. In effect, the primary sound is reflected back upstream.

The monopole attenuator is equivalent to an impedence change in the duct. This causes a redistribution of the energy in the system without necessarily causing the energy to be dissipated.

Let us now consider an analysis of the operation of a conventional monopole. Note that the upstream radiation from the secondary source acts as an acoustic feedback signal, and the microphone detects this along with the primary sound. A block diagram of the relationship between the primary sound P and secondary sound C is shown in Fig. 2.9.

With reference to Fig 2.9 it can be seen that the transfer function of the conventional monopole is as follows(24):-

$$G(s) = \frac{C(s)}{P(s)} = \frac{-e^{-sD}}{1 + e^{-2sD}} \qquad (2.1)$$

where D= time delay 1/c sec.

C(s) = cancelling sound.

P(s) = primary sound.

The magnitude and phase of the transfer function G(s) is(24):-

$$|G(j\omega)| = 1/2\mathrm{Sin}(\omega D)$$

$$\angle G(j\omega) = \pi/2 \qquad (2.2)$$

It can be seen from equation (2.2) that the acoustic feedback modifies the phase of the output from the loudspeaker with respect to the phase of the input signal to the microphone, changing it from a linear function of frequency (i.e. a time delay 1/c), to a constant value of $\pi/2$, which corresponds to a physical delay of $-3\pi/2$(24).

Full cancellation can only occur at one particular frequency, that is, when the phase of the primary sound arriving at the loudspeaker is $-\pi/2$ with respect to its phase at the microphone(24). This occurs for the frequency at which f=1/4D, and corresponds to the particular frequency for which the microphone-loudspeaker spacing is $\lambda/4$ (24).

Also, there will be particular frequencies at which the upstream radiation from the loudspeaker is in phase with the the primary sound arriving at the loudspeaker , and for these frequencies there will be no cancellation. It can be seen then that the conventional monopole cannot provide attenuation over a broadband, but is limited to a narrow band of operation(24).

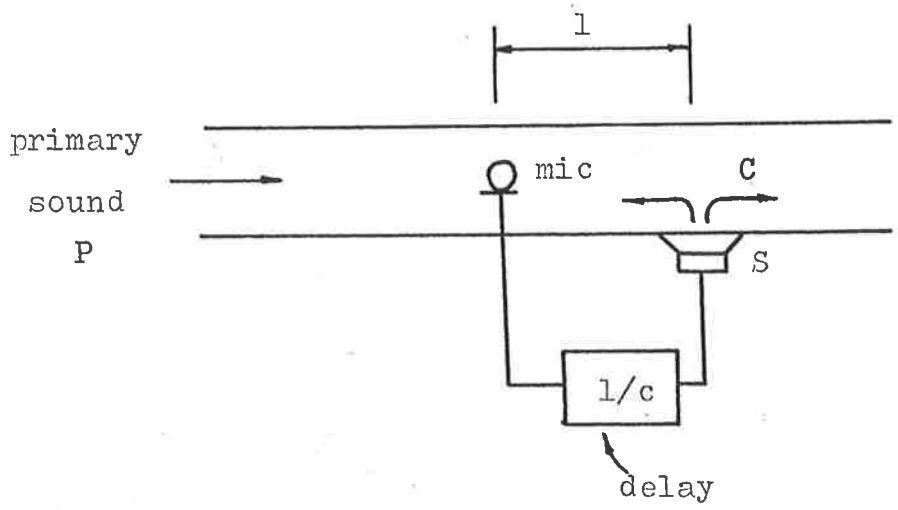

FIG 2.8: Conventional Monopole Canceller

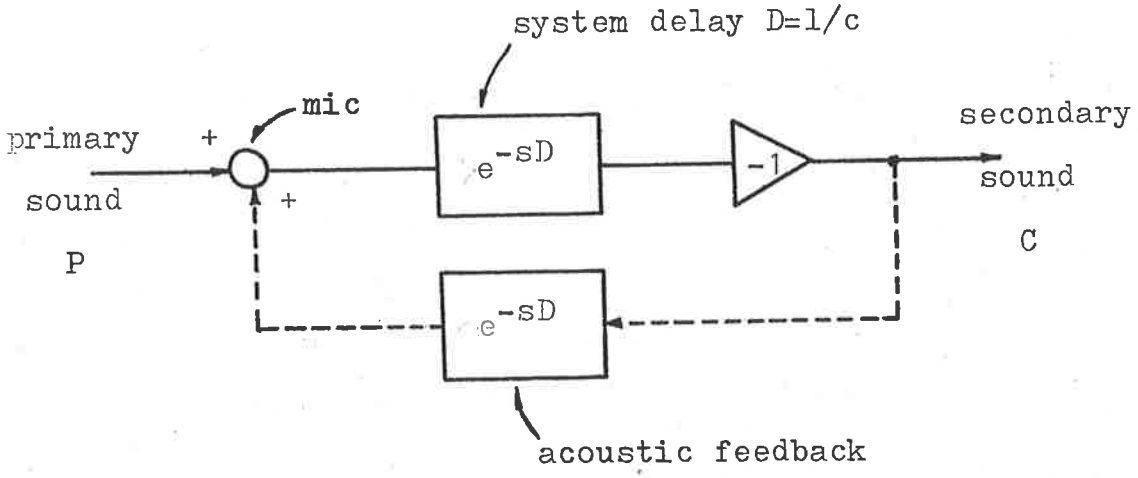

FIG 2.9: Block Diagram of Conventional Monopole*

* Taken from Ref(24)

2.5.3 THE CHELSEA MONOPOLE SOUND CANCELLER:-

The approach taken by Eghtesadi and Leventhall in overcoming the feedback problems associated with the conventional monopole that ultimately lead to a narrowband of operation, was to include a compensating circuit to counteract the acoustic feedback. This new arrangement is known as the Chelsea Monopole. The compensating circuit consisted of an electrical feedback path that was the negative of the acoustic feedback path(24). A diagram of the Chelsea Monopole is shown in Fig 2.10, and a block diagram of the relationship between the primary sound P and secondary sound C is shown in Fig. 2.11.

In the ideal case, (i.e. the electrical compensating path is exactly the negative of the acoustic feedback path), it can easily be seen from Fig. 2.11 that the transfer function, and magnitude and phase of the transfer function of the Chelsea Monopole are as follows :-

$$G'(s) = C(s)/P(s) = -e^{-sD}$$

$$|G'(j\omega)| = 1 \qquad (2.3)$$

$$\angle G'(j\omega) = \pi - \omega D$$

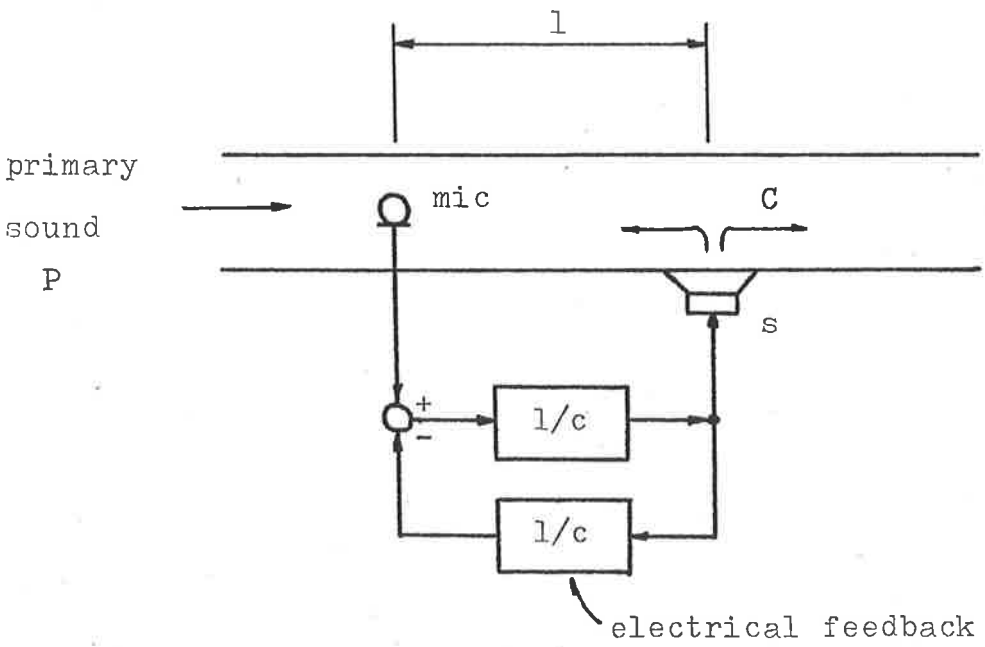

FIG 2.10: The Chelsea Monopole Sound Canceller

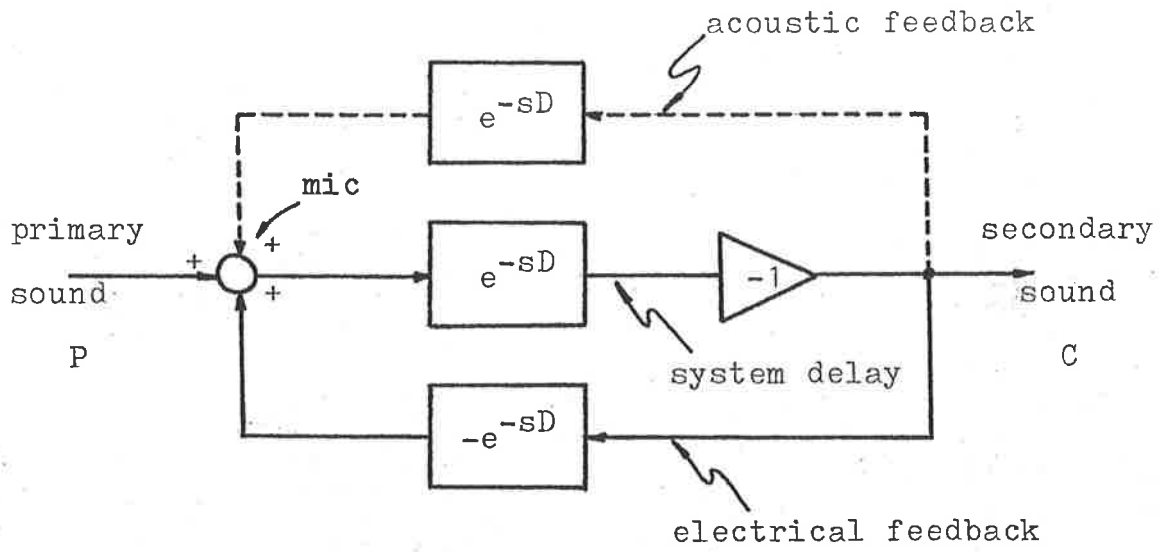

FIG 2.11: Block Diagram of the Chelsea Monopole*

* Taken from Ref(24)

the driving source inside the duct produce fluctuations which reduce the attenuation.

(2) The electronic system does not provide the precise amplitude and phase response that is required.

(3) The microphone and power amplifier do not maintain an ideal response.

In experimental tests of their Chelsea Monopole, Eghtesadi and Leventhall(24) were able to obtain 5 to 18dB of attenuation between 90 and 200Hz for a 30Hz bandwidth random noise, and 5 to 10dB of attenuation between 40 and 200Hz for a 100Hz bandwidth random noise.

2.5.4 THE TIGHT COUPLED ATTENUATOR:-

Eghtesadi, Hong and Leventhall(25) introduced the Tight Coupled Attenuator as an extension to the Chelsea Monopole system proposed by Eghtesadi and Leventhall. Trinder and Nelson(26) have also theoretically analysed such a system, and investigated the optimum placement of the sensing microphone.

Trinder and Nelson(26) point out that it was Olson and May (4,5) who first used a tightly coupled monopole arrangement. Olson and May developed a simple technique of applying closed loop feedback of a microphone signal to a loudspeaker via an inverting amplifier. The microphone was placed close to the loudspeaker, and a sound pressure null was produced at the microphone. The system operated on the "virtual earth principle" which is familiar from operational amplifier theory(26).

In this section we shall consider Eghtesadi, Hong and Leventhall's treatment of the theory. Refer to Figures 2.10, and 2.11 showing the Chelsea Monopole, and the block diagram of the secondary source and compensating network. As we bring the sensing microphone closer to the loudspeaker, which

corresponds to reducing the length of the delay D, then the transfer function of the Chelsea Monopole elements (e^{-sD}) approaches unity(25). At zero separation ($D=0, e^{-j\omega D}=1$), the system block diagram is as shown in Fig 2.12.

If we treat the electrical and acoustic paths in Fig 2.11 separately, then we can write the transfer function for a Chelsea Monopole as follows(25):-

$$G_e(s) = \frac{-e^{-sD}}{1-e^{-2sD}}$$

$$G_a(s) = e^{-sD}$$

$$G'(s) = \frac{G_e(s)}{1 - G_e(s)G_a(s)} \qquad (2.4)$$

From equation (2.4) it can be seen that as the delay D approaches zero, the transfer function of the electrical path $G_e(s)$ approaches infinity. In practice, this amounts to $G_e(s)$ being a high gain amplifier(25). Thus, a practical tight coupled monopole attenuator can be constructed using only a high gain amplifier as shown in Fig 2.13. This system has the transfer function(25):-

$$G''(s) = \frac{C(s)}{P(s)} = \frac{-A}{1 + A} \qquad (2.5)$$

Equation (2.5) reduces to -1 as required when A approaches infinity.

So far, our analysis has assumed the use of ideal components. However, Eghtesadi, Hong and Leventhall have shown that even when the loudspeaker response and acoustic interactions in the duct are taken into account, the system transfer function will still approach -1 as required as long as the ampli-

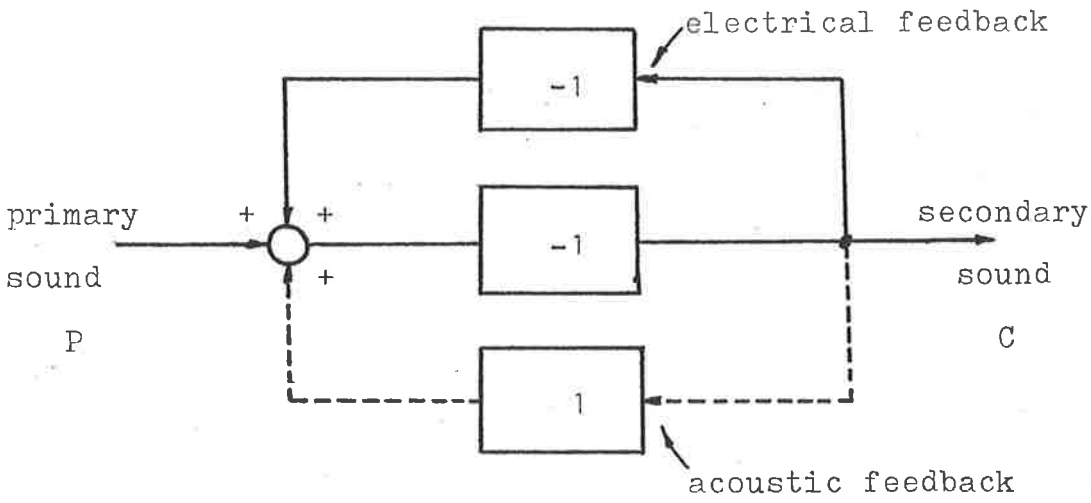

FIG 2.12: Block Diagram of Ideal Tight Coupled Attenuator*

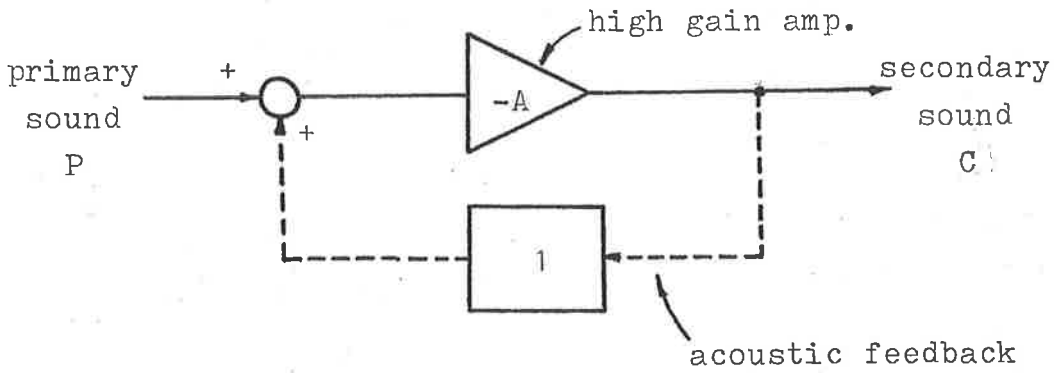

FIG 2.13: Block Diagram of Practical Tight Coupled Attenuator*

* Taken from Ref(25)

fier gain A is large(25).

Under experimental conditions Eghtesadi, Hong and Leventhall found that the stability of the tight coupled attenuator depended on the gain of the feedback loop. Below a certain gain setting the attenuator system was found to be stable (25). However, is was found that there were still limitations to the performance of the system(25):-

(1) Cross modes are present in the near field radiation from the loudspeaker, and these are sensed by the microphone. Trinder and Nelson(26) have investigated the influence of the loudspeaker near field on the sensing microphone. They have demonstrated that the contribution of the transverse modes can be minimized by placing the microphone just below the centre line of the duct.

(2) The frequency response of the loudspeakers can change.

Both Eghtesadi, Hong and Leventhall(25), and Trinder and Nelson(26) have reported quite good results using tight coupled systems. Leventhall(4) has reported the development of a monopole device that is one metre in length and can produce 30dB of attenuation from 31.5 Hz up to high frequencies.

So far, tight coupled attenuators have only been applied in situations in which there is no airflow. However, it would be expected that they would be reasonably insensitive to this. The main advantage of tight coupled systems seems to lie in their simplicity, and that they can use low quality components without demanding high precision in amplitude and phase response(25).

2.5.5 THE CHELSEA DIPOLE:-

In 1976 Leventhall of Chelsea College introduced the theo-

retical aspects of a new type of active attenuator known as the Chelsea Dipole. The practical implementation and development of this device was followed up by Eghtesadi(20,21,22).

Although the secondary source proposed by Leventhall was dipole in nature, it did not produce unidirectional radiation as did Swinbanks dipole (see section 2.5.8), but instead radiated in both the upstream and downstream directions.

The most radical feature of the new system was the placement of the sensing microphone. In an attempt to isolate the microphone from the acoustic feedback from the secondary sources it was placed midway between them. The distance between the two secondary sources is chosen to be $\lambda_o/2$ where $f_o=\lambda_o/c$ is the central operating frequency. A diagram of the Chelsea Dipole sound canceller is shown in Fig 2.14.

When the Chelsea Dipole system is correctly energised, the sound radiating from the two secondary sources s1 and s2 should cancel in the microphone region, and hence the microphone will sense only the incident primary sound(20,21,22).

The secondary sources s1 and s2 radiate in both the upstream and the downstream directions. In the upstream direction the radiation from the secondary sources interferes with the primary sound causing standing waves. In the downstream direction the sum of the radiation from both sources is given by(21,22):-

$$s_x = Ae^{j(\omega t-kx)}\left(e^{-j(kl/2)} - e^{j(kl/2)} \right)$$

$$|s_x| = 2|\mathrm{Sin}(kl/2)|$$

$$\angle s_x = -\pi/2 \qquad \text{(2.5a)}$$

where k = wave number.

l = separation between s1 and s2.

A = constant.

From equation (2.5a) we can see that the downstream radiation from the secondary sources has a constant phase shift of $-\pi/2$, and a frequency dependent amplitude response. The requirements that must be met by the system for perfect cancellation to occur are(20,21,22):-

(1) The input to the loudspeakers from the microphone must be delayed by 90^{o}.

(2) The phase shifter must have a transfer function with modulus $1/2\mathrm{Sin}(\omega/4f_{o})$ where f_{o} is the centre frequency of the system.

Although a theoretical analysis of the ideal system shows that the Chelsea Dipole should operate over a wide range of frequencies, in practice there are some practical limitations that reduce the bandwidth. Eghtesadi and Leventhall(21,22) have found that there are three different factors of primary importance that affect the operation of their system; The centre frequency, the bandwidth, and the level of attenuation.

(1) Centre Frequency:

This is usually chosen to coincide with the highest peak in the primary sound spectrum. The centre frequency f_{o} determines the distance between the secondary sources, and the exact form of the compensation circuit required(21,22).

Once the centre frequency of the system has been chosen, then the centre frequency of the actual system can be caused to deviate by a change in air flow in the duct, a change in air temperature, and an error in the placement of the secondary sources(21,22).

(2) Bandwidth:

The bandwidth of the ideal system is largely determined by the half sine response of the secondary sources in the downstream direction, and this in turn is determined by their spacing. In practice, the bandwidth of the system is limited

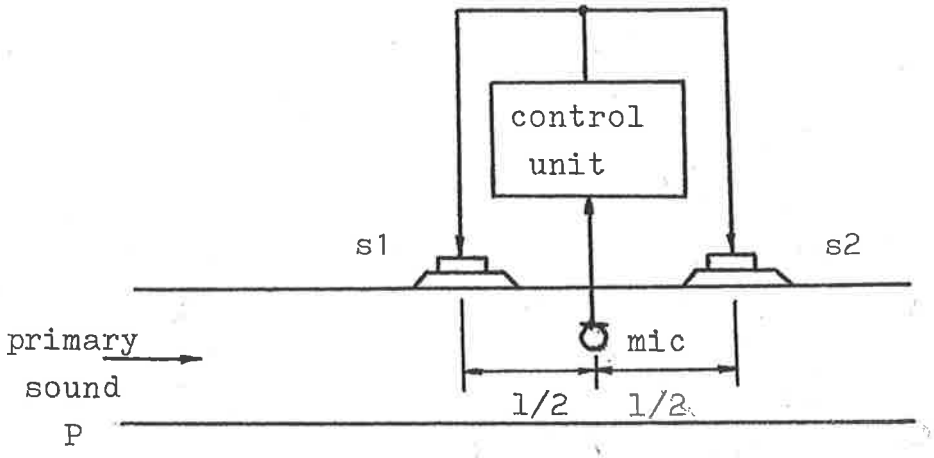

FIG 2.14: The Chelsea Dipole*

* Taken from Ref(20)

further by the following factors(21,22):-

(a) The compensation network requires very high gains, corresponding to the poles of $\frac{1}{2}\sin(\omega/4f_o)$. This has a significant effect on the compensating circuit, and it cannot provide 90^o phase shift at frequencies close to $2f_o$.

(b) The lack of accuracy in positioning the secondary sources and microphone introduces a variable phase shift directly related to frequency. This means that the signals from the secondary sources no longer sum to zero at the microphone, and acoustic feedback occurs. This causes stability problems that effect the upper and lower frequencies of operation.

(c) The response of the secondary sources fluctuate due to the non-ideal nature of the frequency response of the individual loudspeakers, and also due to the acoustical interactions inside the duct.

(3) Level of Attenuation:

The level of attenuation that can be obtained is linked to how accurately the anti-phase sound can be produced. Factors that influence the level of attenuation are(21,22):-

(a) The actual bandwidth of the system. This is determined by the centre frequency, and half sine response, and also the compenastion network.

(b) Inaccuracies in the positioning of the loudspeakers and microphone that result in acoustic feedback to the microphone.

In experimental tests of their Chelsea Dipole canceller, Eghtesadi and Leventhall were able to obtain 10-30dB of attenuation in the range from 500 to 1500Hz, the centre frequency being 1000Hz(21,22).

2.5.6 GENERAL PROPERTIES OF TRIPOLE ABSORBERS:-

The active sound absorbing system proposed by Jessel known as the Jessel System(6,8,9,20) is shown in Fig. 2.15. In general, the tripole (s1,s2,s3) shown in this diagram can be considered to be constructed from a dipole (s1,s2) and the monopole s3 acting as separate entities. This dichotomy of construction gives the acoustic tripole some well defined properties(20).

The Jessel tripole absorber can be analysed by treating the radiation from the monopole and dipole separately, and adding the contributions to get the nett result. If we consider only the dipole, then the radiation from the dipole in the downstream direction is given by(20):-

$$s_{xD} = Ae^{j(\omega t-kx)}\left(e^{-j(kl/2)} - e^{j(kl/2)}\right)$$

$$|s_{xD}| = 2\,|\mathrm{Sin}(kl/2)|$$

$$\angle s_{xD} = -\pi/2$$

where k = wave number.

l = separation of s1 and s2.

(2.6)

The radiation from the dipole in the upstream direction s_{-xD} has the same amplitude response, but has the phase $\angle s_{-xD} = \pi/2$. Thus it can be seen that the radiation from the dipole in the downstream direction is $-\pi/2$ out of phase with the input to the dipole, and $-\pi$ out of phase with the upstream radiation. The radiation from the monopole on the other hand has the same phase in both the upstream and downstream directions(20).

Now, if the dipole is compensated for its half-sine

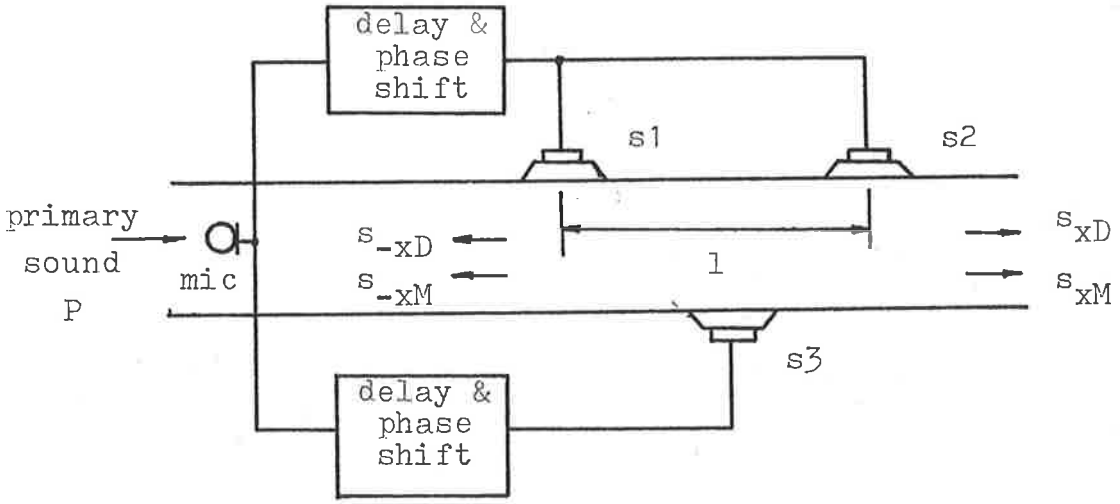

FIG 2.15: The Jessel System*

* Taken from Ref(20)

** Taken from Ref(9)

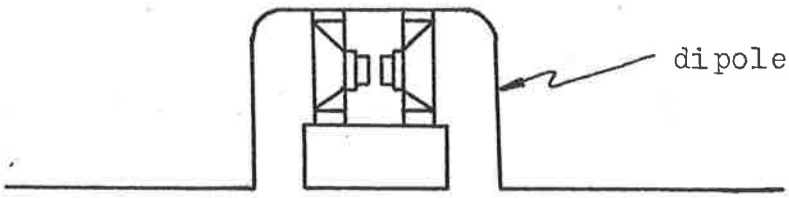

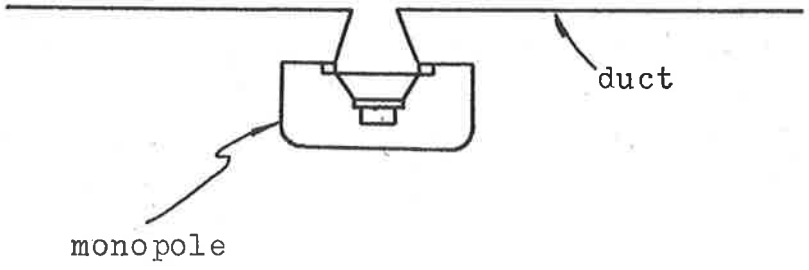

FIG 2.16: Canevet's Acoustic Tripole**

amplitude response, and if the phase of the monopole is suitably adjusted, the tripole can be set up so that it radiates in only the downstream direction. This will be so if(20):-

(1) The dipole is compensated by the transfer function $1/4\sin(kl/2)$.

(2) The input to the monopole is multiplied by $\frac{1}{2}$ and the phase of the monopole is adjusted so that the downstream radiation from the monopole s_{xM} is in phase with the downstream radiation from the dipole s_{xD}. This means that the upstream radiations s_{-xD} and s_{-xM} will then cancel.

If the tripole has been set up so that it radiates in only the downstream direction, it can be used as a sound absorber if the inputs to the dipole and the monopole are phase shifted by $-\pi/2$ and also if a delay is included to account for the separation between the microphone and the tripole.

2.5.7 PRACTICAL IMPLEMENTATION OF THE JESSEL SYSTEM:-

In 1968, Jessel and Mangiante(6) first attempted the practical implementation of the Jessel System. Initially they concentrated on constructing a unidirectional tripole. In these initial experiments, no sensing microphone was used and the driving signal for the secondary source was obtained from the oscillator driving the primary source(6).

With this arrangement they were able to obtain 50dB of attenuation for single 1000Hz tones. However, standing waves were observed in the upstream direction indicating that the source was not truly unidirectional(6).

In a second attempt in 1972 Jessel and Mangiante modified the feeding arrangement to the tripole, making it more flex-

ible and tuned it for unidirectionality. With this arrangement they were able to considerably reduce the standing waves, and still obtain 50dB of attenuation at a single frequency.

Canevet(9) repeated the single frequency experiments that Jessel and Mangiante had conducted in 1972, and obtained 50dB of attenuation at 300Hz. However, Canevet found that this system was narrowband, and once tuned to a particular frequency would behave poorly at other frequencies. There were also problems in that the loudspeakers he was using were inefficient below 300Hz. For these reasons, Canevet attempted to construct a broadband tripole system.

Canevet first attempted to construct a broadband acoustic dipole. The arrangement that he selected consisted of two identical loudspeakers mounted back to back in an enclosure. This arrangement had good symmetry properties, and the loudspeaker dimensions were not restricted so that low frequency absorbers could be constructed(9). To complete the tripole an identical loudspeaker was placed on the opposite side of the duct. This arrangement is shown in Fig. 2.16.

With this new tripole arrangement, Canevet set up an autonomous cancellation system(9), which included a sensing microphone upstream from the secondary sources to provide the driving signal for these sources. For single frequency sounds, superimposed on airconditioner noise, Canevet was able to obtain attenuation of approximately 40dB in the 100-800Hz frequency range(9). For narrowband noise he found that the system could produce approximately 15dB of attenuation, however the performance deteriorated significantly as soon as the bandwidth was appreciably broadened(9).

Canevet suggested that this was mainly due to the separation of the monopole and dipole when forming the tripole. For

this reason he developed another tripole source, this time with the dipole and the monopole integrated in the same enclosure. With this arrangement Canevet was able to obtain 10-15dB of attenuation of broadband noise in the range 70-300Hz(9).

2.5.8 SWINBANKS THEORETICAL INVESTIGATION:-

In 1972, Swinbanks(11) published a rather extensive work entitled "The Active Control of Sound Propagation in Long Ducts". In this paper the problem that he considered was the cancellation of a plane wave disturbance propagating down a duct that contained a fluid flowing steadily and uniformly with a Mach number M less than one. This investigation was prompted by the need to control very low frequency pressure fluctuations in a large gas pipeline.

In his paper Swinbanks(11) does not refer to the work of Jessel and Mangiante(6). However, he does insist that his secondary sources be unidirectional so that they radiate in the downstream direction only, and thus are able to absorb the incident primary sound.

Swinbanks main contribution to the field of active sound cancellation was the arrangement for the secondary sources and sensing microphones that he developed. He started by considering an arbitary distribution of point sources around an arbitary duct wall, and from there deduced the most suitable arrangement to meet his systems requirements.

Swinbanks objective was to find the distribution of point sources that would generate a plane wave interfering with the incident wave and thus reduce its effect. As he was only interested in plane waves, it was a requirement of his system that this point source distribution did not exite any propa-

gating transverse modes. He set out by considering that this arbitary point source distribution could be regarded as a superposition of annular source rings. In this case, the contribution to the plane wave term made by the rings depends on total source strength, but the distribution around the circumference determines which of the transverse modes will be generated.

Swinbanks first determined the distribution that would not allow transverse modes to propagate, and showed that there was a certain frequency $f_u(M)$ above which a single ring must excite propagating transverse modes no matter how the circumferential distribution is chosen. For a square duct Swinbanks showed that the best arrangement was four point sources placed symmetrically around the duct walls. In this case, $f_u(M) = 2.8 f_c(M)$ where $f_c(M)$ is the fundamental cutoff frequency of the duct. Thus providing the source array is made up from ring sources of the type mentioned above, and providing only frequencies below $f_u(M)$ are of interest, it is necessary to consider only the total source strength m(t) of each ring, and its corresponding distribution to the plane wave.

Swinbanks next turned to the problem of producing a unidirectional output from his secondary source array. He found that by using two separated ring sources it was possible to generate such a unidirectional output. However, this arrangement was found to operate satisfactorally over only a certain limited frequency range. It was found that by adding another source ring it was possible to extend this frequency range.

Swinbanks also considered the case when there was uniform flow with mach number M. In this case the modes which are excited by a given ring source remain the same, so that the previous choice of ring source distribution is not affec-

ted, although the upper operating limit $f_u(M)$ is reduced by a factor of $(1-M)^{\frac{1}{2}}$.

We shall now consider an active sound cancellation system of the type proposed by Swinbanks(11) in which the secondary source is comprised of two ring sources. We shall assume that there is no airflow in the duct and thus M=0. A diagram of this systen is shown in Fig 2.17. The signal to drive these secondary sources is obtained from a microphone placed a distance a upstream from the source s1. Swinbanks showed that there will be zero output from the secondary source combination s1 and s2 in the upstream direction if the sources are driven such that(11,12,23):-

$$s2(t) = -s1(t - b/c) \qquad \text{where } c = \text{speed of sound.} \qquad (2.7)$$

When the secondary sources are energised in the above manner, there is an output in the downstream direction which is dependent on the angular frequency of the sound wave in the following manner(11,12,23):-

$$s_D(\omega) \propto \text{Sin}(\omega D/2)\text{Cos}(\omega(t - (x-b)/c - D/2)) \qquad \text{where } D = 2b/c \qquad (2.8)$$

A plot of the expression given in equation (2.8) is shown in Fig 2.18. As can be seen from Fig. 2.18 the Swinbanks active (two ring) attenuator displays a half sine frequency response in the downstream direction as have other multiple source cancellers such as the Chelsea Dipole and the Jessels Tripole. One way that has been used to determine the useful frequency range of a unidirectional source(12,23) is to determine the range over which the output is greater than that for a single source. The ratio of the output from Swinbanks uni-

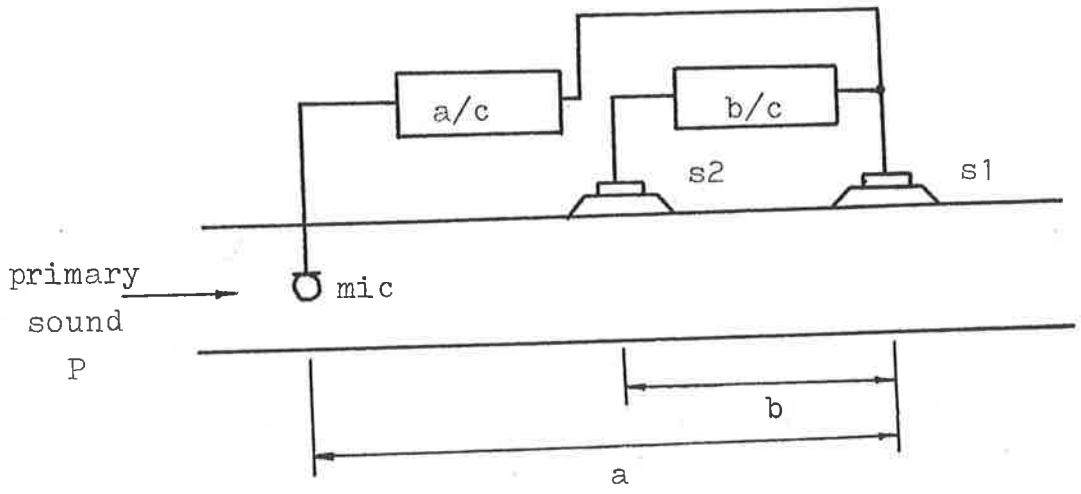

FIG 2.17: Swinbanks Active Sound Attenuator*

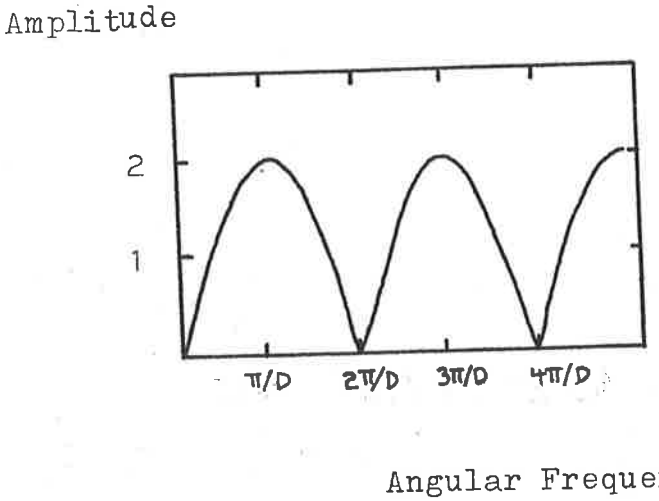

FIG 2.18: Downstream Frequency Response of Secondary Source**

* Taken from Ref(20)

** Taken from Ref(12)

directional source in the downstream direction to the output of a monopole is given by(12,23):-

$$R = \frac{\text{Downstream output from Swinbanks}}{\text{Downstream output from monopole}} = 2\text{Sin}(\omega D/2) \qquad \text{——————(2.9)}$$

This gives a useful frequency range of Swinbanks two ring source as(23):-

$$\pi/3D < \omega < 5\pi/3D \qquad \text{——————————(2.10)}$$

This gives a fundamental interval of $2\frac{1}{2}$ octaves for such a two ring source. The corresponding figure for a three ring source is 3 octaves(23). However, the shape of the downstream frequency response is not really satisfactory for broadband active absorption, and in practical cases the response of the secondary sources would have to be compensated for by using an equalizer circuit.

For the two ring canceller there are three requirements that must exist for cancellation to take place(20,23):-

(1) The output from the sensing microphone must be delayed by a time equal to a/c.

(2) Before being fed to the secondary source, the signal should be passed through an equalizing circuit with the frequency response $1/2\text{Sin}(\omega D/2)$.

(3) The input signal to s1 should be delayed by a time b/c and inverted before being fed to s2.

In his paper, Swinbanks(11) proposed a sound cancelling system based on a three ring secondary source. Although this system was essentially similar to the two ring system described above, it did not include compensation for the half sine response. He suggested that a directional microphone be used to sense the incident sound so that the effects of acoustic

feedback could be minimised. This directional microphone could be constructed in an identical manner to the way in which the unidirectional secondary sources were constructed.

2.5.9 EXPERIMENTAL INVESTIGATION OF SWINBANKS WORK:-

In 1976, Poole and Leventhall(12) conducted an experimental investigation of the active attenuation system proposed by Swinbanks(11). The experimental rig used by Poole and Leventhall was very similar to that proposed by Swinbanks, except that it used a two ring source. The sensing microphone that was used was unidirectional, and two types were tested. The first was a directional cardoid microphone, and the second a two ring microphone array a' la Swinbanks.

In initial experiments the system was tuned to a particular frequency by adjusting the long delay (a/c), or the microphone position, and the gains of the amplifiers feeding the secondary sources. However, this method of setting up eliminated the phase and amplitude errors for one frequency only, and although good performance (40-50dB of attenuation in the range 140 - 200 Hz) can be obtained for this frequency, amplitude and phase errors seriously effect performance at other frequencies(12,13). Thus, using this system Poole and Leventhall could only obtain narrowband absorption centered on the set up frequency.

Due to the fact that the first system that they tested was only capable of narrowband absorption, Poole and Leventhall (13) decided that it was necessary to try and construct a broadband system. This time they employed an equalizer circuit to compensate for the half sine response of the directional microphone and loudspeaker combinations, and also to compensate for the intrinsic frequency response of the loudspeakers

and microphones. With this improved system Poole and Leventhall were able to obtain a significantly improved range of operation, with an attenuation in excess of 20dB being obtained from 50 to 200Hz. Although these results were quite encouraging, Poole and Leventhall felt that the performance of the canceller could be improved in some respects.

Firstly they considered that the design of the transducers could be improved. In particular, it was felt necessary to design the loudspeakers with a resonant frequency below the lowest frequency of operation.

Secondly, they noted that the speed of sound in the duct was a function of temperature and air flow rate. Due to the nature of the construction of the canceller, any change in speed of sound in the duct requires an adjustment of the system parameters. Poole and Leventhall suggested that the required compensation could be obtained by using flow and temperature sensors, or perhaps some form of closed loop control.

2.5.10 BEYOND SWINBANKS - GENERAL N-SOURCE ACTIVE CANCELLERS:-

We have seen in the previous section that Poole and Leventhall have conducted experiments using a Swinbanks type sound canceller employing a two ring secondary source. Eghtesadi and Leventhall(23) found that although the two ring source could produce a unidirectional output with cardoid directivity, there were still a number of problems with this arrangement.

(1) The frequency response of the secondary source in the downstream direction is a sinusoidal function of frequency. This limits the useful range of operation and it is necessary to provide an electronic compensating system with a transfer function that is the inverse of

this half sine frequency response.

(2) The cardoid radiation pattern of the two ring source results in reflections inside the duct, the effects of which are difficult to predict(23).

Swinbanks(11) showed that by adding an extra ring source to the dipole arrangement, the bandwidth could be increased, but there was no attempt to investigate the practical application or performance of this system.

Recently, Eghtesadi and Leventhall(23) have investigated the extension of Swinbanks work to a general N-source system. Berngier and Roure(14) have also considered this problem, but their analysis went no further than three sources.

For an N-source sound canceller, we have N secondary sources located in the duct uniformly spaced by a distance b. Such an N-source cancellation system is shown in Fig. 2.19. Eghtesadi and Leventhall have shown that to obtain a unidirectional secondary source array giving zero output in the upstream direction, and some frequency dependent output in the downstream direction, then the component sources must bear the following relation(23):-

$$s_1(t) = -(s_2(t+b/c) + s_3(t+2b/c) + \ldots + s_n(t+(n-1)b/c)) \qquad (2.11)$$

Thus, the sources should each be delayed by b/c with respect to the previous one, and the sum of the sources s_2 to s_n in the upstream direction is equal and opposite to s_1. To achieve this the amplitudes of s_2 to s_n can all be scaled down by a factor 1/(N-1). Note however that this is not the only arrangement that will result in unidirectionality. Berenger and Roure(14) show that the sum of the amplification constants must be zero. The summed output of the N-source

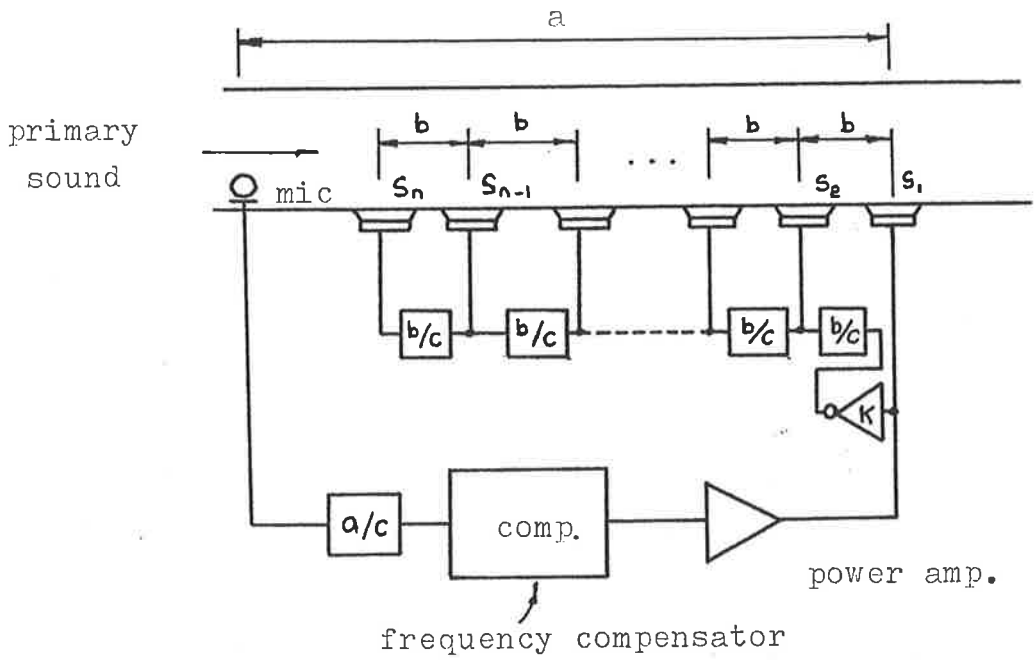

FIG 2.19: The N-Source Active Sound Canceller

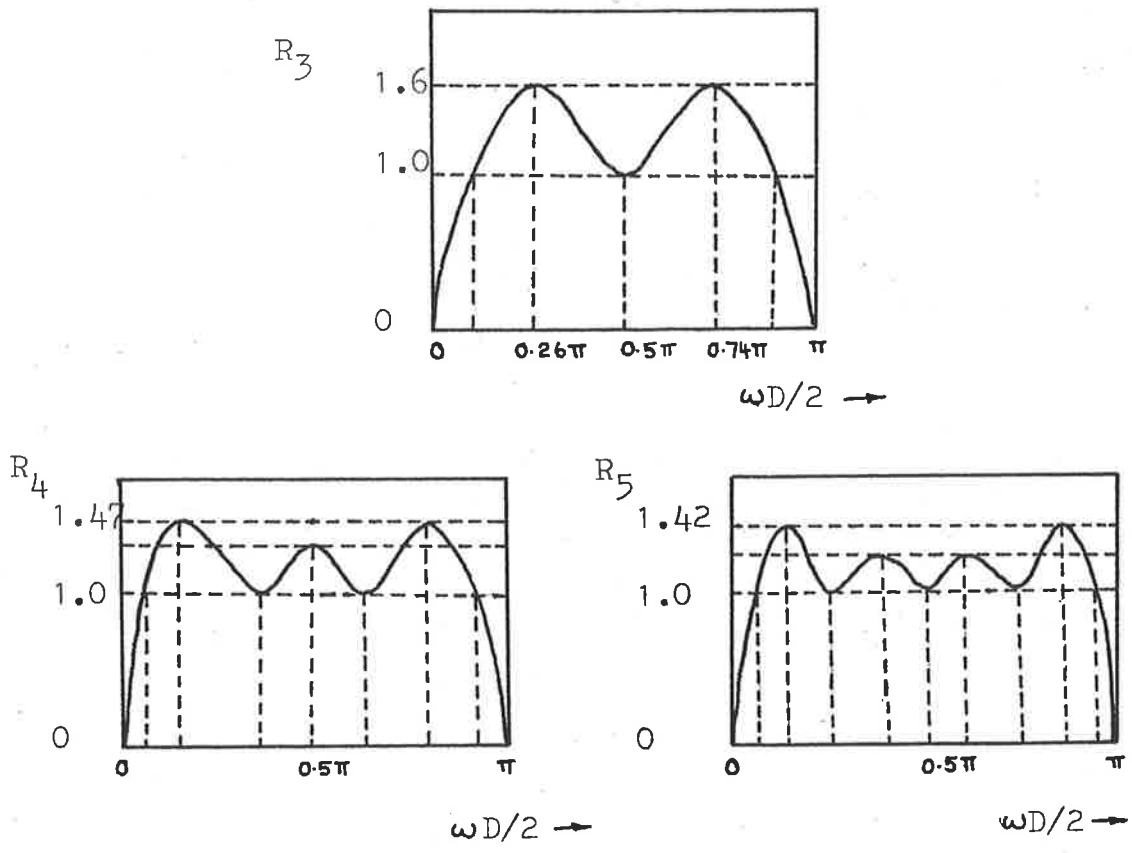

FIG 2.20: Downstream Amplitude Response of Secondary Source for Different Values of N

array in the downstream direction is given by(23):-

$$s_x = Ae^{j(\omega t-kx)}\left(1 - (1/N-1)(e^{-j2\omega b/c} + e^{-j4\omega b/c} + \ldots \right.$$

$$\left. \ldots + e^{-j(N-1)\omega b/c}\right) \qquad \text{——————(2.12)}$$

where k = wave number.

Taking the Laplace Transform of equation (2.12) we obtain the following expression(23):-

$$\left.\begin{aligned} R_x(s) &= 1 - (1/(N-1))R_1(s) \\ \text{where } R_1(s) &= (e^{-sND} - e^{-sD})/(e^{-sD} - 1) \\ D &= 2b/c \end{aligned}\right\} \text{——(2.13)}$$

This response is a function of two parameters, the frequency and the number of sources N. The magnitude of this overall response is given by (23):-

$$|R_x(j\omega)| = \left[1 + \frac{\text{Sin}^2((N-1)\frac{1}{2}\omega D)}{(N-1)^2\text{Sin}^2(\frac{1}{2}\omega D)} - \frac{2\text{Sin}((N-1)\frac{1}{2}\omega D)\text{Cos}(\frac{1}{2}N\omega D)}{(N-1)\text{Sin}(\frac{1}{2}\omega D)} \right]$$

$$\text{——————(2.14)}$$

The useful frequency range of the N-source array is the range over which $|R_x| > 1$ (23). Eghtesadi and Leventhall(23) have outlined a method by which one can solve an expression to obtain these frequency limits. For values of N larger than 2, the bandwidth is increased. Eghtesadi and Leventhall have calculated the bandwidth for values of N up to 8, and these results are shown in Table 2.1. The amplitude response for values of N=3,4, and 5 are shown in Fig. 2.20.

Adding to the number of secondary sources in the array increases the bandwidth, and also reduces the level of deviations of the amplitude response. However, it is still necessary to use an electronic equalizer circuit to compensate for

No. of Sources	No. of octaves	f_o=300Hz	
		f_l	f_u
2	2.33	100	500
3	3.00	66	534
4	3.33	48	552
5	3.70	42	558
6	4.00	35.4	564.6
7	4.21	31.5	568.5
8	4.41	27	573

TABLE 4.1: Useful Bandwidth of N-Source Arrays*

f_o= centre frequency

f_l= lower limit of frequency range

f_u= upper limit of frequency range

* Taken from Ref(23)

the secondary source response(23).

Another advantage of increasing the number of sources is that the directivity of the secondary source is sharpened, and there are less reflections and other acoustical problems inside the duct(23).

The N-source cancellation system gives the promise of wideband active cancellation, but as yet the literature shows no reports of a practical system being implemented with any more than two sources.

2.5.11 DIGITAL SOUND CANCELLERS - THE ANTI-PHASE PATH:-

Most of the researchers that have been discussed so far have aimed to generate the anti-sound required for cancellation by correctly delaying the incident sound wave recorded at a sensing microphone, or changing its phase so that it is an exact anti-phase copy of the primary sound arriving at the secondary sources when played back through those secondary sources.

When multiple source secondary arrays are used they have a frequency dependent amplitude response, and this must be compensated for by using an equalizing circuit if broadband operation is desired. If a monopole secondary source is used, a compensating circuit must be employed to negate the effect of the acoustic feedback.

Although most of the researchers have used compensating circuits to overcome the frequency dependence due to the geometrical arrangement of their cancelling systems, few have attempted to compensate for the intrinsic frequency responses of the system elements such as the loudspeakers and microphones.

Eghtesadi and Leventhall(13,22,23) have indicated that

non-idealities in the response of the system components leads to a reduction in the bandwidth of the attenuation that can be obtained. With the introduction and development of digital techniques (i.e. digital filtering, FFT's) some researchers have been developing systems that rely on what we will call the "anti-phase path" to generate the anti-sound. The anti-phase path takes into account not only the time delay, and the frequency dependent response of the secondary source array, but also the intrinsic frequency response of the system components.

The Ross Algorithm:

Ross's introduction to the field of active noise cancellation came when he investigated the problem of the cancellation of transformer noise(16). The approach taken by Ross in this case was very similar to that adopted by Conover(3), except that he obtained the driving signal for his system from microphones placed to sense the incident sound wave rather than filtering out the harmonics from the power supply.

Ross next tackled the classic problem of the cancellation of sound propagating down an airconditioning duct(18,19). This time his approach was to sense the incident sound with a microphone and process the signal with a digital filter that would compensate for all of the system non-idealities.

To obtain the desired filter characteristic required a knowlege of the frequency response of the individual system elements. As this would require many measurements, Ross devised a scheme by which the required characteristic could be obtained by taking only three measurements. The measurement procedure that Ross employed was to record the required signals , transform them to the frequency domain, obtain the anti-phase transfer function, and transform this back to the

time domain to give the impulse response of the required digital filter.

Once he had set up his system, Ross was able to obtain 15-20 dB of attenuation over a three octave range.

Ross also applied this technique to the cancellation of noise in a lobby(17) with some success.

A Broadband Active Attenuator:

More recently, Shepherd and La Fontain(15) have used a transversal filter to compensate for the effects of the secondary source response and system non-idealities.

These researchers first compensate for the frequency response of the directional microphone and loudspeaker arrays using an equalizer circuit. Next, an adjustable gain and phase is inserted between the sensing microphone and the secondary source array. The gain and phase are then adjusted so that at individual frequencies a null is found at the output of the duct. In this way, the required frequency characteristic for the controller that is used to generate the anti-phase path is obtained. Once this characteristic has been obtained, a minicomputer is used to determine the tap weights of a 32 tap transversal filter so that this filter approximates the required characteristic as closely as possible.

Although Shepherd and La Fontain's system is rather complicated to set up initially, they have reported good results; 10-30dB of attenuation over a range 30-650Hz(15).

In (15) Shepherd and La Fontain investigate the accuracy with which the required controller characteristic can be reproduced with respect to the attenuation that can be obtained. They show that if approximately 20dB of attenuation is desired, then the accuracy of sensing and reproduction must

be within 1dB on amplitude, and 5 degrees on phase angle.

Shepherd and La Fontain(15) and Eghtesadi and Leventhall (22) point out that the loudspeaker is responsible for much of the system's departure from ideal behaviour. Shepherd and La Fontain have employed velocity feedback on their loudspeaker units in an attempt to give them a better response.

Shepherd and La Fontain have also investigated the use of their system in a duct with air flow. They found that this reduced the attenuation that they could obtain in the range 30-650Hz to 14.5dB at 8.6m/s and to 7dB at 20m/s. Part of the reason for this degredation in performance is the turbulence generated by the air flow in the duct, and part is due to the fact that the controller characteristic was determined for no air flow and is no longer optimum.

2.5.12 SUMMARY

Whether or not we are considering cancellation systems that absorb the incident sound wave(6,9,11,12,13,23,25), or merely reflect it (1,2,20,21,24,25,26), it is evident that all practical systems that have been proposed have followed similar lines of development, and have come up against similar practical problems.

When the various systems were first investigated they were found to be narrowband in nature, and therefore not useful in most practical applications. It has been the desire to produce a practical wideband active sound canceller that has been the driving force behind research efforts in the field of active sound cancellation over the last decade or so.

The first attempts that researchers made to increase the bandwidth of their systems was to compensate for the frequency

dependence of the radiation from the secondary sources in the downstream direction (sound absorbers), or the upstream direction (monopole systems). This dependence was largely due to the geometrical arrangement of the system and the secondary sources. However, even after these attempts most researchers found that their systems still had a somewhat limited band of attenuation.

Eghtesadi and Leventhall(22,23) noted that the attenuation bandwidth is also limited by the intrinsic frequency response of the system components such as microphones and loudspeakers, and acoustic interactions within the duct. The latest work on practical active sound cancellers has attempted to compensate for these non-idealities.

Most of the systems that have been proposed have only been tested under experimental conditions in which there was no air flow in the duct. Some researchers such as Shepherd and La Fontain(15), and Ross(18,19) have tested their systems in ducts with air flow, but have found that the performance of the system is degraded under these conditions.

All of the systems discussed involve elements such as time or phase delays that are a function of the speed of the sound in the duct. If this speed changes due to a change in the velocity of the air, or a change in air temperature, then the systems can no longer be expected to provide optimum performance.

Another problem that is associated with air flow that has been noted by Ross(42), and Shepherd and La Fontain(15) is the turbulence that is created by the flow of air in the duct. The turbulence acts as a noise input to the sensing microphone and this can also degrade the performance of the canceller.

To accommodate the changes that are brought about by the

changes in system parameters such as velocity of air flow, or temperature, a number of researchers have studied closed loop or adaptive schemes. The development of such systems is outlined in the next chapter.

3. THE DEVELOPMENT OF ACTIVE ADAPTIVE SOUND CANCELLERS

3.1 INTRODUCTION AND OVERVIEW

It has already been noted in Chapter 2 that changes in system parameters such as temperature and air flow velocity that affect the speed of sound in the duct can lead to a degredation in the performance of the sound canceller. Appart from some of the monopole systems, all of the systems discussed in Chapter 2 were open loop, that is they did not rely on the feeeback of an error signal obtained from the residual noise left after cancellation had been attempted to adjust their performance. These open loop cancellers were set up to operate under a certain set of conditions, and could not respond to changes in system parameters. If the sytem parameters were to change, then the open loop cancellers could no longer provide optimum performance.

It is for this reason that recent research in the field of active sound cancellation has concentrated on the development of closed loop adaptive systems. These systems monitor the residual sound left after cancellation has been attempted, and feed this signal back to a controller that can adjust the parameters of the anti-phase path. A major advantage of these adaptive systems is that they require no initial knowlege of the system in which they are operating, and can adjust to meet changes in the system parameters, thus maintaining optimum performance.

In general Adaptive Sound Cancellers are based on some form of adaptive algorithm, and due to the complicated nature of these algorithms they are run on mini or microcomputers. The development of Digital Signal Processing has been crucial

to the development of these adaptive sound cancellers.

In this chapter we shall look at the adaptive sound cancelling systems that have already been proposed and tested, and also take a look at the future directions that these systems may take.

Firstly, in Section 3.2 we shall look at systems that have been designed to cancel repetitive noise. These systems represent a radical departure from "conventional" active sound cancellers in that they adaptively construct a cancelling signal, rather than adaptively constructing an anti-phase path that acts on the primary sound to form the anti-sound. These systems rely on the fact that some of the low frequency noises that are required to be cancelled are repetitive in nature. A team of researchers from Essex University have had considerable success with these systems, and have explored many applications.

In Section 3.3, we look at work undertaken by Ross who has developed a closed loop adaptive version of the sound canceller discussed in Section 2.5.11, and in Section 3.4 we look at further work undertaken by the researchers at Essex University, this time on the cancellation of random noise propagating down ducts.

One adaptive scheme that has recently been proposed by Burgess, and that seems well suited to the problem of cancelling sound propagating down a duct, is one that employes the LMS algorithm. This algorithm updates a transversal filter that is required to approximate the anti-phase path. The work of Burgess is an extension of Sondhi's adaptive echo canceller that was used to cancel echoes on long distance telephone lines, and also from the theory of the Adaptive Noise Canceller developed by Widrow et al. Warnaka et al have developed practical systems based on the LMS algorithm. The development

of LMS adaptive sound cancellers is described in Section 3.5.

Finally in Section 3.6 we look at the possibilities for the future development of Adaptive Sound Cancellers.

3.2 THE ADAPTIVE CANCELLATION OF REPETITIVE NOISE

In 1976, a research group at Essex University noted that a high proportion of unwanted noise and vibration produced by machines is of a periodic nature. Based on this observation they proposed a new method for generating the anti-sound which they termed "Waveform Synthesis"(27,28). The Essex Team found that by storing the noise made during one firing cycle, that of the next cycle could be predicted with better than 95% accuracy. Any remaining error could be dealt with in the following cycle(27,28).

For the case of cyclic noise the Essex team have developed adaptive active attenuators, and have investigated many practical situations in which these can be applied. At the heart of the Essex system is the so called Adaptive Waveform Synthesiser, a microprocessor based unit in which the signal processing is performed(27,28).

Ross(36,37) has also carried out work on the adaptive cancellation of repetitive noise, and in (36) looks at a number of algorithms that can be used to achieve this.

An example of the application of the Essex teams Adaptive Waveform Synthesiser is an adaptive silencer for a diesel engine exhaust. A diagram of this system is shown in Fig 3.1.

The cancelling waveform in the adaptive silencer is synchronised with the cyclic noise from the diesel engine by sensing the motion of the engine using a toothrate sensor. The synchronising signal, along with the residual noise sensed

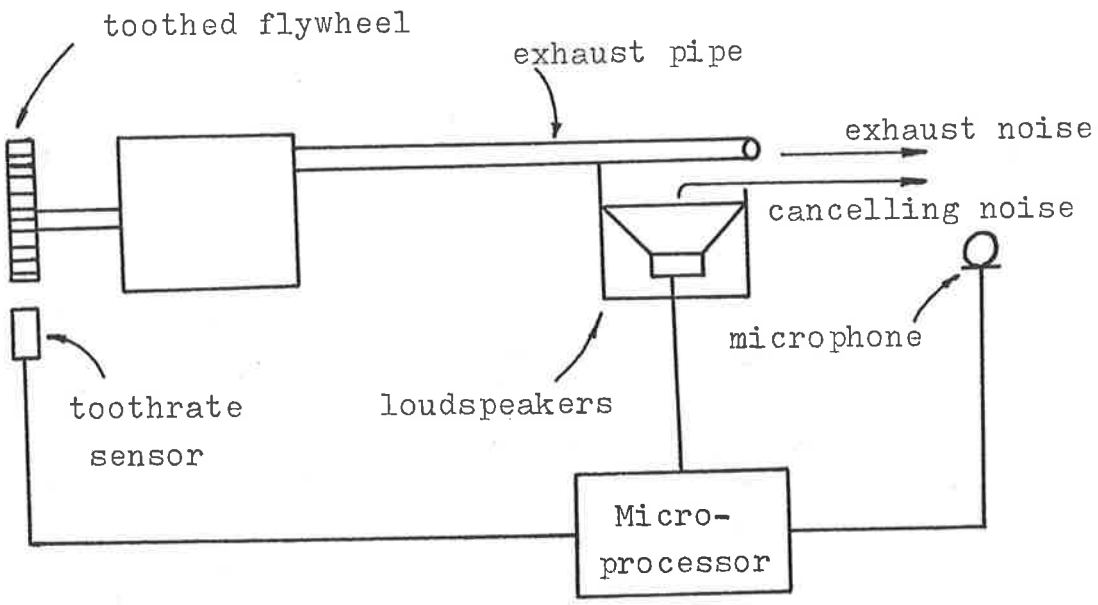

FIG 3.1: Noise Canceller for Diesel Engine*

* Taken form Ref(27)

at the outlet to the duct is fed into an algorithm controlled by the waveform systhesiser(27).

The waveform synthesiser starts from a zero cancelling waveform, and thereafter adjusts each portion of the wave in turn by subtracting the residual microphone signal from the appropriate part of the cancelling waveform, ready for the following repeat cycle. The first algorithms that were developed by the Essex team relied on the residual noise power only, and adjustments of the synthesised waveform segments were made on a trial and error basis(27). Ross(36) also describes similar algorithms.

More recent algorithms that have been developed by the Essex team make use of information contained in the residual waveform shape, or transform the residual waveform into the frequency domain to extract phase and magnitude information. Unfortunately however no detailed information on these algorithms is available.

A unique feature of the Essex system is that it is highly selective with regards to the noise that it cancels. The more accurately the waveform synthesiser is synchronised to the incident sound, the greater is the selectivity. This is found to be particularly useful in certain applications where there is annoying low frequency noise to be cancelled but it is still necessary to respond to speech and warning signals.

Other applications that the Essex team have found for their adaptive waveform synthesiser include a light active ear defender that they claim will give 40dB of attenuation up to 1000Hz, and the cancellation of ship engine noise in the funnel. This last application has required the development of special high power, low frequency loudspeakers but has been quite successful in field tests.

3.3 THE ROSS ADAPTIVE ALGORITHM FOR SOUND IN DUCTS

We have already seen in section 2.5.11 that Ross has developed and tested a non-adaptive sound canceller based on the digital signal processing of various signals in the frequency domain to obtain the transfer function of the anti-phase path. In (36 and 37), Ross describes an extension of his digital sound canceller(17,18,19) in which an adaptive algorithm is used to update the transfer function of the anti-phase path to acccount for changes in the system parameters. A block diagram of the system developed by Ross is shown in Fig 3.2.

With reference to Fig 3.2; The detector signal D is processed by the controller T to produce the cancelling signal S. The net signal received at P, the detector signal, and the cancelling signal are given by the following expressions (36, 37):-

$$\left.\begin{aligned} P &= A_{pn}N + A_{ps}S \\ D &= A_{dn}N + A_{ds}S \\ S &= TD \end{aligned}\right\} \qquad (3.1)$$

Eliminating the cancelling signal S from (3.1), we obtain the following expressions for P and D:-

$$\left.\begin{aligned} D &= A_{dn}N/(1 - TA_{ds}) \\ P &= \left[\frac{A_{pn}N - T(A_{ds}A_{pn} - A_{ps}A_{dn})}{1 - TA_{ds}}\right]N \end{aligned}\right\} \qquad (3.2)$$

It can be seen from (3.2) that if the controller transfer function is chosen to be:

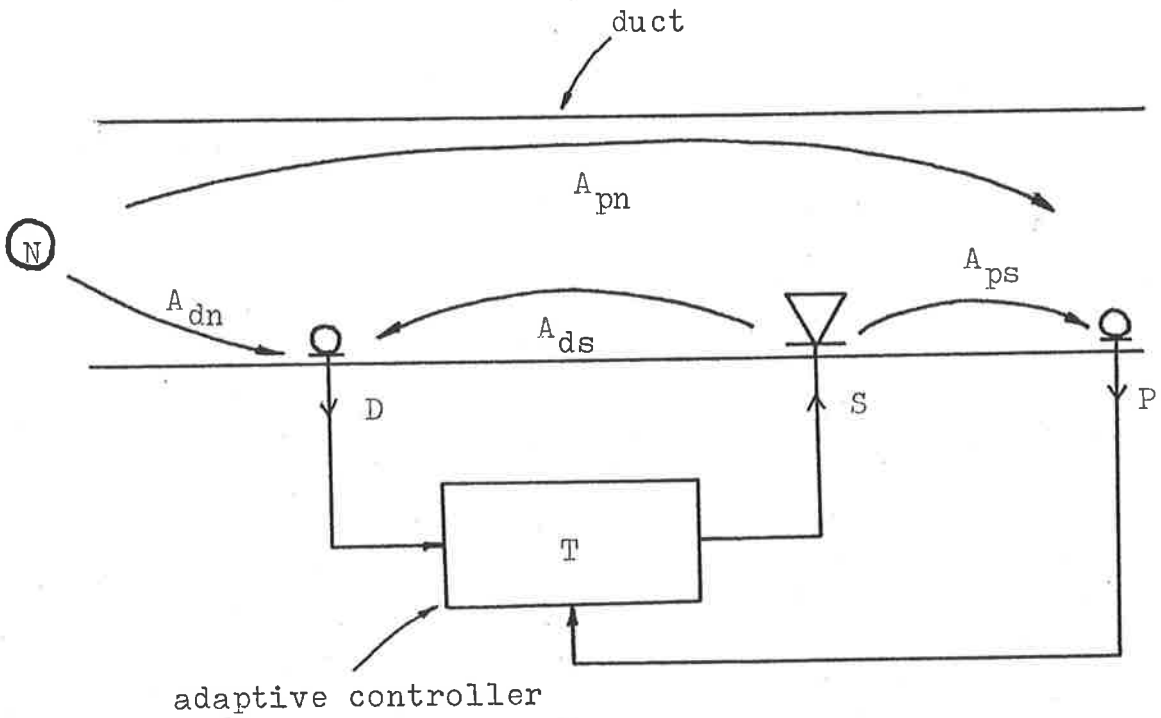

FIG 3.2: Ross's Adaptive Sound Canceller

N = Noise source

D = Detector signal

S = Cancelling signal

P = Error Signal

A_{pn} = Transfer function between N and P

A_{dn} = Transfer function between N and D

A_{ps} = Transfer function between S and P

A_{ds} = Transfer function between S and D

$$T = \frac{A_{pn}}{A_{ds}A_{pn} - A_{ps}A_{dn}} \qquad (3.3)$$

then P=0, and we would get perfect cancellation. If it were possible to continually measure all of the quantities on the R.H.S. of equation (3.3), then it would be possible to adjust T so that P would always equal zero. However, during operation of the canceller we only have access to the signals D,S and P. To develop an adaptive algorithm from equation (3.3) Ross proceeds as follows: Before the controller is switched on, the microphones will hear the noise source only. These microphone signals $A_{pn}N$ and $A_{dn}N$ can be used to construct a filter F with the characteristic A_{pn}/A_{dn}. Using the filter F, Ross(36,37) shows that:-

$$\frac{FTD}{FD - P} = \frac{A_{pn}}{A_{ds}A_{pn} - A_{ps}A_{dn}} \qquad (3.4)$$

The L.H.S. of equation (3.4) is the required canceller characteristic to give perfect cancellation. The expression (3.4) will however only yield perfect cancellation so long as A_{pn} and A_{dn} do not change from the values used to calculate F. In a practical application in which system parameters change with time this will not be the case. For this reason, Ross proposed an algorithm to update the system controller. At the i^{th} iteration, this algorithm is as follows(36,37):-

$$D_i = \left[\frac{A_{dn}}{1 - A_{ds}T_i}\right]N$$

$$P_i = \left[\frac{A_{pn} - T_i(A_{ds}A_{pn} - A_{ps}A_{dn})}{1 - A_{ds}T_i}\right]N \qquad (3.5)$$

cont.

$$T_{i+1} = \frac{T_i}{A_{dn} - FA_{pn} + FT_i(A_{ds}A_{pn} - A_{ps}A_{dn})}$$

$$= \frac{T_i}{1 - F(A_{pn}/A_{dn})(1 - (T_i/T_a))} \qquad (3.5)$$

Where T_a = Actual controller characteristic required for perfect cancellation

According to Ross, his algorithm will converge if the following conditions are met(36,37):-

$$|\beta_i| > \frac{2|\alpha|}{1-|\alpha|} \quad ; \quad |\alpha| < 1$$

where $\alpha = F(A_{dn}/A_{pn}) - 1$

$$\beta_i = (T_i/T_a)$$

$$\varepsilon_i = T_i - T_a$$

$$\varepsilon_{i+1} = \frac{\alpha}{\alpha - \beta_i(\alpha+1)}\varepsilon_i \qquad (3.6)$$

Ross does not describe in any of his papers the basis on which he choses the expression in equation (3.5) to update the controller T. If, as would seem likely he uses the following expression:-

$$T_{i+1} = \frac{FT_iD_i}{FD_i - P_i} \qquad (3.7)$$

then it is difficult to see how he arrives at the expression given in equation (3.5). None the less, Ross has conducted experimental tests using this algorithm, and reported quite

good results(36,37).

In these tests, (cancelling noise in a wind tunnel), Ross uses a minicomputer to run his adaptive algorithm, and store the three signals required for his calculations. Ross collects data for 16 seconds, and then calculates a new controller characteristic using this data. Although the data collection is time consuming, Ross reports that the controller characteristic converges after only a few iterations.

In these tests Ross was able to obtain 11.2dB of attenuation from 40 to 160Hz.

3.4 THE ESSEX SYSTEM FOR CANCELLING RANDOM SOUND IN DUCTS

In addition to the work on the cancellation of repetitive noise, the Essex team has also developed adaptive systems for the cancellation of random noise propagating down a duct. A diagram of this system is shown in Fig 3.3. This system is different to the one in which waveform synthesis is used as it generates an anti-phase path rather than building up a cancelling waveform(27).

The Essex duct noise cancellation system uses two time domain filters. The first of these is used to generate the anti-phase path, and the second is used to cancel out the effect of the acoustic feedback from the loudspeaker(27).

The time domain filters operate by continually convolving the sensed primary signal with the impulse response of the filter. The microprocessor updates the impulse response of the filters on a trial and error basis. Early prototypes of this system used the average residual noise power to guide the adaptation, but more recent systems use the phase and amplitude information that can be extracted from the residual signal.

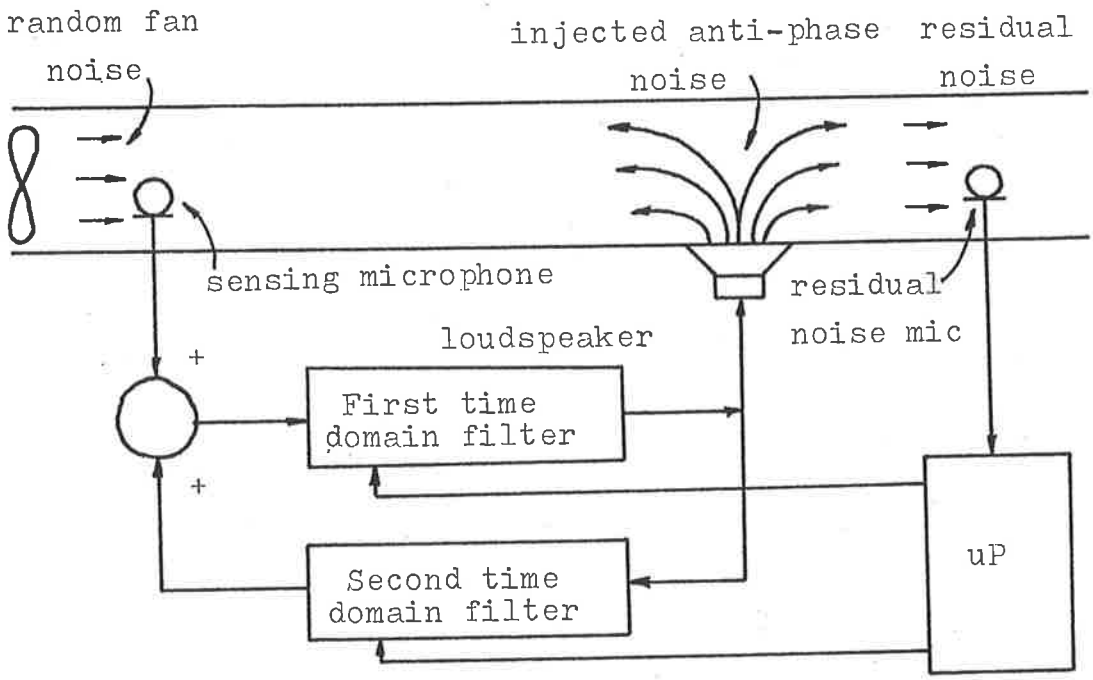

FIG 3.3: The Essex System for Cancelling Random Noise in Ducts*

* Taken from Ref(27)

3.5 ADAPTIVE LMS SOUND CANCELLERS

3.5.1 INTRODUCTION:-

The time domain Adaptive Least Mean Square (LMS) Cancellers are a result of the application of the Adaptive Echo Canceller developed by Sondhi and Presti(31,35), and the Adaptive Noise Canceller developed by Widrow et al(39,40) to the problem of the cancellation of sound propagating down a duct.

The Adaptive Echo Canceller was introduced by Sondhi and Presti(31) in 1966, and further developed by many other researchers(32,33,34,35). The Adaptive Echo Canceller was used to cancel out an echo on a telephone line by subtracting from the incoming speech signal an estimate of the echo derived from the outgoing speech signal. The operation of the Adaptive Echo Canceller is described in Section 3.5.2.

The Adaptive Noise Canceller has been widely used in signal processing applications, and was based on the LMS adaptive algorithm introduced by Widrow and Hoff(39) in 1960. The LMS algorithm is very similar in form to the equations that govern the operation of the Adaptive Echo Canceller. In Section 3.5.3 we describe the operation of a special form of the Adaptive Noise Canceller.

The similarity of adaptive echo cancellation and adaptive noise cancellation to the problem of cancelling a sound propagating down a duct led Burgess(42) to apply a blend of the two to form his Adaptive Sound Canceller. Burgess conducted computer simulations on a simplified version of the Adaptive Sound Canceller, and found that due to its construction it had properties that differed slightly from those of the Adaptive Noise Canceller.

At about the same time, Warnaka et al(29,43,44,48) begun work on their Adaptive Acoustic Canceller, that was similar to the Adaptive Sound Canceller but was developed into a working practical system. The work of Burgess, and Warnaka et al that led to the development of practical LMS adaptive sound cancellers is described in Section 3.5.4. A more detailed mathematical analysis of these systems is given in chapter 4.

3.5.2 BEGINNINGS I - THE ADAPTIVE ECHO CANCELLER

In the mid 1960's when telecommunications satellites were first introduced, problems with echoes degrading the quality of telephone conversations became more pronounced. The echo suppresion techniques that had been used previously to suppress echoes on terrestrial lines were found to be inadequate to cope with the long round trip delays (approx. 600-1200ms) that resulted when telecommunications satellites were used(31, 35).

Echoes on telephone lines arise when there is a transition between a two wire circuit (used for local calls), and a four wire circuit (used for long distance calls). This transition takes place at a junction known as a hybrid, and the echoes occur as a result of imperfect matching at this hybrid(31,35). A diagramatic representation of the production of echoes on a telephone line is shown in Fig 3.4.

In 1966 Sondhi and Presti, and independently Becker and Rudin introduced an adaptive device based on a suggestion by J.L. Kelly and B.F. Logan that aimed to cancel out the echo by subtracting from the incoming speech signal an estimate of the echo derived from the outgoing speech signal(31,35).

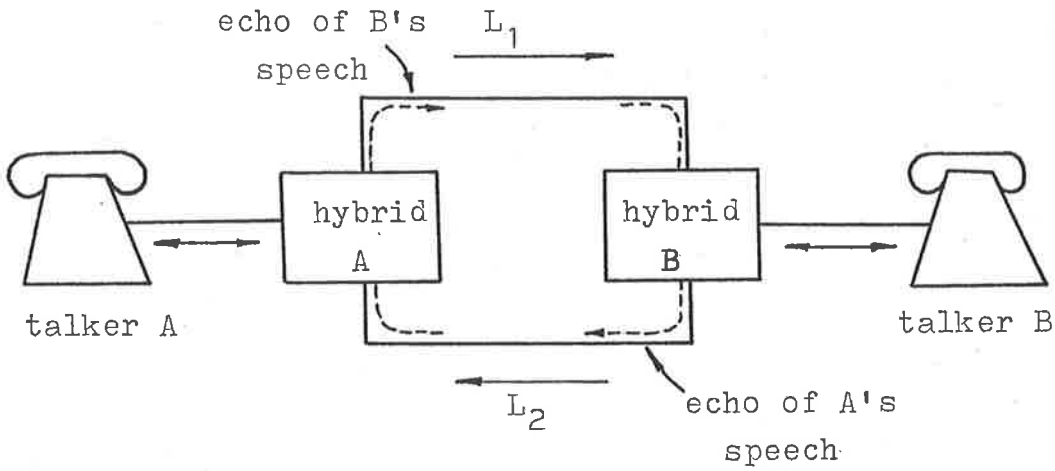

FIG 3.4: Production of Echoes on a Telephone Line

To generate the estimate of the echo Sondhi and Presti first aimed to estimate the parameters of a model for the echo path. The model that was used was a simple tapped delay line, or Finite Impulse Response (FIR) filter. The estimate of the echo was obtained by passing the outgoing speech signal through the FIR filter(31,35).

The first echo cancellers that were proposed relied upon an impulse to be sent, and the impulse response of the echo path to be recorded. This impulse response was then used to determine the elements of the FIR filter. However, in practice it was found that the echo path could change with time, and so it would be necessary to update the estimated echo path from time to time to account for this. It was for this reason that adaptive echo cancellers were proposed. One such adaptive echo canceller is described by Sondhi in (31). The echo canceller proposed in this case was analogue in nature and a diagram of the system is shown in Fig 3.5.

With reference to Fig 3.5, the signal x(t) is the speech signal of speaker A, and y(t) is the sum of the echo z(t) of A's speech and a component n(t). In the case when A alone is talking, n(t) is just low level circuit noise, but during periods of double talking n(t) will be predominately B's speech which may be large compared to the echo(31).

In the system proposed by Sondhi(31), the FIR filter generates the estimate $\hat{z}(t)$ of the echo according to the following equation:-

$$\hat{z}(t) = \sum_{n=0}^{N-1} \hat{h}_n(t)x(t-nT)$$

where $\hat{h}_n(t)$ is gain of the n^{th} tap in FIR estimate of echo path.
$x(t)$ is outgoing speech signal. (3.8)

The control loop uses the error e(t) to update the FIR filter tap gains, and hence the estimate of the echo. Ideally, the system should drive itsealf to the condition e(t)=n(t). The input to the n^{th} integrator in Fig 3.5 is $d\hat{h}_n/dt$, and thus the tap weights $\hat{h}_n$ satisfy the following set of differential equations(31):-

$$
\begin{aligned}
&d\underline{\hat{h}}/dt = KF(e)\underline{X} \\
&\text{where } \underline{X} = \left[x(t), x(t-T), \ \ldots\ , x(t-(N-1)T)\right]^T \\
&\qquad \underline{\hat{h}} = \left[\hat{h}_0(t), \hat{h}_1(t), \ \ldots\ , \hat{h}_{N-1}(t)\right]^T \\
&\qquad K = \text{constant} \\
&\qquad F(e) = \text{monotonic non-decreasing and odd function of the error } e(t)
\end{aligned}
\qquad \Big\} \quad (3.9)
$$

In (31) Sondhi shows that for a suitable choice of the function F(e) the adaptive echo canceller will converge so that the estimated echo is a good estimate of the actual echo, and he calculates the bounds on the convergence rate.

Sondhi's proposal for an adaptive echo canceller has been followed up by many researchers(32,33,34,35), and although the basic configuration of the canceller has not changed, the FIR filter has come to be implemented in digital form. A digital implementation of the echo canceller is shown in Fig 3.6. The update equation used in this case is (35):-

$$
\begin{aligned}
&\underline{\hat{h}}_{m+1} = \underline{\hat{h}}_m + KF(e_m)\underline{X}_m \\
&\text{where } \underline{\hat{h}}_m = \left[\hat{h}_0, \hat{h}_1, \ \ldots\ , \hat{h}_{N-1}\right]_m^T \\
&\qquad \underline{X}_m = \left[x(n), x(n-1), \ \ldots\ , x(n-(N-1))\right]_m^T \\
&\qquad K = \text{constant} \\
&\qquad F(e_m) = \text{function of the error}
\end{aligned}
\qquad \Big\} \quad (3.10)
$$

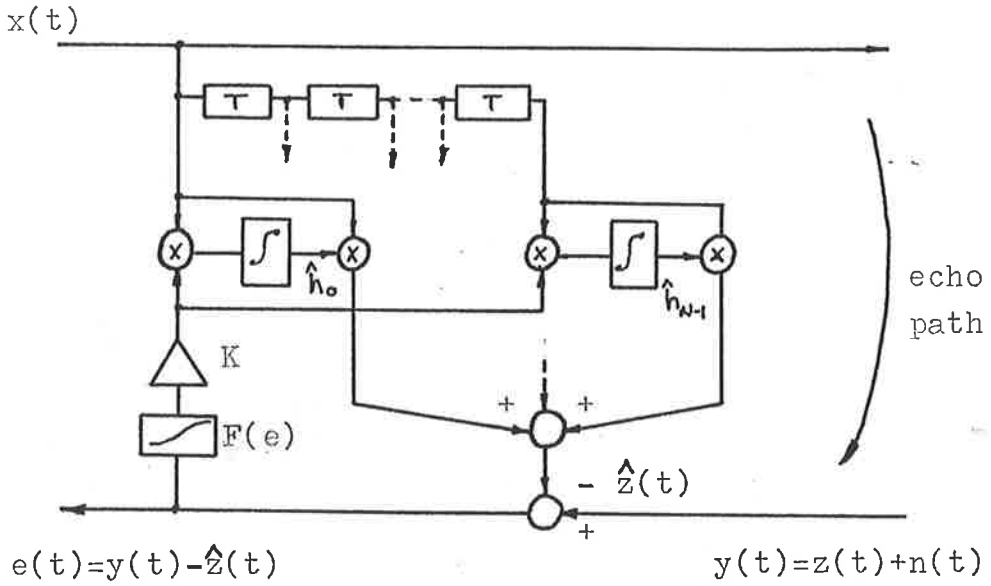

FIG 3.5: Sondhi's Adaptive Echo Canceller*

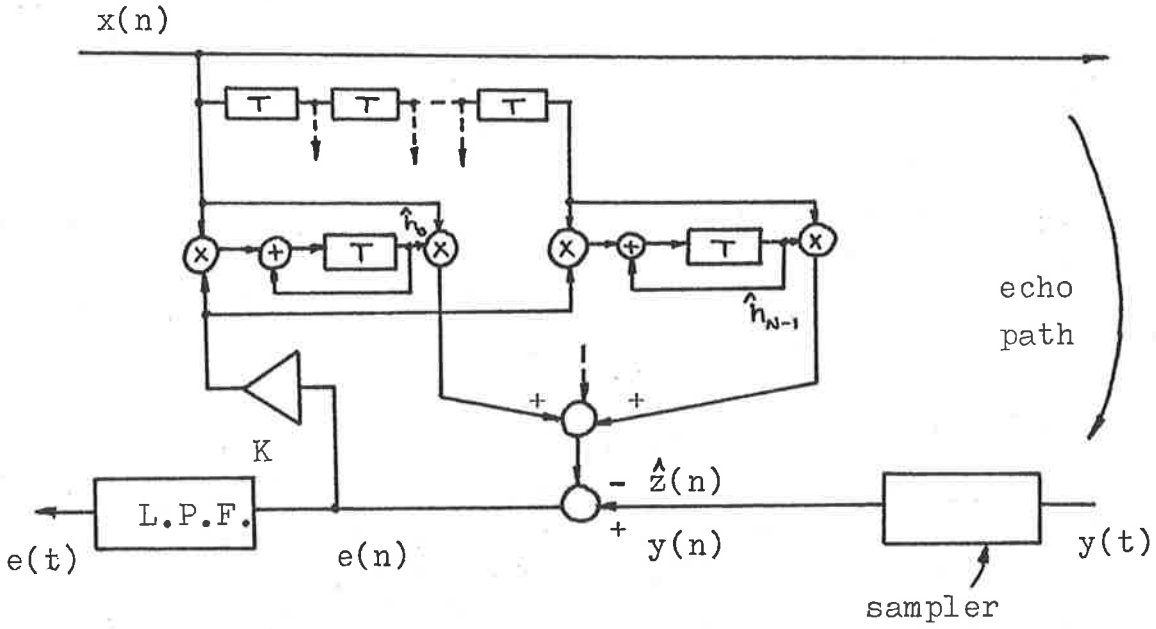

FIG 3.6: A Digital Adaptive Echo Canceller**

* Taken from Ref(31)

** Taken from Ref(35)

The properties of this digital algorithm have been discussed in many references(32,33,34,35), and it can be shown that in many cases it will converge, and a reasonable estimate of the impulse response can be obtained.

A careful study of echo cancellation reveals that this problem is very similar to that of the cancellation of sound propagating down a duct. Both require that an anti-noise path (echo path or anti-phase path) model be estimated so that an estimate of the anti-noise (echo or anti-sound) can be generated from the incident signal (outgoing speech signal , or primary sound). In both cases, due to changes that occur in the system parameters it is desirable that adaptive schemes be used to update the estimate of the anti-noise path.

It is not surprising then that some of the modern Adaptive Sound Cancellers have been based on Sondhi's Adaptive Echo Canceller.

3.5.3 BEGINNINGS II - THE ADAPTIVE NOISE CANCELLER:-

In this section, we shall consider the operation of a simple Adaptive Noise Canceller that is based on the Widrow-Hoff Least Mean Square (LMS) algorithm. The block diagram of a time domain Adaptive Noise Canceller is given in Fig 3.7. In this noise canceller, the LMS adaptive algorithm is used to update the coefficients of a transversal filter W that is used to estimate some transfer function H.

The time domain LMS algorithm was first introduced by Widrow and Hoff in 1960(39), and since then has found many applications in signal processing, estimation and control(40). One such of these applications is the Adaptive Noise Canceller. We will be considering a special case of the adaptive noise

canceller in this section; one in which both the signal to be cancelled d_n, and the input to the transversal filter x_n are obtained directly from the same signal s_n. (In a more general ANC, the signal x_n need only be correlated with some noise component of s_n). By processing the signal x_n with the transversal filter W, an estimate y_n of the desired response d_n is obtained, and the residual error e_n is used to drive the LMS algorithm.

With reference to Fig 3.7, the output of the transversal filter, y_n is given by:-

$$y_n = \underline{W}_n^T \underline{X}_n$$

$$\text{where } \underline{W}_n = \left[w_0, w_1, \cdots, w_{N-1} \right]_n^T$$

$$\underline{X}_n = \left[x_n, x_{n-1}, \cdots, x_{n-N+1} \right]^T \qquad (3.11)$$

and the residual error e_n is given by:-

$$e_n = d_n - y_n$$

$$= d_n - \underline{W}_n^T \underline{X}_n \qquad (3.12)$$

The LMS algorithm is a steepest descent algorithm that aims to minimize the mean square error ($E(e_n^2)$) with respect to the filter taps, or weight vector $\underline{W}$. The steepest descent algorithm for adjusting the transversal filter taps of our noise canceller is given by:-

$$\underline{W}_{n+1} = \underline{W}_n - \mu \underline{g}_n$$

$$\text{where } \underline{g}_n = E(\partial e_n^2 / \partial \underline{W}_n)$$

$$= -E(2 e_n \underline{X}_n) \qquad (3.13)$$

$E(\ )$ means take the expectation of $(\ )$

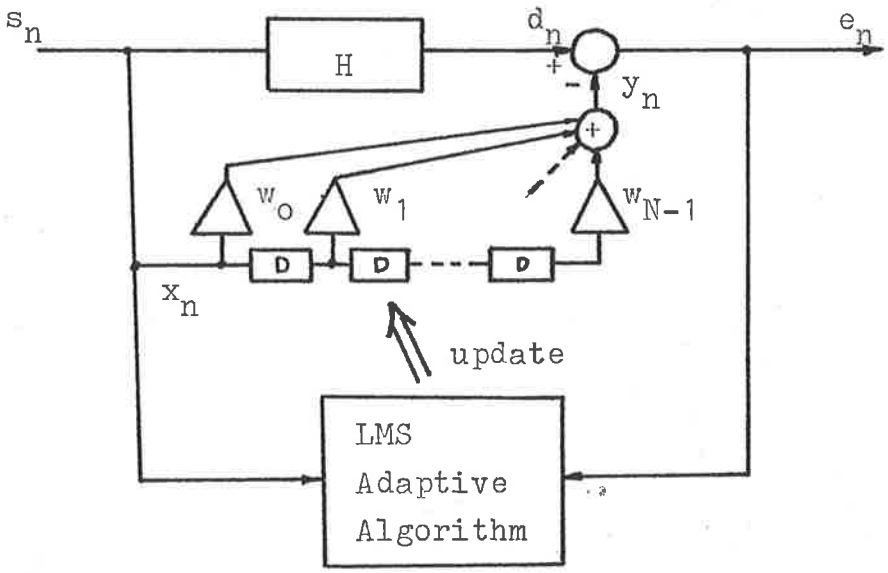

FIG 3.7: An Adaptive Noise Canceller

The LMS algorithm applied to the noise canceller thus becomes:-

$$\underline{W}_{n+1} = \underline{W}_n + 2\mu E(e_n \underline{X}_n) \qquad (3.14)$$

Now, assuming that $\underline{W}_n$ and $\underline{X}_n$ are independent from each other, we can expand the gradient term $E(e_n \underline{X}_n)$ in (3.14) as follows(41):-

$$\begin{aligned} E(e_n \underline{X}_n) &= E\left((d_n - \underline{W}_n^T \underline{X}_n)(\underline{X}_n) \right) \\ &= E(d_n \underline{X}_n) - E(\underline{X}_n \underline{X}_n^T)\underline{W}_n \end{aligned} \qquad (3.15)$$

Substituting for $E(e_n \underline{X}_n)$ into equation (3.14) yields:-

$$\begin{aligned} &\underline{W}_{n+1} = \underline{W}_n - 2\mu(\underline{\underline{R}}\underline{W}_n - \underline{\alpha}) \\ &\text{where} \quad \underline{\underline{R}} = E(\underline{X}_n \underline{X}_n^T) \\ &\qquad\quad \underline{\alpha} = E(d_n \underline{X}_n) \end{aligned} \qquad (3.16)$$

By decoupling the set of equations given in (3.16), Widrow et al(41) have obtained the stability limits for this algorithm as a function of the convergence factor μ. They have shown that for convergence to take place, μ must lie within the following limits(41):-

$$\begin{aligned} &0 < \mu < 1/\lambda_{max} \\ &\text{where } \lambda_{max} \text{ is the largest} \\ &\qquad \text{eigenvalue of } \underline{\underline{R}} \end{aligned} \qquad (3.17)$$

For the case when $\underline{X}_n$ is an N×N vector, (3.16) can be decoupled into N separate scaler equations. Each of these has its own stability limits with respect to the parameter μ, and also its own convergence rate. Widrow et al(41) have shown that for slow adaptation, the time constant for the convergence of the p^{th} mode is given by:-

$$\tau_p = 1/2\mu\lambda_p \qquad (3.18)$$

where λ_p is the eigenvalue of the p^{th} mode

In the time domain implementation of the Adaptive Noise Canceller, it is not possible to actually separate these N different modes, and thus the stability is dependent on the maximum eigenvalue, and the convergence is regulated by the most slowly converging mode . Widrow et al(41) have shown that the convergence rate is dependent on the condition number $(\lambda_{max}/\lambda_{min})$ of the data auto-correlation matrix $\underline{\underline{R}}$. For a small condition number, the algorithm will converge quickly, but for a large condition number the algorithm will converge more slowly.

In practical implementations of the Adaptive Noise Canceller, the Noisy Gradient LMS algorithm of Widrow-Hoff(41) is used to update the weight vector. In this algorithm the gradient of the mean square error $E(e_n\underline{X}_n)$ is replaced by its instantaneous estimate $e_n\underline{X}_n$. The update equation for the weight vector then becomes:-

$$\underline{W}_{n+1} = \underline{W}_n + 2\mu e_n\underline{X}_n \qquad (3.19)$$

Widrow et al(41) have suggested that the stability of this algorithm can be assured if the convergence factor satisfies:-

$$0 < \mu < 1/Tr(\underline{\underline{R}}) \qquad (3.20)$$

Burgess(42), and Bitmead and Anderson(57) suggest a normalized form of the algorithm given in (3.19). The normalized algorithm and its stability limits are as follows:-

$$\underline{W}_{n+1} = \underline{W}_n + 2\mu e_n\underline{X}_n/\underline{X}_n^T\underline{X}_n \qquad (3.21)$$

$$0 < \mu < 1$$

The limits for μ in this case are not exact, but convergence is assured if it lies within these limits.

The time domain Adaptive Noise Canceller is basically a signal processing problem, and only electrical signals are involved. This means that we have direct access to the signals s_n and e_n, and that we can subtract y_n directly from d_n.

In the next section we shall consider the application of the the adaptive noise canceller to the problem of cancelling sound propagating down a duct. This is not simply a signal processing problem as the entity to be controlled is not directly accessible, but must be sensed through transducers, and "acoustic addition" must be used rather than direct subtraction.

3.5.4 THE ADAPTIVE LMS SOUND CANCELLER IN A DUCT:-

The LMS algorithm, and the concept of adaptive echo cancellation was first extended to the field of Adaptive Sound Cancellation by Burgess(42) in 1981. Warnaka et al(43,44,48) have taken a similar approach to Burgess, and have built and successfully tested systems based on the LMS algorithm.

The Adaptive Sound Canceller differs from the adaptive noise canceller in that we are no longer dealing entirely with electrical signals, but instead we use a combination of electrical and acoustical signals. We sense the incident and residual field, and inject the cancelling signal with electro-acoustic transducers, and we also have delays associated with the sound propagating down the duct. These delays and transducers have associated with them a frequency dependent transfer function. As a result of these transfer functions the adaptive noise canceller as described in Section 3.5.3 cannot

be directly applied to the problem of cancelling sound propagating down a duct, but must be modified somewhat. These modifications impose extra limits on the performance of the adaptive sound canceller.

The scheme proposed by Burgess(42) was a blend of Sondhi's adaptive echo canceller(31,35), and the Adaptive Noise Canceller based on the Widrow-Hoff LMS algorithm. Burgess conducted a theoretical analysis, and subsequent computer simulation of a somewhat simplified version of an adaptive sound canceller in a duct. A diagram showing the general arrangement of an adaptive sound canceller is given in Fig 3.8, and the block diagram that Burgess used as the basis of his simulations is shown in Fig 3.9.

In Fig 3.9 the blocks H2 and H3 represent the loudspeaker and the error sensing microphone respectively, and H4 is equal to the combination of H2 and H3 in series. The transfer function H4 has been included so that the problem can be formulated in terms of the adaptive noise canceller. Figure 3.9 is a simplified representation of the adaptive sound canceller shown in Fig 3.8 in that Burgess has ignored the effect of the primary sound sensing microphone, and the acoustic delays between the two microphones and the loudspeaker.

The update algorithm that has been proposed by Burgess is as follows(42):-

$$\left.\begin{aligned} \underline{W}_{n+1} &= \underline{W}_n - 2\mu\epsilon_n\underline{r}_n \\ \text{where } \underline{r}_n &= \left[r_n, r_{n-1}, \cdots, r_{n-N+1}\right]^T \\ \underline{W}_n &= \left[w_0, w_1, \cdots, w_{N-1}\right]_n^T \end{aligned}\right\} \quad (3.22)$$

Burgess has investigated the performance of the algorithm given in equation (3.22) by computer simulation. He has found

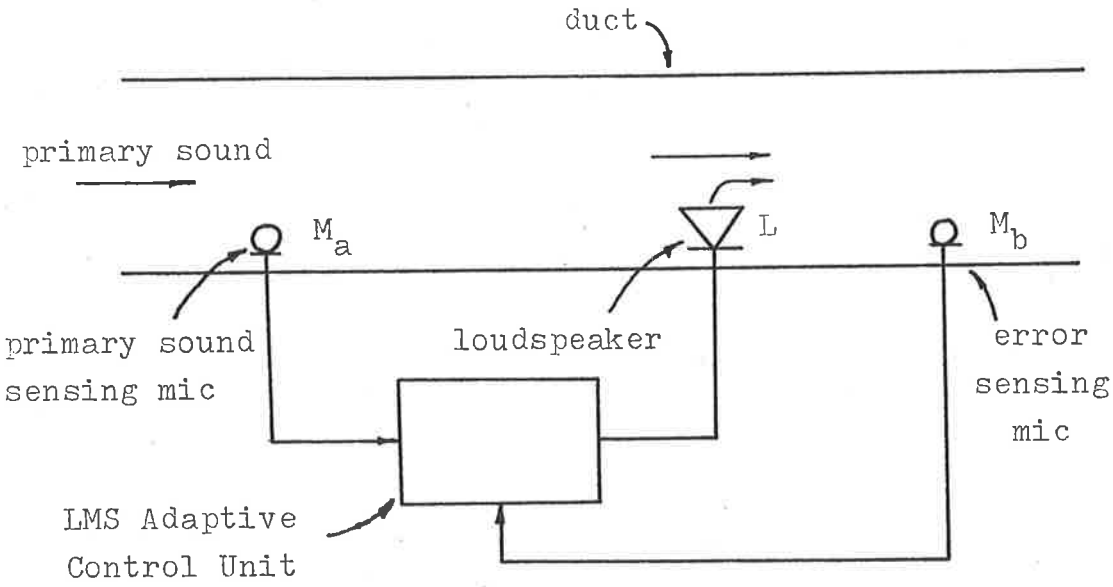

FIG 3.8: General Arrangement of Adaptive Sound Canceller

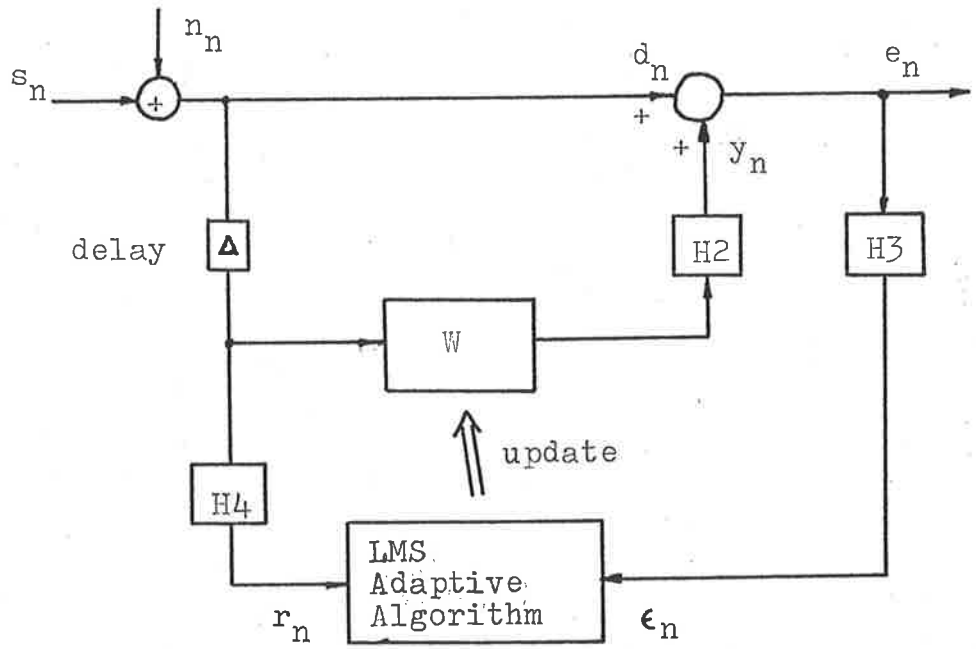

FIG 3.9: Adaptive Sound Canceller Proposed by Burgess

that the convergence rate and stability of the algorithm depends upon μ the convergence constant, N the length of the transversal filter W, the frequency of the input s_n, the signal to noise ratio, and on the relationship between the blocks H4,and H2 and H3(42).

The most obvious dependence is that of the convergence rate and stability on the constant μ. For small values of μ, the algorithm converges slowly and for large values of μ there is a fast convergence rate. However, if μ is made too large the algorithm becomes unstable(42). This is familiar from the theory of operation of the adaptive noise canceller (40,41).

Another interesting dependence noted by Burgess was that of the relation of H4 to H2 and H3. In his simulation, Burgess used simple time delays to represent these transfer functions. He found that if H4 was exactly equal to H2 and H3 then the system behaved as expected (i.e. like an adaptive noise canceller). However, if H4 was different to H2 and H3 then the system converged more slowly, and furthermore if the difference between these time delays became equal to $\frac{1}{4}$ the period of the input sinusoid,the system became unstable(42). Burgess did not offer a theoretical explanation for this instability, and took his development of the Adaptive Sound Canceller no further than these computer simulations. A model of a practical Adaptive Sound Canceller based on the LMS algorithm is analysed in detail in Chapter 4, and from this analysis the reason for the instability observed by Burgess becomes evident.

Warnaka et al(29,43,44,48) have investigated the application of the LMS algorithm to practical adaptive sound cancellers in ducts. This work has involved the investigation of the arrangement of secondary sources and duct geometry to get

good acoustic mixing of the primary and secondary sound fields (29), and the development of the Adaptive Acoustic Canceller(43,44,48) which is based on a modified form of the Widrow-Hoff LMS algorithm, and similar to the Adaptive Sound Canceller proposed by Burgess(42).

The system proposed by Warnaka et al differs from that proposed by Burgess in that it takes into account all of the practical effects associated with implementing an LMS adaptive sound canceller in a duct. For instance, the Adaptive Acoustic Canceller takes into consideration the frequency response of the microphones and loudspeakers, and the acoustic delays between the microphones and loudspeakers.

Warnaka et al have reported quite good results for their Adaptive Acoustic Canceller; 40-50dB of attenuation for low frequency sinusoids, and 20-30dB of attenuation for broadband random noise(44).

3.6 THE FUTURE OF ACTIVE ADAPTIVE SOUND CANCELLATION

Although adaptive sound cancelling systems such as those developed by the Essex team(27,28), Warnaka et al(43,44,48), and Ross(36,37) have been tested in practical applications, and in some cases appear to perform quite well, some of the algorithms used suffer from inherent limitations. It may be possible that new algorithms will show superior performance.

The algorithms developed by the Essex team, and Ross to cancel repetitive noise are of no use when random noise is to be cancelled. Also, we have seen from the computer simulations conducted by Burgess that the sound cancelling systems based on the time domain LMS algorithm can become unstable if incorrect modelling of certain transfer functions takes place. This problem is studied in more detail in

Chapter 4.

So far, most of the successful adaptive cancellers have been based on time domain algorithms. Ross(36) has proposed an algorithm in which certain calculations are performed in the frequency domain, however due to the long data aquisition times the actual convergence time of the algorithm is quite long. Recently there has been quite a lot of discussion of frequency domain algorithms in the signal processing literature. In general, these algorithms have an advantage over the time domain algorithms in that they have faster convergence rates, which means that they can adapt more quickly to changes in system parameters. With powerful signal processing chips becoming available commercially, it should be possible to apply these algorithms to adaptive sound cancelling.

We have already seen in Section 3.5 that the time domain LMS algorithm can be applied to the problem of adaptive sound cancellation. It should also be possible to apply the frequency domain LMS algorithm to this problem. The time domain signals that are available to the adaptive sound canceller can be transformed to the frequency domain using block transforms such as the FFT, or by using running transforms such as Frequency Sampling Filters(47,72). In both cases, the frequency domain LMS algorithm has the advantage over its time domain counterpart in that it has a faster convergence rate. The application of frequency domain LMS algorithms to adaptive sound cancellation is considered is Chapter 6.

It may also be possible to employ different algorithms in the frequency domain other than LMS algorithms. Bogner(45) has suggested the use of hill climbing algorithms in conjunction with Frequency Sampling Filters, and Shepherd and La Fontain have suggested the use of the Simplex Algorithm(46).

As yet there have been no reports of attempts to implement

an adaptive sound canceller based on a frequency domain algorithm. The implementation of practical adaptive sound cancellers based on frequency domain adaptive algorithms is considered in Chapter 6.

4. TIME DOMAIN ADAPTIVE LMS SOUND CANCELLERS

4.1 INTRODUCTION - ADAPTIVE SOUND CANCELLATION IN DUCTS:-

As we have seen in Chapter 3, researchers in the field of Active Sound Cancellation have been concentrating on the development of adaptive systems that can self-adjust to meet changes in the operating conditions and thus maintain optimum performance. In this chapter we will be considering an adaptive system based on the Time Domain Adaptive LMS algorithm. The development of Adaptive LMS Sound Cancellers has been described in Section 3.5, and a diagram of the general arrangement of an Adaptive LMS Sound Canceller is given in Fig 3.8.

In Fig 3.8, M_a and M_b are unidirectional microphones that sense sound incident from the upstream direction only, and L is a unidirectional loudspeaker that injects the anti-sound into the duct so that it propagates in the downstream direction only. Unidirectional microphones are used to prevent acoustic feedback from the loudspeaker to M_a, and from reflections at the end of the duct to M_b. The unidirectional loudspeaker is used so that the Adaptive Sound Canceller absorbs the incident sound rather than reflecting it back upstream.

In Section 3.5.3 we looked at the theory of operation of the Adaptive Noise Canceller on which the LMS Adaptive Sound Canceller is largely based. When the Adaptive Noise Canceller is applied to the problem of cancelling sound propagating down a duct, the sound signal that is to be cancelled s_n, and the residual error signal e_n that are used to drive the LMS algorithm are no longer directly available, but must be

sensed using a microphone. Also, the cancelling signal y_n can no longer be directly subtracted from the desired response d_n, but must be added acoustically to it using a loudspeaker system. This means that y_n must be an exact anti-phase copy (anti-sound) of the incident sound for perfect cancellation to take place.

A block diagram representation of a practical Adaptive Sound Canceller based on the time domain LMS algorithm is shown in Fig 4.1. In this diagram the blocks M_a and M_b represent the incident sound and residual error sensing microphones respectively, and the block L represents the loudspeaker that is used to inject the cancelling sound into the duct. All of these elements have frequency dependent amplitude and phase characteristics.

The blocks D_1 and D_2 represent the acoustic delays that occur due to the physical separation of the microphones and loudspeakers in the duct. These delays may change during the course of operation due to temperature or air speed changes, and the system is required to track these changes to maintain optimum performance.

The practical Adaptive Sound Canceller also includes the estimated delays $\hat{D}_1$ and $\hat{D}_2$ and the estimated transfer functions $\hat{L}$ and $\hat{M}_b$. The estimated delay $\hat{D}_1$ is included so that the transversal filter $\underline{W}$ does not have to compensate for the delay D_1 as this would require too many taps. It is not immediately obvious why the estimates $\hat{L}$, $\hat{D}_2$ and $\hat{M}_b$ have been included. In part, the explanation is that they allow the Adaptive Noise Canceller to be applied to the Adaptive Sound Canceller, but to determine their actual effect requires a detailed mathematical analysis of the system. This analysis is undertaken in section 4.2 and 4.3.

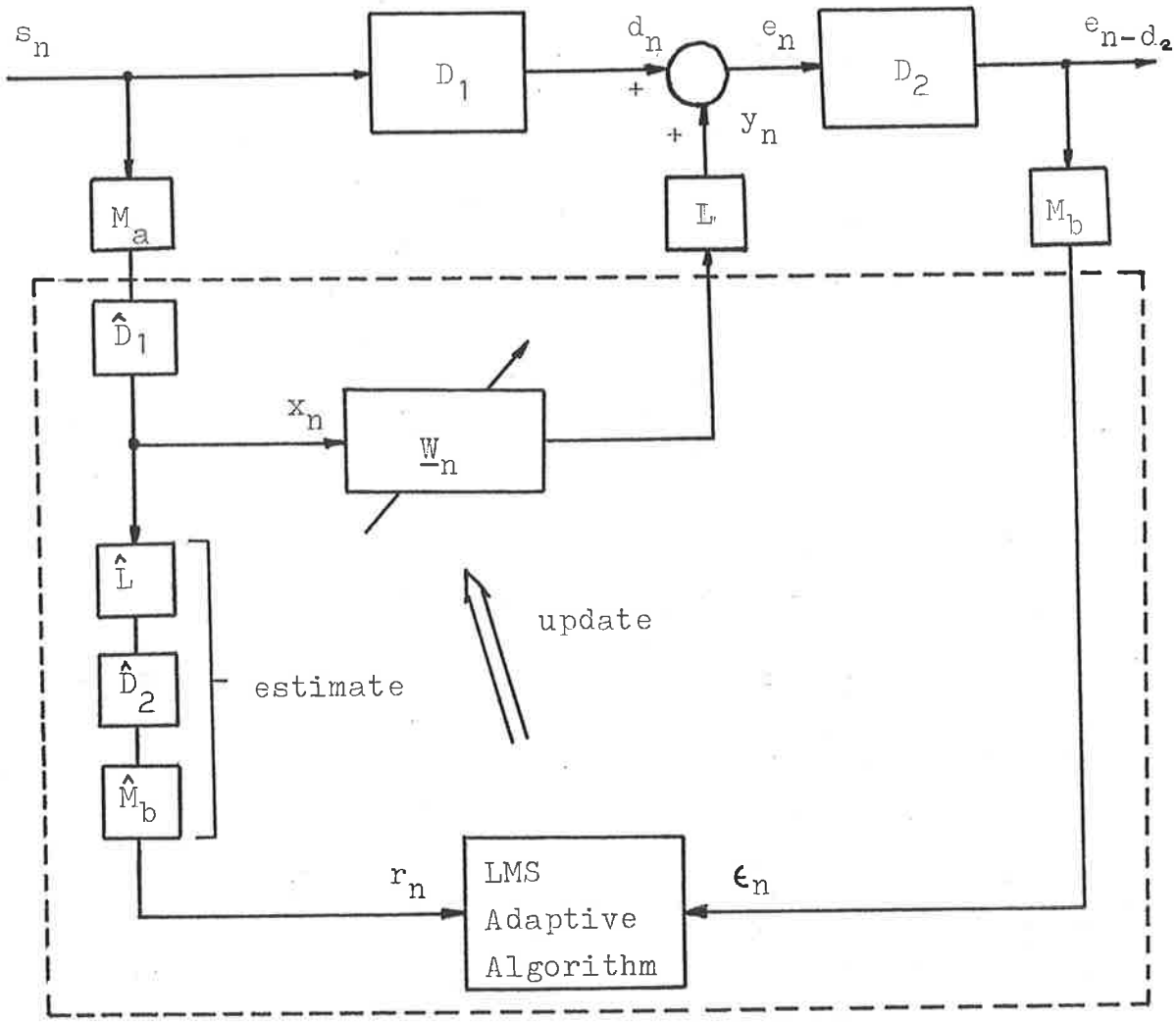

FIG 4.1: Practical LMS Adaptive Sound Canceller

Note: D_1 and D_2 are transfer functions representing acoustic delays in the duct.

$\hat{D}_1$ and $\hat{D}_2$ are estimates of D_1 and D_2.

d_1 and d_2 are discrete delays corresponding to D_1 and D_2, i.e. delay/D where D is the sampling period. $\hat{d}_1$ and $\hat{d}_2$ are estimates of d_1 and d_2

When the delays D_1 and D_2, and the transfer functions L and M_b are initially estimated it is possible for errors to occur. It is also likely that during the course of operation of the sound canceller that these parameters will change, and thus the estimates $\hat{D}_1$, $\hat{D}_2$, $\hat{L}$ and $\hat{M}_b$ will differ from the actual values; that is, mismatches will occur in the estimates of these transfer functions.

In the following sections we will be investigating the performance of the practical Adaptive Sound Canceller as shown in Fig 4.1. In particular we will be interested in the convergence rate and the stability of the adaptive algorithm as a function of various canceller parameters such as the convergence factor μ, system delays, and the mismatch in the estimation of transfer functions.

In section 4.2 we investigate the stability and convergence of a practical LMS Adaptive Sound Canceller based on the LMS algorithm as was used in equation (3.16). This work is based on the work of Kabal(13) who investigated the stability of Adaptive LMS Equalizers using delayed adjustment, and Morgan(5) who investigated Multiple Correlation Cancellation Loops with Filters in their Auxiliary Paths, and is an extension of the work of Burgess(42) who conducted computer simulations of simplified versions of the Adaptive Sound Canceller considered in this chapter.

The algorithm considered in Section 4.2 requires a knowledge of the correlation function of the input signal (primary sound) to calculate the gradient of the mean square error. In practical applications of the Adaptive Sound Canceller, these correlation functions are usually unknown and so the gradient of the mean square error is replaced by its instantaneous estimate, resulting in the so called Noisy Gradient

LMS algorithm. In Section 4.3 we investigate the stability and convergence of a practical LMS Adaptive Sound Canceller based on the Noisy Gradient LMS algorithm.

In sections 4.2 and 4.3 the effect of the mismatch in estimation of system parameters D_2, L and M_b on the performance of the LMS algorithm is investigated. In Section 4.4 we consider the mismatches that may occur in practice.

Finally, in Section 4.5 we look at possible extensions that may be made to the time domain LMS Adaptive Sound Canceller shown in Fig 4.1 to improve its performance.

4.2 THE STABILITY AND CONVERGENCE OF THE PRACTICAL LMS ADAPTIVE SOUND CANCELLER

4.2.1 INTRODUCTION:-

An inspection of Figures 3.7, and 4.1 shows that the Adaptive Sound Canceller (ASC) is more complex than the Adaptive Noise Canceller (ANC). This is because in the ASC we have acoustic delays associated with the duct, and also the sound must be sensed and controlled by electro-acoustic transducers.

As the ASC is more complex than the ANC, we also require a more complicated adaptive LMS update algorithm. Extending the algorithm given by Burgess(42) to the ASC shown in Fig 4.1, the update equation for the weight vector of the transversal filter $\underline{W}$ becomes:-

$$\left.\begin{aligned} \underline{W}_{n+1} &= \underline{W}_n - 2\mu E(\epsilon_n \underline{r}_n) \\ \text{where } \underline{W}_n &= \left[w_0, w_1, \cdots, w_{N-1}\right]_n^T \\ \underline{r}_n &= \left[r_n, r_{n-1}, \cdots, r_{n-N+1}\right]^T \end{aligned}\right\} \quad (4.1)$$

From Fig 4.1 we can see that the error signal ϵ_n, and the incident sound vector $\underline{r}_n$ available to the LMS algorithm are given by:-

$$\epsilon_n = e_{n-d_2} * m_b$$

$$\therefore \epsilon_n = (\underline{X}^T_{n-d}\underline{W}_{n-d_2} * l + d_{n-d_2}) * m_b$$

$$\therefore \epsilon_n = d_{n-d_2} * m_b + \underline{X}^T_{n-d}\underline{W}_{n-d_2} * l * m_b$$

$$\underline{r}_n = \underline{X}_{n-\hat{d}_2} * \hat{l} * \hat{m}_b \qquad (4.2)$$

where l and m_b are impulse responses of L and M_b

$\hat{l}$ and $\hat{m}_b$ are estimates of l and m_b

$\underline{X}_n = [x_n, x_{n-1}, \cdots, x_{n-N+1}]^T$

d_2 = delay in discrete time i.e. delay/D

where D is the sampling interval.

$\hat{d}_2$ = estimate of d_2

* represents correlation

Expanding the expected square error gradient term in (4.1) we obtain:-

$$E(\epsilon_n \underline{r}_n) = E\left[(d_{n-d_2} * m_b + \underline{X}^T_{n-d_2}\underline{W}_{n-d_2} * l * m_b)(\underline{X}_{n-\hat{d}_2} * \hat{l} * \hat{m}_b)\right]$$

$$= E\left[(d_{n-d_2} * m_b)(\underline{X}_{n-\hat{d}_2} * \hat{l} * \hat{m}_b)\right] + E\left[(\underline{X}^T_{n-d_2}\underline{W}_{n-d_2} * l * m_b)(\underline{X}_{n-\hat{d}_2} * \hat{l} * \hat{m}_b)\right] \qquad (4.3)$$

where E() is the expectation of ()

Substituting for $E(\epsilon_n \underline{r}_n)$ into equation (4.1) we obtain:-

$$\underline{W}_{n+1} = \underline{W}_n - 2\mu(\underline{\underline{A}}\underline{W}_{n-d_2} + \underline{c})$$

$$\text{where } \underline{\underline{A}} = E\left[(\underline{X}_{n-d_2} * l * m_b)(\underline{X}^T_{n-\hat{d}_2} * \hat{l} * \hat{m}_b)\right]$$

$$\underline{c} = E\left[(d_{n-d_2} * m_b)(\underline{X}_{n-\hat{d}_2} * \hat{l} * \hat{m}_b)\right] \qquad (4.4)$$

Although equation (4.4) is of a similar form to the equivalent ANC expression equation (3.16), the matricies $\underline{\underline{A}}$ and $\underline{c}$ are more complicated than $\underline{\underline{R}}$ and $\underline{\alpha}$, and dependent on a larger number of parameters. As a result of this, the performance of the algorithm (4.4) is dependent on a larger number of parameters. In particular, we will see in the following sections that the convergence factor μ, the delay d_2, and the mismatch (see below) all have an important influence on the stability and convergence of the adaptive algorithm.

In the practical ASC, the acoustic delay d_2 between the cancelling loudspeaker and the error sensing microphone means that the LMS algorithm only has access to a delayed error signal. The effect of this is to reduce the stability limits for the convergence factor μ. The effect of the delayed error signal on the performance of the LMS adaptive algorithm is considered in Section 4.2.2.

When talking about mismatch, we refer to the collective error in the estimation of the loudspeaker and error sensing microphone transfer functions, and the delay d_2. This mismatch can be expressed as a simple phase and gain at a single frequency, or in general by a mismatch transfer function M defined as follows:-

$$M = LD_2M_b - \hat{L}\hat{D}_2\hat{M}_b \qquad (4.5)$$

As an introduction to the effect of mismatch on the performance of the adaptive LMS algorithm, in Section 4.2.3 we consider a system with a purely sinusoidal input signal. In this case we can consider the mismatch to be represented by a phase and a gain only.

Next, in Section 4.2.4 we consider the effect of a general mismatch on the performance of the ASC for any input signal.

This work is based largely on the work of Morgan(51) who conducted an analysis of multiple correlation cancellation loops with a filter in the auxiliary path. In (51) Morgan included a general linear filter directly after the transversal filter, and investigated the effect of this filter on the stability and convergence of the LMS algorithm. To determine stability, Morgan considered the complex eigenvalues of the data correlation matrix, an important part of this work being to define a relationship between the complex eigenvalues and the cross-power spectrum formed by feeding the input signal through the linear filter that had been introduced into the auxiliary path. In our analysis, we extend the work of Burgess(42) by including an estimate of the cumulative transfer function LD_2M_b between the input to the transversal filter, and the input to the LMS adaptive algorithm. (Burgess used only simple delays to represent L and M_b, and made no attempt to conduct a theoretical analysis of the effect of mismatch). It is then the mismatch between the the estimated transfer function $\hat{L}\hat{D}_2\hat{M}_b$ and the actual transfer function LD_2M_b which becomes the "filter in the auxiliary path" as considered by Morgan. We then follow Morgan's analysis to determine the stability limits of the LMS algorithm with respect to the mismatch.

Finally, in section 4.2.5 we consider the effect of the mismatch on the residual error signal.

4.2.2 THE EFFECT OF THE DELAY D_2 ON THE PERFORMANCE OF THE ADAPTIVE SOUND CANCELLER:-

In this section, we will be considering the stability of the algorithm given in equation (4.4) as a function

of the delay d_2. Due to the presence of this delay in the ASC, the adaptive algorithm only has available to it a delayed version of the residual error signal, and as we shall see the effect of this is to reduce the stability margins for the convergence factor μ.

This section is largely an adaptation of the work carried out by Kabal(59) on the stability of Adaptive LMS Equalizers using delayed adjustment.

In Section 3.5.3, we saw that the stability of the ANC update equation (3.16) is dependent on the eigenvalues of the data auto-correlation matrix $\underline{\underline{R}}$. Again, in this section we will be looking at eigenvalues to determine stability, but in this case they will be the eigenvalues of the data correlation matrix $\underline{\underline{A}}$.

With reference to equation (4.4), it can be seen that the optimum weight vector, (i.e. the one for which there is no error term in (4.4)) is given by(59):-

$$\underline{W}^* = -\underline{\underline{A}}^{-1}\underline{c} \qquad (4.6)$$

Now, in order to determine the stability of equation (4.4) it is desirable that it be decoupled into a set of N scalar equations. To accomplish this we use the orthonormal matrix $\underline{\underline{P}}$ that diagonalizes the correlation matrix $\underline{\underline{A}}$; $\underline{\underline{P}}$ being defined as follows(59):-

$$\underline{\underline{A}} = \underline{\underline{P}}^{-1}\underline{\underline{V}}\underline{\underline{P}} \qquad (4.7)$$

where $\underline{\underline{V}}$ is a diagonal matrix of the eigenvalues of $\underline{\underline{A}}$.

Multiplication of the vector $\underline{W}$ in equation (4.4) by $\underline{\underline{P}}$ yields the decoupled vector $\underline{W}'$. Thus, with reference to equation

(4.7) we can write a decoupled version of equation (4.4) as follows(59):-

$$\underline{\underline{P}}\underline{W}_{n+1} = \underline{W}'_{n+1} = \underline{W}'_n - 2\mu\left[\underline{\underline{V}}\underline{W}'_{n-d_2} + \underline{\underline{P}}\underline{c}\right] \qquad (4.8)$$

We now define the weight vector error $\underline{h}_n$(59):-

$$\left.\begin{aligned} \underline{h}_n &= \underline{W}'_n - \underline{W}'^{*} \\ \text{where } \underline{W}'_n &= \underline{\underline{P}}\underline{W}_n \\ \underline{W}'^{*} &= \underline{\underline{P}}\underline{W}^{*} \end{aligned}\right\} \qquad (4.9)$$

Now, from (4.7) and (4.6) it can be shown that(59):-

$$\left.\begin{aligned} \underline{\underline{P}}\underline{c} &= \underline{\underline{V}}\underline{\underline{P}}\underline{\underline{A}}^{-1}\underline{c} \\ \underline{\underline{P}}\underline{c} &= -\underline{\underline{V}}\underline{W}'^{*} \end{aligned}\right\} \qquad (4.10)$$

Thus, substituting for $\underline{\underline{P}}\underline{c}$ into (4.8) we obtain(59):-

$$\left.\begin{aligned} \underline{h}_{n+1} &= \underline{h}_n - 2\mu(\underline{\underline{V}}\underline{W}'_{n-d_2} - \underline{\underline{V}}\underline{W}'^{*}) \\ &= \underline{h}_n - 2\mu\underline{\underline{V}}\underline{h}_{n-d_2} \end{aligned}\right\} \qquad (4.11)$$

Now, as $\underline{\underline{V}}$ is a diagonal matrix, the system of equations (4.8) have been decoupled and we can treat each one separately. Thus we have(59):-

$$\left.\begin{aligned} h_{i,n+1} &= h_{i,n} - 2\mu\lambda_i h_{i,n-d_2} \\ \text{where} \quad & i = 1, \ldots, N \\ & \lambda_i \text{ are the eigenvalues of} \\ & \text{the correlation matrix } \underline{\underline{A}}. \end{aligned}\right\} \qquad (4.12)$$

Taking the Z-Transform of the i^{th} equation, we obtain the transform function $H_i(z)$ (59):-

$$H_i(z) = \frac{z^{d_2+1} h_i(0)}{z^{d_2+1} - z^{d_2} + 2\mu\lambda_i} \qquad (4.13)$$

We define the polynomial F(z) such that(59):-

$$F(z) = z^{d_2+1} - z^{d_2} + \beta \qquad (4.14)$$

where $\beta = 2\mu\lambda_i$

Thus for stability of equation (4.4) all of the roots of F(z) must lie within the unit circle(59). By putting $z=e^{j\phi}$ into (4.14) we can determine the values of β for which F(z) has roots on the unit circle. Substituting for z into (4.14) we obtain(59):-

$$e^{j\phi(d_2+1)} - e^{j\phi d_2} + \beta = 0 \qquad (4.15)$$

Now, $\beta = 2\mu\lambda_i$ where the λ_i are eigenvalues of the correlation matrix $\underline{\underline{A}}$. It can be seen from equation (4.4) that in general $\underline{\underline{A}}$ will not be a symmetric matrix, and thus the eigenvalues can in general be complex and of the form $\lambda_i = a_i + jb_i$. Equating real and imaginary terms in equation (4.15) we obtain(59):-

$$2\mu a_i = \cos(\phi d_2) - \cos(\phi(d_2+1)) \qquad -a$$

$$2\mu b_i = \sin(\phi d_2) - \sin(\phi(d_2+1)) \qquad -b \qquad (4.16)$$

From equation (A1.8) Appendix 1, we see that the value of μ that yields marginal stability for expression (4.14) is:-

$$\mu = \frac{1}{\lambda_i} \sin\left[\frac{\arctan(a_i/-b_i)}{2d_2+1}\right] \qquad (4.17)$$

where $\lambda_i = a_i + jb_i$

$i = 1, \ldots, N$

Thus the stability limit for equation (4.14) becomes:-

$$0 < \mu < \frac{1}{|\lambda|_{max}} \; Sin\left[\frac{\arctan(a_i/-b_i)}{2d_2 + 1}\right] \qquad (4.18)$$

$$\text{where } |\lambda|_{max} = |a_i + jb_i|_{max}$$

$$i = 1, \ldots, N$$

For the case when all the eigenvalues of $\underline{\underline{A}}$ are real, (i.e. when we have only the delay d_2 in the ASC), equation (4.18) becomes(59):-

$$0 < \mu < \frac{1}{|\lambda|_{max}} \; Sin\left[\frac{\pi}{2(2d_2 + 1)}\right] \qquad (4.19)$$

In (59), Kabal shows that it is also possible to use root locus techniques to obtain the stability limits of equation (4.13), but this method yields the same results. They do however give an insight into the convergence rate, and also the envelope of the weight vector error. Root locus techniques are considered in Appendix 2.

The stability limits obtained in (4.19) for the Adaptive Sound Canceller are very similar to those for the Adaptive Noise Canceller, but the extra sine term in (4.18) accounts for the fact that only a delayed version of the residual error signal is available to the algorithm. The effect of the delay is to impose a stricter limit on the convergence factor μ. For the purpose of building a practical ASC it is desirable to make the delay d_2(i.e. the spacing between the error sensing microphone and loudspeaker) as small as possible. However, there may be an acoustic limitation to the amount by which this spacing can be reduced.

4.2.3 THE EFFECTS OF MISMATCH FOR A PURELY SINUSOIDAL INPUT SIGNAL :-

In this section we wish to investigate the effect of a mismatch on the performance of the LMS Adaptive Sound Canceller for a purely sinusoidal input. As we will be working at a single frequency f_o, we can represent the mismatch as a simple gain and phase delay.

We shall use the simplified block diagram as shown in Fig 4.2 in this case as neglecting M_a, L and M_b will make no difference to our analysis. The simplified version of the LMS update algorithm that applies to Fig 4.2 is:-

$$\underline{W}_{n+1} = \underline{W}_n - 2\mu E(e_{n-d_2}\underline{r}_n) \qquad (4.20)$$

Expanding the expected error square gradient term in (4.20) we have:-

$$E(e_{n-d_2}\underline{r}_n) = mE(d_{n-d_2}\underline{X}_{n-\hat{d}_2}) + mE(\underline{X}^T_{n-d_2}\underline{W}_{n-d_2}\underline{X}_{n-\hat{d}_2})$$

$$\text{where } \hat{d}_2 = d_2 + \Delta_2 \qquad (4.21)$$

Thus we can write (4.20) as:-

$$\underline{W}_{n+1} = \underline{W}_n - 2\mu m(\underline{\underline{A}}\underline{W}_{n-d_2} + \underline{c})$$

$$\text{where } \underline{\underline{A}} = E(\underline{X}_{n-d_2}\underline{X}^T_{n-\hat{d}_2})$$

$$\underline{c} = E(d_{n-d_2}\underline{X}_{n-\hat{d}_2}) \qquad (4.22)$$

To simplify our analysis further we shall assume that the delay $d_2 = 0$ as we realy only wish to consider the effect of the mismatch. Under this simplification, equation (4.22) becomes:-

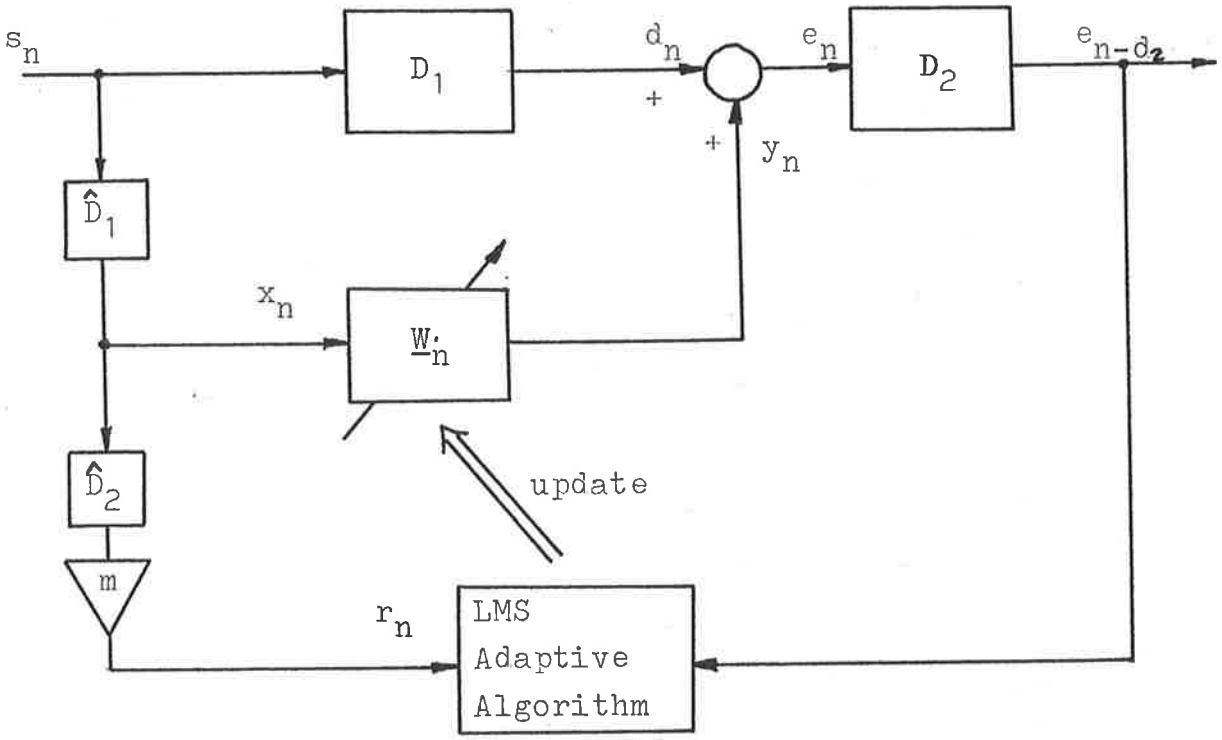

Note: $\hat{d}_1 = d_1$

$\hat{d}_2 = d_2 + \Delta_2$

FIG 4.2: Simplified Block Diagram of ASC

$$\underline{W}_{n+1} = \underline{W}_n - 2\mu m(\underline{\underline{A}}\underline{W}_n + \underline{c})$$

where $\underline{\underline{A}} = E(\underline{X}_n \underline{X}^T_{n-\Delta_2})$

$\underline{c} = E(d_n \underline{X}_{n-\Delta_2})$ ——— (4.23)

We can rearrange (4.23) to yield:-

$$\underline{W}_{n+1} = (\underline{\underline{I}} - 2\mu m\underline{\underline{A}})\underline{W}_n - 2\mu m\underline{c} \qquad \text{——— (4.24)}$$

Now, in a similar way to that used in Section 4.2.2 we can use the orthonormal matrix $\underline{\underline{P}}$ to transform (4.24) and so obtain a set of decoupled equations. The transformation matrix $\underline{\underline{P}}$ was defined as follows:-

$$\underline{W}' = \underline{\underline{P}}\underline{W}$$

$$\underline{\underline{A}} = \underline{\underline{P}}^{-1}\underline{\underline{V}}\underline{\underline{P}}$$

where $\underline{\underline{V}}$ is the diagonal matrix of eigenvalues of $\underline{\underline{A}}$. ——— (4.25)

In general, the matrix $\underline{\underline{A}}$ will be non-symmetric and thus its eigenvalues will in general be complex. Thus we shall represent the eigenvalues of $\underline{\underline{A}}$ as $\lambda_i = a_i + jb_i$. Premultiplying equation (4.24) by the matrix $\underline{\underline{P}}$ yields:-

$$\underline{W}'_{n+1} = (\underline{\underline{I}} - 2\mu m\underline{\underline{V}})\underline{W}'_n - 2\mu m\underline{\underline{P}}\underline{c} \qquad \text{——— (4.26)}$$

It can be easily seen from (4.26) that the algorithm will be stable as long as(51):-

$$\left|\underline{\underline{I}} - 2\mu m\underline{\underline{V}}\right| < \underline{\underline{I}}$$

$$\therefore \left|1 - 2\mu m\lambda_i\right| < 1 \ , \ i = 1, \ \ldots \ , N \qquad \text{——— (4.27)}$$

The expression in equation (4.27) can be given a geometrical interpretation(51). A diagram showing this interpretation is given in Fig 4.3. The algorithm will be stable if for

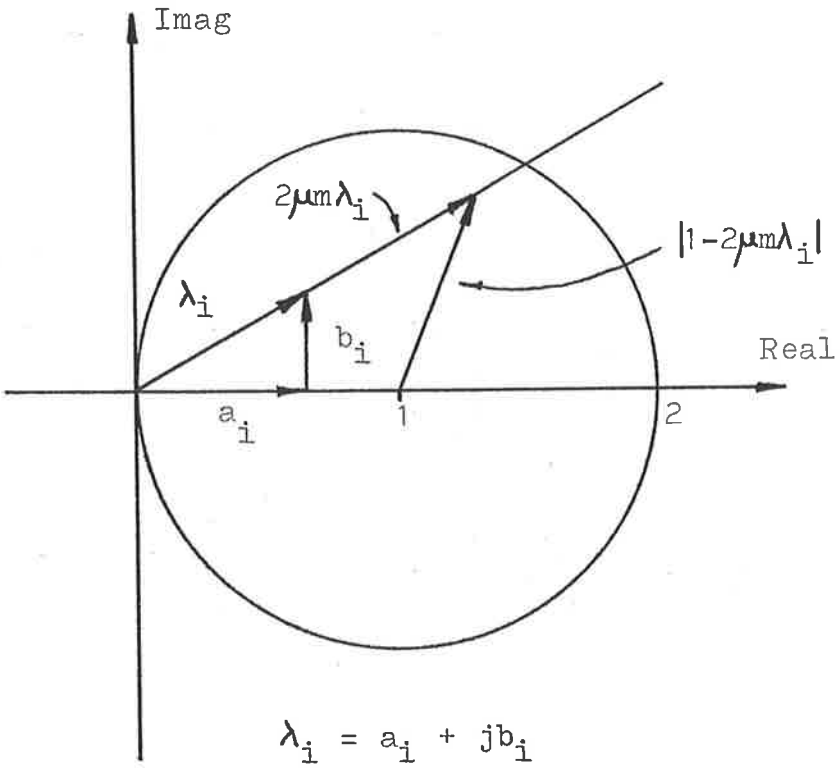

FIG 4.3: Geometrical Interpretation of Equation (4.27)

all the complex eigenvalues of the correlation matrix $\underline{\underline{A}}$, the vector $1 - 2\mu m\lambda_i$ lies within the unit circle centered on (1,0) in the complex plane. Substituting the real and imaginary components of the eigenvalue λ_i into equation (4.27) and expanding we get:-

$$\left.\begin{aligned} &\sqrt{(1 - 2\mu m a_i)^2 + (2\mu m b_i)^2} < 1 \\ &\therefore (1 - 2\mu m a_i)^2 + (2\mu m b_i)^2 < 1 \\ &\therefore \mu < \left(\frac{1}{m}\right)\left[\frac{a_i}{(a_i)^2 + (b_i)^2}\right] \\ &\therefore \mu < \left(\frac{1}{m}\right)\left[\frac{a_i}{|\lambda_i|^2}\right] \\ &i = 1, \ldots, N \end{aligned}\right\} \qquad (4.28)$$

Thus, if we constrain μ to be positive, then the stability limits for the convergence factor μ are:-

$$0 < \mu < \left(\frac{1}{m}\right)\left[\frac{a_i}{|\lambda_i|^2}\right]_{min} \qquad (4.29)$$

Equation (4.29) gives the stability limits for μ given some matrix $\underline{\underline{A}}$ with eigenvalues $\lambda_i = a_i + jb_i$ and assuming that μ must be positive. Now, we wish to set μ at some positive constant value and consider how the stability of the algorithm is dependent on the mismatch.

It can be seen from (4.29) that the mismatch in the gain m has the effect of reducing the stability for μ in proportion to the mismatch. We can see from equations (4.27), (4.28) and (4.29) that if μ is set at a positive constant value within the limits set in (4.29), then the algorithm will

converge as long as the real part of λ_i is positive. It can also be seen from equation (4.23) that the matrix $\underline{\underline{A}}$ is a function of the mismatch Δ_2, and thus the eigenvalues λ_i are also a function of the mismatch.

For our special case of a purely sinusoidal input we have:-

$$s_n = \text{Cos}(\omega_o nT) \qquad \text{——————————} \quad (4.30)$$

The auto-correlation function for a sinusoid of angular frequency ω_o is given by:-

$$R_{ss}(i) = \tfrac{1}{2}\text{Cos}(\omega_o iT) \qquad \text{——————————} \quad (4.31)$$

If we take the special case of N=2, then in general we can write the $\underline{\underline{A}}$ matrix as:-

$$\underline{\underline{A}} = \begin{bmatrix} R_{xx}(\Delta_2) & R_{xx}(1+\Delta_2) \\ R_{xx}(\Delta_2-1) & R_{xx}(\Delta_2) \end{bmatrix}$$

$$= \tfrac{1}{2}\begin{bmatrix} \text{Cos}(\omega_o\Delta_2 T) & \text{Cos}(\omega_o(1+\Delta_2)T) \\ \text{Cos}(\omega_o(\Delta_2-1)T) & \text{Cos}(\omega_o\Delta_2 T) \end{bmatrix} \qquad \text{——} \quad (4.32)$$

The eigenvalues of the $\underline{\underline{A}}$ matrix in this case are given by:-

$$\lambda = \tfrac{1}{2}\left[\text{Cos}(\omega_o\Delta_2 T) \pm \sqrt{\text{Cos}^2(\omega_o\Delta_2 T) - \text{Sin}^2(\omega_o T)}\right]$$

$$\text{——————————} \quad (4.33)$$

From (4.33) we can see the way in which the mismatch affects the eigenvalues of the $\underline{\underline{A}}$ matrix for the case of a simple sinusoidal input. Instability will occur as a result of

mismatch when the real part of the eigenvalue λ becomes negative. For our special case of a sinusoidal input this will occur when:-

$$|\Delta_2| < f_s/4f_o \qquad (4.34)$$

where f_s = sampling frequency

f_o = input sinusoid frequency

This is in agreement with the results reported by Burgess (42) who conducted computer simulations, and Morgan(51) who carried out a theoretical study.

So we see that instability due to mismatch will occur when the error in the estimation of the delay is equal to one quarter of the period of the input sinusoid, or conversely if it represents a phase shift of greater than $\pm 90^{o}$ at that frequency. It is also interesting to note that this is a cyclic effect, and that we will get bands of stability and instability depending on the magnitude of the mismatch in phase. We get stability when the phasor representing the mismatch is in the 1^{st} or 4^{th} quadrants, and instability when this phasor is in the 2^{nd} and 3^{rd} quadrants.

The effect of mismatch in gain was to reduce the stability limits for the convergence factor μ. This can be taken account of by simply reducing the convergence factor. However, mismatch in phase cannot be accounted for and will always result in instability if greater than the allowable limits.

In this section we have considered the effect of mismatch on the performance of the ASC for a purely sinusoidal input. In practice, we are likely to have a broadband input signal and thus we will also have to consider the effect of the mismatch in gain and phase at these other frequencies.

4.2.4 THE EFFECTS OF A GENERAL MISMATCH ON THE STABILITY OF THE ADAPTIVE SOUND CANCELLER:-

In this section we will be considering the effects of a general mismatch in the estimation of system parameters on the stability of the Adaptive Sound Canceller for any input signal s_n.

We start from the weight vector update equation (4.4) which applies to the practical Adaptive Sound Canceller shown in Fig 4.1. As we have seen in Section 4.2.3 for the simple case of a purely sinusoidal input, it is the effect of the mismatch on the eigenvalues of the data correlation matrix $\underline{\underline{A}}$ that determines the dependence of the algorithm stability and convergence on that mismatch. We shall start by considering this dependence. From (4.4), the cross correlation matrix $\underline{\underline{A}}$ is given by:-

$$\underline{\underline{A}} = E\left[(\underline{X}_{n-d_2} * l * m_b)(\underline{X}^T_{n-\hat{d}_2} * \hat{l} * \hat{m}_b)\right] \qquad (4.35)$$

If we define the following quantities;

$$\left.\begin{aligned} h &= l * m_b \\ \hat{h} &= \hat{l} * \hat{m}_b \end{aligned}\right] \qquad (4.36)$$

then we can rewrite (4.35) as follows:-

$$\underline{\underline{A}} = E\left[(\underline{X}_{n-d_2} * h)(\underline{X}^T_{n} - \hat{d}_2 * \hat{h})\right] \qquad (4.37)$$

We can represent the RHS of (4.37) in terms of a cross correlation matrix associated with a mismatch transfer function. A diagram showing this relationship is given in Fig 4.4.

From (4.37) and Fig 4.4 we see that we can think of the

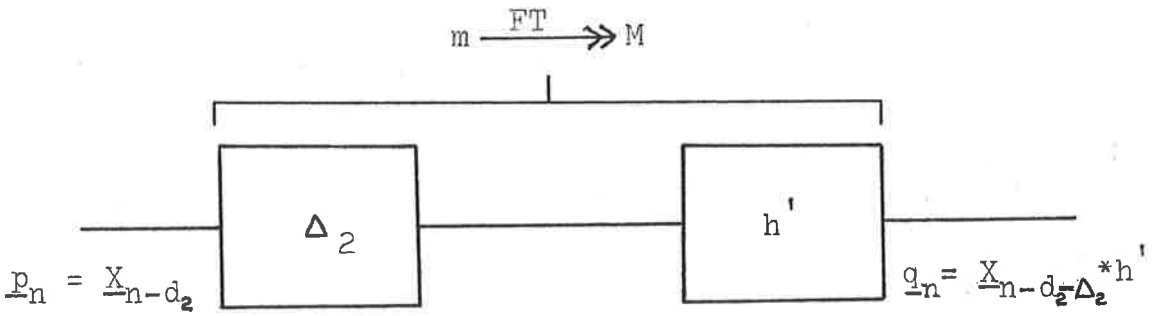

where $h' = h - \hat{h} = (1 * m_b) - (\hat{1} * \hat{m}_b)$

$\hat{d}_2 = d_2 + \Delta_2$

m = mismatch impulse response

M = mismatch transfer function

FT = Discrete Fourier Transform

FIG 4.4: Diagramatic Representation of Equation (4.37)

data correlation matrix $\underline{\underline{A}}$ as being equivalent to the cross correlation matrix of the input signal $\underline{X}_{n-d_2}$ with the convolved version obtained by passing it through the mismatch transfer function M. Thus we could write:-

$$\underline{\underline{A}} = \underline{\underline{R}}_{pq}$$

where $\underline{p}_n = \underline{X}_{n-d_2}$

$\underline{q}_n = \underline{X}_{n-d_2} * m$

m = mismatch impulse response

(4.38)

The elements of the matrix $\underline{\underline{R}}_{pq}$ are given by(51):-

$$r_{kl} = E(p_{n-k}q_{n-l}) = R(k-l)$$

$$= \int_{-1/2T}^{1/2T} S_{pq}(f) e^{-j2\pi(k-l)Tf} df$$

where $S_{pq}(f)$ = sampled cross spectral density function

T = sampling period

(4.39)

If we know the input signal s_n, and thus $\underline{p}_n$ ($\underline{X}_{n-d_2}$), and the mismatch transfer function M, then it would be possible to explicitly calculate $\underline{q}_n$ ($\underline{X}_{n-d_2} * m$) and thus the cross correlation matrix $\underline{\underline{R}}_{pq}(\underline{\underline{A}})$. From this we could calculate the eigenvalues, and thus determine the stability of the system, To follow this procedure however would be time consuming and also we are not likely to be able to obtain the information required (i.e. M). Instead, we wish only to know the effect of the mismatch transfer function M on the eigenvalues of $\underline{\underline{R}}_{pq}$ ($\underline{\underline{A}}$), and thus on system stability.

The eigenvalues of the cross correlation matrix $\underline{\underline{R}}_{pq}$ are related to the maximum and minimum values of the cross

spectral density $S_{pq}(f)$ (51). Also, the cross spectral density function is related to the mismatch transfer function in the following way(51):-

$$S_{pq}(f) = S_{pp}(f)M^{*}(f) \qquad (4.40)$$

where $M^{*}(f)$ is the conjugate of $M(f)$

In (51), Morgan derived the relationship between the maximum and minimum values of his equivalent to the cross spectral density function $S_{pq}(f)$ and the eigenvalues of his equivalent to the data correlation matrix $\underline{\underline{R}}_{pq}$. Using this relationship he was then able to determine the stability limits for the LMS algorithm in terms of the bounds on the cross spectral density function. In our analysis, we will use Morgan's relationship between the bounds on the cross spectral density function and the eigenvalues of the data correlation matrix. However, instead of considering only the bounds of the cross spectral density $S_{pq}(f)$, we will consider the bounds on $S_{pp}(f)$ and $M^{*}(f)$ so that we can see the effect that the mismatch has on the stability of the LMS algorithm.

We shall assume that the power spectral density of p_n can be bounded as follows:-

$$L_1 \leq Re(S_{pp}(f)) \leq U_1 \qquad (4.41)$$

$S_{pp}(f)$ will always be real and positive. The auto-correlation matrix $\underline{\underline{R}}_{pp}$ of p_n will be symmetric, and thus the eigenvalues will be real and positive. Morgan(51) has shown that the eigenvalues of $\underline{\underline{R}}_{pp}$ will be bounded as follows:-

$$L_1 \leq \lambda_{pp} \leq U_1 \qquad (4.42)$$

where $L_1 > 0$

We shall also assume that the mismatch transfer function M is bounded as follows:-

$$\left.\begin{aligned} L_2 \leqslant \mathrm{Re}(M^*(f)) \leqslant U_2 \\ |\mathrm{Im}(M^*(f))| \leqslant V_2 \end{aligned}\right\} \quad (4.43)$$

Now, we wish to consider the eigenvalues of the correlation matrix $\underline{\underline{R}}_{pq}$. We shall assume that the cross spectral density $S_{pq}(f)$ is bounded within the following limits(51):-

$$\left.\begin{aligned} L \leqslant \mathrm{Re}(S_{pq}(f)) \leqslant U \\ |\mathrm{Im}(S_{pq}(f))| \leqslant V \end{aligned}\right\} \quad (4.44)$$

From (4.40), (4.41), (4.42) and (4.43) we can see that:-

$$\left.\begin{aligned} L \geqslant L_1L_2 \\ U \leqslant U_1U_2 \\ V \leqslant U_1V_2 \end{aligned}\right\} \quad (4.45)$$

It follows from (4.45) that:-

$$\left.\begin{aligned} L_1L_2 \leqslant \mathrm{Re}(S_{pq}(f)) \leqslant U_1U_2 \\ |\mathrm{Im}(S_{pq}(f))| \leqslant U_1V_2 \end{aligned}\right\} \quad (4.46)$$

Given the bounds on the cross spectral density in (4.46), we can determine the bounds on the eigenvalues of $\underline{\underline{R}}_{pq}$ by using Morgans relationship. Thus according to Morgan(51) these bounds will be:-

$$\left.\begin{aligned} L_1L_2 \leqslant \sigma \leqslant U_1U_2 \\ |\omega| \leqslant NU_1V_2/\pi \end{aligned}\right\} \quad (4.47)$$

where $\lambda_{pq} = \sigma + j\omega$

N = number of weights.

To simplify our analysis, we shall assume that the delay d_2 is zero, as we only wish to consider the effect of the mismatch in this section. The effect of some finite delay d_2 will be to reduce the margin on the stability limit for the convergence factor as described in section 4.2.2. For $d_2 = 0$, the update algorithm given in equation (4.4) can be rearranged to give:-

$$\underline{W}_{n+1} = (\underline{I} - 2\mu\underline{A})\underline{W}_n - 2\mu\underline{c} \qquad (4.48)$$

Using the orthonormal matrix $\underline{P}$ (as defined previously), to premultiply (4.48) we obtain:-

$$\underline{W}'_{n+1} = (\underline{I} - 2\mu\underline{V})\underline{W}'_n - 2\mu\underline{P}\underline{c}$$

where $\underline{V}$ is a diagonal matrix of the eigenvalues of $\underline{A}$ (4.49)

From (4.49) it can be seen that the algorithm will be stable as long as:-

$$|\underline{I} - 2\mu\underline{V}| < \underline{I}$$

$$|1 - 2\mu\lambda_{pq,i}| < 1 \ , \ i=1, \ \ldots \ ,N \qquad (4.50)$$

From (4.50) we can determine the bounds on the magnitude of the convergence factor μ that should assure convergence of the weight vector update equation. Then, assuming that the convergence factor is set within these limits we can further determine the limits on the mismatch transfer function to assure convergence. With reference to equations (4.28), (4.44) and (4.50) we see that convergence will be assured as long as μ is within the following limits:-

$$0 < \mu < \frac{L}{(U^2 + (NV/\pi)^2)} \qquad (4.51)$$

Morgan in (51) also obtains the result given in (4.51), however he does not show how he derives (4.51) from his equivalent expression to (4.44).

Note that the stability limits given in equations (4.28), and (4.29) for a single frequency input are of a similar form to equation (4.51). The difference is that in (4.51) the bounds of the cross spectral density are used to determine the upper bound of the convergence factor, rather than the real and imaginary components of the eigenvalues. The bounds on the cross spectral density, and the eigenvalues of the data correlation matrix are related by equations (4.44), (4.45) and (4.47). The terms L, U and V in equation (4.51) are chosen to give the lowest possible upper bound for the convergence factor.

We can now extend the result (4.51) that was also obtained by Morgan(51) to take into account the effect of the mismatch on stability. With reference to equations (4.45) and (4.46) we can express the result given in (4.51) as:-

$$0 < \mu < \frac{L_1 L_2}{((U_1 U_2)^2 + (N U_1 V_2/\pi)^2)} \qquad (4.52)$$

Now, we shall assume that the convergence factor μ has been chosen so that it satisfies equations (4.51), or (4.52). It can be seen from (4.50) that instability will occur if the real part of any eigenvalue of $\underline{\underline{A}}$ ($\underline{\underline{R}}_{pq}$) becomes negative. As L_1 will always be positive, it can be seen that the possibility of this occuring first takes place when L_2 is negative. (See equation (4.47)). This will first occur when the arguament of $M^*(f)$, or $M(f)$ is greater than $\pm 90^o$.

Thus we can see that the stability of the weight vector update equation (4.4) is not only dependent on the converge-

nce factor μ, and the delay d_2 but also on the arguament of the mismatch transfer function. In general the stability limits for equation (4.4) could be stated as follows:-

$$0 < \mu < \frac{L_1 L_2}{((U_1 U_2)^2 + (NU_1 V_2/\pi)^2)} \quad \text{Sin}\left[\frac{\pi}{2(2d_2+1)}\right]$$

$$|\measuredangle M(f)| < 90^\circ \quad \text{for all frequencies at which the input signal spectrum is non-zero.}$$

(4.52a)

The stability limit on the arguament of the mismatch transfer function is not a strict limit. The possibility of a mismatch causing instability takes place if the phase of the mismatch transfer function is greater than $\pm 90^\circ$ at any frequency for which the input signal spectrum is non-zero.

To arrive at the expression given in equation (4.52a) we have considered the effect of the mismatch transfer function M on the eigenvalues of the data correlation matrix $\underline{\underline{A}}$. The eigenvalue approach to determine stability of LMS adaptive algorithms is a well established practice, and has been used by many authors(41,51,59 and others).

The form of the data correlation matrix $\underline{\underline{A}}$ (see equation (4.35)) is obtained by extending the simplified analysis of Burgess(42) to cover a practical Adaptive Sound Canceller. It was Burgess who first proposed the idea of including the elements $\hat{L}\hat{D}_2\hat{M}_b$ between the input to the transversal filter and the input to the update algorithm. Burgess however used only simple delays to model L and M_b, and ignored the delays D_1 and D_2 in his model. He did not conduct a theoretical analysis of his system.

It was recognised by the author that the so called mismatch transfer function that is peculiar to the LMS Adaptive Sound Canceller shown in Fig 4.1 was equivalent to the inclusion of a filter in the auxiliary path of a "Multiple Correlation Cancellation Loop", (LMS Algorithm) as described by Morgan(51). A similar analysis to that used by Morgan was used to obtain equation (4.51). The most important part of this analysis was to relate the data correlation matrix $\underline{\underline{A}}$ ($\underline{\underline{R}}_{pq}$) to the cross spectrum of the signal $\underline{X}_{n-d_2}$ convolved with the mismatch transfer function, and further to derive a relationship between the eigenvalues of $\underline{\underline{A}}$ and the bounds of the cross spectral density function $S_{pq}(f)$.

By using equations (4.40), (4.41), (4.42), (4.43) and (4.45), the result in (4.51) was extended by this author to consider the effect of the mismatch on the stability of the LMS algorithm, and in this sense equation (4.52a) is an extension of the work of Morgan.

4.2.5 THE EFFECTS OF A GENERAL MISMATCH ON THE CONVERGENCE OF THE RESIDUAL ERROR:-

In section 4.2.4 we considered the effect of the mismatch on the stability of the LMS adaptive algorithm. Now, we will consider the effect of the mismatch on the residual error, that is, the sound that remains after cancellation has been attempted. An inspection of Fig 4.1 shows that the residual error e_n is given by:-

$$e_n = d_n + \underline{X}_n^T \underline{W}_n * 1 \qquad \text{(4.53)}$$

If we define $\underline{W}^*$ as the optimum weight vector(41), that is, the weight vector for which there is no error term in equation (4.4), then it can be seen from equation (4.4) that:-

$$\underline{W}^* = -\underline{\underline{A}}^{-1}\underline{c}$$

$$d_n = -\underline{X}_n^T\underline{W}^* * 1 \qquad (4.54)$$

Substituting into (4.53) for d_n we can show that:-

$$e_n = \underline{X}_n^T(\underline{W}_n - \underline{W}^*) * 1 \qquad (4.55)$$

We shall call the term $\underline{W}_n - \underline{W}^*$ the weight vector error. It can be seen from equation (4.55) that the form of the residual error is directly related to the weight vector error. We shall consider the effect of the mismatch on the weight vector error, as this will give an indication of the effect of the mismatch on the residual error. In considering the weight vector error we will be following a similar analysis to that of Widrow et al(41), and Morgan(51).

Starting with equation (4.48) we substitute for $\underline{c}$ using equation (4.54), and subtract $\underline{W}^*$ from both sides of the equation. This yields:-

$$\underline{W}_{n+1} - \underline{W}^* = (\underline{\underline{I}} - 2\mu\underline{\underline{A}})\underline{W}_n + 2\mu\underline{\underline{A}}\underline{W}^* - \underline{W}^*$$

$$\underline{W}_{n+1} - \underline{W}^* = \underline{W}_n - \underline{W}^* - 2\mu\underline{\underline{A}}(\underline{W}_n - \underline{W}^*) \qquad (4.56)$$

If we define $\underline{v}_n = \underline{W}_n - \underline{W}^*$ then we can write equation (4.56) as follows:-

$$\underline{v}_{n+1} = (\underline{\underline{I}} - 2\mu\underline{\underline{A}})\underline{v}_n \qquad (4.57)$$

Transforming equation (4.57) into the primed frame of reference using the orthonormal matrix $\underline{\underline{P}}$ as defined in (4.25), we obtain(41):-

$$\underline{v}'_{n+1} = (\underline{\underline{I}} - 2\mu\underline{\underline{V}})\underline{v}'_n$$

$$\therefore \underline{v}'_{n+1} - (\underline{\underline{I}} - 2\mu\underline{\underline{V}})\underline{v}'_n = 0 \qquad (4.58)$$

Equation (4.58) is a homogeneous vector difference equation in the primed, or uncoupled frame. This equation has a simple geometric solution(41,51):-

$$\underline{v}'_n = (\underline{\underline{I}} - 2\mu\underline{\underline{V}})^n \underline{v}'_o$$

$$\text{where } \underline{v}'_o = \underline{W}'_o - \underline{W}'^* \qquad (4.59)$$

From (4.59) it can be seen that the transients in the primed co-ordinates will be geometric, and it is possible to fit an exponential envelope to this geometric sequence(41). In (41) Widrow et al follow through this arguament to estimate the time constant for the i^{th} primed co-ordinate as:-

$$\tau_i = 1/2\mu\lambda_i \qquad (4.60)$$

Now, for a general mismatch, the eigenvalues λ_{pq} of the data correlation matrix $\underline{\underline{A}}$ can be complex. Thus in general the envelope of the i^{th} primed co-ordinate will be of the form:-

$$e^{-2\mu\lambda_{pq,i}} = e^{-2\mu(\sigma_i + j\omega_i)}$$

$$= e^{-2\mu\sigma_i} e^{-j2\mu\omega_i} \qquad (4.61)$$

It can be seen from (4.61) that this envelope will have two general components. One will be an exponential decay with time constant $1/2\mu\sigma_i$, and the other will be a sinusoid of frequency $\mu\omega_i/\pi$.

In general, the response time of the most slowly converging mode (i.e. $e^{-2\mu\sigma_{i(min)}}$) is taken to be indicative of system performance(41,51). The exponential time constant of the slowest mode is given by(41,51):-

$$\tau_{max} = 1/2\mu\sigma_{i(min)} \qquad (4.62)$$

With reference to equations (4.28) and (4.50) we can see

that the exact limits on the convergence factor μ to ensure stability are(51):-

$$0 < \mu < \left[\frac{\sigma_i}{|\lambda_{pq,i}|^2}\right]_{min} \qquad (4.63)$$

Substituting (4.63) into (4.62) then gives(51):-

$$\tau_{max} > \frac{\left[|\lambda_{pq,i}|^2/\sigma_i\right]_{max}}{2\sigma_{i(min)}} \qquad (4.64)$$

For the Adaptive Noise Canceller, the equivalent expressions to (4.63) and (4.64) are(41,51):-

$$0 < \mu < 1/\lambda_{min}$$

$$\tau_{max} > \lambda_{max}/2\lambda_{min} \qquad (4.65)$$

Now, using (4.47) we can rewrite (4.64) to show the effect of the mismatch on the convergence of the weight vector error, and thus through (4.55) the convergence of the error.

$$\tau_{max} > \frac{((U_1U_2)^2 + (NU_1V_2/\pi)^2)}{2(L_1L_2)^2} \qquad (4.66)$$

From (4.66) it can be seen that the mismatch, through U_2, L_2 and V_2 will have an effect on the convergence rate of the weight vector error and residual error, and from (4.61) it can be seen that the mismatch can also introduce an oscillation into the convergence envelope. However, it is difficult to describe in general terms the effect of the mismatch in these respects, but the effect of a particular mismatch could be calculated explicitly in each case.

4.3 THE STABILITY AND CONVERGENCE OF THE PRACTICAL NGLMS ADAPTIVE SOUND CANCELLER

4.3.1 INTRODUCTION:-

In Section 4.2 we investigated the performance of a practical Adaptive Sound Canceller based on the time domain LMS algorithm. The weight vector update equation used in this case, equation (4.1) required the calculation of the mean square error gradient $E(\epsilon_n \underline{r}_n)$. For real time applicatioins of the ASC it is not feasible to calculate the mean, and so the instantaneous square error gradient, $\epsilon_n \underline{r}_n$ is used instead. This leads to the so called Noisy Gradient form of equation (4.1) (41):-

$$\underline{W}_{n+1} = \underline{W}_n - 2\mu\epsilon_n\underline{r}_n$$

$$\text{where } \underline{W}_n = \left[w_0, w_1, \ldots, w_{N-1}\right]_n^T$$

$$\underline{r}_n = \left[r_n, r_{n-1}, \ldots, r_{n-N+1}\right]^T \qquad (4.67)$$

If we substitute for ϵ_n and $\underline{r}_n$ (as given in equation (4.2)) into (4.67), and rearrange we obtain:-

$$\underline{W}_{n+1} = \underline{W}_n - 2\mu(\underline{\underline{A}}_n'\underline{W}_{n-d_2} + \underline{c}_n')$$

$$\text{where } \underline{\underline{A}}_n' = ((\underline{X}_{n-d_2} * \underline{1} * \underline{m}_b)(\underline{X}_{n-\hat{d}_2}^T * \hat{\underline{1}} * \hat{\underline{m}}_b))$$

$$\underline{c}_n' = ((d_{n-d_2} * \underline{m}_b)(\underline{X}_{n-\hat{d}_2} * \hat{\underline{1}} * \hat{\underline{m}}_b)) \qquad (4.68)$$

Although equation (4.68) is of a similar form to equation (4.4), it differs in the respect that $\underline{\underline{A}}_n'$ and $\underline{c}_n'$ are now a function of the time index n.

In Section 4.3 we will be considering the performance of an Adaptive Sound Canceller based on the Noisy Gradient LMS

(NGLMS) algorithm. Due to the time varying nature of the matrix $\underline{\underline{A}}'_n$, the problem of determining the stability of the algorithm is more complicated. Several approaches have been taken to this problem by various authors.

One common approach (49,50,52,53) has been to consider the problem of the stability and convergence of the mean weight vector. For a stationary signal, and a stationary mismatch transfer function this approach yields results that are similar to those obtained in Section 4.2. For a non-stationary signal, or a time varying mismatch transfer function we still have time varying matricies. However, for our applications this time variation is likely to be slow (compared to the rate of convergence) and can most probably be ignored. The stability and convergence of the mean weight vector is considered in Section 4.3.2.

Another approach that has been used with signal processing and control applications of LMS type algorithms has been to use Lyapunov Techniques(56,57) to determine the stability of the algorithm. For the simple case of no delays, and no mismatch Lyapunov Techniques lead to results similar to those obtained in Section 4.2. It would appear however that the extension of these techniques to cover the problem of a practical NGLMS Adaptive Sound Canceller would be rather complicated. The application of Lyapunov Techniques to this problem are considered in section 4.3.3.

A final approach that has been suggested by Wu(54,55) is to try and determine stability directly from equation (4.68) by calculating the time varying eigenvalues of the matrix $\underline{\underline{A}}'_n$. The stability limits for the convergence factor μ can then be calculated from these eigenvalues. This approach is discussed in Section 4.3.4.

4.3.2 STABILITY AND CONVERGENCE OF THE MEAN WEIGHT VECTOR:-

The stability and convergence of the mean weight vector has been investigated by Triechler(49,50), Bershad et al (52), and of the mean weight vector error by Farden(53). To formulate the problem for the Adaptive Sound Canceller we start with equation (4.68) and take the expectation of both sides. This yields:-

$$\left.\begin{aligned} E(\underline{W}_{n+1}) &= E(\underline{W}_n) - 2\mu E(\underline{\underline{A}}_n'\underline{W}_{n-d_2} + \underline{c}_n') \\ &= E(\underline{W}_n) - 2\mu(E(\underline{\underline{A}}_n')E(\underline{W}_{n-d_2}) + E(\underline{c}_n')) \end{aligned}\right\} \quad (4.69)$$

In equation (4.69) we have assumed that $\underline{\underline{A}}_n'$ and $\underline{W}_{n-d_2}$ are uncorrelated. This assumption is not strictly true(53), but it does simplify the analysis, and results obtained under this assumption agree well with experimental results for small values of μ (49,50,52).

By defining the mean weight vector $E(\underline{W}_n)$ as $\overline{\underline{W}}_n$ we can rewrite (4.69) as follows:-

$$\left.\begin{aligned} \overline{\underline{W}}_{n+1} &= \overline{\underline{W}}_n - 2\mu(\underline{\underline{A}}_n\overline{\underline{W}}_{n-d_2} + \underline{c}_n) \\ \text{where } \underline{\underline{A}}_n &= E((\underline{X}_{n-d_2}*1*m_b)(\underline{X}^T_{n-\hat{d}_2}*\hat{1}*\hat{m}_b)) \\ \underline{c}_n &= E((d_{n-d_2}*m_b)(\underline{X}_{n-\hat{d}_2}*\hat{1}*\hat{m}_b)) \end{aligned}\right\} \quad (4.70)$$

The retention of the time index for $\underline{\underline{A}}$ and $\underline{c}$ is in recognition of the fact that the primary input sound s_n (and thus $\underline{X}_n$) may be non-stationary, or the mismatch transfer function may be time varying. In both of these cases the matrix $\underline{\underline{A}}_n$ will be time varying. However, this time variation would be at a much slower rate than that of $\underline{\underline{A}}_n'$.

For the special case when $\underline{\underline{A}}_n$ and $\underline{c}_n$ are constant with respect to n (i.e. time), equation (4.70) is identical to

equation (4.4) in Section 4.2, except that in this case we are considering the mean and not the actual weight vector. Thus it can be seen that in this case the stability limits for the convergence factor μ, the delay d_2, and the mismatch transfer function will be identical to those obtained in section 4.2.

If the matrix $\underline{\underline{A}}_n$ is time varying, then we have the problem of determining the eigenvalues of a slowly time varying matrix to determine stability. For the purposes of cancelling low frequency sound propagating down a duct, it is unlikely that the time variation in the statistics of the input signal, or the rate of change of the mismatch transfer function will be very large. That is, these changes will be slow in comparison to the convergence rate of the Adaptive Sound Canceller. Under these conditions the algorithm will still be stable so long as the convergence factor satisfies the limits as expressed in equation (4.52a) where in this case $d_2=d_{2(max)}$, and L_1 and U_1 are the minimum and maximum values of the power spectral density of the input signal over time, and the mismatch at no time exceeds the required limits.

However, due to the time variation of $\underline{\underline{A}}_n$ there is an extra constraint placed on the convergence factor μ so that the algorithm can track the changes. Farden(53) sets this limit as:-

$$\mu \gg \max\left(\left|\underline{W}^*_{n+1} - \underline{W}^*_n\right|\right) \qquad (4.70a)$$

where $\underline{W}^*_n$ is the optimal weight vector at time n

The actual choice of μ is arbitary, (within the stability limits), as increasing μ leads to better tracking, but also to a greater mean square error(41). As we envisage only slow

changes of system parameters we would not expect that tracking will be a problem for the Adaptive Sound Canceller.

4.3.3 LYAPUNOV TECHNIQUES APPLIED TO THE STABILITY AND CONVERGENCE OF THE NGLMS ADAPTIVE SOUND CANCELLER:-

In (56) Bitmead and Anderson consider the stability of discrete time varying difference equations using Lyapunov Techniques, and in (57) they consider the stability of a number of different NGLMS algorithms.

Bitmead and Anderson's results apply to a simplified version of equation (4.68), in which there is no delay d_2, and there is no mismatch. For this case, and for a stationary input signal they obtain the following stability limits for the convergence factor μ:-

$$\left.\begin{array}{l} 0 < \mu < 1/P^2 \\ \text{where } |\underline{X}_n| \leq P < \infty \end{array}\right\} \quad (4.71)$$

The number P, which is equal to the maximum value of $|\underline{X}_n|$ is related to the maximum value of the power spectral density of s_n. We have previously seen that the maximum eigenvalue of the data correlation matrix $\underline{\underline{A}}$ can be related to the maximum value of the power spectral density function. Thus it can be seen that (4.71) is similar to equation (4.52a) for a zero delay d_2, and for no mismatch, although it is more conservative as in general $U_1 < P^2$.

Lyapunov Techniques do not appear to be suitable for determining the stability of equation (4.68) when the delay d_2, and the mismatch are taken into account. However, it would seem reasonable to assume that the effect of the delay d_2, and the mismatch transfer function M on the update

equation given in (4.68) would be the same as the effect of these parameters on equation (4.1). Using this assumption we obtain the following stability limits for equation (4.68):-

$$0 < \mu < (1/P^2)\mathrm{Sin}\left[\frac{\pi}{2(2d_2 + 1)}\right]$$

where $|s_n| \leq P < \infty \; \forall \; n$

$|\angle M(f)| < 90^\circ$

for all frequencies at which $S(f)$ is non-zero

(4.72)

4.3.4 TIME VARYING EIGENVALUES AND THE STABILITY OF THE NGLMS ADAPTIVE SOUND CANCELLER:-

In (54) Wu considers the stability of the linear time varying system:-

$$\dot{\underline{x}}(t) = \underline{\underline{A}}(t)\underline{x}(t) \qquad (4.73)$$

In this note Wu shows by example that the stability of (4.73) cannot be determined from the eigenvalues of the matrix $\underline{\underline{A}}(t)$ if the eigenvalues are calculated using the conventional definition. Wu follows up this theme in (55) in which he introduces a new definition for eigenvalues and eigenvectors of a time varying system. Wu's new definition for eigenvalues is:-

$$\underline{\underline{A}}(t)\underline{e}(t) = \lambda(t)\underline{e}(t) + \dot{\underline{e}}(t)$$

where $\lambda(t)$ is time varying eigenvalue

$\underline{e}(t)$ is time varying eigenvector

(4.74)

If this definition is valid then it should be possible to calculate the time varying eigenvalues of the time varying

system matrix $\underline{\underline{A}}(t)$ and thus determine the stability of the adaptive algorithm, and convergence of the weight vector directly from equation (4.68). However, problems arise when actually trying to calculate the eigenvalues as they are not unique, and there would appear to be an infinite number of eigenvector-eigenvalue pairs.

The application of this method to determine the stability of the weight vector update equation requires some basis on which a particular eigenvalue or eigenvector can be chosen. As yet, the theory to do this has not been developed, and so the time varying eigenvalue method of Wu is of little use to determine stability. From our survey, it would seem that the methods described in Section 4.3.2 and Section 4.3.3 equation (4.72) are the most useful for determing stability.

4.4 MISMATCHES AND DELAYS IN PRACTICE

In sections 4.2 and 4.3 we have investigated the performance of the practical LMS Adaptive Sound Canceller as a function of the convergence factor μ, the delay d_2 and the mismatch transfer function M. For the case of the delay d_2, or a mismatch in gain we can always assure stability by making μ small enough. However, when we are considering mismatch in phase when estimating the cumulative transfer function LD_2M_b we must ensure that the phase mismatch is within certain limits as otherwise the algorithm will be unstable independent of the convergence factor.

Mismatches in the estimation of LD_2M_b can occur when the original estimation $\hat{L}\hat{D}_2\hat{M}_b$ is made, due to measurement and modelling errors, but they are more likely to occur during the course of operation of the Adaptive Sound Canceller as

the actual values of L, D_2 or M_b change.

The most likely cause of mismatch is the variation of the delay d_2 as a result of changes in the speed of sound in the duct. Such changes lead directly to a phase mismatch which is a linear function of frequency. The effective speed of sound in a duct is dependent on both the air temperature and the air flow rate, the relationship being(60):-

$$c' = 331.4(1 + M)\sqrt{1 + T/273} \qquad (4.75)$$

where T = temperature in ^{o}C

M = Mach Number v/c

c = $331.4\sqrt{1 + T/273}$

v = speed of air flow ms^{-1}

In this section we will consider the way in which changes in air temperature and air flow rate affect the speed of sound in a duct, and how changes in these parameters affect mismatch and thus the stability of the system.

We shall start by considering the speed of sound in the duct as a function of the temperature and air flow rate that we may expect under operating conditions say for an air-conditioner. A table setting out the variation of the speed of sound in a duct as a function of these parameters is given in Table 4.1.

As an example of the way in which changes in the speed of sound in the duct can affect mismatch and thus system stability we will consider an Adaptive Sound Canceller with the following parameters:-

Normal operating temperature = $30^{o}C$

Maximum operating temperature = $50^{o}C$

Minimum operating temperature = $10^{o}C$

Normal air flow rate = 10 ms^{-1}

T (^{o}C)	v=0ms^{-1}		v=5ms^{-1}		v=10ms^{-1}		v=20ms^{-1}	
	M ($\times10^{-1}$)	c (ms^{-1})	M ($\times10^{-1}$)	c (ms^{-1})	M ($\times10^{-1}$)	c (ms^{-1})	M ($\times10^{-1}$)	c (ms^{-1})
0	0	331.4	0.150	336.4	0.300	341.3	0.600	351.3
10	0	337.4	0.148	342.4	0.296	347.4	0.593	357.4
20	0	343.3	0.146	348.3	0.291	353.3	0.583	363.3
30	0	349.1	0.143	354.1	0.286	359.1	0.573	369.1
40	0	354.9	0.141	359.9	0.282	364.9	0.564	374.9
50	0	360.5	0.139	365.5	0.277	370.5	0.555	380.5
60	0	366.0	0.137	371.0	0.273	376.0	0.546	385.0

TABLE 4.1: Variation of Sound Speed with Temperature And Air Flow Rate

Maximum air flow rate = $20ms^{-1}$
Minimum air flow rate = $0ms^{-1}$
Sampling Frequency = 2000Hz
Maximum operating frequency = 500Hz

(4.76)

From (4.76) and Table 4.1 we can see that the maximum variations in the speed of sound in the duct are as follows:-

$T_{min} = 10^{o}C$ $v_{min} = 0ms^{-1}$ $c_{min} = 337.4ms^{-1}$

$\Delta c = 21.7ms^{-1}$

$T_{op} = 30^{o}C$ $v_{op} = 10ms^{-1}$ $c_{op} = 359.1ms^{-1}$

$\Delta c = 21.4ms^{-1}$

$T_{max} = 50^{o}C$ $v_{max} = 20ms^{-1}$ $c_{max} = 380.5ms^{-1}$

From this we can see that the maximum variation in the speed of sound in the duct is $21.7ms^{-1}$. Now, we wish to see how this will affect the mismatch at different frequencies and for different distances of separation between the loudspeaker and the error sensing microphone (which determines the length of the delay d_2).

We have seen from Sections 4.2 and 4.3 that the possibility of instability due to mismatch first arises when the mismatch in phase at any frequency is equal to 90^{o}. The most critical frequency in this respect is the highest frequency of operation. Assuming that we use the value of d_2 for normal operating conditions, then the mismatch Δ_2 (in seconds) is given by:-

$$\Delta_2 = d\Delta c/c' c_{op}$$

where d = distance between L and M_b

c_{op} = speed of sound under normal operating conditions

c' = speed of sound in duct

$\Delta c = c_{op} - c'$

(4.77)

Expressing (4.77) as a phase difference we have:-

$$\Delta\phi_2 = \Delta_2 f(360^o) \qquad (4.78)$$

where f = frequency of sound

In table 4.2 we show the dependence of the phase mismatch $\Delta\phi_2$ on the distance of separation d, and the frequency of operation f for the worst operating conditions as shown in (4.76). This dependence is shown in graphical form in Fig 4.5.

For our example we can see that for spacings up to 2m, we do not get enough mismatch in delay, even under the most extreme conditions, to cause instability. It should be noted however that some of the phase mismatch will be due to variations and incorrect modelling of the loudspeaker and microphone transfer functions. The shaded region in Fig 4.5 shows the amount by which these characteristics can vary at different frequencies for a spacing of 2 meters before instability can result.

It can be seen from equation (4.77) that the absolute value of the mismatch in the delay d_2 is dependent on the magnitude of variations in the operating conditions. The actual value of phase mismatch that results from these variations is dependent on the separation of the loudspeaker and error sensing microphone, and the frequency. Ideally, this spacing should be as small as possible. However, there may be acoustic limitations as to how small this spacing can be made.

Freq. (Hz)	Separation d (m)			
	0.5	1.0	1.5	2.0
100	3.24^{o}	6.44^{o}	9.68^{o}	12.89^{o}
200	6.48^{o}	12.89^{o}	19.37^{o}	25.78^{o}
300	9.72^{o}	19.33^{o}	29.05^{o}	38.66^{o}
400	12.96^{o}	25.78^{o}	38.74^{o}	51.55^{o}
500	16.20^{o}	32.22^{o}	48.42^{o}	61.44^{o}
Δ_2 (msec)	0.09	0.18	0.27	0.36

TABLE 4.2: Phase Mismatch Vs Separation and Frequency

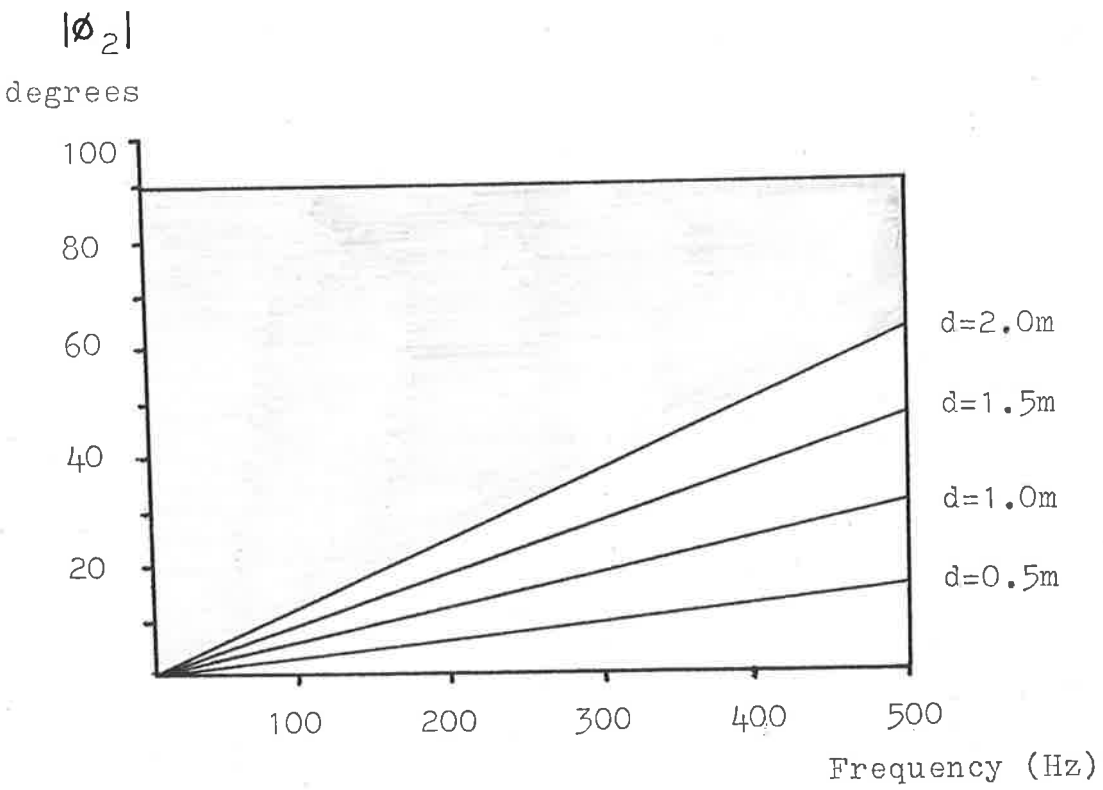

FIG 4.5: Phase Mismatch Vs Frequency

4.5 EXTENSIONS TO THE ADAPTIVE LMS SOUND CANCELLER

4.5.1 INTRODUCTION:-

In Section 4.2 and 4.3 we have investigated the performance of the practical Adaptive Sound Canceller as shown in Fig 4.1 as a function of various system parameters. In particular, the dependence of the stability of the system on the delay d_2, the convergence factor μ, and the mismatch transfer function M were investigated.

The approach taken in the theorectical investigations of sections 4.2 and 4.3 was to calculate the eigenvalues of the data correlation matrix $\underline{\underline{A}}$ for a certain set of operating conditions, and from these eigenvalues determine stability. In Section 4.3 when investigating the stability of the Adaptive Sound Canceller based on the NGLMS algorithm we saw that some techniques did not require the eigenvalues to be explicitly calculated but required the maximum value of $|\underline{X}_n|$ to be known.

In practical situations, it may not always be possible to calculate the correlation matrix $\underline{\underline{A}}$ and thus the eigenvalues, and it may not even be possible to determine the maximum value of $|\underline{X}_n|$. If these are not known then the choice of μ will be made more complicated. In Section 4.5.2 we will look at some modifications that can be made to the NGLMS algorithm to overcome this problem.

In Section 4.1 it was noted that our analysis assumed that the Adaptive Sound Canceller shown in Fig 4.1 used ideal unidirectional microphones and loudspeakers. In practical situations it is not possible to achieve this ideality and thus some acoustic feedback will result between the loudspeaker and the incident sound sensing microphone which

degrades the performance of the canceller. One way of overcoming this problem is to feed back an electrical signal to negate the effect of the acoustic feedback. In Section 4.5.3 we look at a method of doing this using an adaptive LMS filter so that we can track changes in the acoustic feedback path.

In Sections 4.2.3, 4.2.4 and 4.3 we considered the convergence and stability of the Adaptive Sound Canceller as a function of the mismatch transfer function, and in Section 4.4 we looked at the mismatch that was likely to occur in practice. A large proportion of this mismatch was due to the variation in the system delay d_2. In these sections it was assumed that the cumulative estimate $\hat{L}\hat{D}_2\hat{M}_b$ remained constant and that the mismatch would vary during the course of operation as the true values varied around the estimate. To keep the mismatch as small as possible it has been suggested by Warnaka et al(44) that an adaptive LMS filter can be used to obtain the estimate $\hat{L}\hat{D}_2\hat{M}_b$. This approach has been considered in Section 4.5.4.

Taking into account the extensions to the Adaptive Sound Canceller suggested in Sections 4.5.2, 4.5.3 and 4.5.4 we arrive at what we propose is a truly practical system based on the time domain LMS adaptive algorithm. A block diagram of this system is shown in Fig 4.6.

4.5.2 THE NORMALIZED NGLMS ADAPTIVE SOUND CANCELLER:-

A number of authors(42,57) have suggested the use of a normalized NGLMS algorithm in practical applications. One such form of this algorithm is given in equation (4.79) along with the corresponding stability limit for the convergence factor.

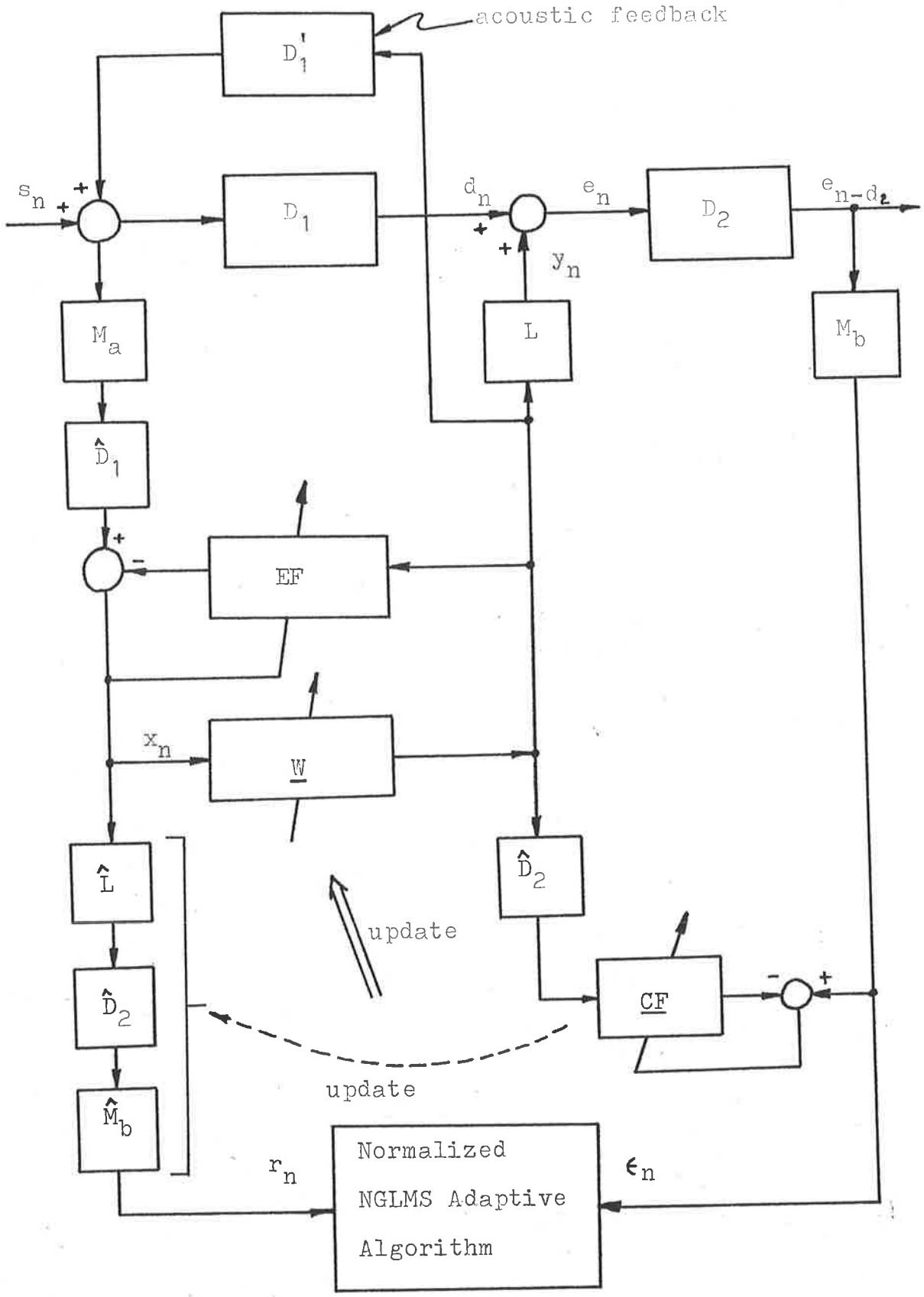

FIG 4.6: Extended Version of Adaptive Sound Canceller

$$\underline{W}_{n+1} = \underline{W}_n - 2\mu\epsilon_n\underline{r}_n/(\underline{r}_n^T\underline{r}_n)$$

$$0 < \mu < 1 \qquad \text{(4.79)}$$

In equation (4.79), the effective convergence constant is $(\mu/(\underline{r}_n^T\underline{r}_n))$ where $\underline{r}_n^T\underline{r}_n$ is the instantaneous estimate of the power in the input signal vector. With reference to equations (4.67) and (4.72) it can be seen that as long as the convergence factor μ is constrained to be less than unity then the effective convergence factor will always be less than $1/P_i^2$ where P_i is equal to the instantaneous value of the magnitude of $\underline{r}_n$, and thus according to (4.72) and assuming zero delay and mismatch the algorithm should be stable. The algorithm given in (4.79) could be stated in a more general way to take into account the effect of the delay d_2, and the mismatch.

$$\underline{W}_{n+1} = \underline{W}_n - 2\mu\epsilon_n\underline{r}_n/(\underline{r}_n^T\underline{r}_n)$$

$$\text{where } 0 < \mu < \sin\left[\pi/2(2d_2 + 1)\right] \qquad \text{(4.80)}$$

$$|\angle M(f)| < 90^\circ$$

One of the main advantages of the algorithm shown in equation (4.80) is that it is no longer necessary to have a knowlege of the eigenvalues of the data correlation matrix, or the maximum value of the magnitude of the input signal vector. Also, we now have in effect an adaptive convergence factor which adjusts to suit the input vector magnitude.

Problems can arise with equations (4.79) and (4.80) when the magnitude of $\underline{r}_n$ is too small. An alternative form has been suggested in (57) to overcome these problems. A small positive constant ε is added to $\underline{r}_n^T\underline{r}_n$ to make this less sensitive to noise when the input signal is small. The new algorithm thus formed is:-

$$\underline{W}_{n+1} = \underline{W}_n - \left[\frac{2\mu\epsilon_n\underline{r}_n}{\varepsilon + \underline{r}_n^T\underline{r}_n}\right]$$

$$\text{where } 0 < \mu < \text{Sin}\left[\pi/2(2d_2 + 1)\right] \qquad \varepsilon > 0 \text{ and small} \qquad \text{(4.81)}$$

4.5.3 ACOUSTIC FEEDBACK COMPENSATION:-

To overcome the problem of acoustical feedback due to the non-ideal properties of the unidirectional loudspeakers and microphones an electrical signal can be fed back and subtracted from the acoustic signal to negate its effect. This was the approach that was taken with the Chelsea Dipole(21,22).

However, a Chelsea Dipole type arrangement would be of limited use in our case, as we have a system that may change with time (due to changes in air speed) and thus we can have a variable acoustic feedback path. Instead of using a constant electrical filter to compensate for the acoustic feedback we can use an adaptive filter to estimate and track any variations in the acoustic feedback path.

The use of such an adaptive compensating filter was first suggested by the Essex Team(27,28) but has also been investigated by Warnaka et al(44) in a practical sytem. The adaptive filter to compensate for acoustic feedback is shown as EF in Fig 4.6.

4.5.4 COMPENSATION FOR THE MISMATCH TRANSFER FUNCTION:-

In a similar way to that in which we used an adaptive LMS filter to compensate for the acoustic feedback, we now wish to use an adaptive filter to obtain an estimate of the cumulative transfer function LD_2M_b. If we can employ an

adaptive filter, then we can track changes in this transfer function and thus we should be able to minimize the amount of mismatch that occurs.

A filter to adaptively estimate the transfer function LD_2M_b is shown as the combination $\hat{d}_2$, CF in Fig 4.6. As shown in Fig 4.6 the filter CF is adaptively updated during the operation of the sound canceller. However in this case, the signal d_n will act as a noise input to the algorithm, and since it is of approximately the same magnitude as y_n and roughly correlated to it, it will mean that a poor estimate may result. The idea of including a compensating filter to condition the error signal was first proposed by Warnaka et al(44), and this system has been reported to perform well in practical situations.

Even if the compensating filter in Fig 4.6 is not used to track the transfer function LD_2M_b, the filter CF could be used to make an initial estimate of this transfer function. If this was the case then it could be arranged so that there was no incident sound in the duct and thus no signal d_n to act as a noise input to the algorithm. This would require that a test signal be played out of the loudspeaker L while the estimation was being made.

In (44) Warnaka et al use a slightly different arrangement of the compensating filter CF. In this case the filter is arranged to adaptively estimate the inverse transfer function of LM_b, and the residual error signal is processed by this filter to compensate for the error sensing microphone and loudspeaker. The arrangement used by Warnaka et al(44) is shown in Fig 4.7. In (44) Warnaka et al do not discuss the theoretical reasons for their inclusion of the compensating filter. However, they do indicate that it helps with

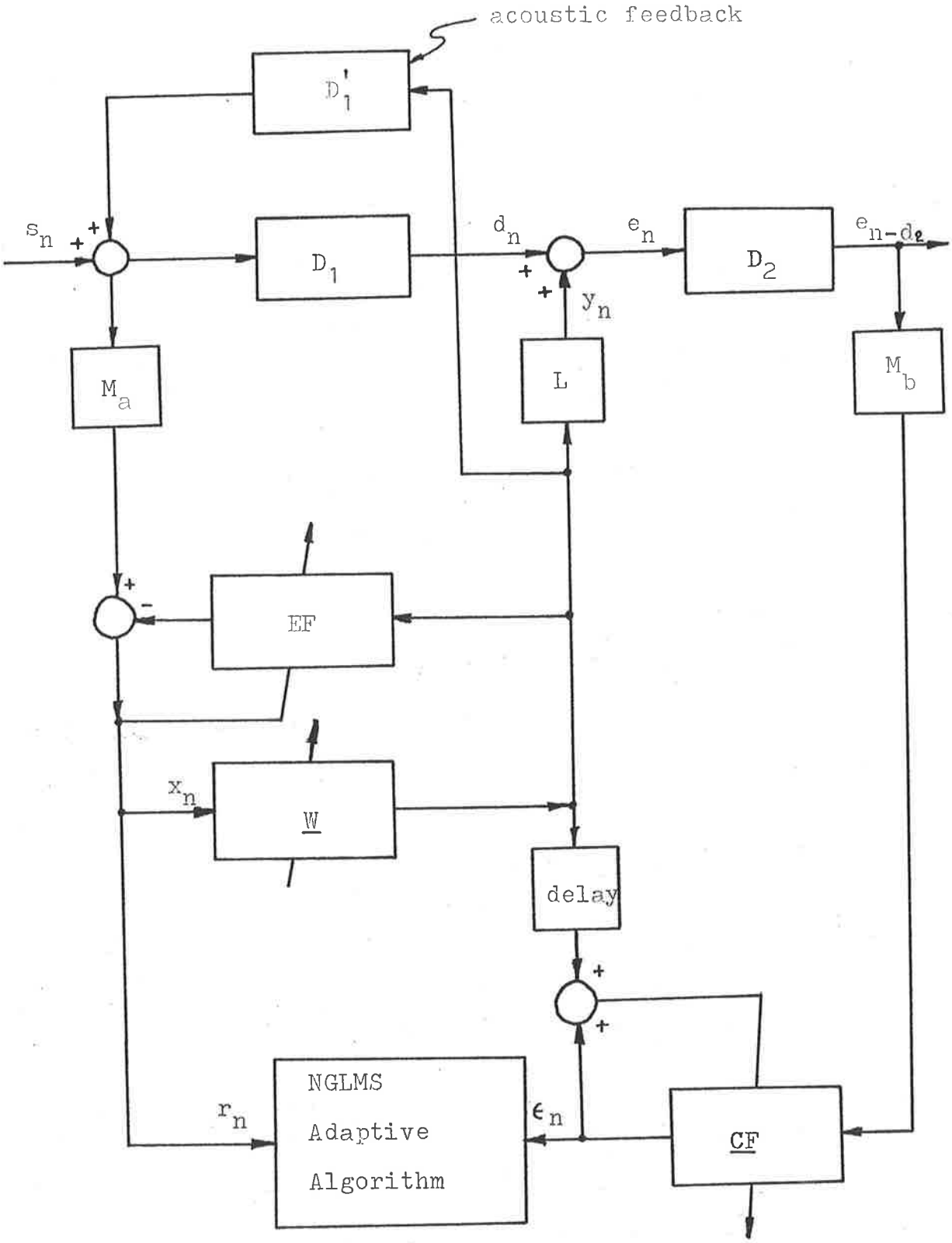

FIG 4.7: Warnaka et al's Adaptive Sound Canceller*

* Based on Fig III Ref(44)

the stability of the LMS algorithm.

We shall now consider briefly the stability of a simplified form of the Adaptive Sound Canceller proposed by Warnaka et al in (44). The Adaptive Sound Canceller to be considered is shown in Fig 4.8. Note that we have omitted the filter EF, but we will assume ideal unidirectional microphones and loudspeakers.

With the arrangement shown in Fig 4.8, we will assume that the LMS algorithm is used to initially estimate the compensating filter transfer function CF. During the course of operation of the ASC the compensating filter will not be updated but will simply be used to condition the error signal. To aid in our analysis we define the following quantities:-

$$\left.\begin{aligned} CF &= (\hat{LM}_b)^{-1} = \text{estimate of } (LM_b)^{-1} \\ cf &= \text{impulse response of CF} \\ M' &= (CF)(LM_b) \\ m' &= \text{impulse response of } M' \end{aligned}\right\} \quad (4.81)$$

The update equation of the transversal filter is:-

$$\underline{W}_{n+1} = \underline{W}_n - 2\mu E(\epsilon_n \underline{r}_n) \quad (4.82)$$

From Fig 4.8 we have:-

$$\left.\begin{aligned} \underline{r}_n &= \underline{X}_{n-\hat{d}_2} \\ \epsilon_n &= e_{n-d_2} * m_b * cf \\ &= (d_{n-d_2} + \underline{X}^T_{n-d_2} \underline{W}_{n-d_2} * l) * m_b * cf \\ &= d_{n-d_2} * m_b * cf + \underline{X}^T_{n-d_2} \underline{W}_{n-d_2} * m' \end{aligned}\right\} \quad (4.83)$$

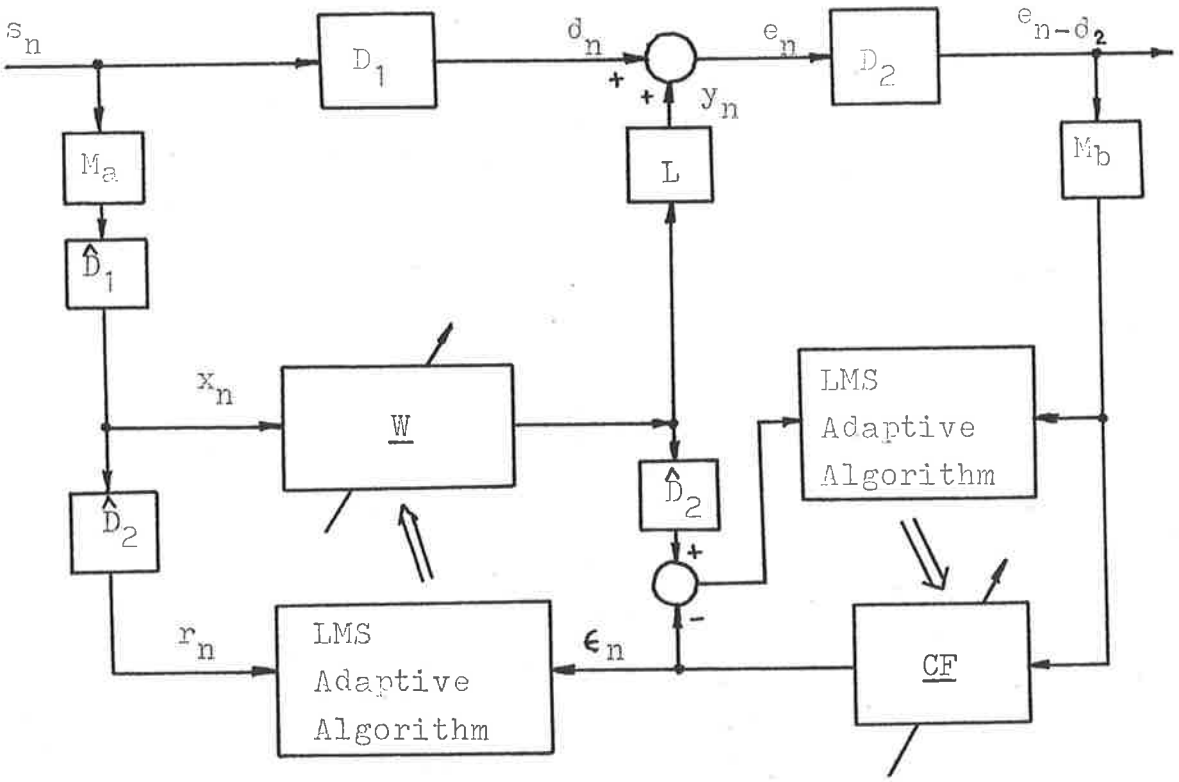

FIG 4.8: LMS Adaptive Sound Canceller Using Compensating Filter

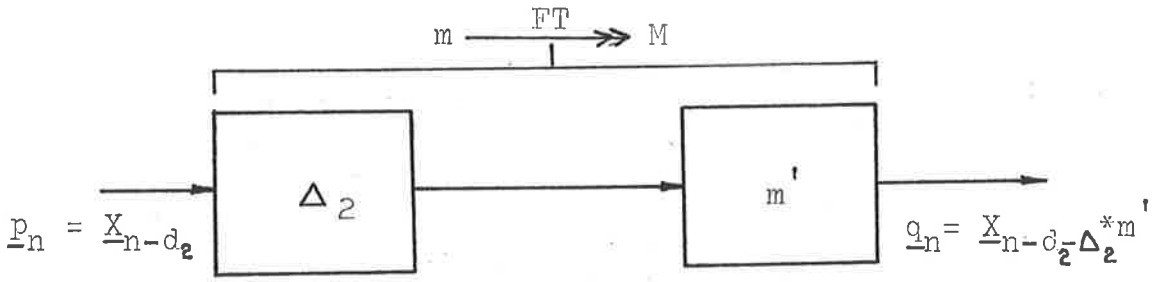

where m = mismatch impulse response

M = Mismatch transfer function

FT = Discrete Fourier Transform

$\hat{d}_2 = d_2 + \Delta_2$

$\underline{\underline{R}}_{pq} = E(\underline{X}_{n-d_2}\underline{X}^T_{n-\hat{d}_2} * m')$

FIG 4.9: Relationship Between Mismatch Transfer Function And Data Correlation Matrix

Now, substituting for $\underline{r}_n$ and ϵ_n into (4.83) we obtain:-

$$\left.\begin{aligned}
\underline{W}_{n+1} &= \underline{W}_n - 2\mu E((d_{n-d_2}{}^{*}m_b{}^{*}cf + \underline{X}^{T}_{n-d_2}\underline{W}_{n-d_2}{}^{*}m')\underline{X}_{n-\hat{d}_2}) \\
&= \underline{W}_n - 2\mu(\underline{\underline{A}}\underline{W}_{n-d_2} + \underline{c}) \\
\text{where } \underline{\underline{A}} &= E(\underline{X}_{n-d_2}\underline{X}^{T}_{n-\hat{d}_2}{}^{*}m') \\
\underline{c} &= E(d_{n-d_2}\underline{X}_{n-\hat{d}_2}{}^{*}m_b{}^{*}cf)
\end{aligned}\right\} \quad (4.84)$$

To determine the stability of equation (4.82) we will need to determine the eigenvalues of the matrix $\underline{\underline{A}}$ in equation (4.84). We can represent the RHS of the expression for $\underline{\underline{A}}$ in terms of a cross correlation matrix associated with a mismatch transfer function in a similar way to that in Section 4.2.4. A diagram showing this arrangement is given in Fig 4.9. It follows from this that the stability of the algorithm given in (4.84) will also depend upon the phase of the mismatch transfer function, the delay d_2, and the convergence factor μ. The stability limits for this algorithm will thus be:-

$$\left.\begin{aligned}
0 < \mu < & \frac{L_1 L_2}{\left[(U_1 U_2)^2 + (NU_1 V_2/\pi)^2\right]} \operatorname{Sin}\left[\frac{\pi}{2(2d_2 + 1)}\right] \\
& |\angle M'(f)| < 90^{\circ} \\
\text{where } & L_2 \leqslant \operatorname{Re}(M'^{*}(f)) \leqslant U_2 \\
& |\operatorname{Im}(M'^{*}(f))| \leqslant V_2 \\
& U_1 \text{ and } L_1 \text{ as defined in (4.41)}
\end{aligned}\right\} \quad (4.85)$$

Thus it can be seen that the Adaptive Sound Canceller shown in Fig 4.8 is very much similar to the one shown in

Fig 4.1, the main difference being in the way in which the mismatch is defined.

5. CONSTRUCTION AND TESTING OF ADAPTIVE SOUND CANCELLER

5.1 DESIGN AND CONSTRUCTION OF ADAPTIVE SOUND CANCELLER

5.1.1 OVERVIEW OF HARDWARE:-

In Chapter 4 we considered the theory of operation of a practical Adaptive Sound Canceller based on the time domain LMS algorithm. In this section we will consider the implementation of such an Adaptive Sound Canceller. An ASC Control Unit was designed and constructed by the author. This unit was designed to be used in conjunction with the test rig employed by Shepherd and La Fontain(15) when testing their broadband active attenuator, but with suitable interfacing could be applied to other systems.

A simplified block diagram of the final design of the Adaptive Sound Canceller Control Unit is shown in Fig 5.1, and photographs of the unit are shown in Fig 5.2. Figure 5.2(a) shows a front view of the canceller, and Fig 5.2(b) gives an oblique view of the canceller showing the TMS1/TMS2 Interface card extracted.

The design shown in Fig 5.1 is based upon two TMS32010 Digital Signal Processing chips; TMS1 has been used to implement the adaptive transversal filter $\underline{W}$, (that approximates the anti-phase path); TMS2 is used to implement the compensating filter $\underline{CF}$ and is also used to communicate with the outside world via an 8225 Programmable Peripheral Interface to a host computer. The two processors TMS1 and TMS2 can 'talk' to each other via a parallel interface.

The arrangement of the Adaptive Sound Canceller in Fig 5.1 is very similar to the one used by Warnaka et al(44), (see

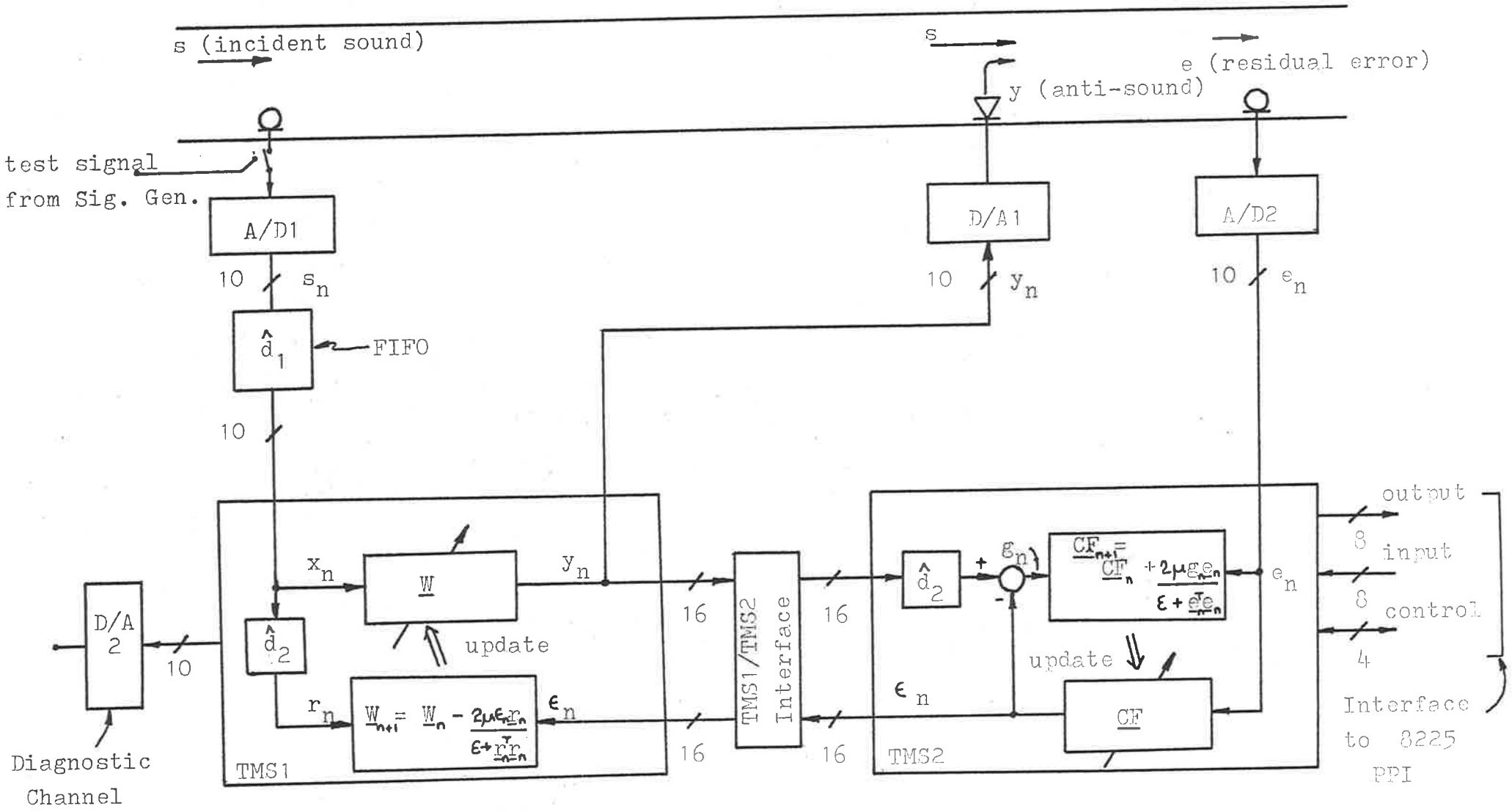

FIG 5.1: Simplified Block Diagram of Adaptive LMS Sound Canceller

Fig 4.7 and Fig 4.8). In this arrangement the compensating filter CF is used to estimate the impulse response of the inverse transfer function $(LM_b)^{-1}$ of the loudspeaker and error sensing microphone. The conditioned error signal ϵ_n is then passed across to TMS1 for use in the weight vector update equation for the transversal filter W. This particular arrangement has been used as it requires less processor memory to implement than an arrangement based on the Adaptive Sound Canceller in Fig 4.6, and the programming is less complicated. (Initially a system was designed based on one TMS32010, and Fig 4.6. The TMS32010 has 144 words of internal data memory and if any extra data memory is required this must be interfaced to the processor. Reading from and writing to external data memory is more time consuming than the same operations performed on internal data memory. Also, shuffling blocks of data between internal and external memory requires more complicated programming and also wastes time. The initial design based on Fig 4.6 would have required external data memory, resulting in a complicated program with long loop times in its sound cancelling mode. The design shown in Fig 5.1 is well suited to using two processors, and requires no external data memory.)

In (44) Warnaka et al have indicated that the compensating filter CF would be continuously updated during the course of operation of the ASC. In our implementation the compensating filter CF is to be initially estimated using a test signal that is played out of the loudspeaker. The compensating filter tap weights are not updated during the course of operation of the sound canceller, the compensating filter being used only to condition the error signal.

The weight vectors of both the transversal filters W and

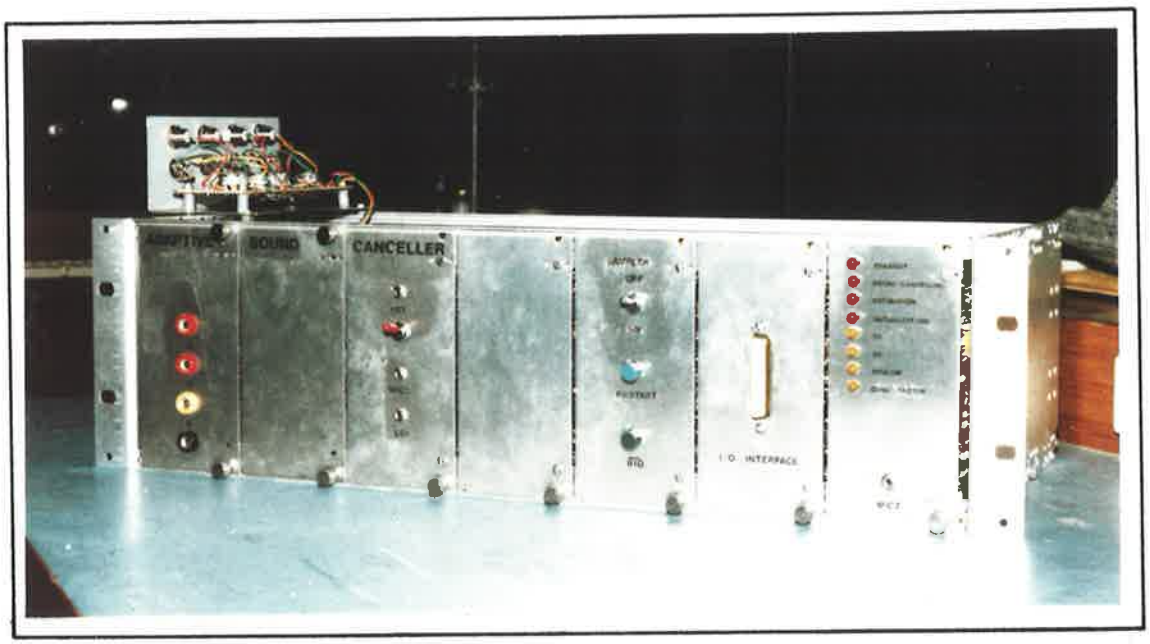

(a)

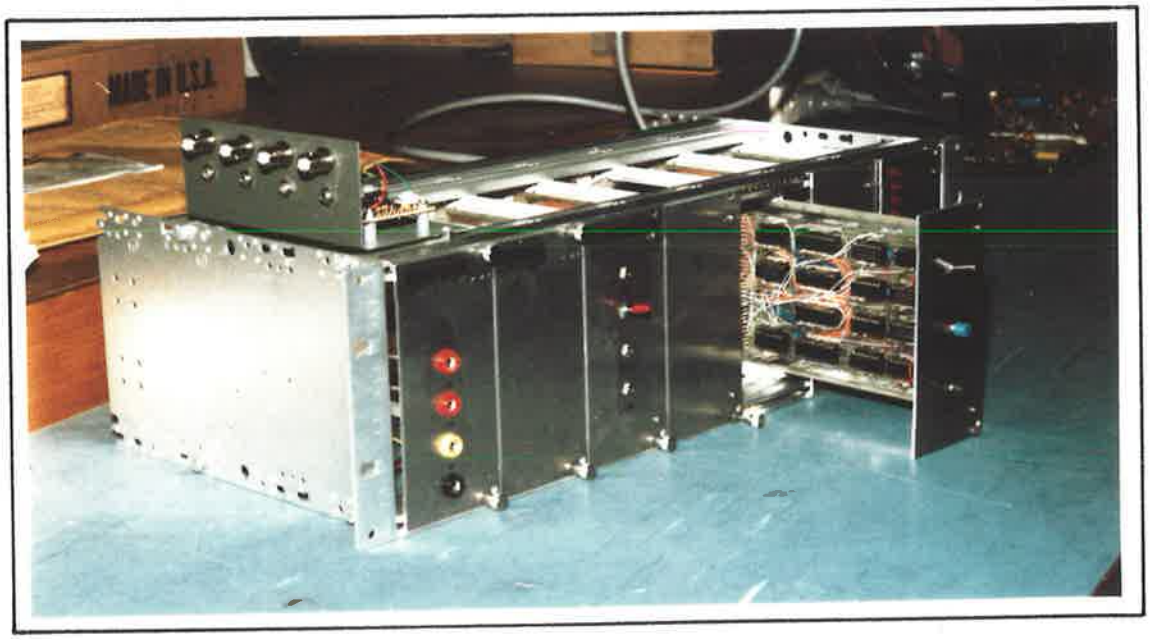

(b)

Fig 5.2: Adaptive Sound Canceller Control Unit

CF are updated using a normalized form of the Noisy Gradient LMS (NGLMS) algorithm. The update equations used are shown in Fig 5.1. Both of the algorithms are similar to equation (4.81). The transversal filter W has 32 taps. This figure was chosen as the broadband attenuator of Shepherd and La Fontain(15) also used 32 taps. The compensating filter was chosen to have 16 taps.

Both processors TMS1, and TMS2 sample the incident sound s, and the residual error signal e respectively at a rate of 2400Hz. This sampling rate was chosen to suit the equipment (i.e. anti-aliasing filters) used by Shepherd and La Fontain. The blocks shown as A/D1 and A/D2 in Fig 5.1 comprise both a sample and hold circuit and a 10-bit analogue to digital convertor. A single sampling clock is used to drive both A/D's in synchronism. The sampling clock starts the conversion process of the A/D's and when conversion is complete, the A/D's interrupt their respective processors and the signal processing, and update algorithms can proceed.

The 10-bit digital to analogue convertor D/A1 is used to transform the digital cancelling signal y_n into its analogue form. The convertor D/A2 is used as a "diagnostic channel" so that the internal workings of the processor can be accessed. The diagnostic channel is used to view the error signal g_n in the estimation stage, and used to follow the adaptation of the weight vector W during the operation of the Adaptive Sound Canceller.

The discrete delay $\hat{d}_1$ has been included in the ASC so that the transversal filter W does not have to account for all of the acoustic delay d_1. This delay has been implemented using a First In First Out (FIFO) memory chip. The FIFO has 512 bytes of memory, and can be configured to act as a variable

length digital delay line. The FIFO has the advantage that it saves wasting internal memory space in the processor TMS1. The delays $\hat{d}_2$ used for estimating both transversal filters $\underline{W}$ and $\underline{CE}$ are digital delay lines implemented internally in processor memory. As the delay $\hat{d}_2$ will in general only be small this does not require much memory.

The incident sound sensing microphone, and the loudspeaker are required to be unidirectional for use with an LMS Adaptive Sound Canceller. Ideally, the error sensing microphone will also be unidirectional so that it does not sense reflections from the end of the duct. (This will be more of a problem at low frequencies.) The microphones and loudspeakers also require anti-aliasing and low pass filters respectively, and analogue interface circuits to the ASC Control Unit. These are not shown in Fig 5.1.

5.1.2 OVERVIEW OF SOFTWARE:-

The software for the Adaptive Sound Canceller has been written in four stages; (1) Initialization, (2) Estimation, (3) Adaptive Sound Cancelling, (4) Readout of results. The programs written for both TMS1 and TMS2 follow this four stage format, and run in parallel. A simplified flow chart of the Adaptive Sound Canceller program is shown in Fig 5.3.

The programs for the ASC were developed using the Texas Instruments TMS320 Emulator kit, and the completed programs stored in PROM.

The user starts the operation of the ASC after power-up by pressing a RESTART button common to both processors. This causes both programs to jump to memory location 0, the beginning of the initialization routine. At the end of each program

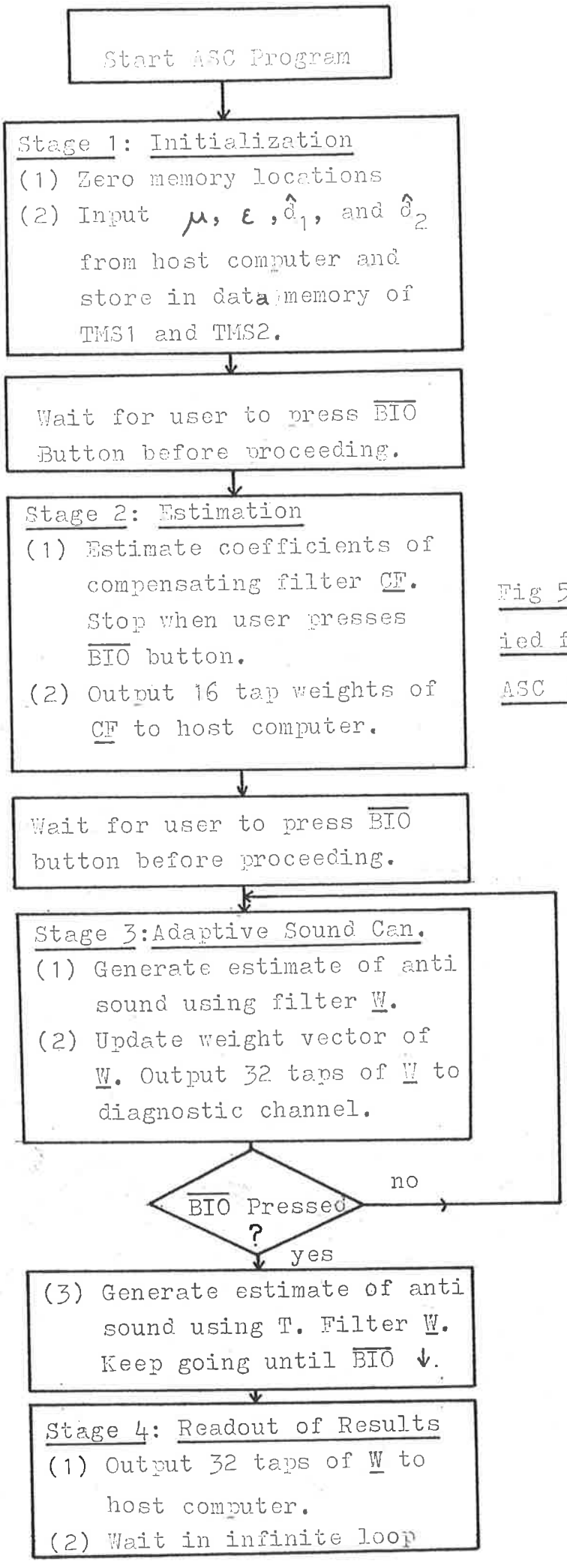

Fig 5.3: Simplified flowchart of ASC Program

stage, both processors wait for the user to press a common $\overline{BIO}$ button before advancing to the next stage. The current status of the Adaptive Sound Canceller is displayed on a set of lamps connected to a status register that is controlled by TMS2.

In this section we will consider the operation of the Adaptive Sound Canceller as it progresses through the four program stages.

Stage 1 - Initialization:

The Initialization stage is entered by pressing a RESTART button that is common to both processors. This causes both TMS320's to commence operation at program memory location 0. In the initialization stage the user enters certain program parameters using a host computer that is connected to TMS2 via the 8225 PPI. The Adaptive Sound Canceller can be connected to any host computer, as long as it has two 8225 PPI's available. The program on the host computer is written so that it prompts the user to enter the required data, and this is then transferred to TMS2.

Four bytes of data are entered; The convergence constant μ, the estimated delays $\hat{d}_1$ and $\hat{d}_2$, and the constant ε. As well as being prompted by the host computer, the ASC displays the data that is required to be entered using its status lamps. The data is first entered into the data memory of TMS2, and is then transferred to TMS1 via the parallel interface.

At the end of the initialization stage both processors wait in a loop for the $\overline{BIO}$ button to be pressed.

Stage 2 - Estimation:

In this stage the compensating filter coefficients are estimated using a normalized NGLMS algorithm. A test signal

(input from a signal generator via A/D1) is played out of the loudspeaker so that this estimation can take place, and there is no primary sound propagating down the duct.

The analogue to digital convertor A/D1 is switched to input the test signal from a signal generator. TMS1 is used simply to digitize the test signal, and then play it out of D/A1. Also, the test signal is transferred across to TMS2 for use in the estimation of CF.

The LMS algorithm run on TMS2 is arranged so that the filter CF estimates the impulse response of the inverse transfer function $(LM_b)^{-1}$. During the estimation process, the error signal g_n is transferred to TMS1 and is output through the diagnostic channel. The estimation process is stopped when the user presses the $\overline{BIO}$ button. (The $\overline{BIO}$ input to both TMS320's acts as a software polled interrupt). The 16 taps of the compensating filter are then output to the host computer (via the 8225 PPI), and displayed.

At the end of the initialization stage both processors wait in a loop for the $\overline{BIO}$ button to be pressed.

Stage 3 - Adaptive Sound Cancellation:

In this stage, TMS1 is used to produce the estimate of the anti-sound by convolving the transversal filter $\underline{W}$ with the input sound signal, and the coefficients of $\underline{W}$ are updated using the normalized NGLMS algorithm. The compensating filter CF on TMS2 is used to condition the error signal e_n, to produce the signal ϵ_n that is used in the update equation for the transversal filter $\underline{W}$. The weights of the compensating filter are not updated during this stage but remain fixed.

The taps of the transversal filter $\underline{W}$ can be observed as as they adapt via the diagnostic channel. At each iteration

the 32 taps are output to the diagnostic channel in succession and so the "impulse response" of the filter can be observed at the output of D/A2 as an analogue signal. The diagnostic channel was found to be a very useful tool for trouble shooting.

The adaptation of the weights can be stopped by pressing the $\overline{\text{BIO}}$ button. Once this has occurred, the transversal filter will still operate but the taps remain fixed. The operation of the sound canceller continues until $\overline{\text{BIO}}$ is again pressed whereupon the final program stage is entered.

Stage 4 - Readout of Results:

In this final stage the coefficients of the transversal filter $\underline{W}$ are transferred from TMS1 to TMS2 , and then to the host computer (via the 8225 PPI) where they are displayed. At the end of stage 4 both processors wait in an infinite loop for the operation of the ASC to be restarted.

5.2 TESTING OF ADAPTIVE SOUND CANCELLER

5.2.1 INITIAL TESTS USING CSIRO DUCT:-

Two test series were conducted using the experimental rig of Shepherd and La Fontain at the CSIRO Division of Energy Technology, Melbourne. The experimental arrangement used for these tests is shown in Fig 5.4. The Adaptive Sound Canceller Control Unit was connected to the rest of the ASC via an analogue interface board to adjust signals to the levels required by the control unit.

The tests were conducted using a 244mm square duct with 25mm thick perspex side walls, and 13mm thick aluminium top and bottom walls. The primary sound was generated using an

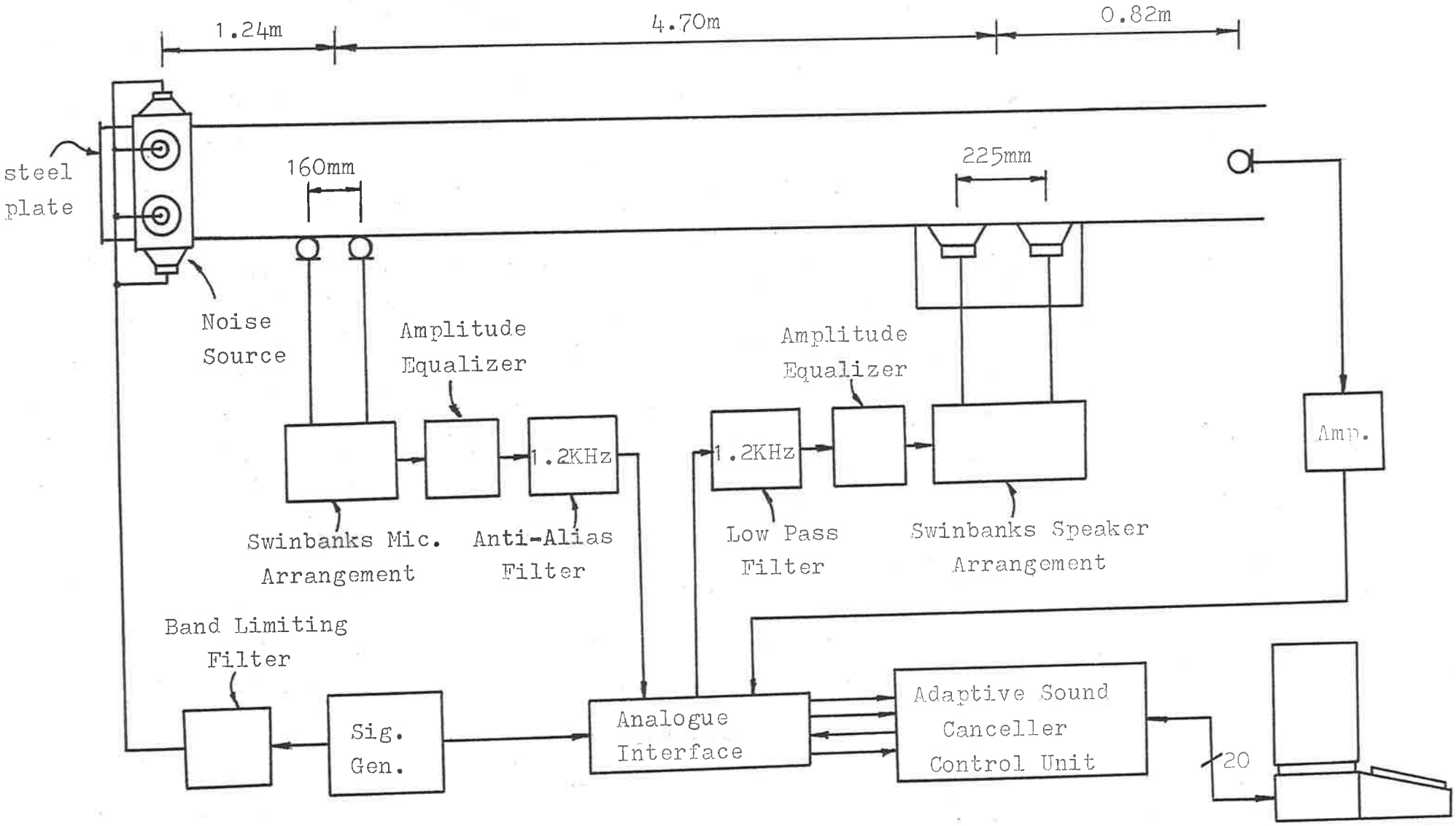

FIG 5.4: Experimental Arrangement for Conducting Tests at CSIRO

array of eight 100mm diameter loudspeakers placed around one end of the duct and driven from a signal generator. Both the incident sound sensing microphone, and the cancelling loudspeakers were two element Swinbanks arrays; The microphone spacing of 160mm gives a centre frequency of 1075Hz, and the loudspeaker spacing of 225mm a centre frequency of 764Hz. The half-sine amplitude response of both arrays is compensated for by an equalizer circuit to flatten out the response. The incident sound sensing microphone and cancelling loudspeaker are separated by 4.7m. This represents an acoustic delay of 13.7ms (for no air flow), equivalent to 32.8 sampling periods of the ASC. The 0.82m spacing between the loudspeaker and error sensing microphone represents an acoustic delay of 2.4 ms and is equivalent to 5.8 sampling periods.

In the first test series the sound canceller was unable to cancel random sound, and could cancel single frequency sounds for a short period only. For single frequency sounds the system eventually became unstable and would "search", somtimes producing cancellation but at most times adding to the sound level.

5.2.2 DIAGNOSTIC TESTS:-

After the initial test series, a diagnostic channel was added to TMS1 so that the impulse response of the transversal filter $\underline{W}$ could be observed as this filter adapted, and so that the error signal from the update algorithm for the compensating filter could be observed during the estimation stage. With the diagnostic channel operational it became evident that a dc drift was being introduced into the tap weights of the transversal filter $\underline{W}$, causing them to eventually run up

against the numerical limits of the accumulator. (Viewed from the diagnostic channel, the impulse response of $\underline{W}$ could be seen to drift downwards in a negative sense until the weights reached the limits of the accumulator, whereafter the impulse response would be random.)

The dc drift was caused by a small dc offset introduced to the input signals x_n and e_n at the analogue to digital convertors due to incorrect alignment of the convertors, or the input signals which were required to have an offset of 2.5v to suit the A/D's. This offset enters the weight vector update equations for $\underline{W}$ via the terms $\underline{r}_n$ and ϵ_n and is added to the weight vector at each iteration, resulting in the observed drift.

To overcome the problem of drift, the dc component of the weight vector was calculated at each iteration, and then subtracted from the individual weights. The update algorithms for both the compensating filter $\underline{CF}$ and the transversal filter $\underline{W}$ were modified in this way to eliminate dc drift.

5.2.3 SECOND SERIES OF TESTS AT CSIRO:-

In the second test series the performance of the Adaptive Sound Canceller was observed for both sinusoidal and random sounds.

For sinusoidal sound signals the ASC was able to obtain an attenuation of 20-40dB in the range 220-280Hz. However, below 220Hz and at most frequencies above 280 Hz the ASC was unable to cancel the primary sound, the sound level being increased.

The impulse response of the compensating filter $\underline{CF}$ and the transversal filter $\underline{W}$ for sinusoidal sound signals are shown

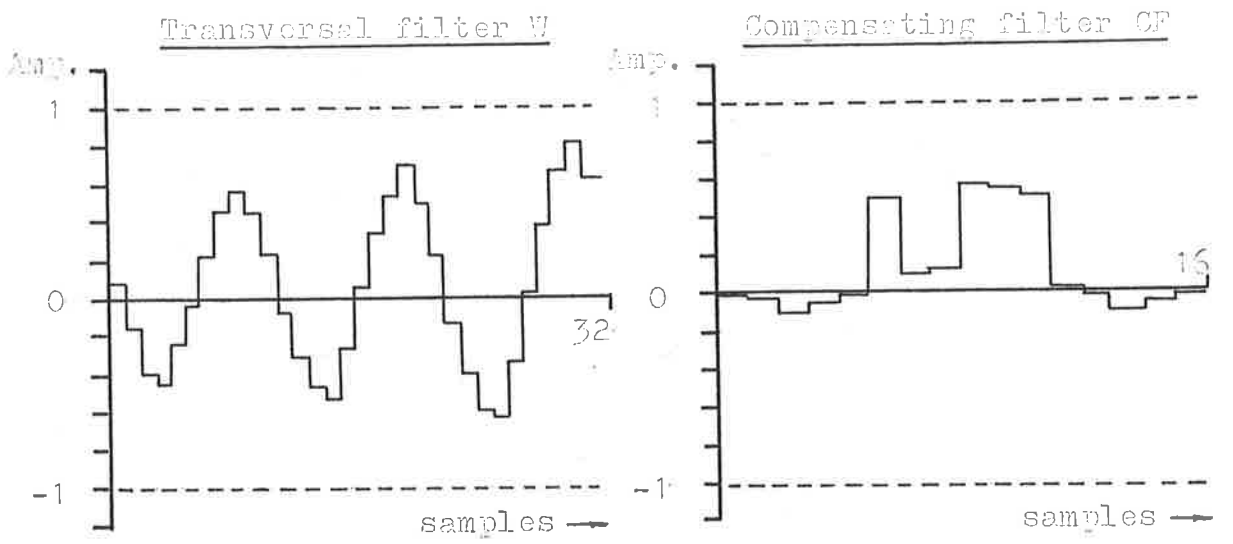

(a) frequency = 220Hz

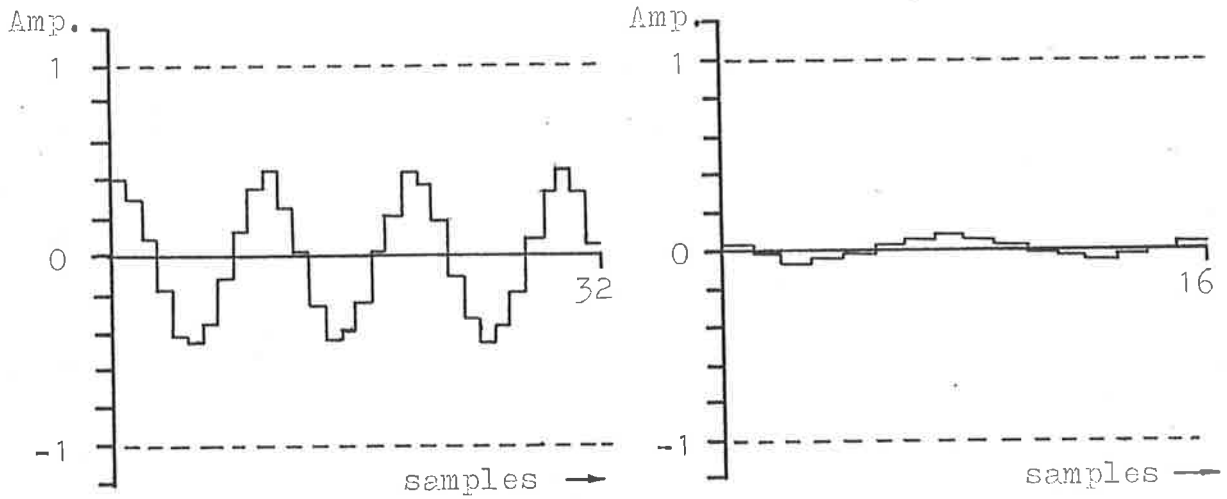

(b) frequency = 248Hz

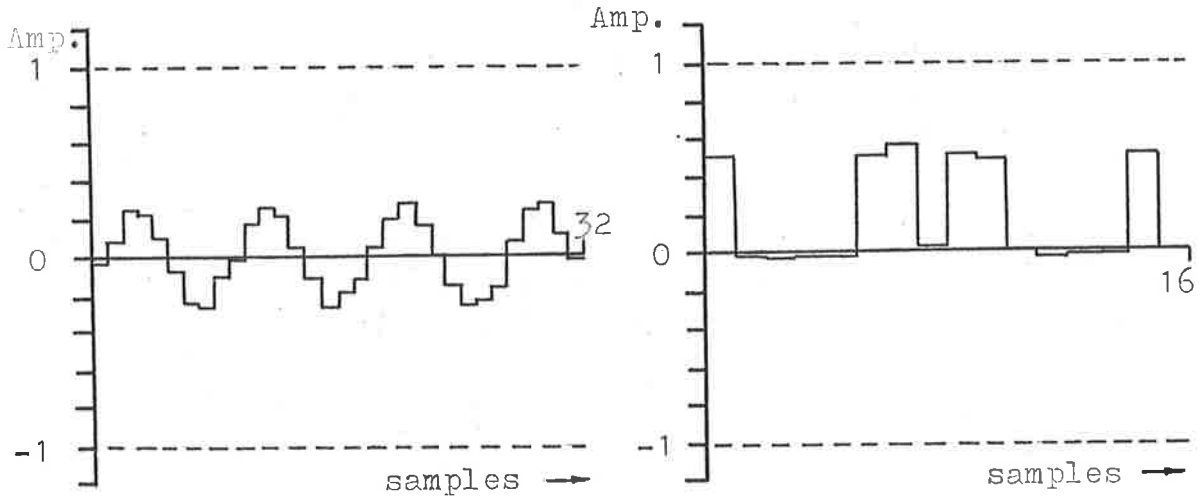

(c) frequency = 272Hz

FIG 5.5:

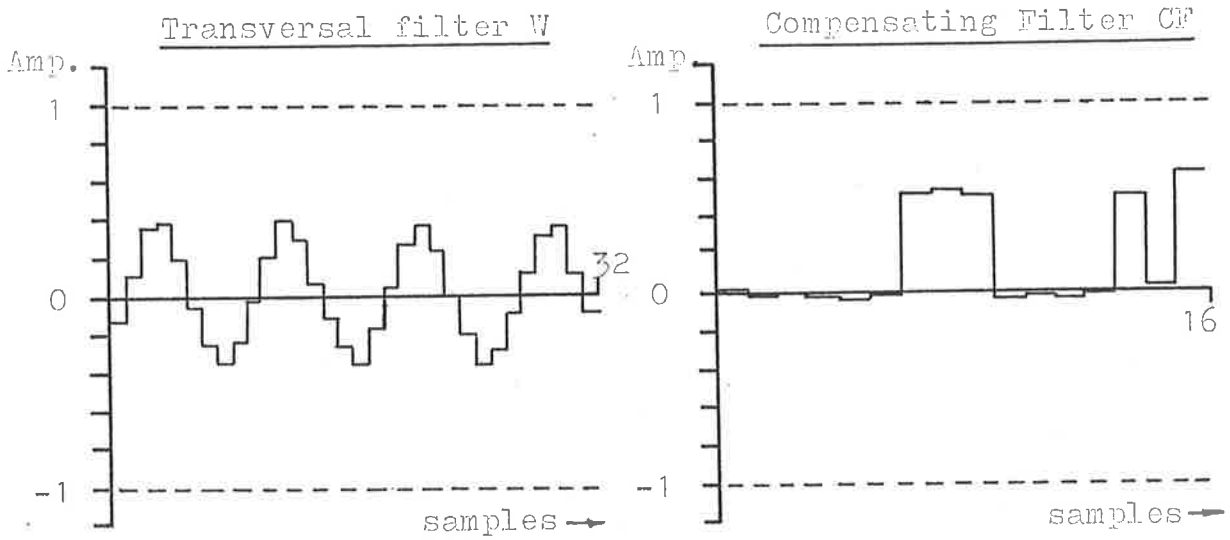

(d) frequency = 280Hz

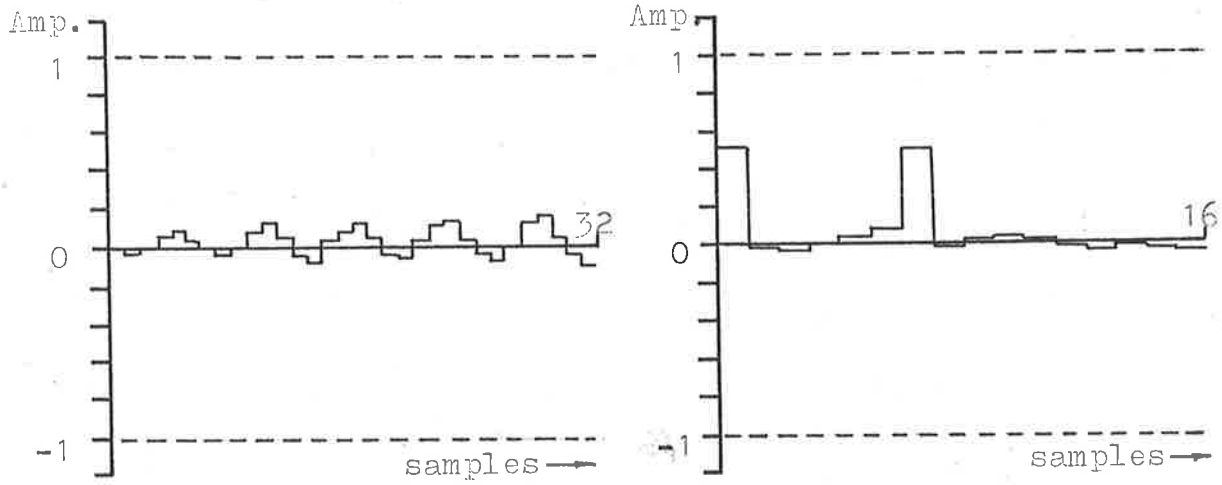

(e) frequency = 400 Hz

FIG 5.5: Normalized Impulse Responses for Transversal Filters W and CF for Sinusoidal Sound Signals

Note: (1) Impulse responses have been normalized to the maximum possible value.
(2) Results for $\mu=8$, $\epsilon=30$, $\hat{d}_1=0$, $\hat{d}_2=12$

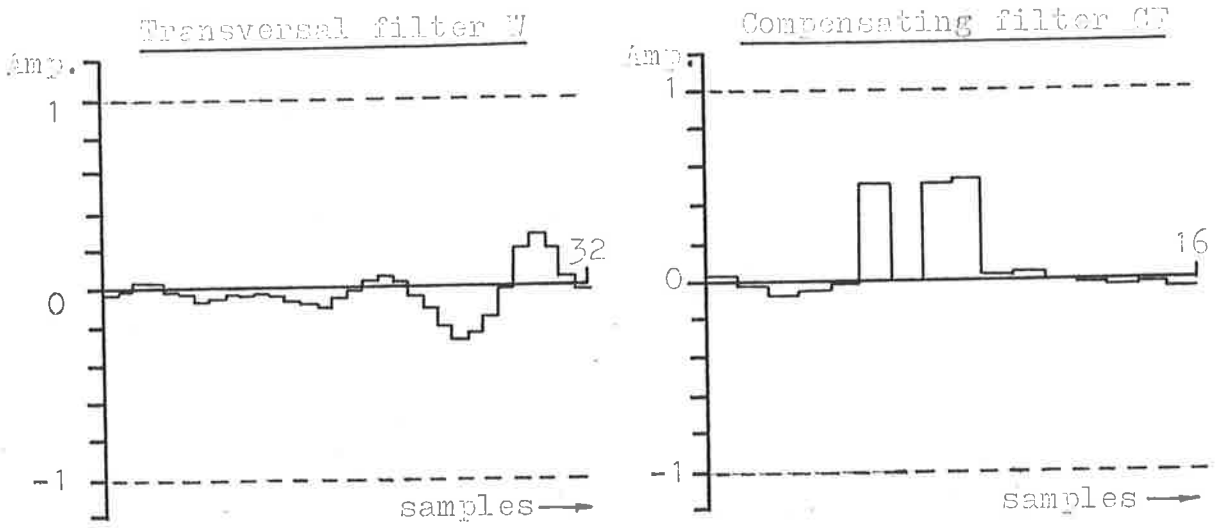

(a) Random signal b/w 40Hz, centered 250Hz

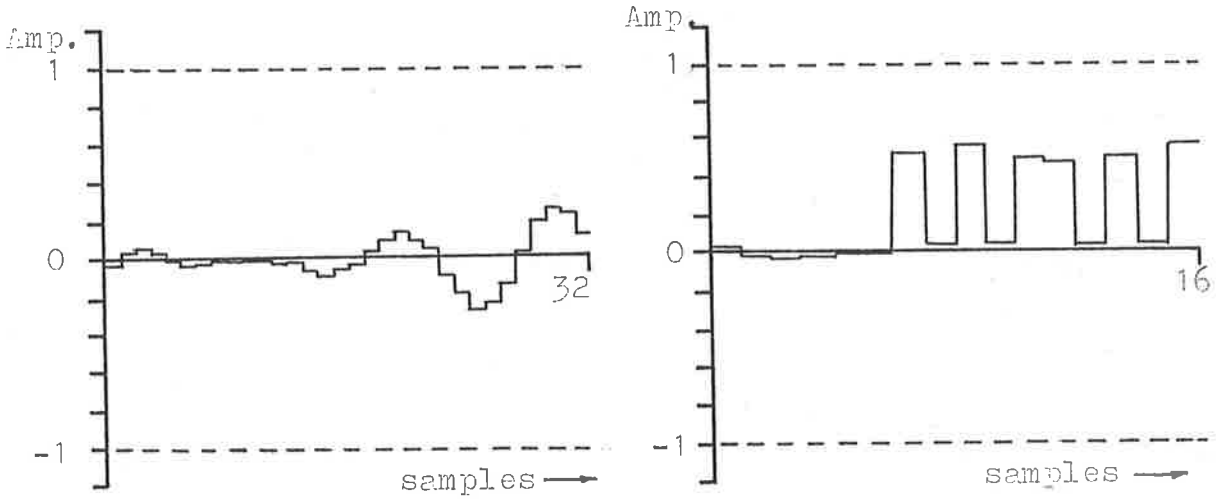

(b) Random signal b/w 75Hz, centered 250Hz

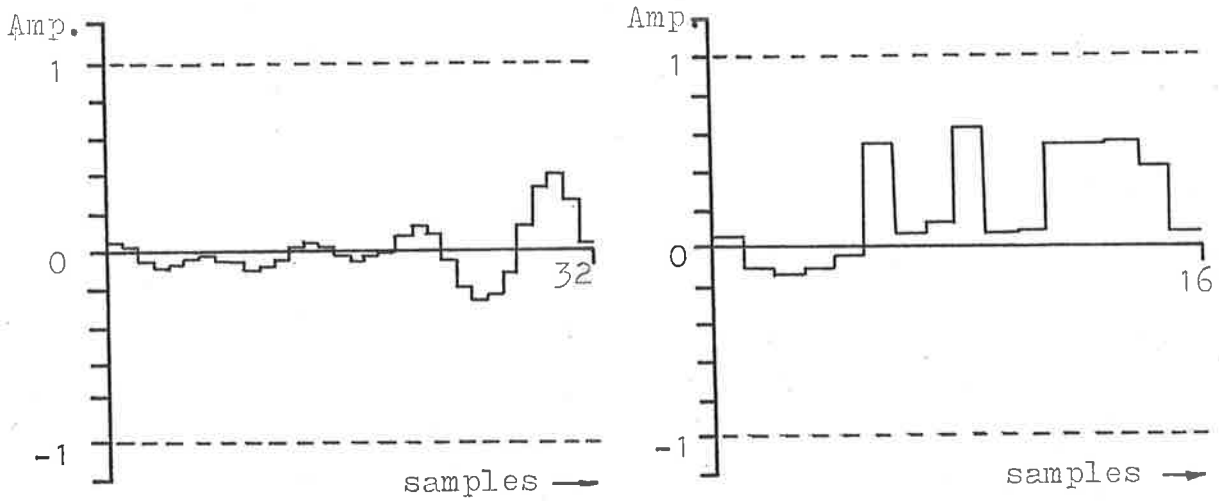

(c) Random signal b/w 95Hz, centered 250 Hz

FIG 5.6: Normalized Impulse Response for transversal Filters W and CF for Random Sound Signals

Note: Results for $\mu=8$, $\epsilon=30$, $\hat{d}_1=0$, and $\hat{d}_2=12$.

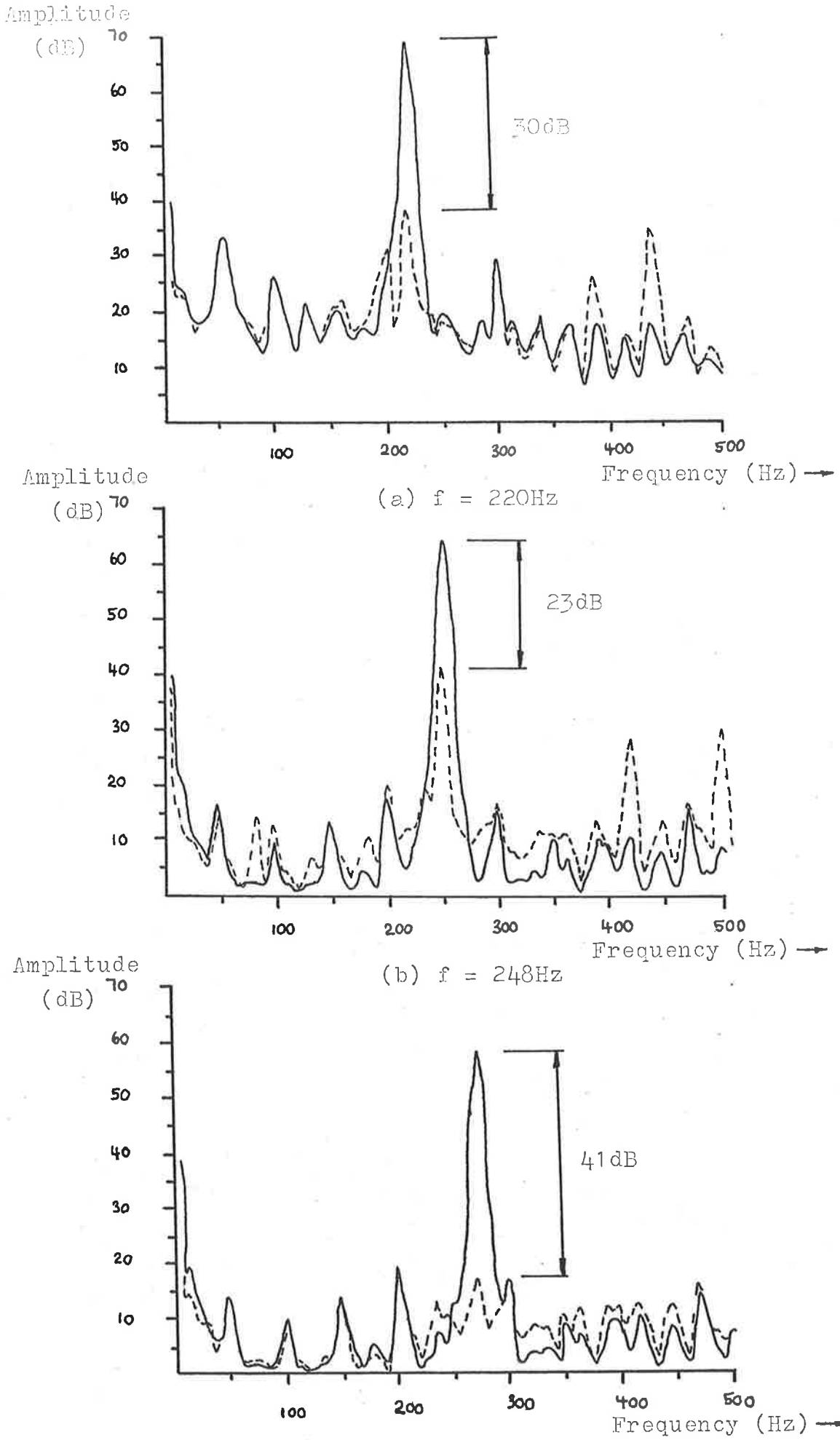
Amplitude (dB)
70
60
50
40
30
20
10
30dB
100
200
300
400
500
Frequency (Hz)
(a) f = 220Hz
Amplitude (dB)
23dB
(b) f = 248Hz
41dB
(c) f = 272Hz

FIG 5.7:

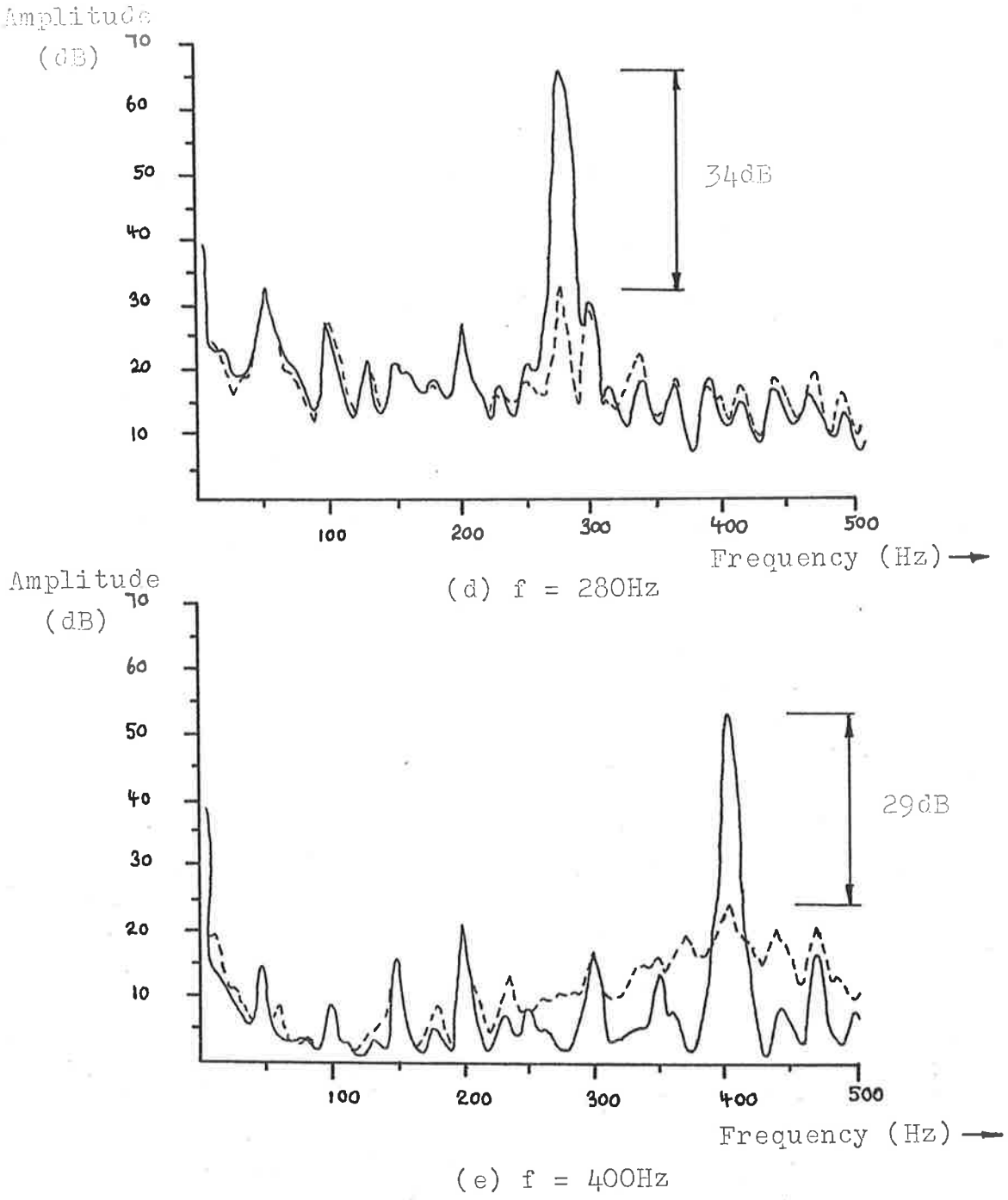

FIG 5.7: Frequency Spectrum of Error Signal for Sinusoidal Sound

——— ASC off

- - - - - - ASC on

Note: Results for μ=8, ϵ=30, $\hat{d}_1$=0, $\hat{d}_2$=12.

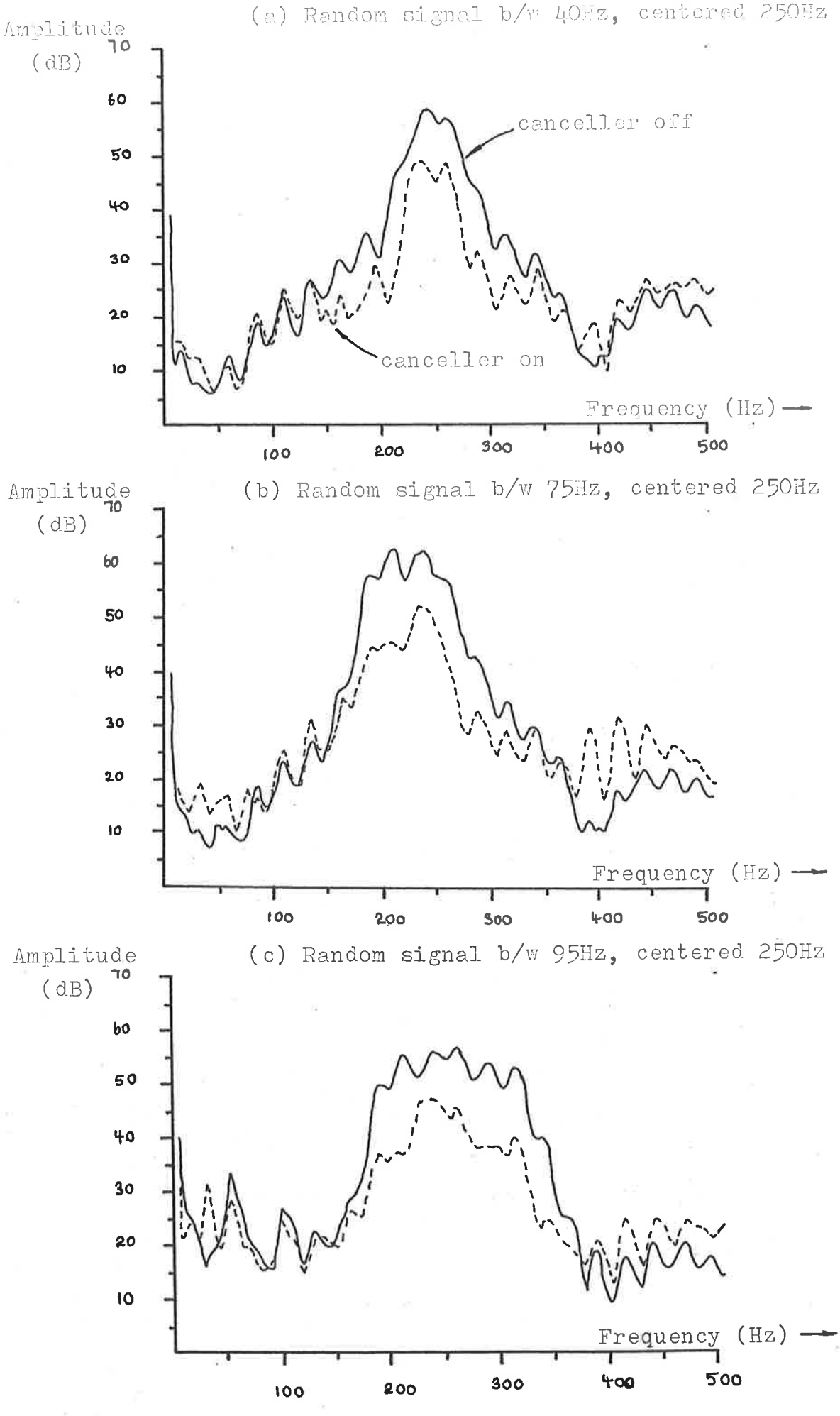

FIG 5.8: Frequency Spectra of Error Signal for Random Sound

in Fig 5.5, and the frequency spectra of the residual error signals with the canceller both on and off are shown in Fig 5.7.

From Fig 5.5 it can be seen that the impulse response of the transversal filter W is (approximately) a truncated sinusoid with the same frequency as the input signal. For the frequencies at which cancellation could not be obtained, the impulse response of the transversal filter W would either become too large in magnitude and overflow the limits of the accumulator, or when the impulse response had reached a certain magnitude the system would ring quite loudly at the input frequency.

In some cases, the impulse response of the compensating filter CF is also a truncated sinusoid, but in most cases they have an irregular shape. However, in all cases the error signal from the update algorithm for CF was observed to converge.

For random sound signals, the widest band of operation that could be achieved was from 160-370Hz for a random sound of bandwidth 95Hz centered on 250Hz. (The random sound was produced by passing the signal from a white noise generator through a band limiting filter.) If the bandwidth of the primary sound signal was increased further, then no cancellation could be obtained and the system would ring loudly at certain frequencies.

The impulse responses of the filters W and CF for different bandwidth signals are shown in Fig 5.6, and the frequency spectra of the corresponding error signals in Fig 5.8.

From Fig 5.6 it can be seen that the impulse response of the transversal filter W has a sinusoidal component of approximately 240Hz. The impulse response of the filter W changes

only silghtly as the bandwidth of the input signal is increased, although the bandwidth of the signal has not changed greatly. The compensating filter on the other hand has an irregular shape and seems to vary as the bandwidth is increased.

5.2.4 TESTS CONDUCTED USING SIMULATION CIRCUIT:-

To see what affect acoustic considerations have on the performance of the ASC Control Unit some tests were conducted using an electronic circuit to simulate the experimental arrangement that had been used in Melbourne. A block diagram of the simulation circuit that was used for these tests is shown in Fig 5.9.

The acoustic delays in the duct have been simulated using a transversal filter chip acting as a tapped delay line, and have been set to be similar to those applicable to the duct in Melbourne. The directional loudspeaker and microphones have been simulated using low pass filters.

The simulation circuit is ideal in the sense that there is no coupling between the "loudspeaker" and the "incident sound sensing microphone", and there can be no reflections of "sound" at the ends of the "duct" as may occur in the real life canceller.

For sinusoidal input signals, attenuations of 22-45dB were obtained in the range 30-290Hz. Above 290Hz the system became unstable and the "sound" level was increased rather than decreased. It is interesting to note that if the canceller was first set up to cancel at a frequency below 290Hz and then the input frequency increased, cancellation could be obtained up to at least 600Hz.

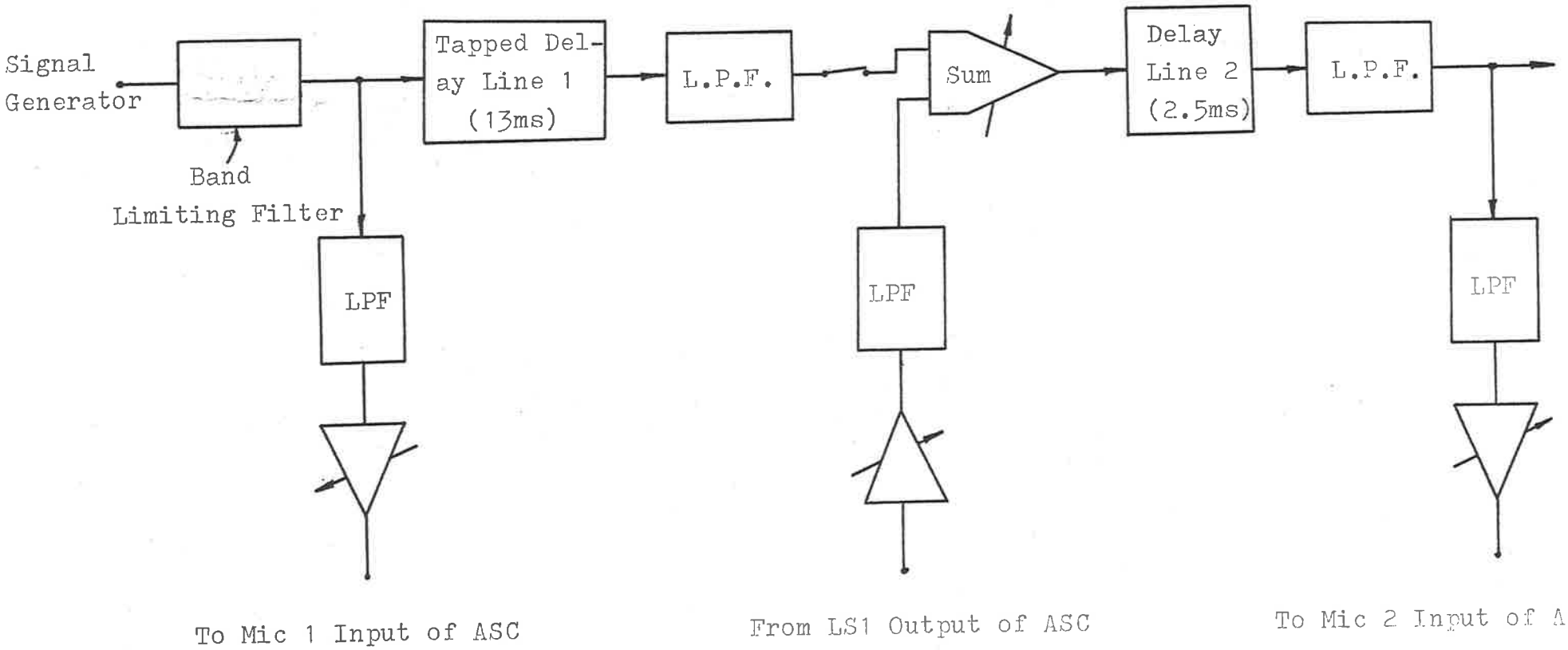

FIG 5.9: Block Diagram of the Simulation Circuit

Tests were also conducted using pseudo random input signals. (The random signals were obtained from a Wavetek model 132 VCG/Noise Generator set to output a pseudo random sequence of length $2^{15} - 1$, and a Noise Frequency of approx. 400Hz. The output from the signal generator was passed through a Krohn-Hite model 3202 filter set to low pass and a cut off frequency in the range 200-400Hz.) The frequency spectra of the residual error signals for two random signals of different bandwidth are shown in Fig 5.10. The spectra shown in Fig 5.10 (a) is for a random signal passed through a low pass filter with a cut off frequency of 250Hz, and the spectra shown in Fig 5.10 (b) are for a random signal passed through a low pass filter with a cut off frequency of 400Hz. (The frequency spectra shown in Fig 5.10 were recorded using a Tektronix 7603 oscilloscope/7L5 Spectrum Analyser combination set to have a Frequency Span of 500Hz, a resolution of 10Hz and a Time/Div setting of 2 sec.)

The best performance that could be obtained was cancellation in the range 60-375Hz for a random signal passed through a filter with a cut off frequency of 400Hz. In this case attenuation of 5-20dB could be obtained in the range 100-360Hz. If the bandwidth of the input signal was increased further, then the system became unstable and cancellation could not be achieved.

5.2.5 COMMENTS ON TEST RESULTS:-

In theory, the Adaptive Sound Canceller should be able to produce attenuation over a wider bandwidth than has been obtained for the tests conducted both in the duct in Melbourne and using a simulation circuit. For tests conducted in the

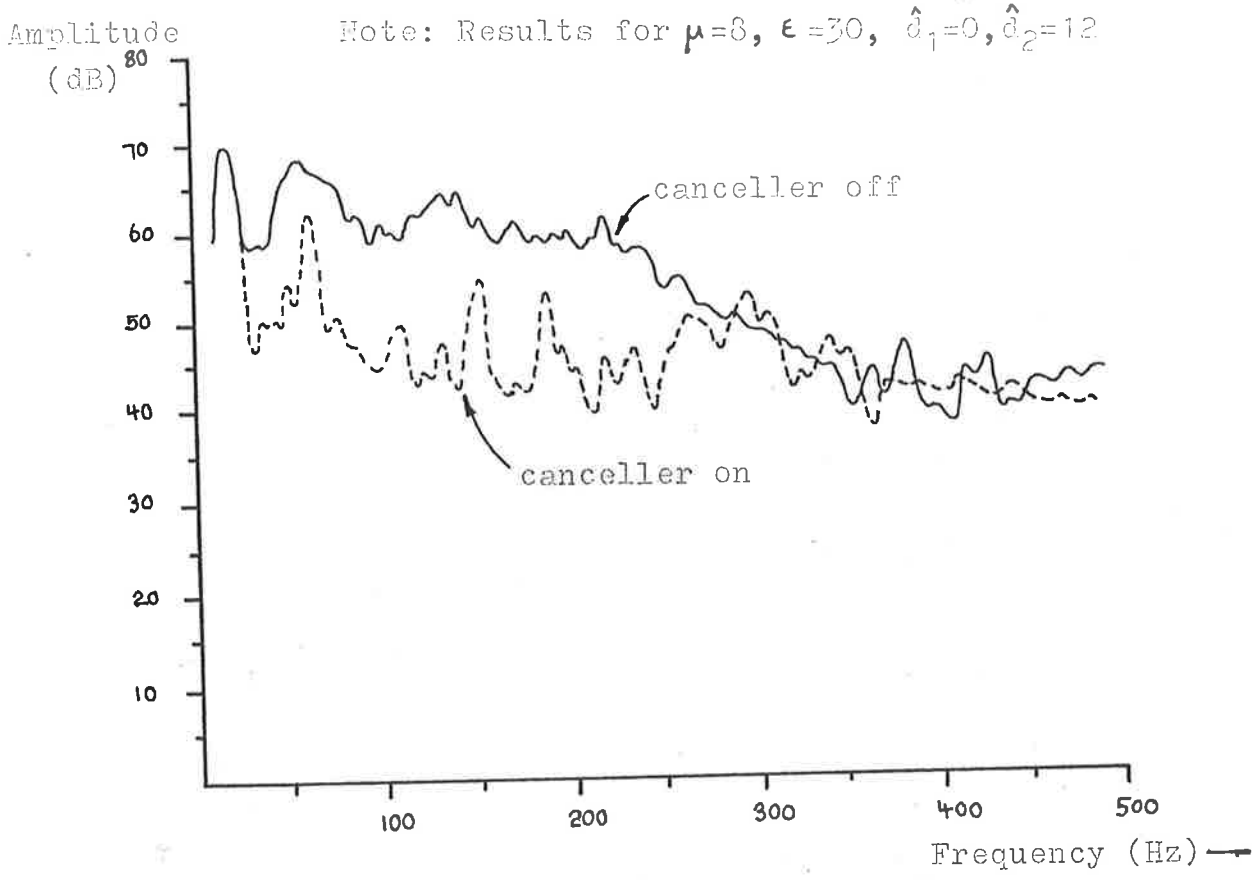

(a) Random Sound, LPF Cutoff freq. 250Hz

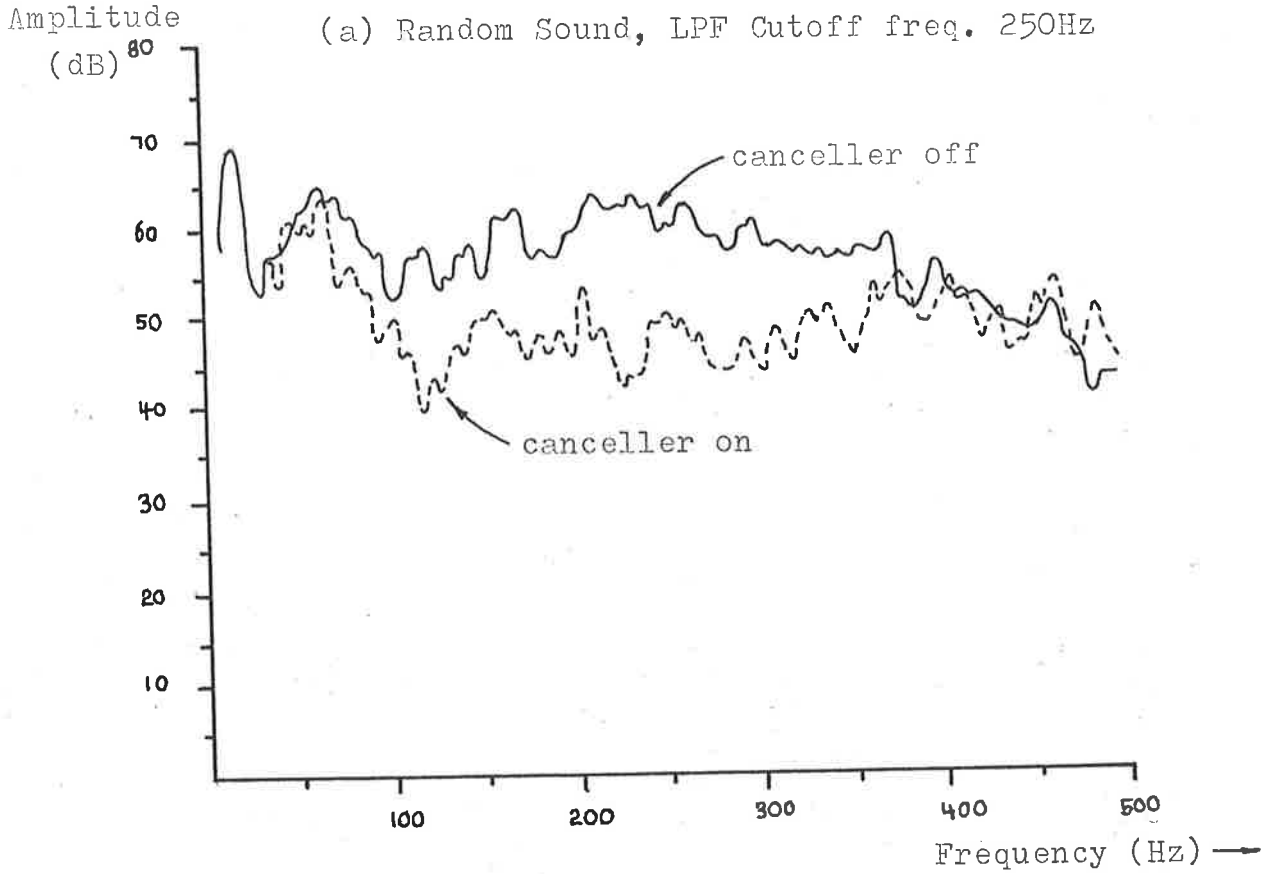

(b) Random Sound, LPF Cutoff freq. 400Hz

FIG 5.10: Frequency Spectrum of Error Signal in Simulated Duct for Random Input Signals

duct in Melbourne cancellation could be obtained over the range 160-370Hz for a random signal of bandwidth 95Hz centered on 250Hz, and for the simulation circuit cancellation could be obtained over the range 60-375Hz for a pseudo random signal passed through a filter with a cut off frequency of 400Hz. In both cases, if the bandwidth of the input signal is increased then cancellation can no longer be obtained.

For tests conducted in both the duct, and simulation circuit, the upper frequency limit at which cancellation takes place is about the same, (approx. 370Hz), but for tests conducted using the simulation circuit better low frequency performance was obtained. This is reflected in the frequency range over which single frequency sinusoids could be cancelled; 220-280Hz for the duct, and 30-290Hz for the simulation circuit.

A possible explanation for the difference in low frequency performance between the two systems is that the duct is subject to acoustic reflections from its ends (especially at low frequencies), and due to this the output from the loudspeaker can be fed back to the incident sound sensing microphone, resulting in a degredation in performance. The simulation circuit on the other hand does not suffer from reflections.

The output end of the duct is open to the air, but at low frequencies has quite a high reflection coefficient; The source end of the duct has been covered by a steel plate which is a good reflector of acoustic waves. At low frequencies reflections from the open end of the duct travel back upstream and are reflected from the steel plate, thereby coupling back into the incident sound sensing microphone. We thus have an acoustic feedback path, and if the loop gain is large enough instability will occur.

To see what effect the acoustic reflections from the end of the duct have on the performance of the ASC, a number of tests were conducted for single frequency sinusoids in which the input signal to the ASC was not obtained from the incident sound sensing microphone but instead from the signal generator. In this case no acoustic feedback can occur. With this arrangement, sinusoidal signals could be cancelled down to about 50Hz.

For both the duct and the simulation circuit the upper frequency limit for which cancellation can be obtained is approximately the same. This suggests that the limitation is due to the internal workings of the ASC Control Unit, and not acoustic considerations.

From Fig 5.5 and Fig 5.6 it can be seen that the shape of the compensating filter impulse response is irregular. For a sinusoidal signal the impulse response of the compensating filter would be expected to also be sinusoidal, and for a random signal it would be expected to have a similar shape to that of the transversal filter $\underline{W}$. In the case of a sinusoidal input it was noted that the error signal from the compensating filter update algorithm converged to zero, and for a random input the error signal was reduced only slightly as the weight vector $\underline{CF}$ adapted. Although the impulse response of $\underline{CF}$ has an irregular shape for a sinusoidal input, it is still possible for the algorithm to converge as long as the transfer function of $\underline{CF}$ has the correct phase and gain at the input frequency. There are many possible impulse responses that would meet this requirement for a given input frequency. For a random signal the impulse response of $\underline{CF}$ must be more precise. Not only must the combination $\hat{D}_2$, $\underline{CF}$ provide the correct delay, but $\underline{CF}$ must also have the correct frequency characteristic (i.e. phase and

gain) over the bandwidth of the input signal. It would seem that for random signals that the correct frequency characteristic cannot be obtained, resulting in a mismatch which we have seen can result in instability. The effect of this mismatch would become more pronounced at higher frequencies.

More work needs to be undertaken to see how the impulse response of the compensating filter behaves during adaptation. To do this a diagnostic channel needs to be installed on TMS2 so that the weights of the compensating filter can be observed at each iteration.

For random signals the best results were obtained with the estimated delay $\hat{d}_1=0$, and the estimated delay $\hat{d}_2=12$. The transversal filter $\underline{W}$ has 32 taps, and the acoustic delay between the incident sound sensing microphone and loudspeaker is equivalent to 32.8 smapling periods. It seems that the taps of the transversal filter $\underline{W}$ are adapting to a solution such that $\underline{W}$ acounts for the acoustic delay in the duct. In the case of the compensating filter $\underline{CF}$, the estimated delay $\hat{d}_2$ is close to the acoustic delay between the loudspeaker and error sensing microphone (5.8 sampling periods) added to one half the length of the filter $\underline{CF}$ (8 sampling periods). More theoretical work needs to be undertaken to understand the performance of the transversal filters $\underline{W}$ and $\underline{CF}$. In particular this work needs to concentrate on the delay that is inherent in the transversal filters after adaptation, and the effect of varying the parameters $\hat{d}_1$ and $\hat{d}_2$. This will be important when considering the physical dimensions (i.e. spacing of loudspeakers and microphones) of practical systems, and the length of the transversal filter $\underline{W}$ and the compensating filter $\underline{CF}$.

6. FREQUENCY DOMAIN ADAPTIVE SOUND CANCELLERS

6.1 INTRODUCTION

In chapters 4 and 5 we considered the theory of operation, and the implementation of an Adaptive Sound Canceller based on the time domain LMS algorithm. In this chapter we will be considering the implementation of an Adaptive Sound Canceller in the frequency domain, and in particular an ASC based on the frequency domain LMS algorithm.

As an introduction to frequency domain adaptive algorithms, in Section 6.2 we consider frequency domain LMS algorithms based on block transforms such as the Fast Fourier Transform.

In most cases, frequency domain LMS algorithms converge at a faster rate than the basic time domain LMS algorithm. The frequency domain is a special case of a general transform domain. In Section 6.3 we investigate transform domain LMS algorithms and compare their convergence properties with the time domain LMS algorithm.

In Section 6.4 we consider Frequency Sampling Filters. A Frequency Sampling Filter is an arrangement to implement a running frequency transform. Running transforms differ from block transforms in that they produce an output at every sampling period, rather than after every N samples.

Finally, in Section 6.5 we consider the implementation of a practical Adaptive Sound Canceller in the frequency domain. Most of this section is occupied with the analysis of an ASC based on the frequency domain LMS algorithm, but a brief look is also taken at some alternative frequency domain algorithms.

This chapter has been included in the thesis to serve as

an introduction to frequency domain Adaptive Sound Cancellers, and is not intended to be a complete treatment of the subject. We have seen in Chapter 4 that the time domain LMS Adaptive Sound Canceller suffers from a stability limit imposed by the mismatch transfer function. It may be possible that a frequency domain ASC can overcome this constraint. However, there is still much work that needs to be undertaken in regard to the theoretical and practical aspects of a frequency domain ASC. Chapter 6 is a first step in this direction, and a pointer to further work that needs to be done.

6.2 FREQUENCY DOMAIN LMS ALGORITHMS

6.2.1 INTRODUCTION:-

There have been two different approaches to adaptive filtering using LMS algorithms in the frequency domain. One approach has been to use the frequency domain via Fast Fourier Transforms (FFT's) to reduce the computational requirement for the time domain LMS algorithm(63,64). The other approach (65,68) has been to use the frequency domain to increase the convergence rate of the LMS algorithm. In this case, special frequency domain algorithms have been proposed. This is opposed to the first case in which frequency domain arithmetic is used to realize time domain algorithms. In some cases (67), both of the objectives computational efficiency and faster convergence have been achieved.

In Section 6.2 we will be looking at some of the frequency domain algorithms that have been proposed. This will not involve a detailed analysis of the algorithms, but will be a brief review and comparison of their properties. In Appendix 3

we derive a basic form of the frequency domain LMS algorithm from first principles.

In Section 6.2.2 we consider frequency domain algorithms that result in a reduction in computation compared to the basic time domain LMS algorithm, and in Section 6.2.3 we consider frequency domain LMS algorithms that have improved convergence rates. In Section 6.2.4 we compare the various frequency domain LMS algorithms that have been proposed.

6.2.2 REDUCTION OF COMPUTATION USING THE FREQUENCY DOMAIN:-

In (63,64, and 67), the underlying incentive for using a frequency domain LMS algorithm is to reduce the amount of computation that is required.

In (63), Dentino et al have proposed that the input data should be processed in blocks of length N using N-point Fast Fourier transforms (FFT's). The resulting N-point frequency domain input vector $\underline{Z}_n$ is "multiplied" by an N-component complex frequency domain weight vector $\underline{W}_n$, and the output is found by inverse transforming this product. A block diagram of the scheme proposed by Dentino et al is shown in Fig 6.1.

In the adaptive filter shown in Fig 6.1 the effect of multiplying the individual elements of the input vector $\underline{Z}_n$ by their corresponding weights, and taking the inverse transform is the same as performing a circular convolution of the input vector with the impulse response of the weight vector(64). As we are working in the frequency domain, the LMS algorithm can be split up into N separate scalar equations. Dentino et al (63) have used the complex LMS algorithm(62) to update the k^{th} component of the weight vector. Thus the algorithm proposed by Dentino et al is as follows:-

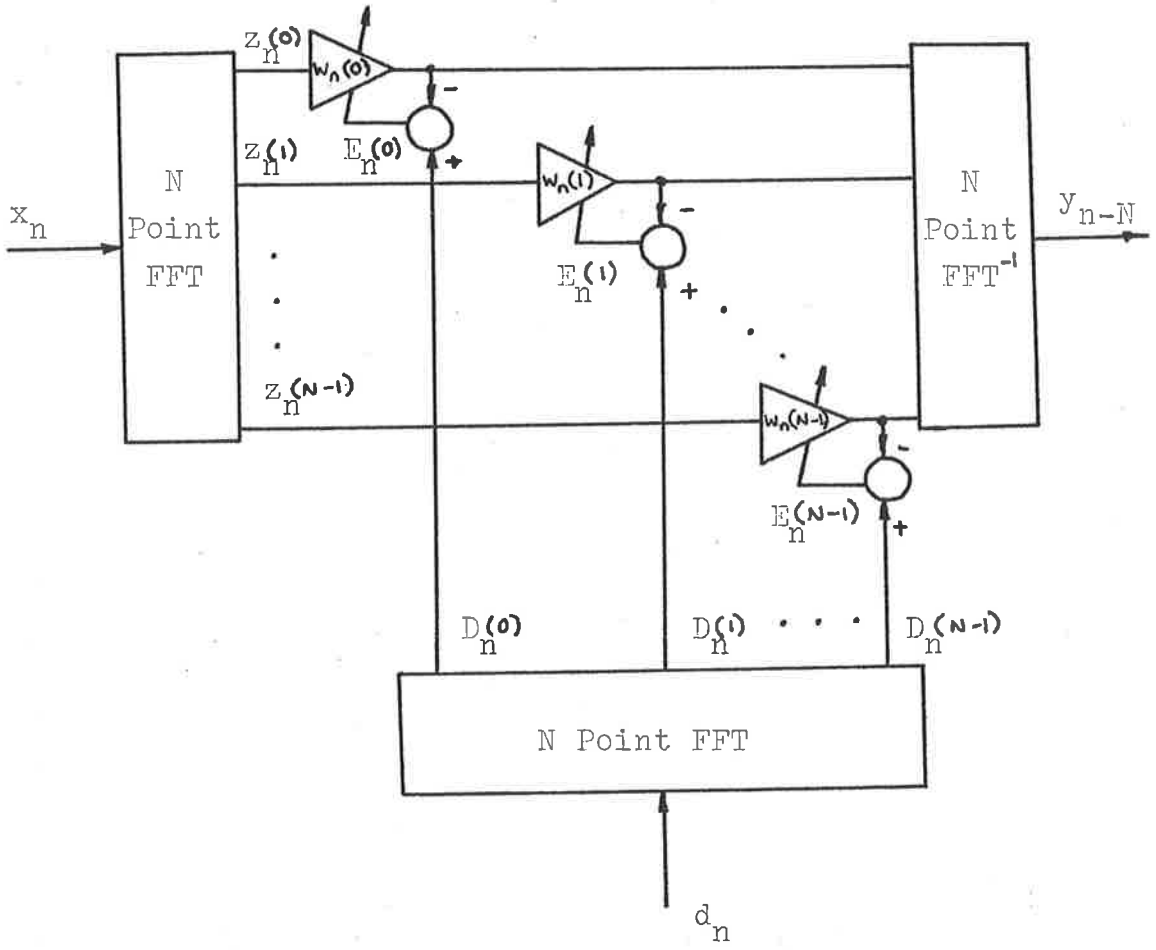

FIG 6.1: Frequency Domain LMS Adaptive Filter of Dentino et al*

* Taken from Ref (63)

$$w_{n+1}(k) = w_n(k) + 2\mu E_n(k) z_n^*(k)$$
$$k = 0, \ldots, N-1 \qquad (6.1)$$

Dentino et al(63) have found that their algorithm promises a significant reduction in computation over the conventional time domain LMS algorithm when the number of weights used exceeds sixteen.

Ferrara(64), and Mansour and Gray(67) have both started with the time domain LMS algorithm and rearranged it so that it can be realized in the frequency domain. The frequency domain algorithm of Dentino et al(63) involves circular convolution of the filter input with the tap weight impulse response, whereas the conventional time domain LMS adaptive filter involves linear convolution(64). This prevents the filter of (63) from converging to the optimal Wiener solution that is attained by the conventional time domain filter(64). Both of the algorithms proposed in (64) and (67) involve linear convolution, and hence the filter coefficients can converge to the Wiener solution(64).

The Fast LMS (FLMS) algorithm (64) uses the FFT to transform the time domain signals, and uses the "overlap save" method to realize the linear convolutions. For the overlap save method, the weight vector must be padded with N zeroes, and 2N-point FFT's must be used(64). The FLMS algorithm requires the calculation of five 2N-point FFT's, two of which are required to impose a time domain constraint in which the last N points of the time domain augmented impulse response are made to be zero(67). For the number of tap weights $N \geq 64$, the FLMS algorithm yields computational savings over the conventional time domain LMS algorithm. However, it will converge at the same rate as the time domain algorithm.

The Unconstrained Frequency domain LMS (UFLMS) algorithm (67) is similar to the FLMS algorithm. However, the time domain constraints on the impulse response have been removed. The UFLMS algorithm requires the calculation of only three 2N-point FFT's, but also requires the time windowing of the error sequence(67). The UFLMS algorithm yields computational savings when the number of tap weights exceeds thirty two.

Both the FLMS and the UFLMS algorithms have weight vector update equations of the form:-

$$\underline{W}_{n+1} = \underline{W}_n + 2\mu\underline{E}_n\underline{Z}_n^* \qquad (6.2)$$

where $\underline{W}_n$, $\underline{Z}_n$ and $\underline{E}_n$ are complex frequency domain vectors of length 2N.

In the UFLMS algorithm, the convergence constant μ is also a vector of length 2N, that is, a separate convergence constant is used for each channel. Mansour and Gray(67) have also investigated the use of an adaptive convergence constant μ_n. This is similar to normalizing the LMS algorithm in each consecutive frequency bin.

The UFLMS algorithm requires less computation than the FLMS algorithm, and it also converges at a faster rate. This is due to the fact that the UFLMS algorithm employs a different convergence factor for each frequency channel, and also because the UFLMS algorithm has been normalized.

For a more comprehensive analysis and comparison of the algorithms considered in this section the reader is referred to a recent study by Clark et al(76).

6.2.3 FASTER CONVERGENCE USING FREQUENCY DOMAIN ALGORITHMS:-

Although the UFLMS algorithm of (67) has resulted in faster

convergence, it has not set out specifically to do so. In (65) Narayan and Peterson aim to directly increase the convergence rate of the LMS algorithm by implementing a frequency domain version of it. The scheme proposed by Narayan and Peterson is shown in Fig 6.2. In this scheme Narayan and Peterson use a form of running transform that produces an output for every sampling interval. They do this by calculating a Discrete Fourier Transform (DFT) at every sampling instant.

We have seen in Section 3.5.3 that the convergence rate of the time domain LMS algorithm is dependent of the condition number ($\lambda_{max}/\lambda_{min}$) of the data correlation matrix $\underline{\underline{R}}$ where $\underline{\underline{R}} = E(\underline{X}_n \underline{X}_n^T)$. This eigenvalue spread can be shown to be bound by the relation(65):-

$$1 \leqslant \frac{\lambda_{max}}{\lambda_{min}} \leqslant \frac{\max\limits_{0 \leqslant \omega \leqslant 2} |X(e^{j\omega})|^2}{\min\limits_{0 \leqslant \omega < 2} |X(e^{j\omega})|^2} \qquad (6.3)$$

where $X(e^{j\omega})$ is the Z-transform of the x_n evaluated at $z = e^{j\omega}$.

Narayan and Peterson (65) suggest that an approach to accelerate the convergence rate of the LMS algorithm would be to reduce the spectral dynamic range of the input signal. It can be seen from (6.3) that this would have the effect of decreasing the eigenvalue spread, or the condition number of the data correlation matrix. The weight vector update equation proposed by Narayan and Peterson is as follows(65):-

$$\underline{W}_{n+1} = \underline{W}_n + 2\mu \underline{\underline{V}}^{-2} e_n \underline{Z}_n^* \qquad (6.4)$$

where $\underline{\underline{V}}^2$ is an N×N diagonal matrix whose $(i,i)^{th}$ component is equal to the power estimate of the i^{th} DFT output $X_n(i)$.

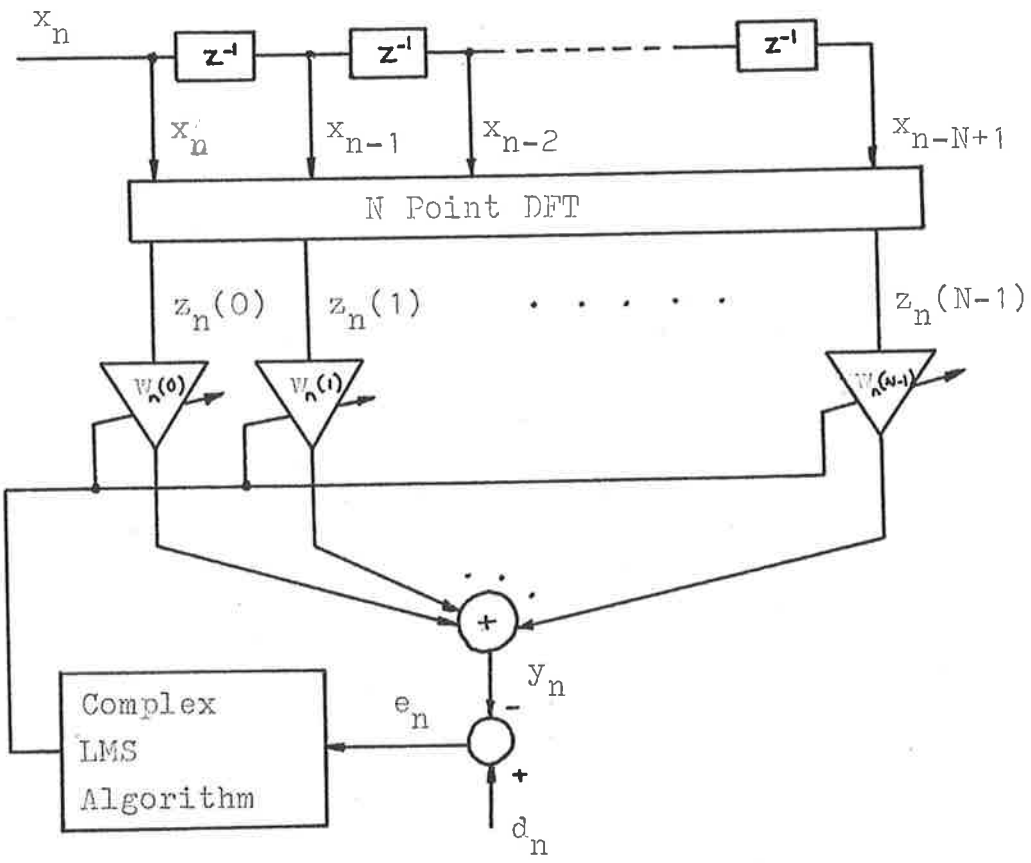

FIG 6.2: Adaptive Scheme of Narayan and Peterson

The use of $\mu\underline{\underline{V}}^{-2}$ in controlling the adaptive step size is functionally equivalent to normalizing the power in each of the DFT bins to unity before weighting(65). This has the same effect as that of prewhitening the input signal, compressing the eigenvalue spread and thus giving faster convergence(65). Really all we have in this case is a normalized form of the LMS algorithm but this time in the frequency domain.

In Section 6.3 we consider transform domain LMS algorithms. The frequency domain LMS algorithm is a special case of such algorithms. In this section we shall consider other possible reasons for the improved convergence rate of the algorithm given in equation (6.4).

In (65) Narayan and Peterson have proposed an algorithm to increase the convergence rate of the LMS algorithm by implementing a frequency domain version of it. Recently, Reddi(77) has proposed a modified version of the time domain LMS algorithm that will converge at the same rate as the algorithm proposed by Narayan and Peterson. The algorithm proposed by Reddi is as follows(77):-

$$\underline{W}_{n+1} = \underline{W}_n + 2\mu e_n \underline{\underline{R}}^{-1} \underline{X}_n \qquad (6.5)$$

$$\text{where } \underline{\underline{R}} = E(\underline{X}_n \underline{X}_n^T)$$

Taking the expectation of both sides of (6.5), and substituting for e_n as given in equation (3.12) and shown in Fig 3.7 we obtain:-

$$E(\underline{W}_{n+1}) = (\underline{\underline{I}} - 2\mu\underline{\underline{R}}^{-1}\underline{\underline{R}})E(\underline{W}_n) + 2\mu\underline{\underline{R}}^{-1}\underline{\alpha} \qquad (6.6)$$

$$\text{where } \underline{\alpha} = E(d_n \underline{X}_n)$$

From (6.6) we can see that the effective data correlation matrix for equation (6.5) is $\underline{\underline{R}}^{-1}\underline{\underline{R}} = \underline{\underline{I}}$. The identity matrix

ofcourse has equal eigenvalues, and thus from (6.3) we would expect a faster convergence rate. It has been shown by Reddi (77) that (6.5) is in fact the time domain equivalent of the frequency domain algorithm proposed by Narayan and Peterson. The effect of both of these algorithms was to prewhiten the input signal. It should be possible then to process the input signal x_n with a whitening filter before allowing it to pass through the transversal filter. This would result in an identity matrix for the data correlation matrix $\underline{\underline{R}}$, and would thus result in faster convergence.

6.2.4 COMPARISON OF FREQUENCY DOMAIN ALGORITHMS:-

Whether or not the frequency domain LMS algorithm requires less computation than its time domain counterpart, it would seem that the most important aspect of the frequency domain algorithms is their potential for increasing the convergence rate of the weight vector. It should be remembered however that it is possible to modify the time domain LMS algorithm so that it will converge at the same rate as the algorithm proposed by Narayan and Peterson(77).

Of the various frequency domain algorithms considered in sections 6.2.2 and 6.2.3 there were in general three types of algorithm proposed:-

$$\begin{aligned}
&\underline{W}_{n+1} = \underline{W}_n + 2\mu e_n \underline{Z}_n^* && \text{a}\\
&\underline{W}_{n+1} = \underline{W}_n + 2\,\underline{\underline{\mu}}_n \underline{E}_n \underline{Z}_n^* && \text{b}\\
&\underline{W}_{n+1} = \underline{W}_n + 2\mu \underline{\underline{V}}^{-2} e_n \underline{Z}_n^* && \text{c}
\end{aligned} \qquad (6.7)$$

The algorithm of (6.7b), (67, and 64 with all elements of μ_n equal to μ) would seem to be the most general as it treats

each frequency channel as being completely independent. It is similar to the algorithm given in (6.7c) in that both are normalized. However, in the latter the effective convergence constant does not change with time, and it uses the time domain error sequence in the update equation. The algorithms (6.7c) and (6.7a) both use the time domain error sequence in the update equation and thus the update equations in each channel are not entirely independent.

The reason for the faster convergence rates of the frequency domain LMS algorithms over that of the conventional time domain LMS algorithm is the reduction in eigenvalue spread of the data correlation matrix that can be obtained. This reduction in eigenvalue spread is the basic mechanism by which the convergence rate is increased.

6.3 TRANSFORM DOMAIN LMS ALGORITHMS

In (68) Narayan et al consider a general Transform Domain equivalent of the time domain adaptive LMS filter. There are a number of possible transforms that can be used, and the Frequency Transform (i.e. FFT and DFT) that we have considered in Section 6.2 was just one of these. As was the case with frequency domain algorithms , transform domain algorithms give the promise of improvements in the convergence rate over that of the conventional time domain LMS algorithm. However, different transform domain algorithms will converge at different rates(68).

We have seen previously that the convergence rate of the time domain LMS algorithm is dependent on the condition number of the data correlation matrix. The approach taken in (68) to accelerate the convergence rate is to transform the input

signal x_n into another domain such that the data correlation matrix of the transformed signal will have a smaller eigenvalue spread. This can be achieved by performing the adaptive filtering in some orthogonal transform domain. The scheme proposed in this case is the same as that shown in Fig 6.2 with the FFT replaced by a general N×N orthogonal transform.

The weight vector update equation proposed by Narayan et al is the same as that used in equation (6.4), but in this case we transform the input vector $\underline{X}_n$ to $\underline{Z}_n$ using some orthogonal transform $\underline{T}$ such that:-

$$\underline{Z}_n = \underline{\underline{T}}\underline{X}_n \qquad (6.8)$$

The new data correlation matrix thus becomes(68):-

$$\underline{\underline{R}}_z = E(\underline{Z}_n \underline{Z}_n^{*T}) = \underline{\underline{T}}\underline{\underline{R}}\underline{\underline{T}}^* \qquad (6.9)$$

$$\text{where} \quad \underline{\underline{R}} = E(\underline{X}_n \underline{X}_n^T)$$

The speed of convergence of the transform domain algorithm now depends upon the eigenvalue spread of $\underline{\underline{R}}_z$, which can be seen from (6.9) is a transformation of the data correlation matrix $\underline{\underline{R}}$. Narayan et al(68) have shown that for a properly chosen orthogonal transform some reduction in eigenvalue spread can be expected, and thus the convergence rate can be increased.

The reduction in eigenvalue spread that can be obtained depends upon the nature of the input signal, and also the transform that is used(68). Narayan et al have compared DFT's and Discrete Cosine Transforms (DCT's) when the input data was speech and found that the DCT's led to a smaller eigenvalue spread. The DCT has the advantage over the DFT in that its outputs are real and no complex arithmetic is involved.

The convergence rate of the LMS algorithm proposed by Narayan et al(68) is further increased by the use of the matrix $\underline{V}^{-2}$ in conjunction with the convergence constant μ. This has the effect of normalizing each channel in the transform domain , and thus results in faster convergence.

6.4 THE FREQUENCY SAMPLING FILTER

6.4.1 INTRODUCTION:-

So far we have considered frequency and transform domain algorithms that calculate the transformed signal from a block of N data. In this section we will consider an arrangement for implementing a running frequency transform known as a Frequency Sampling Filter (FSF). Running transforms differ from block transforms in that they produce an output at every sampling instant rather than after every N samples(74).

Frequency Sampling Filters were introduced in 1967 by Rader and Gold(78), and have since been studied by Bogner(72), and Bitmead and Anderson(47). In Section 6.4.2 we will consider the Frequency Sampling Filter proposed by Bogner(72). Bogner has proposed a modified form of the "conventional" Frequency Sampling Filter that has as its output the conventional FSF output and also a Hilbert Transformed version of it. It is this type of FSF that we shall incorporate in our Adaptive Sound Canceller in Section 6.5.

A block diagram of a general Frequency Sampling Filter is shown in Fig 6.3. The Frequency Sampling Filter can be thought of as being a bank of narrowband filters each centered on some frequency f_k. The output from each of these narrowband filters is multiplied by a complex gain w_k, and the outputs of the

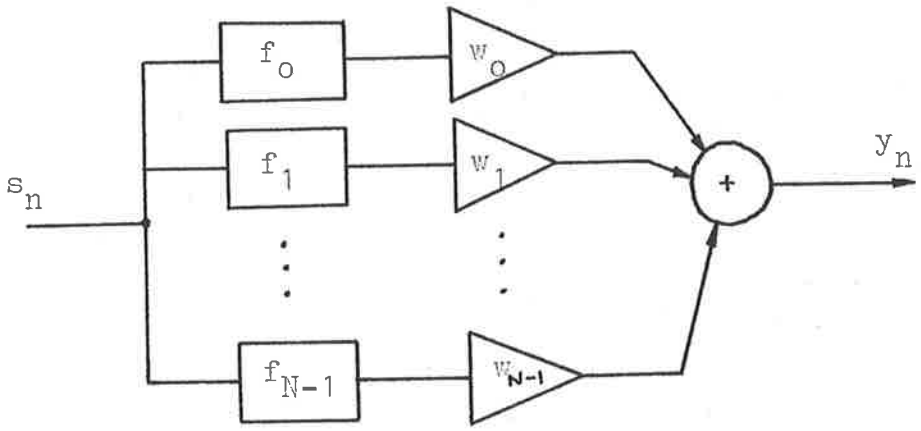

FIG 6.3: A General Frequency Sampling Filter

individual filters summed to produce the FSF output.

The outputs of the elemental filters are approximately independent(47) and so we can treat each frequency channel separately. This means that when we apply Frequency Sampling Filters to problems such as adaptive filtering we can break down possibly large dimensional problems that we have in the time domain into a number of smaller dimensional adaptations in each frequency channel.

6.4.2 IMPLEMENTATION OF FREQUENCY SAMPLING FILTERS:-

In (72) Bogner proposes a modified version of the conventional Frequency Sampling Filter(78). Bogner starts his analysis by considering a Frequency Sampling Filter that is built up from parallel banks of elemental filters whose frequency responses are sinc (or sampling) functions centered on some frequency f_k. The transfer function of these elemental filters is of the form(72):-

$$V_k(f) = \frac{A_k \mathrm{Sin}\left[\pi(f-f_k)/f_o\right] e^{-j2\pi f\tau}}{\pi(f-f_k)/f_o} + \frac{A_k \mathrm{Sin}\left[\pi(f+f_k)/f_o\right] e^{-j2\pi f\tau}}{\pi(f+f_k)/f_o}$$

where A_k = value of amplitude response at f_k

f_k = k^{th} sampling frequency kf_o

f_o = frequency interval between samples

τ = group delay

(6.10)

The elemental impulse responses of the filters $V_k(f)$ are delayed cosines that are truncated to be of length DT; where

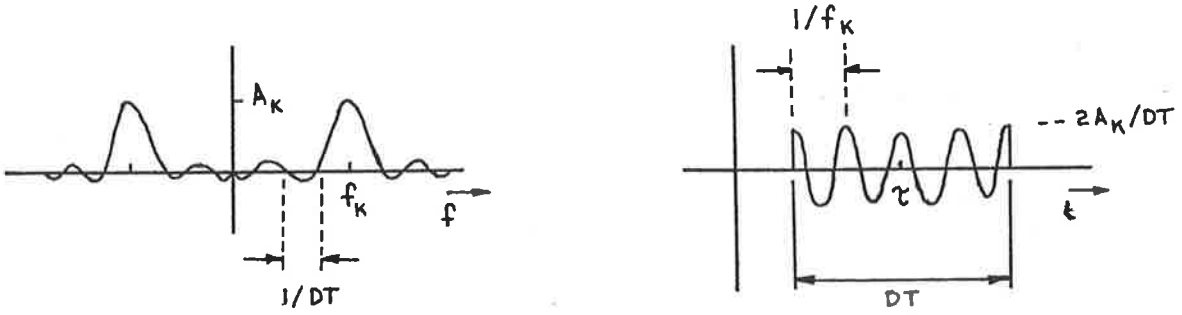

(a) Elemental Frequency Response

(b) Elemental Impulse Response

FIG 6.4: Elemental Responses of the FSF

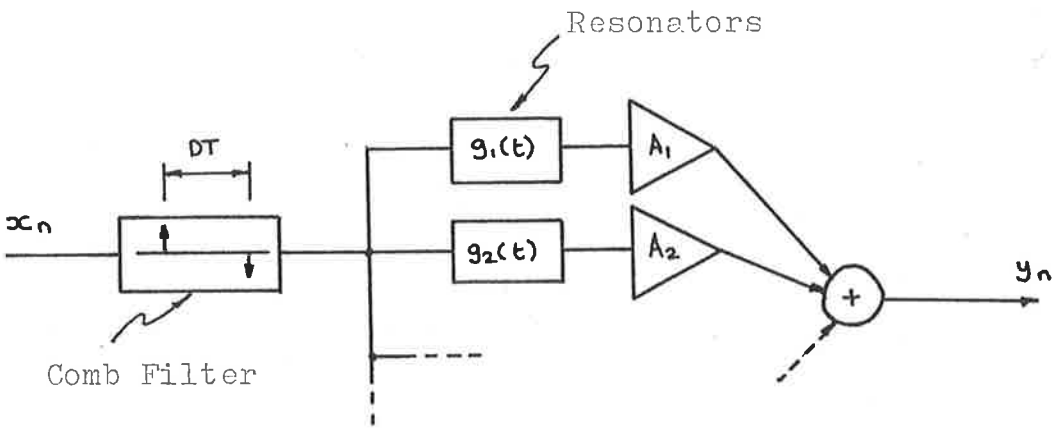

FIG 6.5: Bogners Implementation of FSF

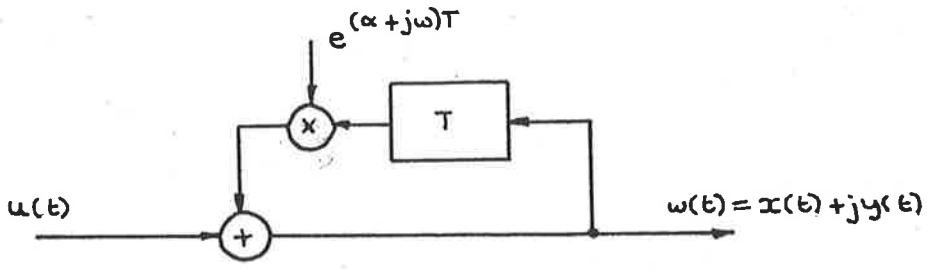

FIG 6.6: Complex Number Resonator

D = delay in samples, and T = sampling period. The elemental transfer function $V_k(f)$, and the elemental impulse response are shown in Fig 6.4a and 6.4b respectively.

Bogner (72) suggests that the elemental filters can be constructed from a comb filter of length DT, followed by a second order resonator whose impulse response is a cosine wave of frequency an integral multiple of 1/DT. The filter as a whole need only use one of these comb filters. A block diagram of this scheme is shown in Fig 6.5.

Bogner (72) then takes the idea of the basic Frequency Sampling Filter further by using a complex number resonator in place of the second order resonator $g_k(t)$. If this is the case then the output at each sampling interval is a complex number whose real part corresponds to the output of a conventional FSF, and whose imaginary part is an approximation to the Hilbert Transform of the real part. The complex number resonator proposed by Bogner is shown in Fig 6.6. The modified Frequency Sampling Filter proposed by Bogner is similar to the "transformed implementation" proposed by Bitmead and Anderson in (47).

6.5 A PRACTICAL FREQUENCY DOMAIN ADAPTIVE SOUND CANCELLER

6.5.1 INTRODUCTION:-

In the preceeding sections we have considered the implementation of Adaptive LMS filters in the frequency and other transform domains. We now wish to consider the implementation of an Adaptive Sound Canceller based on a frequency domain algorithm to estimate the parameters of the anti-phase path.

When constructing the Adaptive Sound Canceller we shall use

Frequency Sampling Filters to transform the time domain signals into the frequency domain. The FSF's have the advantage over the FFT in that they provide a continuous output, and also have a better transient response(47). Bogner (72) has proposed an implementation of the FSF using complex number resonators that should be reasonably easy to implement on processors such as the TMS32010. A block diagram of a general frequency domain Adaptive Sound Canceller is shown in Fig 6.7.

In Section 6.5.2 we shall consider the implementation of an LMS Adaptive Sound Canceller in the frequency domain. As with the time domain LMS Adaptive Sound Canceller we shall consider the stability of the LMS update equation as a function of the convergence constant μ, the delay d_2, and the mismatch. We will see in this section that the frequency domain LMS Adaptive Sound Canceller can be split up into a number of independent LMS algorithms; that is, one for each frequency channel. Each of these channels is very similar to a two tap time domain LMS Adaptive Sound Canceller, but with a narrowband input signal. It is not surprising then that the frequency domain implementation of the LMS Adaptive Sound Canceller suffers from the same limitations as its time domain counterpart in regards to mismatch, but in this case the limits on μ and mismatch apply to each frequency channel independently.

In Section 6.5.3 we consider the implementation of a frequency domain Adaptive Sound Canceller using an adaptive algorithm other than the LMS adaptive algorithm. It may be possible that other algorithms do not suffer from the limitations due to mismatch that are inherent in the LMS algorithm.

We shall briefly consider the application of two possible algorithms to the Adaptive Sound Canceller; The Simplex

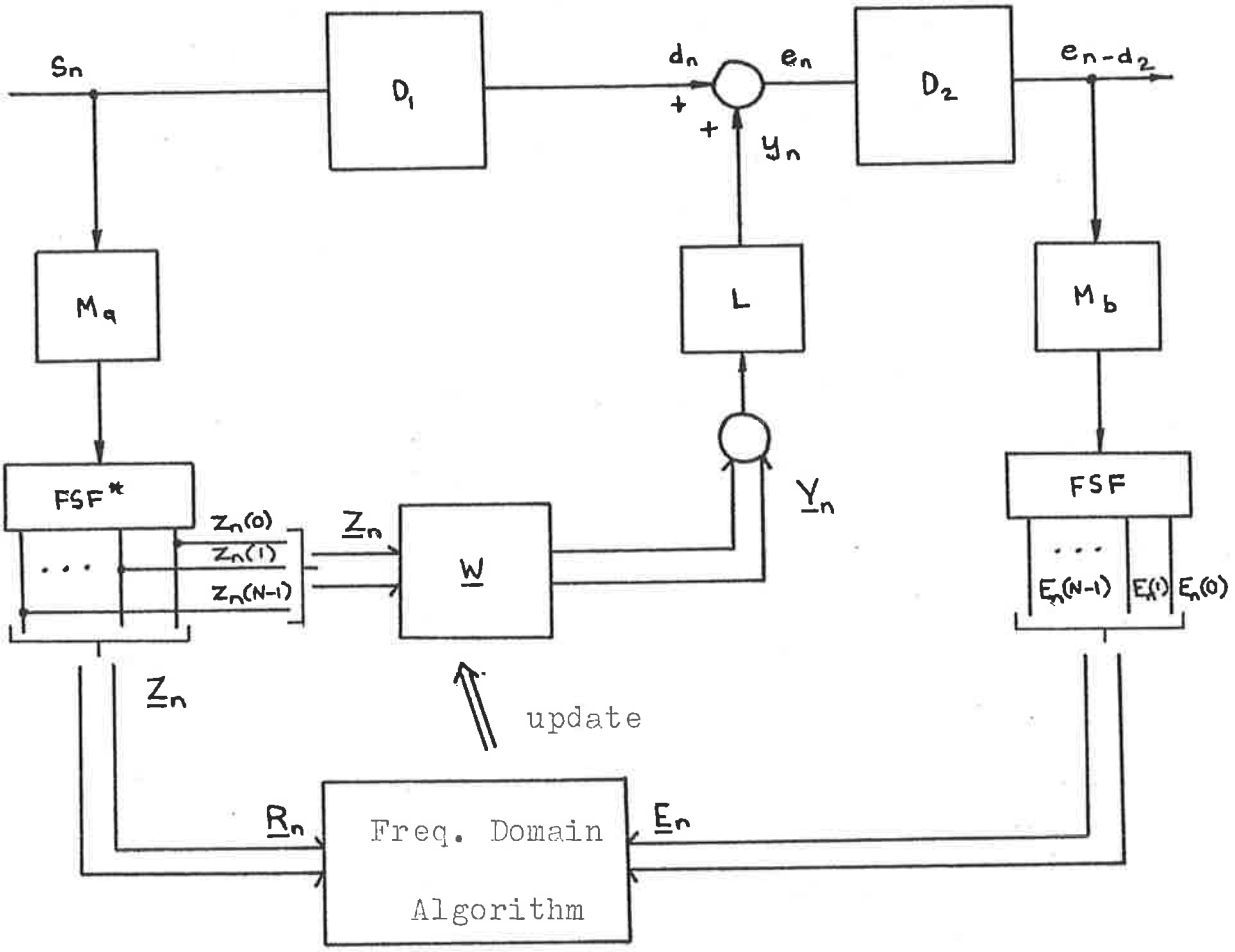

FIG 6.7: General Frequency Domain ASC

algorithm(46) suggested by Shepherd and La Fontain, and some form of Hill Climbing algorithm suggested by Bogner(45).

6.5.2 A PRACTICAL FREQUENCY DOMAIN LMS ADAPTIVE SOUND CANCELLER:-

A block diagram of a frequency domain LMS Adaptive Sound Canceller is shown in Fig 6.8. We shall use Frequency Sampling Filters to transform the signals x_n and e_{n-d_2} into their frequency domain counterparts $\underline{Z}_n$ and $\underline{E}_n$. To transform the input signal x_n we shall use the FSF's proposed by Bogner(72). Each of these filters outputs a frequency smaple, and the estimate of the Hilbert Transform of the frequency sample. To transform the error signal e_{n-d_2} we shall use a conventional Frequency Sampling Filter.

In our analysis of the frequency domain LMS Adaptive Sound Canceller shown in Fig 6.8 we will consider only the k^{th} frequency channel as the weight vector update equations for the different channels are independent. A block diagram of the k^{th} frequency channel is shown in Fig 6.9.

With reference to Fig 6.9, the weight vector update equation for the k^{th} frequency channel is:-

$$\left.\begin{aligned} \underline{W}_{n+1}(k) &= \underline{W}_n(k) - 2\mu(k)\, E_n(k)\, \underline{R}_n(k) \\ \text{where } \underline{W}_n(k) &= \left[w_1(k),\ w_2(k) \right]_n^T \\ \underline{R}_n(k) &= \left[r_{n,1}(k),\ r_{n,2}(k) \right]^T \\ k &= 1, \ldots, N \end{aligned}\right\} \quad (6.11)$$

From Fig 6.9, we can see that $E_n(k)$ and $\underline{R}_n(k)$ are given by:-

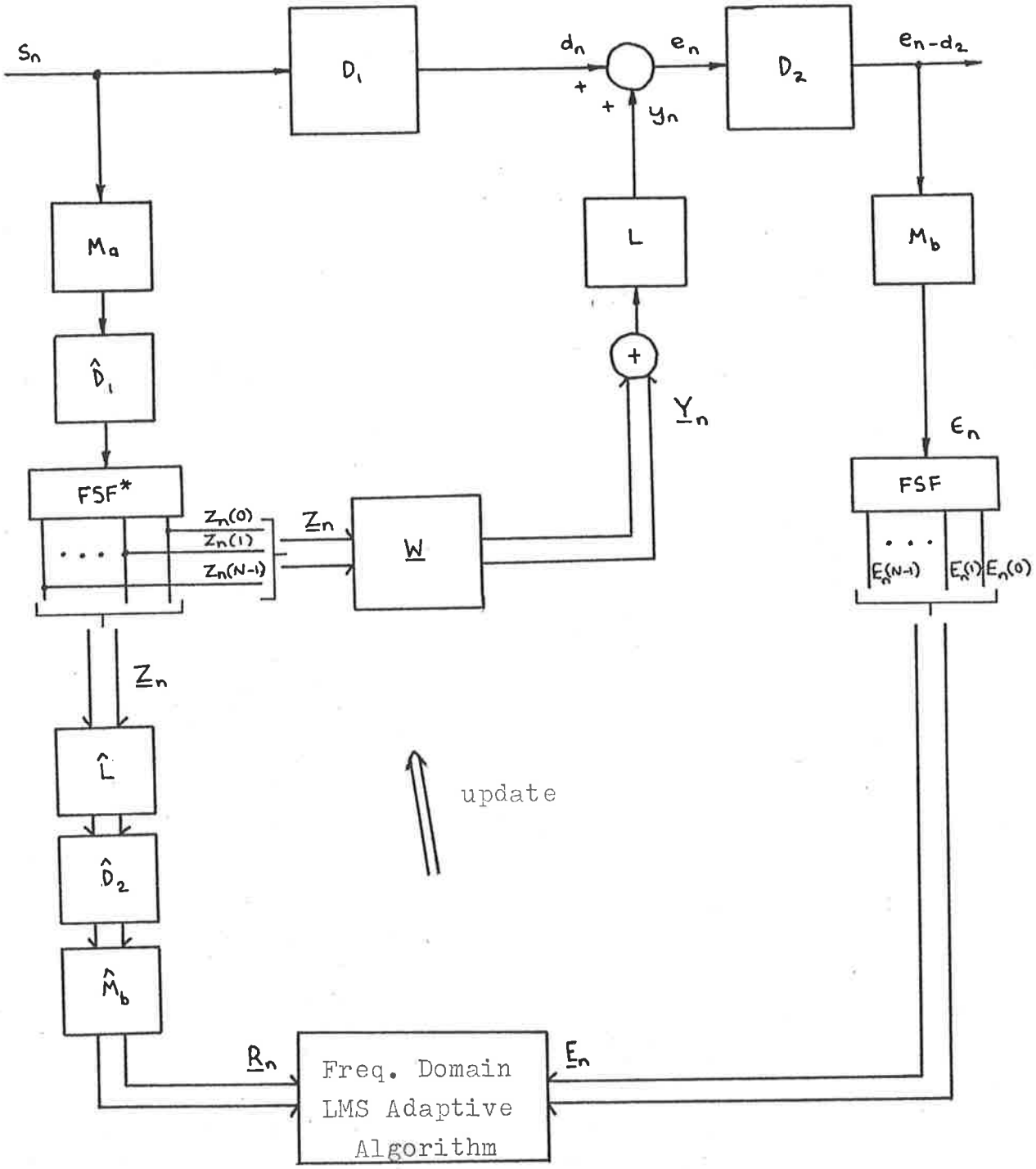

FIG 6.8: Frequency Domain LMS ASC

$$E_n(k) = \left[D_{n-d_2}(k) + Y_{n-d_2}(k) * l\right] * m_b$$

$$= \left[D_{n-d_2}(k) + \underline{Z}^T_{n-d_2}(k)\,\underline{W}_{n-d_2}(k) * l\right] * m_b$$

$$= D_{n-d_2}(k) * m_b + \underline{Z}^T_{n-d_2}(k)\,\underline{W}_{n-d_2}(k) * l * m_b$$

$$\underline{R}_n(k) = \underline{Z}_{n-d_2}(k) * \hat{l} * \hat{m}_b \qquad (6.12)$$

where $l, m_b, d_2, \hat{l}, \hat{m}_b$, and $\hat{d}_2$ are as defined in chapter 4

Substituting for $E_n(k)$ and $\underline{R}_n(k)$ into (6.11) we obtain:-

$$\underline{W}_{n+1}(k) = \underline{W}_n(k) - 2\mu(k)\left[\underline{\underline{A}}_n(k)\,\underline{W}_{n-d_2}(k) + \underline{c}_n(k)\right]$$

where $\underline{\underline{A}}_n(k) = \left[(\underline{Z}_{n-d_2}(k) * l * m_b)(\underline{Z}^T_{n-\hat{d}_2}(k) * \hat{l} * \hat{m}_b)\right]$

$\underline{c}_n(k) = \left[(D_{n-d_2}(k) * m_b)(\underline{Z}_{n-\hat{d}_2}(k) * \hat{l} * \hat{m}_b)\right]$ (6.13)

In (6.11) and (6.13) we have assumed that a NGLMS algorithm has been used. To consider the stability of this algorithm we shall consider the eigenvalues of the cross-correlation matrix $\underline{\underline{A}}(k)$ defined as follows:-

$$\underline{\underline{A}}(k) = E(\underline{\underline{A}}_n(k)) = E\left[(\underline{Z}_{n-d_2}(k) * l * m_b)(\underline{Z}^T_{n-\hat{d}_2}(k) * \hat{l} * \hat{m}_b)\right] \qquad (6.14)$$

It can be seen that equation (6.14) is very similar to equation (4.35) except that now $\underline{X}_n$ has been replaced by $\underline{Z}_n$. In equation (4.35) the vector $\underline{X}_n$ has N elements, and the data correlation matrix is of size N×N. In equation (6.14) the vector $\underline{Z}_n(k)$ has two components , and the data correlation matrix for the k^{th} channel $\underline{\underline{A}}(k)$ is of size 2×2.

We can follow a similar analysis to that in Section 4.2 to determine the stability of the update equation given in

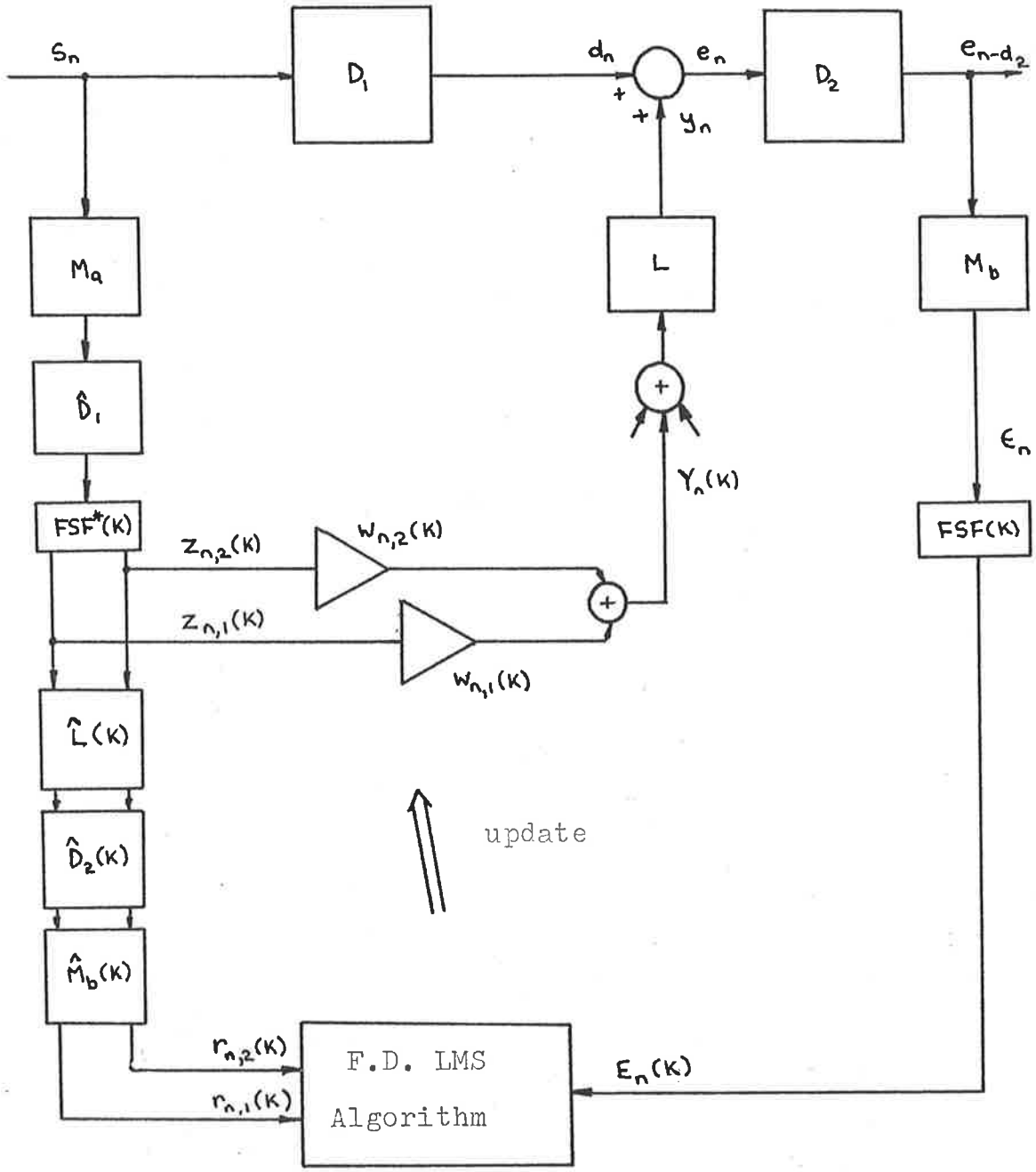

FIG 6.9: K^{th} Channel of Freq. Domain LMS ASC

(6.11). The signals $z_{n,1}(k)$ and $z_{n,2}(k)$ are time varying narrowband signals. Thus it can be seen that each frequency channel is equivalent to a time domain LMS Adaptive Sound Canceller with only two taps, and a narrowband input signal. It follows from this that the stability limit for the k^{th} channel of the frequency domain LMS Adaptive Sound Canceller is the same as that expressed in equation (4.52a) except that in this case the input signal vector $\underline{X}_n$ is now $\underline{Z}_n(k)$, the convergence constant μ is now $\mu(k)$, and we need only consider the mismatch over the bandwidth of the k^{th} channel.

For the frequency domain LMS Adaptive Sound Canceller as a whole to be stable, the stability limit as expressed in (4.52a) must be satisfied in each frequency channel. However, if the stability limit is not satisfied in one of the frequency channels this should not effect the performance of the other channels.

The frequency domain implementation of the LMS Adaptive Sound Canceller has a number of advantages over the time domain implementation, and a number of possible disadvantages:

(1) The frequency domain LMS Adaptive Sound Canceller will be more complicated to implement than its time domain counterpart, especially if broadband operation is required. The bandwidth over which sound attenuation is required, and the spacing of the frequency channels will determine the number of elemental FSF's that need to be employed, and thus the complexity of the system. More work needs to be undertaken to determine the spacing of the frequency channels that is required for good cancellation. This work will also need to consider the possibility of interference between adjacent channels.

(2) The frequency domain LMS Adaptive Sound Canceller will converge at a faster rate than the time domain Adaptive Sound Canceller, and thus will have better tracking properties.

(3) As the frequency domain LMS Adaptive Sound Canceller is split up into a number of separate frequency channels, it will only become unstable in the channels for which the stability condition (i.e. convergence constant and mismatch) is not met. The time domain LMS Adaptive Sound Canceller on the other hand will become unstable due to mismatch if for any frequency of operation the mismatch is too large.

(4) The 'anti-phase path' of an Adaptive Sound Canceller is required to accommodate the acoustic propagation delay d_1 between the incident sound sensing microphone, and the cancelling loudspeaker. For a purely sinusoidal signal this amounts to providing the correct gain and phase shift at the frequency of the input sinusoid. However, for random signals the 'anti-phase path' must provide the delay d_1, as well as the correct phase and gain required to produce the anti-sound over the bandwidth of operation of the canceller.

The frequency domain LMS Adaptive Sound Canceller has only two taps $w_1(k)$ and $w_2(k)$ in each channel. These taps can only provide a phase shift of $\pm 180^{o}$. The comb filter which forms part of the Frequency Sampling Filter will provide a certain fixed delay depending on its length. Any extra delay that is required will have to be accounted for by a delay line at the input to the FSF. The length of this delay line may need to be adaptively updated to account for changes in the speed of

sound in the duct.

The 'anti-phase path' of the time domain LMS Adaptive Sound Canceller is formed from a transversal filter, or tapped delay line. The transversal filter is more easily able to provide the variable delay d_1 than the frequency domain LMS Adaptive Sound Canceller.

In this section, we have investigated the stability of the k^{th} frequency channel of a frequency domain LMS Adaptive Sound Canceller, and found that it is a similar problem to the stability of a time domain LMS Adaptive Sound Canceller. However, we have also seen that there is more work that needs to be undertaken to determine the performance of the overall frequency domain LMS Adaptive Sound Canceller.

6.5.3 FREQUENCY DOMAIN A.S.C. USING OTHER ALGORITHMS:-

We have seen in Section 6.5.2 that the frequency domain LMS Adaptive Sound Canceller suffers from some of the same problems as the time domain LMS Adaptive Sound Canceller. If some algorithm other than the LMS algorithm is used to update the weight vector then it may be possible to overcome problems such as mismatch that can result in instability for the LMS algorithm.

In this section we will briefly consider two algorithms that are possible candidates for replacing the LMS algorithm; The Simplex algorithm of Nelder and Mead(46), and a Hill Climbing algorithm proposed by Bogner(45).

The Simplex Algorithm:

The Simplex algorithm(46) is a method to minimize a function of N variables. In the case of an Adaptive Sound Canceller

the variables are the tap weights and the delay d_1, and the function to be minimized is the mean square error. The Simplex algorithm starts with a set of N variables, (i.e. tap weights and delay d_1) that have a certain function value (i.e. mean square error). From here, by reflection, contraction and expansion of the starting point (or simplex), the algorithm searches for a new point that has a lower function value. The algorithm proceeds in this manner until a minimum value is found.

The application of this algorithm to Adaptive Sound Cancellation was first suggested by Shepherd and La Fontain of the CSIRO Division of Energy Technology.In the system proposed by Shepherd and La Fontain a non-adaptive transversal filter is first tuned to provide optimum cancellation for no air flow in the duct. The Simplex algorithm is then used to adaptively update a phase and gain to account for changes in the speed of sound in the duct.

It may be possible to use the Simplex algorithm to update the tap weights and delay d_1 for a frequency domain Adaptive Sound Canceller. Such a system would not appear to suffer from problems associated with mismatch although there may be other problems peculiar to the Simplex algorithm.

A Hill Climbing Algorithm:

The scheme proposed by Bogner(45) involves the adjustment of a complex weight vector H(k) in each frequency channel. The algorithm searches along orthogonal directions $\mathrm{Re}|H(k)|$ and $\mathrm{Im}|H(k)|$ to minimize a measure of the error in each frequency channel $E_n(k)$. With reference to Fig 6.7, Bogner suggested that a suitable measure of the error to use would be $|E_n(k)|/|Z_n(k)|$.

The Hill Climbing algorithm proposed by Bogner will not be affected by mismatch. However, as yet the stability and convergence properties of the algorithm have not been investigated.

7. SUMMARY AND CONCLUSIONS

We have considered the active adaptive cancellation of low frequency sound propagating down a duct. The main body of work for this thesis consists of a theoretical analysis, and implementation of a practical Adaptive Sound Canceller based on the time domain LMS algorithm. This work is contained in chapters 4 and 5 of the thesis respectively.

The Adaptive Sound Canceller (ASC) that has been studied is shown in Fig 4.1, and is an extension of the simplified ASC proposed by Burgess in 1981 and shown in Fig 3.9. The Adaptive Sound Canceller proposed by Burgess was an extension of the Adaptive Noise Canceller of Widrow et al that has found wide application in signal processing and control. An Adaptive Noise Canceller that is very similar to the ASC of Fig 4.1 is shown in Fig 3.7. The Adaptive Noise Canceller is a signal processing application of the LMS algorithm and involves only electrical signals.

In the case of the Adaptive Sound Canceller, the LMS algorithm used to update the weight vector does not have direct access to the sound in the duct that is to be cancelled, but must sense this sound using electro-acoustic transducers. The cancelling signal cannot simply be subtracted from the sound in the duct, but must be added acoustically using a loudspeaker. Also, the duct has associated with it acoustic propagation delays. Due to the delay between the cancelling loudspeaker and the error sensing microphone the LMS algorithm has access to a delayed error signal only.

Because of the electro-acoustic transducers, and delays that are peculiar to the Adaptive Sound Canceller, an estimate of the cumulative transfer function LD_2M_b (Fig 4.1) is

included in the system. The input signal to the transversal filter $\underline{W}$ is passed through this estimated transfer function before being input to the LMS update algorithm. The estimated transfer function $\hat{L}\hat{D}_2\hat{M}_b$ can differ from the actual transfer function LD_2M_b either because of an incorrect initial estimate, or due to the fact that the actual transfer function may change during the course of operation of the ASC. The difference between the estimated, and actual transfer function is known as mismatch.

In Chapter 4 we have conducted a mathematical analysis of the ASC shown in Fig 4.1. This analysis aimed to determine the stability and convergence properties of the weight vector update equation for the ASC given in equation (4.1). The stability of this equation was found to be dependent on the convergence factor μ, the discrete delay d_2, and the mismatch transfer function M in the following way:-

$$0 < \mu < \frac{L_1 L_2}{(U_1 U_2)^2 + (NU_1 V_2/\pi)^2} \operatorname{Sin}\left[\frac{\pi}{2(2d_2+1)}\right]$$

and

$$|\angle M(f)| < 90^\circ \text{ for all frequencies at which the input signal spectrum is non-zero.}$$

where $M(f) = LD_2M_b - \hat{L}\hat{D}_2\hat{M}_b$

= Mismatch Transfer Function

L_1, U_1 as defined in (4.41)

L_2, U_2, V_2 as defined in (4.43)

(7.1)

It can be seen from (7.1) that the effect of the delay d_2

has been to reduce the stability limits on the convergence constant μ by a factor $\text{Sin}(\pi/2(2d_2+1))$. The mismatch imposes another stability limit which is independent of the convergence constant. If the phase of the mismatch transfer function is not within $\pm 90^{\circ}$ then there is a possibility that the algorithm will become unstable independent of the convergence constant.

In practical applications, a modified form of the update equation given in (4.1) is used. The mean square error gradient term $E(\epsilon_n \underline{r}_n)$ is replaced by its instantaneous estimate $\epsilon_n \underline{r}_n$, which is known as the Noisy Gradient form of the algorithm. This algorithm is given as equation (4.67). To determine the stability and convergence properties of equation (4.67), we can consider the stability of the mean weight vector. This analysis leads to a very similar stability condition to that given in equation (7.1).

From our analysis of the Adaptive Sound Canceller shown in Fig 4.1 it became evident that it would be necessary to keep the mismatch in phase between the transfer functions LD_2M_b and $\hat{L}\hat{D}_2\hat{M}_b$ as small as possible. In section 4.5.4 we considered two possible schemes for reducing the mismatch; One scheme involved estimating the transfer function LD_2M_b using an LMS algorithm, and the second scheme, proposed by Warnaka et al involved estimating the transfer function $(LM_b)^{-1}$ using an LMS algorithm, and conditioning the error signal with a compensating filter. The stability of the system proposed by Warnaka et al was considered in section 4.5.4. The stability condition is identical to that given in equation (7.1) except that the mismatch transfer function is defined in a silghtly different way.

In Chapter 5 we considered the implementation of a practi-

cal LMS Adaptive Sound Canceller that uses the time domain LMS algorithm to update the weights of a 32 tap transversal filter that is used to approximate the anti-phase path. The design included a compensating filter that was used to condition the error signal and reduce the effect of mismatch.

In tests conducted in a duct in Melbourne using the experimental rig of Shepherd and La Fontain, the band of attenuation that could be obtained 160-370Hz was somewhat less than that expected from theory. For tests conducted using a simulation circuit, improved low frequency performance could be obtained (i.e. cancellation down to 60Hz for random signals), but the upper frequency limit was about the same as for the duct.

The poor low frequency performance in the duct appears to be caused by reflections from the ends of the duct that cause coupling from the cancelling loudspeaker to the incident sound sensing microphone. The effect of reflections from the ends of the duct on the performance of the Adaptive Sound Canceller needs to be studied in more detail. In particular, the effect of the termination at the source end of the duct should be given more consideration. In the tests that were conducted this termination was a steel plate that reflected sound strongly. This would not be the case for a true practical application, but there is still likely to be some reflection.

The upper frequency limit on the performance of the Adaptive Sound Canceller seems to be due to the internal workings of the ASC Control Unit. For random signals the error from the compensating filter update algorithm does not converge properly, and so it would seem that there is still some mismatch present. This mismatch could account for the poor performance of the canceller for input signals with appreciable components above 370Hz. More work needs to be

undertaken here to study the behaviour of the compensating filter weights during the adaptation process. A diagnostic channel could be added to TMS2 to allow the impulse response of the compensating filter to be observed as the adaptation proceeds.

In Chapter 6 we have considered the implementation of an Adaptive Sound Canceller based on the frequency domain LMS algorithm. The ASC that we consider employes Frequency Sampling Filters to transform the broadband sound signals into a number of narrowband signals in the separate frequency channels. The overall weight vector update equation for the frequency domain ASC can be split up into separate two tap update equations in each frequency channel.

The analysis of the time domain ASC conducted in Chapter 4 can be applied to the update equations used for each frequency channel. It turns out that the same stability condition applies to each frequency channel as applied to the time domain ASC, except that in this case we have only two weights and we need only consider the mismatch over the narrow frequency band of the channel in question.

There is still much work that needs to be done in regard to the practical implementation of Adaptive Sound Cancellers using frequency domain algorithms. An important aspect of this work will be to investigate the relationship between the frequency channels. In our analysis so far we have assumed that they are independent. We may find in practice that there is interference between the channels that can affect the performance of the ASC. A related matter is the spacing between the frequency channels that is required to ensure that a good level of attenuation is achieved.

APPENDIX 1

A1: SOLUTION OF EQUATION (4.16)

We wish to find the solution for ϕ in the following equation:-

$$2\mu a = \cos(\phi d_2) - \cos(\phi(d_2 + 1)) \quad -a$$
$$2\mu b = \sin(\phi d_2) - \sin(\phi(d_2 + 1)) \quad -b \qquad \text{(A1.1)}$$
$$\text{where } \lambda = a + jb$$

Using: $\sin(u) - \sin(v) = 2\sin\frac{1}{2}(u-v)\cos\frac{1}{2}(u+v)$

$$\cos(v) - \cos(u) = 2\sin\tfrac{1}{2}(u+v)\sin\tfrac{1}{2}(u-v)$$

we can rewrite (A1.1) as follows:-

$$2\mu a = 2\sin\tfrac{1}{2}(\phi(2d_2 + 1))\sin\tfrac{1}{2}(\phi) \quad -a$$
$$2\mu b = -2\cos\tfrac{1}{2}(\phi(2d_2 + 1))\sin\tfrac{1}{2}(\phi) \quad -b \qquad \text{(A1.2)}$$

Now, dividing (A1.2a) by (A1.2b) we obtain:-

$$a/-b = \tan\tfrac{1}{2}\phi(2d_2 + 1) \qquad \text{(A1.3)}$$

Taking the arctan of (A1.3) and rearranging yields:-

$$\phi = (2/(2d_2 + 1))(\arctan(a/-b) \pm n\pi) \qquad \text{(A1.4)}$$

Based on Kabals analysis(59), we chose n=0 to yield the value of ϕ and λ for which all roots of equation (4.14) lie inside the unit circle. Thus we have:-

$$\phi = 2\gamma/(2d_2 + 1)$$
$$\text{where } \gamma = \arctan(a/-b) \qquad \text{(A1.6)}$$

Substituting into equation (A1.2) for ϕ we obtain:-

$$\mu a = \mathrm{Sin}\left[\tfrac{1}{2}(2d_2+1)(2\gamma/(2d_2+1))\right]\mathrm{Sin}\left[2\gamma/2(2d_2+1)\right]$$

$$\therefore \mu a = \mathrm{Sin}(\gamma/(2d_2+1))\mathrm{Sin}\gamma \qquad -a$$

$$\mu b = -\mathrm{Sin}\left[2\gamma/2(2d_2+1)\right]\mathrm{Cos}\left[\tfrac{1}{2}(2d_2+1)(2\gamma/2(2d_2+1)\right]$$

$$\therefore \mu b = -\mathrm{Sin}(\gamma/(2d_2+1))\mathrm{Cos}\gamma \qquad -b$$

(A1.6)

Squaring, adding and taking the square root of equations (A1.6a) and (A1.6b) we obtain:-

$$\mu\sqrt{a^2 + b^2} = \mathrm{Sin}(\gamma/(2d_2 + 1)) \qquad \text{(A1.7)}$$

Thus we obtain:-

$$\mu = (1/|\lambda|)\mathrm{Sin}(\gamma/(2d_2 + 1))$$

where $\lambda = a + jb$

$$\gamma = \arctan(a/-b) \qquad \text{(A1.8)}$$

APPENDIX 2

A2: ROOT LOCUS TECHNIQUES APPLIED TO STABILITY OF LMS ALGORITHM WITH DELAY IN THE ERROR PATH

In Section 4.2.2 we considered the effect of the delay d_2 on the performance of the Adaptive Sound Canceller. Following the analysis of Kabal(59) we obtained the following expression for the i^{th} element of the decoupled weight vector error:-

$$H_i(z) = \frac{z^{d_2+1} h_i(0)}{z^{d_2+1} - z^{d_2} + 2\mu\lambda_i} \qquad \text{(A2.1)}$$

The stability of equation (A2.1) can be determined by considering the roots of the equation:-

$$F(z) = z^{d_2+1} - z^{d_2} + \beta \qquad \text{(A2.2)}$$

where $\beta = 2\mu\lambda_i$

One method of finding the roots of (A2.2) that result in marginal stability was given in Section 4.2.2. Kabal(59) has also suggested that Root Locus techniques can be used to consider the stability of equation (A2.2). In this section we look at some specific examples to see how root locus techniques can be applied, and also consider the most general case.

Example 1:

In the first example we consider the special case when the delay d_2 is zero. Thus equation (A2.2) becomes:-

$$F(z)\big|_{d_2=0} = z - 1 + \beta \qquad \text{(A2.3)}$$

Now, for $\beta = 0$, F(z) has the root z=1, and in the general case the root is $z=1-\beta$. A plot showing the variation in root position with β is given in Fig A.1. From the root locus plot we observe the following:-

(1) For $\beta=0$ we are on the margin of stability as the root lies on the unit circle.

(2) For $0 < \beta < 1$, the weight vector error will follow a simple exponential decay, the time constant decreasing as β approaches 1.

(3) For $1 < \beta < 2$, the weight vector error will still converge exponentially, however it will also oscillate with the frequency $f_s/2$. As β approaches 2 the time constant will approach ∞.

(4) For $\beta > 2$ the weight vector diverges.

Example 2:

In this example we consider the case when $d_2=1$. Thus equation (A2.2) becomes:-

$$F(z)\Big|_{d_2=1} = z^2 - z + \beta \qquad \text{(A2.4)}$$

For $\beta=0$, F(z) has the roots z=0,1 , and in the general case the roots are given by:-

$$z = (1 \pm \sqrt{1 - 4\beta})/2 \qquad \text{(A2.5)}$$

The root locus plot for (A2.4) showing the variation of root position as β varies is given in Fig A.2. From the root locus plot we observe the following:-

(1) For $0 < \beta < \frac{1}{4}$ the weight vector error converges exponentially there being two time constants involved.

(2) For $\frac{1}{4} < \beta < 1$ the weight vector error still converges however it also oscillates. At $\beta=1$ the weight vector

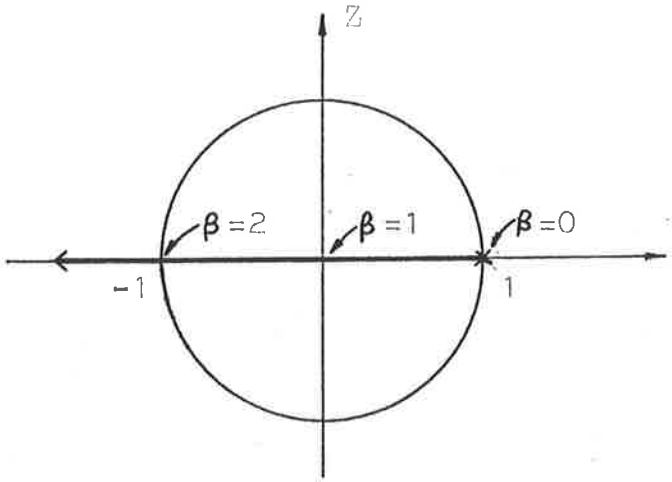

FIG A.1: Root Locus Plot For $d_2 = 0$

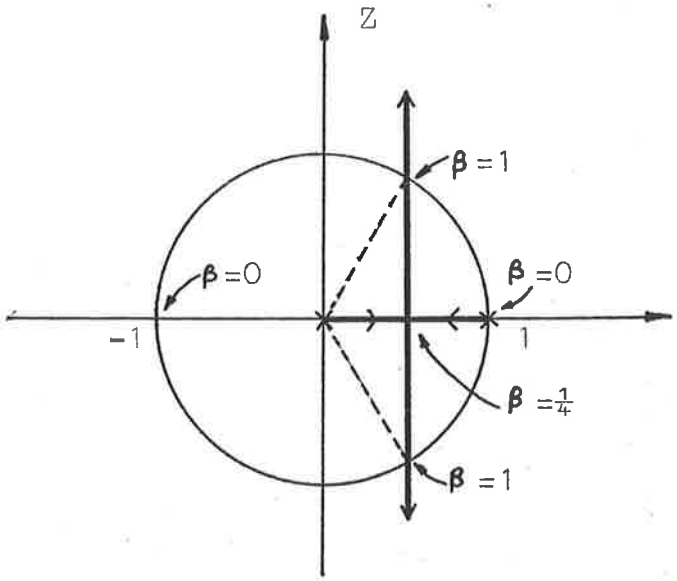

FIG A.2: Root Locus Plot For $d_2 = 1$

error is marginally stable, and oscillates at a frequency of $f_s/6$.

(3) For $\beta > 1$ the weight vector error diverges.

In the general case for any delay d_2, then if $\beta = 0$ $F(z)$ has d_2 roots at zero and one root at $z = 1$. As β increases one of the roots at $z=0$, and the root at $z=1$ move towards each other along the z-axis. These two roots meet and form a complex conjugate pair that cross the unit circle at $\phi = \pm\pi/(2d_2 + 1)$ (59). The other d_2-1 roots move out radially from the origin(59).

It can be seen that the root locus technique yields the same stability limits for β (or μ) as the analysis in Section 4.2.2. However, they give more insight into the nature of the convergence envelope of the weight vector error as μ is varied.

APPENDIX 3

A3: THE FREQUENCY DOMAIN LMS ALGORITHM

In this appendix we shall derive the basic frequency domain LMS algorithm for the Adaptive Noise Canceller shown in Fig A3.1. In this ANC we use the frequency transform FT to transform the time domain signals into N complex frequency domain signals. We shall assume that the frequency transform outputs a new set of frequency samples every sampling period.

The derivation that we shall follow is based on that of Widrow, McCool and Ball(62). With reference to Fig A3.1 we start by defining the following:-

$$\underline{W}_n = \left[w_n(0), w_n(1), \ \ldots \ , w_n(N-1)\right]^T$$

$$\underline{Z}_n = FT(x_n) = \left[z_n(0), z_n(1), \ \ldots \ , z_n(N-1)\right]^T$$

$$\underline{E}_n = FT(e_n) = \left[E_n(0), E_n(1), \ \ldots \ , E_n(N-1)\right]^T$$

$$\underline{Y}_n = FT(y_n) = \left[Y_n(0), Y_n(1), \ \ldots \ , Y_n(N-1)\right]^T$$

where $w_n(k)$, $E_n(k)$, $Z_n(k)$ and $Y_n(k)$ are complex.

$$w_n(k) = w_{nr}(k) + jw_{ni}(k)$$

$$z_n(k) = z_{nr}(k) + jz_{ni}(k)$$

$$E_n(k) = E_{nr}(k) + jE_{ni}(k)$$

$$Y_n(k) = Y_{nr}(k) + jY_{ni}(k)$$

(A3.1)

When the signals x_n and e_n are transformed into the frequency domain they result in the formation of N complex signals. We also have N complex weight vectors. As we now have N

channels, and each channel has its own complex weight, we can treat each channel separately. Keeping this in mind, the output vector $\underline{Y}_n$, and the error vector $\underline{E}_n$ are given by the following expressions:-

$$\underline{Y}_n = \begin{bmatrix} Y_n(0) \\ \vdots \\ Y_n(N-1) \end{bmatrix}$$

where $Y_n(k) = w_n(k)\, z_n(k)$

$k = 0, \ldots, N-1$

$$\underline{E}_n = \begin{bmatrix} E_n(0) \\ \vdots \\ E_n(N-1) \end{bmatrix}$$

where $E_n(k) = D_n(k) - w_n(k)\, z_n(k)$

$k = 0, \ldots, N-1$ (A3.2)

In the time domain Adaptive Noise Canceller we aimed to minimize the mean square error $E(e_n^2)$. In the frequency domain, as we have complex terms in the error vector, we aim to minimize $E(E_n(k)\, E_n^*(k))$. Thus, the LMS update equation for the Adaptive Noise Canceller shown in Fig A3.1 is:-

$$w_{n+1}(k) = w_n(k) - 2\mu E\left[\partial(E_n(k)\, E_n^*(k))/\partial w_n(k)\right]$$

where $E_n^*(k) = E_{nr}(k) - jE_{ni}(k)$

$k = 0, \ldots, N-1$ (A3.3)

Expanding the mean square error gradient term in equation (A3.3) we have:-

$$\frac{\partial(E_n(k)\,E_n^*(k))}{\partial w_n(k)} = \frac{\partial(E_n(k)\,E_n^*(k))}{\partial w_{nr}(k)} + j\frac{\partial(E_n(k)\,E_n^*(k))}{\partial w_{ni}(k)} \qquad \text{(A3.4)}$$

With reference to equations (A3.1) and (A3.2) we can expand the terms on the RHS of (A3.4) as follows(62):-

$$\frac{\partial(E_n(k)\,E_n^*(k))}{\partial w_{nr}(k)} = E_n(k)\frac{\partial E_n^*(k)}{\partial w_{nr}(k)} + E_n^*(k)\frac{\partial E_n(k)}{\partial w_{nr}(k)}$$

$$= E_n(k)\,(-z_n^*(k)) + E_n^*(k)\,(-z_n(k))$$

$$\frac{\partial(E_n(k)\,E_n^*(k))}{\partial w_{ni}(k)} = E_n(k)\frac{\partial E_n^*(k)}{\partial w_{ni}(k)} + E_n^*(k)\frac{\partial E_n(k)}{\partial w_{ni}(k)}$$

$$= E_n(k)\,(jz_n^*(k)) + E_n^*(k)\,(-jz_n(k))$$

$$\text{where } E_n^*(k) = D_n^*(k) - W_n^*(k)\,z_n^*(k) \qquad \text{(A3.5)}$$

Using (A3.5), and substituting (A3.4) into (A3.3) we obtain:-

$$w_{n+1}(k) = w_n(k) + 2\mu E(E_n(k)\,z_n^*(k))$$

$$k = 0, \ldots, N-1 \qquad \text{(A3.6)}$$

In practical applications a Noisy Gradient form of the algorithm given in (A3.6) can be used:

$$w_{n+1}(k) = w_n(k) + 2\mu E_n(k)\,z_n^*(k)$$

$$k = 0, \ldots, N-1 \qquad \text{(A3.7)}$$

We can write equation (A3.7) in vector form as follows:-

$$\underline{W}_{n+1} = \underline{W}_n + 2\mu \underline{\underline{I}}\,\underline{E}_n \underline{Z}_n^{*T} \qquad \text{(A3.8)}$$

We can extend equation (A3.8)to include a separate convergence constant for each frequency channel:

$$\underline{W}_{n+1} = \underline{W}_n + 2\underline{\underline{U}}\,\underline{E}_n \underline{Z}_n^{*T} \qquad \text{(A3.9)}$$

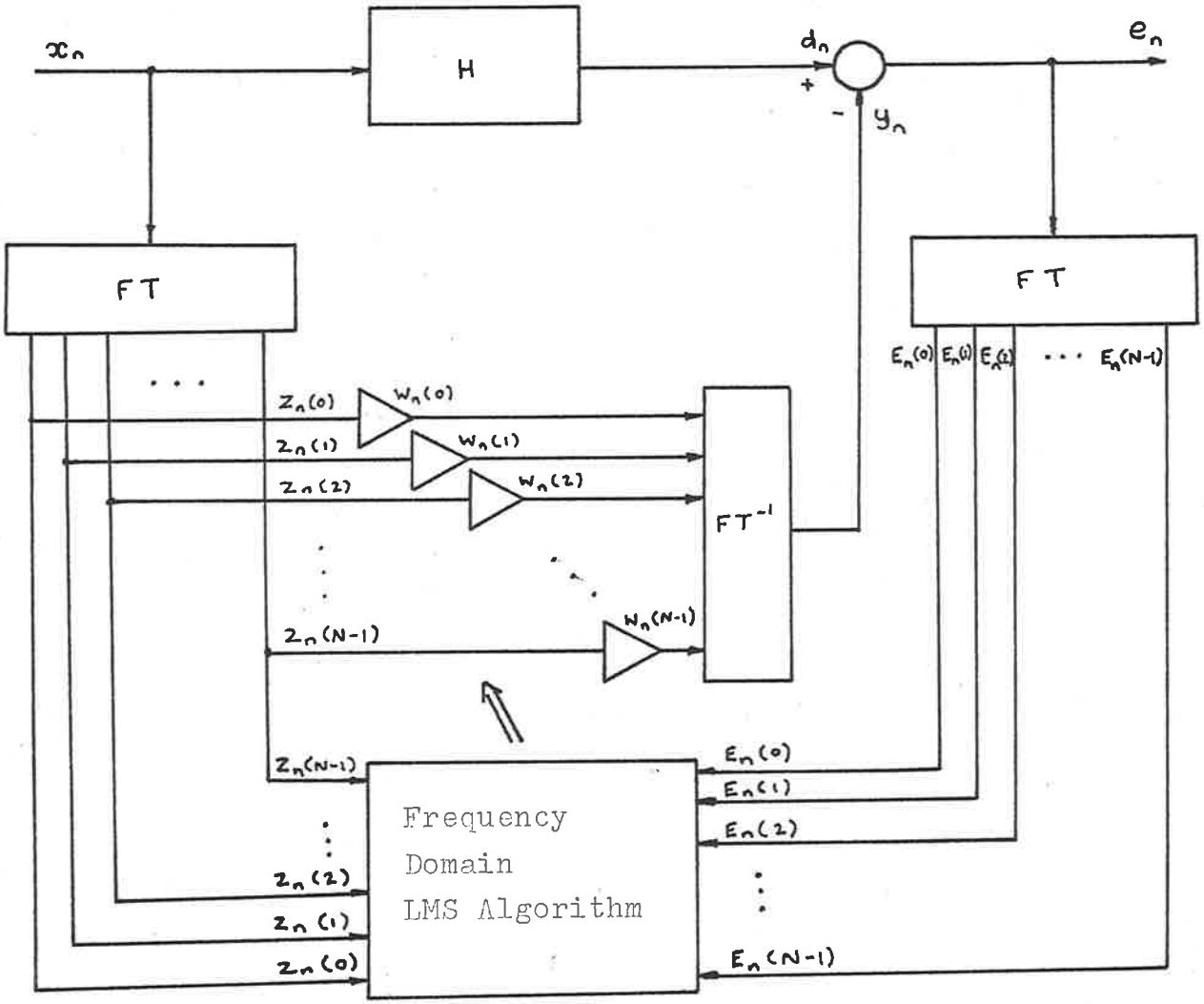

FIG A3.1: Frequency Domain Adaptive Noise Canceller

REFERENCES

(0): BRONER N.
"The Effects of Low Frequency Noise on People - A Review"
J. Sound & Vib., Vol 58, No 4, (1978), 483-500

(1): OLSON H.F., MAY E.G.
"Electronic Sound Absorber"
J. Acoust. Soc. Am., Vol 25, No 6, (1953), 1130-1136

(2): OLSON H.F.
"Electronic Control of Noise, Vibration and Reverberation"
J. Acoust. Soc. Am., Vol 28, No 5, (1956), 966-972

(3): CONOVER W.B.
"Fighting Noise With Noise"
Noise Control, Vol 92, (1956), 78-82

(4): LEVENTHALL H.G.
"Active Attenuators: Histroical Review and Some Recent Developments"
Inter-Noise 1980, Miami, USA

(5): WARNAKA G.E.
"Active Attenuation of Noise - The State of the Art"
Noise Cont. Eng., Vol 18, No 3, (1982),100-110

(6): JESSEL, M.J.M., MANGIANTE G.A.
"Active Sound Absorbers in An Air Duct"
J. Sound & Vib.,Vol 23, No 3, (1972), 383-390

(7): KEMPTON A.J.

"The Ambiguity of Acoustic Sources - A Possibility For Active Control"

J. Sound & Vib., Vol 48, No 4, (1976), 475-483

(8): MANGIANTE G.A.

"Active Sound Absorption"

J. Acoust. Soc. Am., Vol 61, No 6, (1977), 1516-1523

(9): CANEVET G.

"Active Sound Absorption In An Air Conditioning Duct"

J. Sound & Vib., Vol 58, No 3, 333-345

(10): JESSEL M.J.M., ANGEVINE O.L.

"Active Acoustic Attenuation of a Complex Noise Source"

Inter-Noise 1980, Miami, USA

(11): SWINBANKS M.A.

"The Active Control of Sound Propagation in Long Ducts"

J. Sound & Vib., Vol 27, No 3, (1973), 411-436

(12): POOLE J.H.B., LEVENTHALL H.G

"An Experimental Study of Swinbanks Method of Active Attenuation of Sound in Ducts"

J. Sound & Vib., Vol 49, No 2, (1976), 257-266

(13): POOLE J.H.B., LEVENTHALL H.G.

"Active Attenuation of Noise in Ducts"

J. Sound & Vib., Vol 57, No 2, (1978), 308-309

(14): BERENGIER M., ROURE A.
"Broad-Band Active Sound Absorption in a Duct Carrying Uniformly Flowing Fluid"
J. Sound & Vib., Vol 68, No 3, (1980), 437-449

(15): LA FONTAIN R.F., SHEPHERD I.C.
"An Experimental Study of A Broadband Active Attenuator For Cancellation of Random Noise In Ducts"
J. Sound & Vib., Vol 91, No 3, (1983), 351-362

(16): ROSS C.F.
"Experiments on the Active Control of Transformer Noise"
J. Sound & Vib., Vol 61, No 4, (1978), 473-480

(17): ROSS C.F.
"Demonstration of Active Control of Broadband Sound"
J. Sound & Vib., Vol 74, No 3, (1981), 411-417

(18): ROSS C.F.
"Application of Digital Filtering to Active Control of Sound"
Acoustica, Vol 51, (1982),135-140

(19): ROSS C.F.
"An Algorithm for Designing a Broadband Active Sound Control System"
J. Sound & Vib., Vol 80, (1982), 373-380

(20): EGHTESADI Kh.
"Attenuation of Noise By Active Methods"
Noise & Vib. Bulletin, Oct 1979, 234-238

(21): EGHTESADI Kh., LEVENTHALL H.G.
"Active Attenuation of Noise: The Chelsea Dipole"
J. Sound & Vib., Vol 75, No 1, (1981), 127-134

(22): EGHTESADI Kh., LEVENTHALL H.G.
"The Effects of Non-Ideal Elements and Geometry on the Performance of the Chelsea Dipole Active Attenuator"
J. Sound & Vib., Vol 91, No 1, (1983),1-10

(23): EGHTESADI Kh., LEVENTHALL H.G.
"A Study of N-Source Active Attenuator Arrays For Noise In Ducts"
J. Sound & Vib., Vol 91, No 1, (1983), 11-19

(24): EGHTESADI Kh., LEVENTHALL H.G.
"Active Attenuation of Noise - The Monopole System"
J. Acoust. Soc. Am., Vol 71, No 3, (1982), 608-611

(25): EGHTESADI Kh., HONG W.K.W., LEVENTHALL H.G.
"The Tight-Coupled Monopole Active Attenuator in A Duct"
Noise Cont. Eng. J., Vol 20, No 1, (1983), 16-20

(26): TRINDER M.C.J., NELSON P.A.
"Active Noise Control in Finite Length Ducts"
J. Sound & Vib., Vol 89, No 1, (1983), 95-105

(27): CHAPLIN G.B.B.
"The Essex Systems of Active Cancellation of Noise and Vibration"
Wolfson Centre, Dept. EES, Essex University, Oct 1981

(28): CHAPLIN G.B.B.
"Anti-Noise - The Essex Breakthrough"
Chartered Mech. Eng., Jan 1983, 41-47

(29): WARNAKA G.E.
"Acoustic Mixing in Active Attenuators"
Inter-Noise 1980, Miami, USA,683-688

(30): SHORT W.R.
"Global Low Frequency Active Noise Attenuation"
Inter-Noise 1980, Miami, USA, 695-698

(31): SONDHI M.M.
"An Adaptive Echo Canceller"
Bell Syst. Tech. J., Vol 46, No 3, (1967),497-511

(32): DUTTWEILLER D.L.
"A Twelve Channel Digital Echo Canceller"
IEEE Trans. Com., Vol 26, No 5, (1978), 647-653

(33): GITLIN R.D., WEINATEIN S.B.
"The Effects of Interference on the Tracking Capability of Digitally Implemented Echo Cancellers"
IEEE Trans. Com., Vol 26, No 6, (1978),833-839

(34): WHERMANN R., VAN DER LIST J., MEISSNER P.
"A Noise-Insensitive Compromise Gradient Method for the Adjustment of Adaptive Echo Cancellers"
IEEE Trans. Com., Vol 28, No 5, (1980),753-758

(35): SONDHI M.M., BERKLEY D.A.
"Silencing Echoes on the Telephone Network"
Proc. IEEE, Vol 68, No 8, (1980), 949-963

(36): ROSS C.F.
"An Adaptive Digital Filter for Broadband Active Sound Control"
J. Sound & Vib., Vol 80, No 3, (1982), 381-388

(37): ROSS C.F.
"Active Control of Sound"
PHD Dissertation, Queens College Cambridge, Jul. 1980

(38): ROSS C.F.
"Active Control of Repetitive Noise"
Fortschritte Der Akustik - FASE/DAGA '82, 333-337

(39): WIDROW B., HOFF M.
"Adaptive Switching Circuits"
In IRE WESCON Conv. Rec., Pt. 4, (1960), 96-104

(40): WIDROW B., GLOVER J.R., MCCOOL J.M., KAUNITZ J., WILLIAMS C.S., HEARN R.H., ZEIDLER J.R., DOMG E. GOODLIN R.C.
"Adaptive Noise Cancelling: Principles and Applications"
Proc. IEEE, Vol 63, No 12, (1975), 1692-1716

(41): WIDROW B., MCCOOL J.M., LARIMORE M.G., JOHNSON C.R.
"Stationary and Non-Stationary Learning Characteristics of the LMS Adaptive Filter"
PROC. IEEE, Vol 64, No 8, (1976), 1151-1162

(42): BURGESS J.C.
"Active Adaptive Sound Control in a Duct: A Computer Simulation"
J. Acoust. Soc. Am., Vol 70, No 3, (1981), 715-726

(43): WARNAKA G.E., TICHY J., POOLE L.A.
"Improvements in Adaptive Active Attenuators"
Inter-Noise 1981, 307-311

(44): POOLE L.A., WARNAKA G.E., CUTTER R.C.
"The Implementation of Digital Filters Using a Modified Widrow-Hoff Algorithm for the Adaptive Cancellation of Acoustic Noise"
Procs. IEEE ICASSP 84, San Diego Mar. 1984.

(45): BOGNER R.E.
"Proposals For Signal Processing For Active Attenuation of Noise in Ducts"
Electrical Eng. Dept., Adelaide University, 1980

(46): NELDER J.A., MEAD R.
"A Simplex Method for Function Minimization"
Computer J., Vol 7, No 4, (1956), 308-313

(47): BITMEAD R.R., ANDERSON B.D.O.
"Adaptive Frequency Sampling Filters"
IEEE Trans. ASSP, Vol 29, No 3, (1981), 684-693

(48): WARNAKA G.E., POOLE L.A., TICHY J.
"Transient Response in Active Systems"
Inter-Noise 1982, San Francisco, USA

(49): TRIECHLER J.R.
"Transient and Convergent Behaviour of the Adaptive Line Enhancer"
IEEE Trans. ASSP, Vol 27, No 1, (1979), 53-62

(50):TRIECHLER J.R.
"Response of Adaptive Line Enhancer to Chirped and Doppler Shifted Sinusoids"
IEEE Trans. ASSP, Vol 28, No 3, (1980), 343-348

(51):MORGAN D.R.
"An Analysis of Multiple Correlation Cancellation Loops With A Filter in the Auxiliary Path"
IEEE Trans. ASSP, Vol 28, No 4, (1980), 454-467

(52): BERSHAD N.J., FEINTUCH P.L., REED F.A., FISHER B.
"Tracking Characteristics of the LMS Adaptive Line Enhancer - Response to a Linear Chirp Signal in Noise"
IEEE Trans. ASSP, Vol 28, No 5, (1980), 504-515

(53): FARDEN D.C.
"Tracking Properties of Adaptive Signal Processing Algorithms"
IEEE Trans. ASSP, Vol 29, No 3, (1981),439-446

(54): WU M.Y.
"A Note on Stability of Linear Time-Varying Systems"
IEEE Trans. Auto. Cont., Vol 19, (1974),162

(55): WU M.Y.
"A New Concept of Eigenvalues and Eigenvectors and Its Application"
IEEE Trans. Auto. Cont., Vol 25, No 4, (1980), 824-826

(56):BITMEAD R.R., ANDERSON B.D.O.
"Lyapunov Techniques for the Exponential Stability of Linear Difference Equations With Random Coefficients"
IEEE Trans. Auto. Cont., Vol 25, No 4, (1980), 782-787

(57): BITMEAD R.R., ANDERSON B.D.O.
"Performance of Adaptive Estimation Algorithms in Dependent Random Environments"
IEEE Trans. Auto. Cont., Vol 25, No 4, (1980), 788-793

(58): MORI T., FUKUMA N., KUNAHARA M.
"Delay-Independent Stability Criteria For Discrete Delay Systems"
IEEE Trans. Auto. Cont., Vol 27, No 4, (1982), 964-966

(59): KABAL P.
"The Stability of Adaptive Minimum Mean Square Error Equalizers Using Delayed Adjustment"
IEEE Trans. Com., Vol 31, No 3, (1983), 430-432

(60): BERANEK L.L.
"Acoustics"
McGraw-Hill , (1954)

(61): WIDROW B., WALACH E.
"Adaptive Signal Processing For Adaptive Control"
Procs. IEEE ICASSP 84, San Diego Mar. 1984.

(62): WIDROW B., MCCOOL J., BALL M.
"The Complex LMS Algorithm"
Proc. IEEE, Vol 63, Apr. 1975, 719-720

(63): DENTINO M., MCCOOL J., WIDROW B.
"Adaptive Filtering in the Frequency Domain"
Proc. IEEE, Vol 66, No 12, (1978), 1658-1659

(64): FERRARA E.R.
"Fast Implementation of LMS Adaptive Filters"
IEEE Trans ASSP, Vol 28, No 4, (1980), 474-475

(65): NARAYAN S.S., PETERSON A.M.
"Frequency Domain Least Mean Square Algorithm"
Proc. IEEE, Vol 69, No 1, (1981),124-126

(66): REED F.A., FETINUCH P.L.
"A Comparison of the LMS Adaptive Cancellers Implemented in the Frequency Domain, and the Time Domain"
IEEE Trans. ASSP, Vol 29, No 3, (1981), 770-775

(67): MANSOUR D., GRAY A.H.
"Unconstrained Frequency-Domain Adaptive Filter"
IEEE Trans. ASSP, Vol 30, No 5, (1982),726-734

(68): NARAYAN S.S., PETERSON A.M., NARASHIMA M.J.
"Transform Domain LMS Algorithm"
IEEE Trans. ASSP, Vol 31, (1983), 609-615

(69): OGUE J.C., SATIO T., HOSHIKO Y.
"A Fast Convergence Frequency Domain Adaptive Filter"
IEEE Trans. ASSP, Vol 31, No 5, (1983), 1312-1314

(70) CLARK G.A., PARKER S.R., MITRA S.K.
"A Unified Approach to Time- and Frequency- Domain Realization of FIR Adaptive Filters"
IEEE Trans. ASSP, Vol 31, No 5, (1983), 1073-1083

(71): LEE J.C., UN C.K.
"On the Convergence Behaviuor of Frequency-Domain LMS Adaptive Digital Filters"
Procs. IEEE ICASSP 84, San Diego Mar. 1984

(72): BOGNER R.E.
"Frequency Sampling Filters - Hilbert Transformers and Resonators"
Bell Syst. Tech. J., Vol 48, (1969), 501-510

(73): NATARAJAN T., AHMED N., RAO K.R.
"Discrete Cosine Transforms"
IEEE Trans. Comp., (1974), 90-93

(74): STULLER J.A.
"Generalized Running Discrete Transforms"
IEEE Trans. ASSP, Vol 30, No 1, (1982), 60-68

(75): CROCKER M.J., KESSLER F.M., PRICE A.J.
"Noise and Noise Control Vol I and II"
CRC Press 1982

(76): CLARK G.A., PARKER S.R. MITRA S.K.
"A Unified Approach to Time- and Frequency Domain Realization of FIR Adaptive Digital Filters"
IEEE Trans. ASSP, Vol 31, No 5, (1983), 1073-1083

(77): REDDI S.S.
"A Time-Domain Adaptive Algorithm for Rapid Convergence"
Proc. IEEE, Vol 72, No 4, (1984), 533-535

(78): RADER C.M., GOLD B.
"Digital Filter Design Techniques in the Frequency Domain"
Proc. IEEE, Vol 55, No 2, (1967), 149-171